Structure/Function Studies of Rat Uncoupling Protein in Yeast Mitochondria

by

Debra Lynn Murdza-Inglis

A Thesis

Submitted to the School of Graduate Studies

in Partial Fulfillment of the Requirements

for the Degree

Doctor of Philosophy

McMaster University,

STRUCTURE/FUNCTION STUDIES OF RAT UCP IN YEAST MITOCHONDRIA

DOCTOR OF PHILOSOPHY (1995)
(Biochemistry)

McMASTER UNIVERSITY
Hamilton, Ontario

TITLE: Structure/Function Studies of Rat Uncoupling Protein in Yeast Mitochondria

AUTHOR: Debra Lynn Murdza-Inglis, B.Sc. (McMaster University)

SUPERVISOR: Dr. K.B. Freeman, Professor

NUMBER OF PAGES: xix, 182

ABSTRACT

Uncoupling protein (UCP) is one of a family of mitochondrial transport proteins involved in energy metabolism. It is specific to brown adipose tissue mitochondria where it has the primary function in mammals of non-shivering thermogenesis. Heat production is achieved by uncoupling oxidative phosphorylation. It has been suggested that UCP serves the uncoupling role by providing a regulated pathway for proton re-entry back into the mitochondrial matrix. UCP also transports monovalent anions electrophoretically, such as chloride and alkylsulfonates, but the physiological role of anion transport is not yet known, although models based on UCP-catalyzed anion transport for uncoupling have been put forth. Both proton and anion transport are inhibited by purine nucleoside di- and triphosphates, but only proton transport is activated by fatty acid. The detailed mechanisms of ion transport and their regulation remain unknown.

Our approach to studying UCP independently from all other brown adipose tissue mitochondrial protein components was to functionally express UCP in a novel cellular environment. The initial goal of this project was to establish an expression system in yeast to determine whether UCP was responsible for the nucleotide-sensitive ion permeabilities observed in brown adipose tissue mitochondria. Establishing a functional yeast expression system would also allow structure/function relationships of UCP to be explored using site-directed mutagenesis of the UCP cDNA.

An expression system for UCP in yeast was developed by inserting the rat UCP cDNA into a *Saccaromyces cerevisiae/Escherichia coli* shuttle vector under transcriptional control or the inducible *GAL* 1 promoter and transforming yeast strain JB516 (*MATa, ura3, ade1, leu2, his4, gal$^+$*) with this construct. High level expression of rat UCP in yeast mitochondria was achieved by altering the region around the start codon in the rat UCP cDNA to one resembling a highly expressed yeast gene. Expression of 70-100 μg UCP/mg mitochondrial protein is reported, a level similar to that found in brown adipose tissue mitochondria of cold adapted rats. Functional assays were developed for UCP in yeast mitochondria to measure fatty acid-activated, GDP-inhibited uncoupling of yeast mitochondria and to measure GDP bound to yeast mitochondria containing UCP. Oleate-activated uncoupling that was reversed by GDP was observed and specific for yeast mitochondria containing UCP. In addition, GDP was found to bind specifically to yeast mitochondria containing UCP with a comparable affinity to that found for brown adipose tissue mitochondria, although the level of binding was lower.

Past chemical modification studies on UCP using cysteine and arginine modifying reagents suggested that these residues had functional significance with respect to ion transport and their regulation. However, the specific location of these residues could not be determined. Photoaffinity labelling with purine nucleotide analogs showed that the third domain of UCP was involved in purine nucleotide binding, but these studies also did not identify functionally important residues. The yeast expression system was used in conjuction with site-directed mutagenesis of the UCP cDNA to identify functionally important residues in UCP.

Initial studies focused on the cysteines of UCP, all seven of which are conserved in UCP in all species studied to date. Each cysteine was changed independently to serine. Yeast mitochondria containing independently each mutant form of UCP showed fatty acid-activated, GDP-inhibited uncoupling. Cysteine 253 was modified further to alanine and phenylalanine to further investigate the role of this residue since cysteine 253 had been covalently labelled with a purine nucleotide analogue. These substitutions were also without effect on UCP function in yeast mitochondria. From the cysteine studies, it appears that none of the seven cysteines in UCP serve a critical role in fatty-acid activated, GDP-inhibited uncoupling. The next study investigated the role of arginine 276 in UCP. This residue was mutated to both glutamine and leucine. Yeast mitochondria containing the mutant proteins showed normal fatty acid-activated uncoupling, but the inhibitory effect of GDP was lost. Arginine 276 was therefore found to be involved in purine nucleotide regulation of UCP, but presently, it is not known if this residue is involved directly in the binding of purine nucleotides or in propogating the response in the protein to bound nucleotide.

ACKNOWLEDGEMENTS

I would like to express my most sincere thanks to my thesis supervisor, Dr. Karl B. Freeman. He not only provided expert guidance, critical evaluations and support throughout my research on this challenging project, but he also provided me with many opportunites to grow as a scientist and an individual. I will miss being part of his laboratory, and I will certainly miss his witty stories. I would also like to thank my supervisory committee members, Dr. J. Capone, Dr. R. Bell and Dr. S. Bayley, for their valuable discussions and suggestions throughout this work.

I would also like to make special mention to Ms. Hansa Patel, who taught me basic laboratory practices when I started as a summer student many years ago, and continued to offer her excellent technical assistance throughout this work. Her friendship, guidance and support will always be greatly appreciated. I must also thank my collaborators in Dr. K. D. Garlid's laboratory, M. Modriansky, D. E. Orosz, P. Jezek, G. Woldegiorgis and K.D. Garlid for their contributions to our publications, and for continuing with this reasearch.

I gratefully acknowledge The Medical Research Council of Canada for their generous support of a Studentship throughout this research.

I extend my sincere gratitude to Lisa Kush for all her help and patience in the preparation of this thesis and throughout this work. I would also like to thank my co-workers for providing a stimulating and enjoyable work atmosphere. Sincere thanks are extended to fellow students Karen Craig, Geoff Werstuck, Dan Syroid, Richard Tapping, Dino Trigatti, Jae-Ho Yoo, Tina McCallum, Richard Pfeutzner, Susanna Reichling and Alex Balogh. To the office staff who were never too busy to listen or help, Barbara Sweet, Bonnie Murphy and Dale Tomlinson, thank you.

Lastly, my deepest thanks are extended to my family. Thank you Dad for instilling in me the desire to always strive to do my best and for your encouragement over the years. Thank you to my brothers Steve and Peter, and their families, and my mother- and father-in-law for their love and support over the years. Last but not least, I would like to thank my husband Rob, not only for his encouragement throughout the years, but also for helping me to enjoy life outside the laboratory.

I would like to dedicate this thesis in memory of my mother, who knew from the time I was ten years old that I was destined for a career in research. She was right!

TABLE OF CONTENTS

LIST OF FIGURES

LIST OF TABLES

LIST OF ABBREVIATIONS

AAC	ADP/ATP carrier
ADP	adenosine diphosphate
AMP	adenosine monophosphate
ala	alanine
arg	arginine
ATP	adenosine triphosphate
bis-acrylamide	N,N'-methylene bis-acrylamide
BSA	bovine serum albumin
cAMP	cyclic AMP
CCCP	carbonylcyanide-m-chlorophenylhydrazone
C-terminal	carboxyl-terminal
cDNA	complementary DNA
CDTA	trans-1,2-diaminocyclohexane-N,N,N'N'-tetra-acetic acid
CHO	Chinese hamster ovary
Ci	curie
CoA	coenzyme A
cys	cysteine
$\Delta\mu_{H+}$	proton electrochemical potential or proton motive force
dATP	deoxyadenosine triphosphate

DNA	deoxyribonucleic acid
DTT	dithiothreitol
ECL	enhanced chemiluminesence
EDTA	ethylenediamine tetraacetic acid
ELISA	enzyme-linked immunosorbent assay
EtOH	ethanol
gal	galactose
G3PDa	glyceraldehyde-3-phosphate dehydrogenase
GDP	guanosine diphosphate
h	hour
HEPES	N-2-hydroxethylpiperazine-N'-2-ethane
kcal	kilocalorie
K_d	dissociation constant
kDa	kilodalton
K_i	inhibition constant
K_M	Michaelis Menten constant
LB	Luria-Bertani
M	molar
min	minute
mol	mole
MOPS	3[N-morpholino]propanesulphonic acid
mRNA	messenger RNA

mV	millivolt
nmol	nanomol
NP-40	Non-idet 40
N-terminal	amino-terminal
PAGE	polyacrylamide gel electrophoresis
PEG	polyethylene glycol
phe	phenylalanine
PiC	phosphate carrier
PMSF	*para*-methylsulphonylfluoride
PTP	phosphate transport protein
RCR	respiratory control ratio
RF	replicative form
RNA	ribonucleic acid
S	substrate
SDS	sodium dodecyl sulphate
sec	second
ser	serine
T4	bacteriophage T4
T7	bacteriophage T7
TBE	Tris-borate-EDTA
TE	Tris-EDTA
TEMED	N,N,N'N'-tetramethylethylenediamine

Tris	Tris(hydroxymethyl)aminomethane
v/v	volume per total volume
V_{max}	maximum velocity
UCP	uncoupling protein
UCP_d	uncoupling protein dimer
UCP_m	uncoupling protein monomer
wt	wild type
w/v	weight per total volume

INTRODUCTION

The primary function of brown adipose tissue in mammals is to produce heat, either to maintain or raise body temperature, known as non-shivering thermogenesis, or to waste food energy, known as diet-induced thermogenesis (reviewed in Himms-Hagen, 1990). Heat is produced by brown adipose tissue due to the action of a mitochondrial inner membrane protein unique to this tissue known as uncoupling protein (UCP) or thermogenin. UCP has a molecular mass of 32kDa and is thought to function in the inner membrane as a dimer, as discussed later in the introduction.

1.1 MITOCHONDRIAL OXIDATIVE PHOSPHORYLATION

In all mitochondria, the inner membrane is relatively impermeable to charged species. During mitochondrial respiration, as electrons are transferred from the substrate being oxidized through the electron transport chain (respiratory chain) and finally onto oxygen, protons are pumped out from the mitochondrial matrix across the mitochondrial inner membrane into the intermembrane space (Figure 1-1). Because the inner membrane is relatively impermeable to protons, a proton electrochemical gradient is established across the inner membrane that serves to temporarily store the energy released from substrate oxidation. When protons flow down their electrochemical gradient re-entering the mitochondrial matrix, energy is released. If protons re-enter the matrix through the ATP synthase, the energy released is used to drive ATP synthesis. Mitochondria are under respiratory control when substrate oxidation occurs only in response to

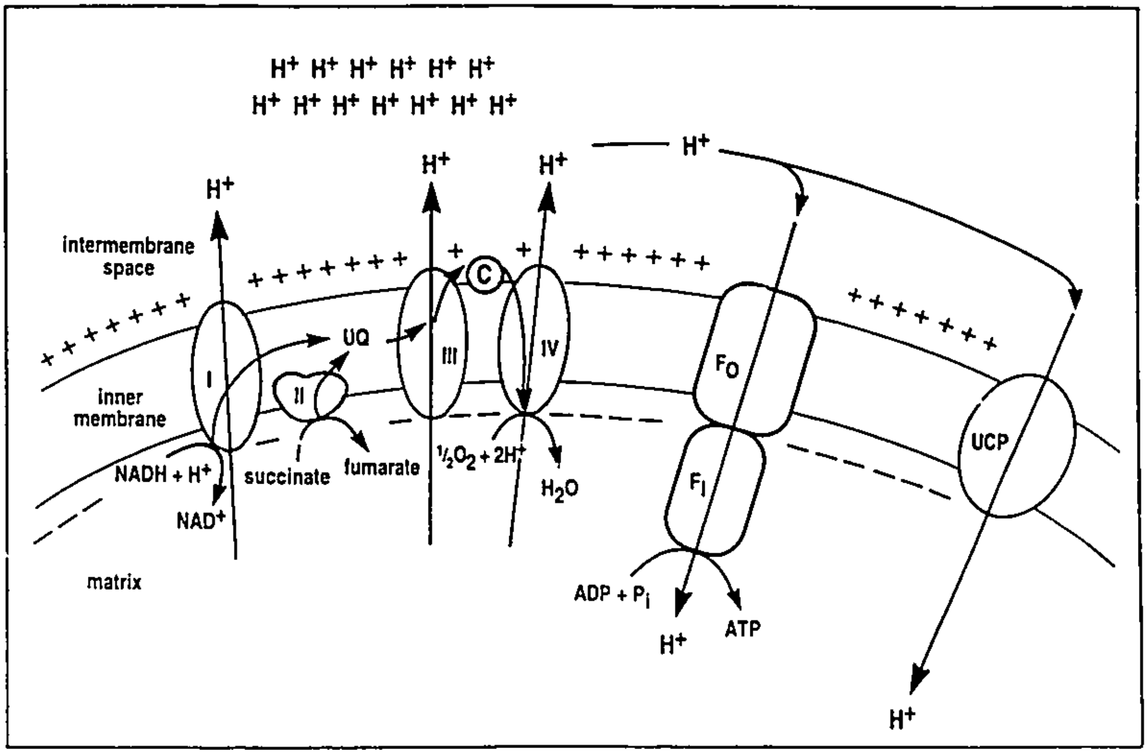

Figure 1-1. Mitochondrial Oxidative Phosphorylation (Modified from Lehninger et al., 1993)

Electrons from NADH or other oxidizable substrates are transferred through the complexes of the respiratory chain (I,II,III,IV) to oxygen. Electrons reach ubiquinone (UQ) via complexes I and II. UQH_2 is a mobile carrier of electrons. It passes electrons to complex III, which in turn passes them to cytochrome *c*, another mobile carrier. Complex IV transfers electrons from reduced cytochrome *c* to oxygen. As electrons flow through complex I, III and IV, protons are pumped by the complexes from the matrix into the intermembrane space, forming a proton electrochemical gradient across the inner membrane. The energy released as protons re-enter the matrix through the ATP synthase (F_0F_1) is used to drive ATP synthesis. If protons re-enter the matrix through an alternate pathway (UCP) rather than through the ATP synthase, the released energy is dissipated as heat.

phosphorylation of ADP to ATP so that proton extrusion (through the respiratory chain) is balanced by proton re-entry (through the ATP synthase). Under these circumstances, oxidation and phosphorylation are coupled by the proton electrochemical gradient and, therefore, the mitochondria are termed coupled. If protons re-enter the matrix by an alternate pathway rather than through the ATP synthase, substrate oxidation will still occur in response to proton re-entry into the matrix, but without phosphorylation of ADP by the ATP synthase. Under these circumstances, oxidation and phosphorylation are not coupled to each other through the proton electrochemical gradient and, therefore, these mitochondria are termed uncoupled. Uncoupled mitochondria lack respiratory control because oxidation occurs in the absence of phosphorylation. In brown adipose tissue mitochondria, UCP provides an alternate pathway for protons to re-enter the matrix such that the ATP synthase is bypassed. Without the synthesis of ATP, the energy released from the proton electrochemical gradient is dissipated as heat. Brown adipose tissue UCP is so named because of its uncoupling effect on oxidative phosphorylation. UCP is also known as thermogenin due to the heat generated by its mitochondrial uncoupling action.

1.2 ACTIVATION OF NON-SHIVERING THERMOGENESIS

Non-shivering thermogenesis can be activated in newborns and rodents by exposure to cold due to the activation of UCP present in brown adipose tissue mitochondria (reviewed in Himms-Hagen, 1990; Nedergaard and Cannon, 1992). A cold stimulus causes the release of noradrenaline from the sympathetic nerves directed to brown adipose tissue. Of the adrenergic receptors on the brown adipocyte, interaction of noradrenaline with the β_3-type appears to be the most relevant to induce the acute thermogenic response in hamsters and rats (Arch *et al.*, 1984; Arch, 1989; Mohell and Dicker, 1989; Zhoa *et al.*, 1994), although β_1-adrenergic receptors may also be involved in the rat (Granneman and Whitty, 1991; Scarpace and Matheny, 1991; Gourbern *et al.*, 1993). Interaction of noradrenaline with β-receptors increases adenylate cyclase activity which increases the cellular cAMP level which in turn triggers a cAMP-dependent cascade of events. The cAMP activates a protein kinase which in turn activates a lipase that releases free fatty acid from the triacylglycerol stores in the brown adipocyte. Some of the free fatty acid released by the lipase activates UCP present in the mitochondrial inner membrane. The mechanism of fatty acid activation of UCP at present is unknown, but is discussed in sections **1.3.1 Fatty Acid Activation of UCP** and **1.5 UCP AS A FATTY ACID ANION TRANSPORTER**. Activated UCP provides an alternate pathway for protons to re-enter the mitochondrial matrix, thus dissipating the energy from oxidation that was stored in the proton electrochemical gradient as heat. Most of the released fatty acids are oxidized by β-oxidation to provide fuel for the mitochondrial respiratory chain directly in the form of reduced coenzymes and indirectly in the form of acetyl-CoA which enters the citric acid cycle. Since the respiratory chain operates at an accelerated rate in response to the dissipation of the proton electrochemical gradient due to the action of UCP, this accelerates all of the mitochondrial dehydrogenases of the citric acid cycle (for isocitrate, oxoglutarate, succinate and malate) that deliver reduced coenzymes to the respiratory chain (Himms-Hagen, 1990). In addition to activating UCP present in brown adipose tissue mitochondria, cold exposure also causes an increase in the thermogenic response in mammals by increasing the amount of brown adipose tissue in the animal and by increasing the level of UCP in brown adipose tissue (reviewed in Himms-Hagen, 1990).

1.3 REGULATION OF PROTON CONDUCTANCE

Early in the study of brown adipose tissue mitochondria, it was determined that respiratory control of uncoupled brown adipose tissue mitochondria was gained by removal of endogenous fatty acid (either by albumin addition or β-oxidation) and by addition of purine nucleoside di- or triphosphates (reviewed in Nicholls *et al.*, 1986). The mechanisms by which fatty acids and purine nucleotides regulated the proton conductance of the inner membrane of brown adipose tissue mitochondria was studied in a series of experiments initiated by Nicholls using Syrian hamster (Nicholls, 1974a, Rial *et al.*, 1983) and guinea pig (Nicholls, 1977) brown adipose tissue mitochondria. In these studies, proton conductance was measured as the proton current carried back across the mitochondrial inner membrane, in the absence of ATP synthesis, per unit of proton electrochemical potential (nmol H^+/min/mg mitochondrial protein/mV). Proton current was calculated from the mitochondrial respiratory rate. They also characterized the conductance as either ohmic, which means that there is a linear relation between respiration and proton electrochemical potential, $\Delta\mu_{H+}$, or non-ohmic, where the respiratory rate increases without a proportional increase in membrane potential. The membrane potential where conductance changes from ohmic to non-ohmic is termed the breakpoint potential.

Rat liver mitochondria show a low ohmic conductance of 0.13 nmol H^+/min/mg/mV up to 180 mV, above which the proton conductance increases in a non-ohmic fashion (Nicholls, 1974b). The membrane potential where the transition from ohmic to non-ohmic conductance occurs is known as the breakpoint potential, which is approximately 180 mV in rat liver mitochondria (Nicholls, 1974b). The maximum $\Delta\mu_{H+}$

maintained across rat liver mitochondria is 230 mV (Nicholls, 1974b). Nicholls (1974a; 1977) found that isolated brown adipose tissue mitochondria could not maintain a $\Delta\mu_{H+}$ across the inner membrane in the presence of endogenous fatty acid and in the absence of GDP, therefore the proton conductance was unmeasurably high. Addition of albumin to brown adipose tissue mitochondria to bind fatty acid lowered the conductance across the inner membrane such that a relatively high ohmic conductance (3.8 and 16 nmol H^+/min/mg/mV in hamster and guinea pig brown adipose tissue mitochondria respectively) was established (Nicholls, 1974a; Nicholls, 1977). In the presence of albumin, the inner membrane was able to maintain a $\Delta\mu_{H+}$ of 80 mV (Nicholls, 1974a; Nicholls, 1977). Addition of both albumin and GDP substantially lowered the proton conductance of the inner membrane of brown adipose tissue mitochondria such that it mimicked that measured for rat liver mitochondria (Nicholls, 1974a; Nicholls, 1977; Rial *et al.*, 1983). A low ohmic conductance of 0.8 and 0.7 nmol H^+/min/mg/mV in hamster and guinea pig brown adipose tissue mitochondria respectively was established up to 180 mV, above which a high non-ohmic conductance was observed (Nicholls, 1974a; Nicholls, 1977; Rial *et al.*, 1983). Under these conditions, the mitochondrial inner membrane was able to maintain a maximum membrane potential of 230 mV. In the presence of albumin and GDP, addition of exogenous fatty acid to respiring brown adipose tissue mitochondria did not restore the higher ohmic conductance observed in the absence of GDP, but fatty acid addition *did over-ride* the inhibitory effect of GDP by increasing the non-ohmic proton conductance and decreasing the breakpoint potential (Rial *et al.*, 1983). It should be emphasized that in non-respiring mitochondria where the membrane potential is low and well below the breakpoint potential, fatty acid *can not over-ride* the inhibitory effect of GDP (Rial *et al.*, 1983).

1.3.1 Fatty Acid Activation of UCP

The effect of fatty acids on brown adipose tissue mitochondria have been studied in detail. Fatty acid stimulation of proton conductance in brown adipose tissue mitochondria increases with fatty acid chain length and requires an unesterified carboxyl group on the fatty acid (Rial *et al.*, 1983). Rial *et al.* (1983) reported respiratory rate increases of approximately 300% above the basal rate in the presence of GDP in brown adipose tissue mitochondria isolated from cold-adapted hamsters with the addition of myristic (14:0), palmitic (16:0), palmitoleic (16:1) and oleic (18:1) acids. Cunningham *et al.* (1986) found that palmitate uncoupled brown adipose tissue mitochondria isolated from cold-adapted guinea pigs in a partially saturable manner, requiring 100 nM free palmitate for half-maximal response. However, palmitate was ineffective at this concentration as an uncoupler of brown adipose tissue mitochondria in the presence of very low levels of UCP, when mitochondria were isolated from warm-adapted animals (Cunningham *et al.*, 1986). Fatty acid activation of proton flux across lipid membranes in proteoliposomes reconstituted with purified UCP has now been reported by several groups (Strieleman *et al.*, 1985; Jezek *et al.*, 1990; Katiyar and Shrago, 1991; Murdza-Inglis *et al.*, 1994; Winkler and Klingenberg, 1994). In a recent study by Winkler and Klingenberg (1994) fatty acids were found to stimulate proton flux in proteoliposomes reconstituted with UCP in parallel to results found for fatty acid respiratory stimulation of brown adipose tissue mitochondria (Rial *et al.*, 1983). Activation of proton flux in proteoliosomes required fatty acids with a chain length of at least C-8 reaching a maximum at C-14 for saturated fatty acids, with maximum activation also observed for long chain unsaturated fatty acids (oleic and linoleic). As in brown adipose tissue mitochondria, blockage of the free carboxyl group of the fatty acid prevented activation of proton flux (Winkler and Klingenberg, 1994).

1.3.2 GDP Inhibition of UCP

Nicholls (1976) first showed that brown adipose tissue mitochondria isolated from cold-adapted animals bound higher levels of GDP in comparison to brown adipose tissue mitochondria isolated from warm-adapted animals. The binding of 8-azido-ATP, a photoaffinity analogue of ATP, to brown adipose tissue mitochondria was used to identify a 32 kDa protein (UCP) as the unique purine nucleotide receptor in brown adipose tissue mitochondria (Heaton *et al.*, 1978). It has since been shown that GDP binding to and UCP levels in brown adipose tissue mitochondria vary depending on the thermogenic state of the animal, with the highest levels of both found in thermogenically active animals (reviewed in Trayhurn and Milner, 1989). In addition, the molar ratio of GDP bound per $UCP_{monomer}$ to brown adipose tissue mitochondria is highest in mitochondria isolated from cold-adapted animals when the proton conductance of the inner membrane is highest and lowest in mitochondria isolated from thermoneutral animals when the proton conductance of the inner membrane is lowest (reviewed in Trayhurn and Milner, 1989).

Changes in the level of GDP bound to brown adipose tissue mitochondria without changes in UCP levels (referred to as masking and unmasking of GDP binding sites on UCP) have been documented in several studies where bound GDP and UCP levels were quantified in parallel (reviewed in Trayhurn and Milner, 1989). Masking of GDP binding sites is observed in mitochondria taken from cold-adapted animals that have been rewarmed for a brief time period. These mitochondria show both a decrease in GDP binding level and a decrease in proton conductance without a change in UCP level (Swick and Swick, 1986; Peachey *et al.*, 1988; Goubern *et al.*, 1992). Conversely, unmasking of GDP binding sites is observed in mitochondria taken from warm-adapted animals that have been exposed briefly to the cold. These mitochondria show both an increase in GDP binding and an increase in proton conductance without an increase in UCP level (Desautels *et al.*, 1978; Gribskov *et al.*, 1986; Swick and Swick, 1986; Trayhurn *et al.*, 1987; Peachey *et al.*, 1988; Henningfeld and Swick, 1991). Due to the masking and unmasking of GDP binding sites on UCP, purine nucleotide binding to brown adipose tissue mitochondria is now used as an index of the activity of the proton conductance pathway in brown adipose tissue mitochondria, rather than as a measure of the amount of UCP present in the mitochondria. Masking and unmasking of GDP binding sites is thought to reflect inactivation and activation of UCP respectively (Trayhurn and Milner, 1989). The mechanism of masking and unmasking GDP binding sites on UCP is not known. It has been suggested that these changes may be enzyme-mediated because of the unmasking effect observed for UCP isolated from Mg^{2+} treated brown adipose tissue mitochondria (Swick and Swick, 1988; Henningfield and Swick, 1991). Unmasking of GDP binding sites induced by magnesium treatment of brown adipose tissue mitochondria was dependent on the time of treatment and concentration of magnesium used. Due to masking and unmasking of GDP binding sites on UCP, the molar ratio of GDP bound to active UCP is still not certain, ranging between 0.5 to 1 mol GDP per mol $UCP_{monomer}$ in mitochondria isolated from cold-adapted animals (reviewed in results section **3.3.1 GDP Binding to Brown Adipose Tissue Mitochondria**).

The affinity of purine nucleotides for purified UCP and UCP present in brown adipose tissue mitochondria is dependent on the pH of the binding medium (Nicholls, 1976, Klingenberg, 1988, Rafael *et al.*, 1994). The pH dependence of purine nucleotide binding to UCP was first shown using hamster brown adipose tissue mitochondria, where the K_d for GDP binding to the mitochondria increased from 4.2 μM at pH 6.7 to 34 μM at pH 7.9, an eight-fold reduction in the binding affinity (Nicholls, 1976). A more detailed binding study using purified hamster UCP over a pH range of 5-8 showed that the affinity was highest and pH independent between pH 5.5-6.5, but became pH dependent and decreased above pH 6.8 (Klingenberg, 1988). These results were confirmed for rat UCP using membrane particles isolated from rat brown adipose tissue (Rafael *et al.*, 1994).

1.4 UCP AS A MEMBER OF THE MITOCHONDRIAL CARRIER FAMILY

Uncoupling protein is one of the many transport proteins that are present in the mitochondrial inner membrane. The hydrophobic core of biological membranes creates a permeability barrier for the passage of charged species. Transport of positively or negatively charged or zwitterionic metabolites across the mitochondrial inner membrane is catalyzed by specific transport proteins, ten of which have been purified from animal mitochondria: ADP/ATP carrier (AAC), phosphate carrier (PiC; in yeast, PTP), UCP, oxoglutarate carrier, citrate transport protein, dicarboxylate carrier, pyruvate carrier, carnitine carrier, aspartate/glutamate carrier and ornithine carrier (reviewed in Palmieri, 1994). These mitochondrial carrier proteins have a narrow range of molecular mass from 28 to 34 kDa as measured by SDS-PAGE (Palmieri, 1994).

Five of these carriers have been sequenced to date; AAC, PiC, UCP, the oxoglutarate carrier and the citrate transport protein (Aquila *et al.*, 1982; Runswick *et al.*, 1987; Ridley *et al.*, 1986; Runswick *et al.*, 1990; Kaplan *et al.*, 1993). The sequenced proteins appear to form a family based on their primary amino acid sequence and proposed membrane structure (Aquila *et al.*, 1987). It was proposed that these carrier proteins have a tripartite structure, containing three related domains of approximately 100 residues with significant internal amino acid homology among the domains (Saraste and Walker, 1982). Based on hydropathy plots of the proteins and sequence alignment of the three domains, a transmembrane arrangement of the carriers was proposed (Saraste and Walker, 1982) as illustrated for UCP in Figure 1-2 (Klingenberg, 1990; Nedergaard and Cannon, 1992; Mayinger and Klingenberg, 1992; Klingenberg, 1993): each 100 residue domain contains two transmembrane amphipathic α-helices which are connected by a hydrophilic section of 35 to 40 residues (regions A,B,C in Figure 1-2) with each domain being connected by a shorter hydrophilic section (regions a,b in Figure 1-2).

It is now thought that both the N- and C-terminal ends of the carriers and the two short hydrophilic segments (regions a and b in Figure 1-2) connecting the three domains reside on the cytosolic side of the mitochondrial inner membrane (reviewed in Palmieri, 1994). It is also thought that each hydrophilic segment connecting the transmembrane helices within each domain (regions A, B and C in Figure 1-2) are on the matrix side of the mitochondrial inner membrane with part of each segment looping up into the membrane region between the amphipathic helices forming a pocket in the membrane (reviewed in Palmieri, 1994).

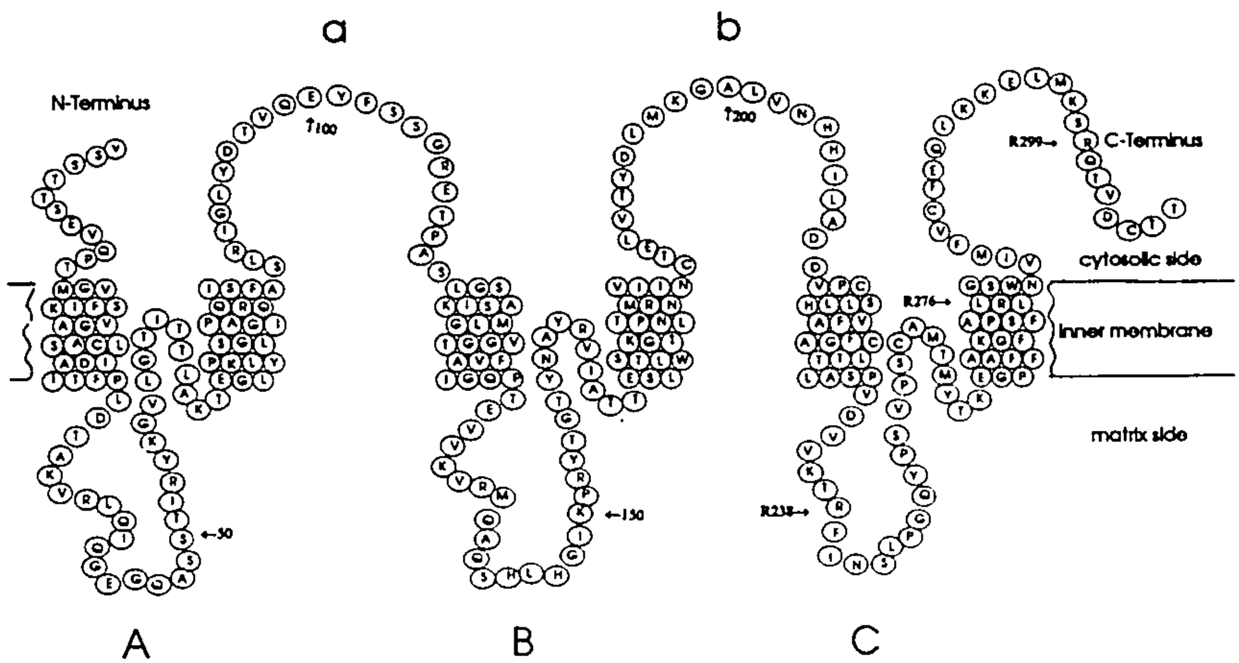

Figure 1-2. Putative Transmembrane Disposition Model of UCP in the Mitochondrial Inner Membrane

This putative transmembrane disposition model of UCP is based on the model proposed by Nedergaard and Cannon (1992) with the addition of matrix loops A, B and C depicted as looping up into the mitochondrial inner membrane, as proposed for UCP and AAC by Klingenberg (1990, 1993; Mayinger and Klingenberg, 1992). Regions a and b connect the 100 residue domains of UCP, whereas regions A, B and C connect the two transmembrane α-helices within each domain respectively. The N- and C-terminal ends of UCP and regions a and b are thought to reside on the cytosolic side of the inner membrane.

Support for the membrane disposition model of the carriers has come from several studies that examined the accessibility of the proposed extramembranous regions of the carriers to non-permeant probes such as proteolytic enzymes and peptide specific antibodies. Tryptic cleavage of UCP at lys292 in brown adipose tissue mitochondria indicated that the C-terminal end of UCP was directed towards the cytosolic side of the inner membrane (Eckerson and Klingenberg, 1987). This was further verified by the ability of a disulfide cross-link to be formed between C-terminal SH groups of UCP monomers at cys304 which could be removed by trypsin digest (Klingenberg and Appel, 1989). Arg residues in loop A of the AAC were found to reside on the matrix side of the inner membrane due to their accessibility to an arginine-specific endoprotease in inside-out submitochondrial particles only (Brandolin *et al.*, 1989). In similar studies using arg-endoprotease and lys-endoprotease to study the topology of PiC, loop B containing arg140 was found to be on the matrix side of the inner membrane (Capobianco *et al*, 1991) and loop a (containing lys96), loop b (containing lys198) and the C-terminal region (containing lys288) were found to be on the cytosolic side of the inner membrane (Palmieri *et al*, 1993).

The topology of AAC, PiC, the oxoglutarate carrier and UCP have all been studied using antibodies to different segments of the proteins. The N-terminal segment of AAC was found to be on the cytosolic side of the inner membrane from the reactivity of anti-N-terminal antibodies to AAC with frozen/thawed mitochondria (Brandolin *et al.*, 1989). Using antibodies raised against the N- and C-terminal segments of PiC and the oxoglutarate carrier, it was determined that both the N- and C-terminal segments of these proteins are on the cytosolic side of the inner membrane (Capobianco *et al.*, 1991;

Bisaccia *et al.*, 1994). Miroux *et al.* (1992, 1993) were able to verify the orientations of the first, second, third, fourth and sixth predicted α-helices in UCP using antibody back-titration experiments. In these experiments, the immunoreactivity of antibodies in an anti-UCP antibody preparation to individual fusion proteins containing antigenic epitopes of UCP was determined using an ELISA method. The sequence specificity of antibodies in the antibody preparation was determined by the fusion protein bound to the ELISA plate. To determine whether the sequence specific antibody being assayed could react with UCP on the cytosolic or matrix side of the inner membrane, the antibody preparation was incubated with increasing amounts of either brown adipose tissue mitochondria or brown adipose tissue submitochondrial particles respectively (submitochondrial particles contain both rightside-out and inside-out inner membranes). The residual sequence specific antibodies remaining unbound to mitochondria or submitochondrial particles were assayed by ELISA. If submitochondrial particles but not mitochondria decreased the ELISA signal, then the sequence specific antibody reacted to a UCP epitope on the matrix side of the inner membrane. If both submitochondrial particles and mitochondria decreased the ELISA signal, then the sequence specific antibody reacted to a UCP epitope on the cytosolic side of the inner membrane. Since the sequence specific epitope was on the ELISA plate, one could determine the sidedness with respect to the inner membrane of the UCP sequence.

Information on the membrane topology of the mitochondrial membrane carriers has also been gained from covalent binding studies of photoaffinity nucleotide derivatives to AAC and UCP (reviewed in Klingenberg, 1993). Because it was known that purine nucleotides regulate UCP from the cytosolic side of the inner membrane (Nicholls, 1976), but residues in the proposed matrix loop C of UCP were labelled by photoaffinity nucleotide derivatives, Klingenberg proposed that matrix loop C loops up into the membrane area between the transmembrane α-helices 5 and 6 as outlined in Figure 1-2 (Mayinger and Klingenberg, 1992). Because matrix loops B and C were labelled in AAC by the photoaffinity nucleotide derivatives, Klingenberg (1993) has proposed a membrane disposition model for AAC where each matrix loop A, B and C loops up into the membrane area between the transmembrane α-helices, as outlined for UCP in Figure 1-2.

It is thought that the carriers descended originally from a single gene that encoded a protein of 100 amino acids containing two transmembrane helices that formed the ancestral carrier family gene by gene triplication, followed by diversification to form the members of the carrier family (Saraste and Walker, 1982; Runswick *et al.*, 1987, Aquila and Klingenberg, 1987; Kuan and Saier, 1993). Based on the primary sequence of the carriers, UCP is most closely related to the oxoglutarate carrier (Kuan and Saier, 1993) which exchanges oxoglutarate and malate. Palmieri (1994) determined conserved residues among the carrier family by aligning 15 sequences among the 5 carriers. From the sequence alignment, the sequence motif P-h-D/E-h-h-K/R-(20-30 amino acids)-D/E-G-(4 amino acids)-a-K/R-G (h = hydrophobic, a = aromatic) was found to be repeated three times in the carriers, starting at the end of helices I, III and V respectively and ending in the middle of helices II, IV and VI respectively (Figure 1-2). It is likely that the highly conserved residues would not be involved in carrier specificitiy and, therefore, probably serve a structural role in the carriers (Walker and Runswick, 1993; Kuan and Saier, 1993; Palmieri, 1994).

This carrier family is also known as the mitochondrial anion carrier family of proteins because all of the sequenced mitochondrial carriers to date are known to transport anions acrcss the inner membrane. Transport of metabolites by this family occurs as electroneutral antiport or symport of two charged species (oxoglutarate carrier, citrate transport protein, PiC), electrogenic antiport of two charged species (AAC) or electrophoretic uniport (UCP).

The anion permeability of brown adipose tissue mitochondria was first identified by Nicholls and Lindberg (1973) when they found the inner membrane of brown adipose tissue mitochondria was permeable to chloride, bromide and nitrate and that the permeability in non-respiring mitochondria was inhibited by purine nucleotides. Like the fatty acid-induced proton conductance of brown adipose tissue mitochondria, the chloride conductance of brown adipose tissue mitochondria was not inhibited by GDP in respiring mitochondria. Anion transport was demonstrated for purified UCP reconstituted into proteoliposomes, where it was found that UCP catalyzed the transport of a large variety of anions including chloride, alkylsulfonates, oxohalogenides, some monovalent phosphate analogs and pyruvate (Jezek *et al.*, 1990; Jezek and Garlid, 1990). Only monovalent anions were transported and the transport rate of the alkylsulfonates was found to increase with increasing alkyl chain length. In the reconstituted system, anion transport was also inhibited by GDP as in non-respiring brown adipose tissue mitochondria. Furthermore, the monovalent anions that were transported competitively inhibited chloride transport. Based on their results, Jezek and Garlid (1990) suggested that the anions interact with a hydrophobic site in UCP and possibly pass through a hydrophobic channel. Currently, it is not known whether, physiologically, UCP transports protons from the intermembrane space electrophoretically across the mitochondrial inner membrane into the matrix or whether it is strictly an anion transporter, transporting the fatty acid anion electrophoretically out of the matrix into the intermembrane space (Andreyev *et al.*, 1989; Skulachev, 1991).

1.5 UCP AS A FATTY ACID ANION TRANSPORTER

Before examining the possible mechanisms of fatty acid activation of UCP, a general mechanism of fatty acid uncoupling of mitochondria will be examined. Fatty acids are known to be natural uncouplers of oxidative phosphorylation in liver and muscle mitochondria as well as brown adipose tissue mitochondria (reviewed in Wojtczak and Schonfeld, 1993). However, fatty acids have a limited effect on the proton conductance of phopholipid bilayers that are impermeable to the fatty acid anion (Skulachev, 1991). It has been shown that long chain fatty acids cross phospholipid bilayers in the undissociated form with a half-time less than 2 s, whereas the dissociated form crosses slowly, with a half-time of minutes (Kamp and Hamilton, 1992). Therefore, the uncoupling mechanism of fatty acids must differ from that for artificial protonophore uncouplers such as carbonylcyanide-p-trifluoro-methoxyphenylhydrazone (abbreviation FCCP) or carbonylcyanide-m-chlorophenylhydrazone (CCCP) (Andreyev *et al*, 1989; Skulachev, 1991). These uncouplers are weak lipophilic acids that can cross the hydrophobic barrier of the membrane in both their protonated, neutral form and their deprotonated, anionic form because the negative charge of the anion is strongly delocalized over the molecule (reviewed in Nicholls and Ferguson, 1992). Thus, membrane proton conductance is increased by protonophores because the protonated form of the uncoupler can cross the membrane, deprotonate to release the proton, and then the anionic form can diffuse back across the membrane to pick up another proton (Nicholls and Ferguson, 1992).

To explain how fatty acids uncouple mitochondria, Skulachev proposed that uncoupling is catalyzed by a fatty acid anion transport protein present in the mitochondrial inner membrane (Andreyev *et al.*, 1989; Skulachev, 1991). The fatty acid anion would be transported out of the matrix into the intermembrane space where the fatty acid anion would then get protonated and return to the matrix by diffusion across the membrane. A net proton flux into the matrix would result from the fatty acid cycling. Skulachev suggested that fatty acid anion transport could be mediated by the ADP/ATP carrier (AAC) in mitochondria in general, since mitochondrial uncoupling by palmitate was inhibited by inhibitors of the carrier (see Andreyev *et al.*, 1989). He also proposed that fatty acid anion transport in brown adipose tissue mitochondria would be mediated by UCP, a member of the same mitochondrial carrier family as AAC. In support of this theory, the reconstituted AAC has now been shown to mediate fatty acid-activated proton flux in proteoliposomes in a manner that is sensitive to inhibitors of adenine nucleotide transport (Brustovetsky and Klingenberg, 1994). Free fatty acid could not maintain proton flux in liposomes lacking AAC or containing inactive AAC, demonstrating the specific effect of fatty acid on AAC.

At present, the mechanism of fatty acid activation of UCP is not known. To date, saturable binding of fatty acid to UCP has not been demonstrated for UCP in brown adipose tissue mitochondria due to a high level of non-specific fatty acid binding as indicated from binding studies using [^{3}H]palmitate (Cunningham *et al.*, 1986). However, evidence for the existence of a fatty acid binding site on UCP has been reported by Jezek and Freisleben (1994) . Garlid's group has examined the characteristics of anion transport by UCP in detail to gain insight into the mechanism of transport catalyzed by UCP. Purified and reconstituted UCP has been found to transport monovalent anions with hydrophobic anions showing the highest transport rates (Garlid and Jezek, 1990). Similarly to AAC, GDP-sensitive, fatty acid-activated proton flux is observed in proteoliposomes reconstituted with purified UCP (Jezek *et al*, 1994; Murdza-Inglis *et al*, 1994; Winkler and Klingenberg, 1994). Laurate-activated proton flux is inhibited by undecanesulfonate, however, undecanesulfonate itself can not catalyze proton flux across the membrane (Murdza-Inglis *et al.*, 1994). This finding also supports Skulachev's theory for fatty acid anion transport since undecanesulfonate, unlike laurate, does not diffuse across lipid membranes in its protonated form, and therefore, it could not complete the protonophoric cycle required for proton efflux. Recently, Jezek *et al* (1994) using purified, reconstituted UCP have shown that chloride transport is competitively inhibited by fatty acid and noncompetitively inhibited by GDP, laurate-activated proton flux is competitively inhibited by nitrate and hexanesulfonate and laurate-activated proton flux is inhibited by GDP. Taken together, these results indicate that the anion transport pathway is the same as the possible fatty acid binding site and distinct from the nucleotide binding site (Jezek *et al.*, 1994). They propose that UCP is an anion channel designed to transport fatty acid anions and does not transport protons at all, in line with Skulachev's proposed mechanism.

As opposed to Skulachev's proposal for fatty acid anion transport through UCP as the mechanism of fatty acid uncoupling, Winkler and Klingenberg (1994) have proposed that fatty acid anion does not get completely transported across the membrane, but rather, participates in uncoupling by supplying the carboxyl group in the transport channel to act as the proton translocating group. In this model, the carboxyl group of the positioned fatty acid would accept the proton from one side of the membrane and after a protein conformational change, deliver it to the other side of the membrane. Alternatively, the fatty acid may bind in the two half-channels of the transport pathway, thereby supplying both proton accepting and proton delivering carboxyl groups to a central proton translocating g:oup endogenously present in UCP (Winkler and Klingenberg, 1994).

1.6 RATIONALE FOR EXPRESSION OF UCP IN YEAST

Prior to the start of this thesis work, although UCP had been identified as the protein in brown adipose tissue mitochondria that bound purine nucleotides (Heaton *et al.*, 1978), it was not known what role UCP played in the ion conductance properties of the inner membrane. In addition, there were conflicting results over whether proton and chloride transport competed in brown adipose tissue mitochondria (Nicholls and Lindberg, 1973; Kopecky *et al.*, 1984; reviewed in Nicholls *et al.*, 1986 and Nedergaard and Cannon, 1992). Although both proton and chloride transport in brown adipose tissue mitochondria could be inhibited by purine nucleoside di- and triphosphates, only proton transport was activated by fatty acid (reviewed in Nicholls *et al.*, 1986). The mechanisms of fatty acid activation and purine nucleotide inhibition of uncoupling in brown adipose tissue mitochondria as well as the ion transport mechanism were also not known prior to the start of this research project.

1.6.1 Knowledge of Ion Transporting Pathway in Brown Adipose Tissue

At the beginning of this thesis study, it was not known whether both the proton and chloride conductances of the brown adipose tissue mitochondrial inner membrane were due to the action of one protein with a common channel responsible for both conductances or two proteins with individual channels or possibly one protein with two transport channels, one for protons and a second one for anions (reviewed in Nedergaard and Cannon, 1992). Nicholls concluded that proton and chloride transport were competitive because he did not observe swelling of brown adipose tissue mitochondria that was dependent on simultaneous proton and chloride transport. Using his experimental design, the K^+/H^+ antiport ionophore nigericin would transport K^+ into the matrix in an electroneutral exchange for H^+ out of the matrix. If UCP also transported both Cl^- and H^+ into the matrix simultaneously, the overall effect would be an increase of KCl in the matrix which would lead to mitochondrial osmotic swelling (Nicholls and Lindberg, 1973). No swelling was observed when swelling depended on simultaneous transport of both protons and chloride ions, although proton-dependent swelling and chloride-dependent swelling were observed independently. It appeared from these results that both ions were transported through a common pathway. Nicholls suggested that rather than having a common transport pathway for both protons and anions, proton transport could actually be hydroxyl ion transport in the opposite direction, which would have the same uncoupling effect on mitochondria (Nicholls *et al.*, 1984). If this were the case, then one protein (UCP) with an anion transport pathway would account for the observed ion conductances in brown adipose tissue mitochondria. However, Kopeckey *et al.* (1984) observed both proton extrusion (monitored by measuring external pH) and chloride transport (monitored by measuring mitochondrial swelling) simultaneously in brown adipose tissue mitochondria. They concluded that these processess are not competitive and suggested that there were two separate ion-transporting pathways that were both inhibited by GDP. Nicholls disagreed with their interpretation (Nicholls *et al.*, 1986).

1.6.2 Reconstitution of UCP

To determine whether UCP was responsible for the ion conductance properties of the brown adipose tissue mitochondrial inner membrane, these transport properties would have to be observed for UCP independently from all other brown adipose tissue specific mitochondrial components. One way of achieving this is to reconstitute purified UCP isolated from brown adipose tissue mitochondria into phospholipid vesicles. Initial attempts at reconstituting UCP into liposomes using purified UCP failed to consistently demonstrate proton flux inhibited by GDP (Bouillaud *et al.*, 1983). Strieleman *et al.* (1985a) were the first to observe both proton and chloride flux that was inhibited by GDP in proteoliposomes reconstituted with UCP. However, UCP was only partially pure prior to their reconstitution (Strieleman *et al.*, 1985a). They subsequently showed that GDP-sensitive proton conductance but not chloride conductance of UCP containing proteoliposomes was increased by palmitic and oleic acid but not by palmitoyl-CoA. This was the first direct evidence that supported the idea that fatty acids were the physiological activators of UCP. However, because UCP was only partially pure prior to reconstitution, it could not be stated that fatty acid directly activated UCP (Strieleman *et al.*, 1985b). During this time period, Klingenberg and Winkler (1985) only observed GTP-sensitive proton flux in proteoliposomes reconstituted with partially purified UCP, but did not observe chloride flux across the liposomal membrane. Furthermore, fatty acids did not further increase the observed proton flux. Because the isolated UCP used in these reconstitution studies was only partially purified, and both groups observed different ion conductances, it could not be stated unequivocally that the ion conductances in brown adipose tissue mitochondria were due to UCP.

1.6.3 Structure/Function Studies of UCP by Chemical Modification and Protease Digestion of UCP

Chemical modification and protease digestion of UCP in brown adipose tissue mitochondria has been used to demonstrate that UCP was the ion conducting pathway in brown adipose tissue mitochondria, to determine domains in the protein involved in purine nucleotide binding and to distinguish specific types of amino acids involved in GDP binding, ion transport and regulation of fatty acid activation and GDP inhibition of ion transport.

Chymotrypsin treatment of UCP in brown adipose tissue mitochondria, which causes proteolytic fragmentation of UCP, caused a parallel decrease in both proton and chloride ion transport and fatty acid activation of proton transport, indicating that these processes share a common structural element (Fernandez *et al.*, 1987). UCP was shown to exist as a dimer in the inner membrane since a disulfide cross-link could be formed between the C-terminal cysteine residues of the monomers, which indicated that the monomers were in close proximity to each other in the membrane (Klingenberg and Appel, 1989). Since the cross-linking of the monomers did not interfer with GTP binding to the protein or proton transport, and cross-linking could be removed by trypsin digestion, which cleaves the C-terminus of UCP (Eckerskorn and Klingenberg, 1987), it was concluded that the C-terminus of UCP was not involved in either of these processes (Klingenberg and Appel, 1989).

Both arginine and lysine modifying reagents were found to decrease GDP binding to brown adipose tissue mitochondria and/or isolated UCP. GDP binding to brown adipose tissue mitochondria and purified UCP was decreased by the lysine specific reagent 2,4,6-trinitrobenzenesulfonic acid (Lin and Klingenberg, 1982). Although the arginine modifying reagent phenylglyoxal was less effective in decreasing GDP binding to brown adipose tissue mitochondria (Lin and Klingenberg, 1982), Katiyar and Shrago (1989) showed that the arginine modifying reagents phenylglyoxal and 2,3 butanedione could decrease GDP binding to purified UCP. They also showed that arginine modification of UCP had no effect on the reconstituted proton flux, but prevented GDP inhibition of proton flux (Katiyar and Shrago, 1991). Photo-oxidation of brown adipose tissue mitochondria also caused a decrease in GDP binding, with tryptophan likely being the photo-oxidizable amino acid in the purine nucleotide binding site (Lin and Klingenberg, 1982). Diazobenzenesulfonate, which modifies ionizable groups, caused no effect on ion transport or its regulation by fatty acid, but decreased GDP inhibition of transport and both GDP binding affinity and capacity in brown adipose tissue mitochondria (Kopecky *et al.*, 1987).

Using various cysteine modifying reagents, the seven cysteine residues in UCP, all of which are conserved, were implicated in all functions of UCP: GDP binding (Rial and Nicholls, 1986;), proton transport (Jezek, 1987; Jezek and Drahota, 1989), both proton and chloride transport (Rial and Nicholls, 1986) and GDP regulation of ion transport (Rial and Nicholls, 1986; Jezek and Drahota, 1989). Jezek and Drahota (1989) suggested that there were two types of SH groups in UCP, one type (SH_C) associated with proton transport and the other type (SH_B) associated with purine nucleotide binding.

Photoaffinity labelling of UCP using the nucleotide derivatives 8-azidoadenosine 5'-triphosphate (8-azido-ATP), 2-azidoadenosine 5'-triphosphate (2-azido-ATP) and 3'-O-(5-fluoro-2,4-dinitrophenyl)adenosine 5'-triphosphate (FDNP-ATP) localized the purine nucleotide binding region of UCP to the third domain of the protein in matrix loop C (Winkler and Klingenberg, 1992; Mayinger and Klingenberg, 1992). Since it is known that purine nucleotides regulate UCP from the cytosolic side of the inner membrane (Nicholls, 1976) but the region of UCP labelled by the nucleotide derivatives were in the putative matrix loop C, Mayinger and Klingenberg (1992) proposed that matrix loop C loops up into the membrane between putative transmembrane α-helices 5 and 6 to form a nucleotide binding pocket as outline in Figure 1-2.

The limitation of all the chemical modification studies lies in their inability to identify the location of specific amino acid residues involved in any function. In addition, there is an uncertainty of whether the observations were due to loss of a functional group in the protein or due to addition of the chemical groups from the modifying reagents that sterically interfered with function or caused conformational changes in the protein, resulting in loss of function. Although the use of photoaffinity derivatives to probe binding sites for ligands on proteins allows the binding region in the protein to be localized, this technique is limited in that the actual residues involved in binding can not be identified. By changing individual residues in UCP by site-directed mutagenesis, the roles of specific residues in function could be observed with minimal steric interference from the substitution. In addition, because UCP has several functions to be monitored (purine nucleotide binding, ion transport, fatty acid activation of proton transport, purine nucleotide regulation of transport), gross conformational changes in protein structure from the mutagenesis can be ruled out if only one function is modified and the others remain unaffected.

1.6.4 Heterologous Expression of UCP in Yeast

A second approach to studying UCP independently from all other brown adipose tissue mitochondrial protein components other than reconstituting the protein in proteoliposomes is to functionally express UCP in a novel cellular environment. The initial goal of this project was to establish an expression system for UCP to determine whether UCP was responsible for the nucleotide-sensitive ion permeabilities observed in brown adipose tissue mitochondria. Establishing an expression system for UCP also had the advantage of enabling future structure/function studies of UCP to be carried out using site-directed mutagenesis to target the role of specific amino acids in UCP.

A eukaryotic expression system for UCP was chosen such that the functions of UCP could be studied in the host mitochondria as long as import of UCP occurred. Yeast were chosen over mammalian cells due to the ability to establish a stable, high level expression system in yeast using an autonomously replicating plasmid that contains the foreign DNA (reviewed in Emr, 1990; Rose and Broach, 1990). Mammalian cells do not naturally contain autonomously replicating DNA plasmids and therefore, without integration of the foreign DNA into the host genome, expression of foreign DNA from mammalian expression plasmids in mammalian cells is only transient, with the DNA being lost over time (Kaufman, 1990). To establish stable expression of foreign DNA in mammalian cells as opposed to transient expression, the foreign gene must be integrated into the host chromosomal DNA to establish a stable cell line or virus vectors must be used which can have limited host range (Kaufman, 1990). Another advantage of using yeast for foreign gene expression is the ability to put gene expression under control of an inducible promoter in the yeast plasmid, thus avoiding any negative effects of constitutive expression of a foreign gene in the host (Mylin *et al.*, 1990; Price *et al.*, 1990; Etcheverry, 1990). Lastly, transformation of yeast and maintenance of yeast transformants is convenient and inexpensive.

Although UCP is foreign to yeast, it is a member of the mitochondrial carrier family. It was thought that UCP may be targeted to and imported into yeast mitochondria using the same yeast mitochondrial import pathway as used by the yeast AAC, a member of the mitochondrial carrier family. Neither of these proteins contain a cleavable targeting sequence. However, the *Neurospora crassa* AAC, which also lacks a cleavable target sequence, was imported into isolated rat liver mitochondria, indicating that fungal and mammalian mitochondrial import pathways may be conserved (Schleyer *et al.*, 1982). In addition, the human ornithine transcarbamoylase precursor, a mitochondrial matrix enzyme in humans, was imported into the matrix of *Saccaromyces cerevisiae* mitochondria and proteolytically processed into its functional form (Cheng *et al.*, 1987). This finding was significant because the yeast ornithine transcarbamoylase is a cytosolic enzyme lacking a cleavable target sequence, and therefore, the human ornithine transcarbamoylase, which contains a mitochondrial targeting presequence, successfully used the yeast import pathway.

For expression of UCP in yeast, the rat UCP cDNA was cloned into an *S. cerevisiae*/*Escherichia coli* shuttle vector pCGS110 (Figure 1-3). This vector was constructed from the bacterial plasmid pBR322, with additions of the yeast *GAL 1* promoter (Johnston and Davis, 1984), a segment of the endogenous yeast 2 μ plasmid (Futcher, 1988), and the yeast *URA 3* gene (Rose and Broach, 1990) inserted into the plasmid. This vector has all the properties required for propogation in both *E. coli* and *S. cerevisiae* and for selection of bacterial and yeast cells containing the vector (reviewed in Rose and Broach, 1990): a bacterial origin of replication (*ori*), an *E. coli* selectable marker (ampicillin resistance, Ap), a yeast origin of replication and partition system to ensure daughter cells will contain a copy of the vector (both present in the 2 μ segment), a yeast selectable marker (*URA 3*), and an inducible yeast promoter for transcription of UCP cDNA (P_{GAL1}).

1.6.5 Structure/Function Studies of UCP

If a functional expression system for UCP was established, the long term goal of this project was to study structure/function relationships of UCP. This would be accomplished by changing individual amino acid residues in UCP by site-directed mutagenesis of the UCP cDNA and determining the effect of these changes on the function of UCP. Mutagenesis would concentrate on the cysteine and arginine residues in UCP based on the results from chemical modification studies (see section **1.6.3 Chemical Modification of UCP**), as well as their conservation in UCP and their location in UCP based on the putative membrane disposition model (see results sections **3.4.1 Cysteine Residues** and **3.4.2 Arginine Residues** and parts therein for detailed dicussion on rationale for changes).

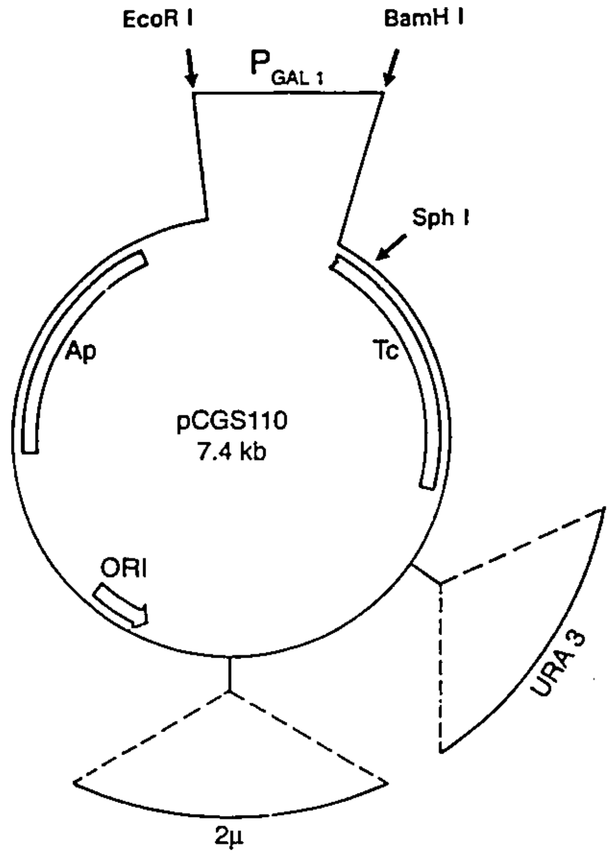

Figure 1-3. ***Saccharomyces cerevisiae/Escherichia coli*** **shuttle vector pCGS110**

This vector was a gift from Dr. D. T. Moir, Collaborative Research Inc. It was constructed from the bacterial plasmid pBR322, with additions of the yeast inducible promoter *GAL* 1, a segment of the endogenous yeast 2 μ plasmid and the yeast *URA 3* gene encoding orotidine-5'-phosphate decarboxylase (the yeast selectable marker). For propagation and selection in *E. coli*, the vector also contains a bacterial origin of replication (*ori*) and ampicillin resistance gene (*Ap*).

MATERIALS AND METHODS

2.1 MATERIALS

2.1.1 Chemicals and Reagents

The following is a list of chemicals and reagents required for this research and the companies from where they were purchased.

Adenine (hemisulfate salt)	Sigma
ADP	Boehringer Mannheim
Agarose	FMC
Albumin, bovine (essentially fatty acid free)	Sigma
Ammonium persulfate	BRL
Ampicillin	Sigma
ATP	Boehringer Mannheim
Bacto-agar	Difco
Bacto-peptone	Difco
Bacto-tryptone	Difco
Carboxyatractyloside	Boehringer Mannheim
CCCP	Sigma
D(+)-galactose	Sigma
D-glucose	BDH
Di-potassium hydrogen orthophosphate	BDH
DL-Lactic acid	Sigma
DTT	Boehringer Mannheim
EDTA	BDH
GDP	Boehringer Mannheim
GTP	Boehringer Mannheim
Glycerol	BDH
Glycine	BDH
HEPES	Sigma
Hydroxylapatite	Calbiochem
L-arginine hydrochloride	Sigma
L-ascorbic acid	Sigma
L-histidine	Sigma
L-leucine	Sigma

L-methionine	Sigma
L-tryptophan	Sigma
Magnesium chloride	BDH
Mannitol	BDH
NCS solubilizer	Amersham
Nonidet P-40 (NP-40)	Sigma
Oleic acid (sodium salt)	Sigma
Oligomycin	Calbiochem
Omnifluor	Dupont
Potassium acetate	BDH
Potassium chloride	BDH
Potassium dihydrogen orthophospate	BDH
Potassium hydroxide	BDH
Skim milk powder	Carnation
Sodium chloride	BDH
Sodium dodecyl sulfate	Gibco BRL
Sodium hydroxide	BDH
Sodium potassium tartrate	Fisher Scientific
Sorbitol	BDH
Succinic acid, disodium salt	Sigma
Sucrose	BDH
Toluene	BDH
Tris	Boehringer Mannheim
Triton X-100	Biorad Laboratories
Yeast nitrogen base w/o amino acids and ammonium sulfate	Difco

2.1.2 Radiochemicals

[2-^{3}H]Adenosine 5'-diphosphate (23 Ci/mmol), [8,5'-^{3}H]guanosine 5'-diphosphate (25-50 Ci/mmol), [9,10-^{3}H(N)]oleic acid (2-10 Ci/mmol) and [^{14}C(U)]sucrose (475 mCi/mmol) were purchased from Dupont NEN. [^{125}I]Protein A labelled with Bolton and Hunter reagent (31 mCi/mg) and [^{35}S]dATPαS (1000 Ci/mmol) were purchased from Amersham.

2.1.3 Antibodies

Anti-rabbit IgG, peroxidase-linked species-specific whole antibody (from donkey) was purchased from Amersham. Monospecific anti-rat UCP antibody from rabbit was prepared in Dr. K. B. Freeman's laboratory.

2.1.4 Western Blot Kits

The Renaissance Western Blot Chemiluminescence Reagents were purchased from Dupont NEN. The ECL Western Blotting Detection Reagents were purchased from Amersham.

2.1.5 Enzymes

Zymolyase-100T was purchased from both ICN Biochemicals and Seikagakgu America. Yeast Lytic Enzyme was purchased from ICN Biochemicals. Restriction endonuclease suppliers included Bethesda Research Laboratories, Boehringer Mannheim, New England Biolabs and Pharmacia Biotech. DNA ligase (T4) was purchased from New England Biolabs and Pharmacia. DNA polymerase I Klenow fragment was purchased from New England Biolabs and polynucleotide kinase was purchased from Pharmacia.

2.1.6 DNA Kits

Qiagen Plasmid Kit and Qiaex DNA Gel Extraction Kit were purchased from Qiagen.

2.1.7 Cloning Vectors and Host Bacterial Strains

M13mp19 was purchased from GIBCO BRL Research Products, Life Technologies, Inc., pGEM^{TM}-5Zf(+) was purchased from Promega and pSPT18-UCP was constructed by Susanna Reichling in Dr. K. B. Freeman's laboratory. Library Efficient HB101 competent cells (F$^-$ *mcr*B *mrr hsd*S20(r_B^-,m_B^-) *rec*A13 *sup*E44 *ara*14 *gal*K2 *lac*Y1 *pro*A2 *rps*L20(Sm^r) *xy*15 λ^-*leu mtl*1), Subcloning Efficiency DH5α Competent cells (F$^-$, ϕ80d*lac*ZΔM15 Δ(*lac*ZYA-*arg*F)U169 *deo*R *rec*A1 *end*A1 *hsd*R17(r_K^-,m_K^+) *sup*E44 λ^-*thi*-1 *gyr*A96 *rel*A1) and JM107 M13 host cells (*end*A1, *gyr*A96, *thi*, *hsd*R17, *sup*E44, *rel*A1, *tra*D36 (r_K^-, m_K^+) Δ(*lac pro*A,B)/F', *pro*A,B, *lac*I^{q}ZΔM15 were purchased from GIBCO BRL Research Products, Life Technologies, Inc.

2.1.8 Yeast Expression Vector and *Saccaromyces cerevisiae* Strains

The *S. cerevisiae/Escherichia coli* shuttle vector pCGS110 was a gift from Dr. D. T. Moir, Collaborative Research Inc. *S. cerevisiae* strains JB516 (*MATa, ura3, ade1, leu2, his4, gal$^+$*) and BF304-15d (*MATa, ura3, leu2, his3, ade1, met14, arg5,6, trp1*) were gifts from Dr. A. B. Futcher. *S. cerevisiae* strains CY22 (*MATa, ura3-52, his4, trp1*), CY21 (*MATα, ura3-52, leu2*) and 699 (*MATa, ura3, leu2, his3, ade2-1, trp1-1, can1-100*) were gifts from K. Nasmyth and K. Ardnt.

2.1.9 Oligodeoxyribonucleotides

Oligodeoxyribonucleotides were purchased from the Central Facility of the Institute for Molecular Biology and Biotechnology at McMaster University and were used in subcloning or to alter the rat UCP cDNA.

PRIMER	OLIGODEOXYRIBONUCLEOTIDE SEQUENCE	PURPOSE
AB264	5'GATCTGCA3'	*Bam*H I/*Pst* I bridge
AB265	5'GATCGTAC3'	*Bam*H I/*Kpn* I bridge
AB439 AB440	5'GACACATAAATAAACAAAATGGTCTCTT3' 3'ACGTCTGTGTATTTATTTGTTTTACCAGAGAAGC5'	increase translation of UCP mRNA in yeast
AB1279	5'TTTCTGCCTCCCTAGCAGAC3'	change cys24 to ser
AB1280	5'CATCAACTCTACAGAGC3'	change cys188 to ser
AB1281	5'CGTCCCCTCCCATTTAC3'	change cys213 to ser
AB1282	5'CGGGTTTTCCACCACAC3'	change cys224 to ser
AB1283	5'ACCCAGCTCTGCAATGAC3'	change cys253 to ser
AB1284	5'GTTTGTGTCCTTTGAAC3'	change cys287 to ser
AB1285	5'CAGTGGACTCCACCACATAG3'	change cys304 to ser
AB1703 AB1704	5'GATCCGAGCTCGTGCATG3' 3'GCTCGAGCAC5'	introduce *Sac* I site into pCGS110
AB1881	5'GAACAGCTGTAGAAAGAGC3'	change lys292 to stop codon
AB2585	5'AGTGTACCCAGCGCTGCAATGACCATG3'	change cys253 to ala
AB2713	5'ACCCAGCTTTGCAATGAC3'	change cys253 to phe
AB2714	5'TTTTCTGCAACTCGGATC3'	change arg276 to gln
AB2715	5'TTTTCTGCTACTCGGATC3'	change arg276 to leu
AB3568	5'GCTGGCATCCAGCAGCAAATCAGCTTTG3'	change arg83 to gln
AB3569	5'ATCTAATGACAAATGTCAT3'	change arg182 to thr
AB3570	5'CCCTGCCAATTACTGTC3'	change his214 to gln
AB3574	5'GCCTTTTTCCAAGGGTTTG3'	change lys268 to gln

2.2 CULTURING OF BACTERIA AND YEAST

2.2.1 Bacterial Growth Medium

Bacterial strains were grown in incubators at 37°C either shaking in liquid medium at 225 rpm or stationary on agar plates. Two types of liquid medium and agar plates were used:

Luria-Bertani (LB) medium: 1% bactotryptone, 0.5% bacto yeast extract, 1% NaCl, pH 7.5, supplemented with ampicillin at 40 µg/ml when required for selection.

2YT medium: 1.5% bactotryptone, 1% bacto yeast extract, 0.5% NaCl, pH 7.5, supplemented with ampicillin at 40 µg/ml when required for selection.

LB amp plates: LB medium supplemented with ampicillin at 40 µg/ml with the addition of 1.5% bactoagar.

Minimal medium agar plates: 20 ml 10X M-9 salts, 3 g agar and 175 ml of water are mixed, autoclaved and cooled to 55°C to which the following sterile solutions are added to a final volume of 200 ml: 0.2 ml 1 M $MgSO_4$, 2 ml 10 mM $CaCl_2$, 2 ml of 20% (w/v) glucose and 0.2 ml of 10 mg/ml thiamine. (10X M-9 salts: 60 g Na_2HPO_4, 30 g KH_2PO_4, 5 g NaCl, 10 g NH_4Cl, H_2O to 1 litre.

Top agar: 1% bactopeptone, 0.8% NaCl, pH 7.5 with the addition of 0.6% bactoagar

2.2.2 Storage of Bacteria

Bacteria were stored either at 4°C on agar plates for up to one month or frozen at -70°C in liquid medium containing 15% glycerol.

2.2.3 Yeast Growth Medium

Yeast strains were grown in incubators at 30°C either shaking in liquid medium at 180 rpm or stationary on agar plates. Two types of liquid medium and agar plates were used:

YPD medium: 1% bacto yeast extract, 2% bacto peptone, 2% glucose, pH 6.5

Ura- selective growth medium: 0.17% yeast nitrogen base, 0.5% $(NH_4)_2SO_4$, 0.005% each of adenine, leucine, histidine, tryptophan, methionine and arginine with 2% lactate and 0.05% glucose as the carbon sources, pH 6.5

YPD plates: 1% bacto yeast extract, 2% bacto peptone, 2% glucose, 2% bactoagar, pH 6.5

Ura- selective plates: 0.17% yeast nitrogen base, 0.5% $(NH_4)_2SO_4$, 0.005% each of adenine, leucine, histidine, tryptophan, methionine and arginine, 2% glucose, 2% bactoagar, pH 6.5

2.2.4 Storage of Yeast

Yeast were stored preferentially at 4°C on agar plates and replated every two months. They were also frozen at -70°C in YPD medium containing 50% glycerol by adding 0.2 ml of an overnight culture to 1.0 ml of YPD containing 60% glycerol.

2.3 CLONING

2.3.1 Restriction Endonuclease Digests

Restriction endonuclease digests were set up in sterile 1.5 ml microcentrifuge tubes with the desired quantity of plasmid DNA, the appropriate buffer as recommended by the manufacturer of the enzyme, the required units of restriction endonucleases and sterile, deionized/distilled water in an appropriate final volume (usually 20-80 µl) as outlined by Sambrook *et al* (1989). The reactions were carried out at 37°C in a water bath for approximately 1 h.

2.3.2 Agarose Gel Electrophoresis

Plasmid DNA or DNA fragments were separated by electrophoresis through 1% agarose gels as outlined by Sambrook *et al* (1989). The buffer used for electrophoresis and to dissolve the agarose was 0.5 X TBE (0.045 M Tris-borate, 0.001 M EDTA). The DNA samples were prepared in a 20 µl final volume containing the required amount of DNA, 4 µl formamide dye mix and sterile, deionized/distilled water. Various combinations of applied voltage and running times were used to separate DNA samples. To visualize the DNA, the gel slabs were first soaked for 15 min in deionized/distilled water containing the fluorescent dye ethidium bromide (0.5 µg/ml) then exposed to UV light.

Low melting agarose gels were also used to separate DNA samples that were to be purified from the gel. The gels were made as described above except low melting point agarose was used. Due to the fragile nature of the gels, they were run in the cold room at low voltage (50 V) for several hours to separate the DNA samples. The DNA was also visualized using ethidium bromide.

2.3.3 Purification of DNA Fragments From Agarose Gels

DNA was purified either from 1% low melting point agarose gels (Sambrook *et al.*, 1989) or from regular agarose gels using the Qiaex method. After the DNA was separated by electrophoresis, the desired DNA bands were cut out from the agarose gel and placed in a sterile microcentrifuge tube (maximum of 2 gel slices per tube). To recover the DNA from the low melting point agarose, 200 µl of 0.2 M Tris-HCl, pH 8.0 and 10 µg tRNA were added to the gel slices and the mixture was heated for 10 min at 65°C. An equal volume of phenol saturated with 0.2 M Tris-HCl, pH 8.0 was then added to denature the proteins, the solution was vortexed and the phases were separated by microcentrifugation for 3 min. The upper aqueous phase was collected and put into a new sterile microcentrifuge tube. After back extraction of the phenol phase with 200 µl of sterile, deionized/distilled water, the aqueous phases were combined. The aqueous solution was extracted two times with an equal volume of phenol:chloroform (1:1) and one time with 500 µl of chloroform. The DNA was precipitated by the addition of one tenth the volume of 3 M sodium acetate, pH 5.2 and one volume of isopropanol. After incubating the sample on ice for 15 min or overnight at -20°C, the DNA was recovered by microcentrifugation for 15 min at 4°C. The DNA pellet was washed once with 70% ethanol, dried under vacuum and dissolved in 20 µl of TE buffer.

Using the Qiaex method, agarose slices containing DNA were solubilized in a high salt buffer in the presence of the Qiaex silicagel particles. The high salt concentration of the buffer disrupts hydrogen bonding between sugars in the agarose, dissociates any DNA binding proteins from the DNA and forces the nucleic acids to adsorb to the Qiaex silicagel particles. The Qiaex particles were then washed with an ethanol-containing buffer to remove salts and dyes and the resultant purified DNA was eluted from the particles using TE buffer.

2.3.4 Ligation of DNA Fragments

Ligation reactions were set up in a 20 µl final volume containing 200 ng of vector DNA with an appropriate amount of insert DNA to establish a 4:1 molar ratio of insert to vector. The appropriate units of T4 DNA ligase and the corresponding ligation buffer were added to the reaction using sterile deionized/distilled water to make up the final volume. The reactions were incubated either overnight at 12°C or for 3 h at 16°C.

2.3.5 Transformation of *E. coli*

Commercially available competent bacterial cells (DH5α or HB101) were used to propogate plasmid DNA by transforming the cells with the desired plasmid. The manufacturer's directions were followed for transformation of the bacteria. The cells were removed from the -70°C freezer and allowed to thaw on ice. The suggested volume of cells was aliquoted into chilled, sterile 1.5 ml microcentrifuge tubes followed by the addition of 1 µl of the ligation reaction (1-10 ng of DNA) to the cells. The cells were then incubated on ice for 30 min, heat shocked for the required time at the appropriate temperature and then put on ice for 2 min. LB or 2YT medium was then added to the cells to a final volume of 1 ml and the cultures were incubated at 37°C with shaking for 1 h. Aliquots of the cultures (100 µl) were spread on LB amp plates and incubated at 37°C overnight to select for transformants.

2.3.6 Plasmid DNA Preparation

Plasmid DNA was prepared on a small scale from overnight bacterial cultures. These cultures were established by inoculating 3 ml volumes of LB or 2YT medium containing ampicillin with single bacterial colonies. After overnight growth of the culture, plasmid DNA was isolated from the cells using the method outlined by Birnboim (1983) or a modified version of the Qiagen protocol for Plasmid Mini preparation.

Following the Birnboim method, bacterial cells were pelleted in microcentrifuge tubes from 1.5 ml of culture by microcentrifugation at maximum speed for 15 s. Each pellet was then suspended in 0.1 ml lysozyme solution and left on ice for 5 min. Alkaline SDS (0.2 ml) was added to the samples and the tubes inverted several times to gently mix the solutions. After leaving the samples on ice for 5 min, 0.15 ml of high salt solution was added, the samples were gently mixed and left on ice for 15 min. The resultant precipitate was pelleted by microcentrifugation for 10 min. The DNA was precipitated from 0.35 ml of supernatant with the addition of 0.9 ml of cold 95% EtOH. After precipitating the DNA on ice for 15 min, the DNA was recovered by microcentrifugation for 10 min. The resultant pellets were dissolved in 0.1 ml acetate-MOPS-CDTA buffer and reprecipitated with 0.2 ml of 95% EtOH. The dried DNA pellets were dissolved in 25-40 µl TE buffer.

Using the Qiagen method, the bacterial cell pellets from 1.5 ml of culture were resuspended in 0.3 ml of buffer P1 containing RNase A, mixed gently with 0.3 ml of buffer P2 (alkaline SDS) then incubated at room temperature for 5 min. Following this, 0.3 ml of buffer P3 (high salt buffer) was added to the samples, the samples were gently mixed by inversion and the resultant precipitate was pelleted by microcentrifugatior for

15 min at 4°C. At this point, the DNA was precipitated directly from 0.8 ml of supernatant with the addition of isopropanol (0.5 volumes) without passing it through a Qiagen-tip. After incubating the samples on ice for 30 min, the plasmid DNA was pelleted by microcentrifugation for 5 min at 4°C. The DNA pellet was washed once with 500 μl of 70% EtOH, dried under vacuum and dissolved in 30 μl of TE buffer.

2.3.7 Sequencing

Dideoxy sequencing was used to determine nucleotide sequences in plasmid constructs. Protocols outlined in the T7Sequencing™ Kit from Pharmacia P-L Biochemicals were followed for single-stranded and double-stranded template sequencing using T7 DNA polymerase and [^{35}S]dATPαS as the radioactive label. After the annealing, extension, labelling and termination reactions were complete, the chain-terminated reaction products were separated by electrophoresis through an 8% polyacrylamide sequencing gel under denaturing conditions as outlined in the Pharmacia protocol. Since [^{35}S]dATP was used for the radioactive label, the gel was soaked for 20 min in 1 liter of 10% acetic acid, 10% methanol in distilled water to remove the urea before the gel was transfered to a sheet of whatman paper. After the gel was dried, it was exposed to X-ray film overnight, then processed and analyzed the next day.

2.3.8 Plasmid DNA Analysis

Isolated plasmid DNA was initially analysed by agarose gel electrophoresis (Sambrook *et al.*, 1989) to determine the size, purity and estimated concentration of each plasmid preparation. To determine whether a plasmid construct contained the desired insert, the plasmid was digested with restriction enzymes and the sizes of the resultant fragments were determined using agarose gel electrophorsesis. Dideoxy sequencing was used to confirm the nucleotide sequence of each new plasmid construct.

2.4 SITE-DIRECTED MUTAGENESIS

2.4.1 Mutagenesis

Oligonucleotide-mediated, site-directed mutagenesis was carried out following the method developed by Kunkel *et al.* (1987). The details of the method are outlined in Sambrook *et al* (1989). The first step required generating and isolating the single-stranded template DNA that contained uracil in place of thymine. This was accomplished by growing recombinant M13 in a *dut*$^{-}$ *ung*$^{-}$ F' strain of *E. coli* in the presence of uracil. The phosphorylated mutagenic oligonucleotide was then annealed to the single-stranded template DNA to serve as a primer for DNA extension. Following primer extension and ligation, the resultant double-stranded DNA was used to transfect *ung*$^{+}$ *E. coli* cells, where uracil-containing DNA was degraded. Library efficient HB101 competent cells (F^{-}) were used following the manufacturer's transformation protocol with JM107 cells (F^{+}) present in the top agar to support plaque formation. Twelve resultant plaques were used to transfect JM107 cultures in order to prepare and sequence the resultant single-stranded phage DNA to determine if the desired mutation was present.

2.4.2 Single-Stranded Phage DNA Preparation

Single-standed M13 phage DNA was prepared from transfected JM107 cells following the method outlined in the BRL instruction manual for M13 cloning /dideoxy sequencing. Cultures of JM107 cells (5ml) were inoculated with a single phage plaque and grown for 6 h at 37°C with vigorous shaking (300 rpm). Phage DNA was prepared from 1.5 ml of the culture. Bacterial cells were pelleted using a microcentrifuge and later used to isolate double-stranded M13 RF plasmid DNA. Single-stranded phage DNA was recovered from the supernatant. The M13 virus was precipitated from the supernatant with PEG/NaCl at room temperature and recovered by microcentrifugation. The viral pellet was then resuspended in TE buffer and extracted with phenol/chloroform (1:1). The upper aqueous phase was extracted with chloroform and the phage DNA was precipitated from the upper aqueous phase using one tenth the volume of 3 M sodium acetate and two volumes of 95% ethanol. The phage DNA was pelleted by microcentrifugation, washed once with cold 80% EtOH, dried under vacuum and resuspended in TE buffer. Dideoxy sequencing of the phage DNA was used to confirm the site-directed mutation.

2.5 ANALYSIS OF PROTEINS

2.5.1 Lowry Protein Assay

The method of Lowry *et al.* (1951) was used for protein determination. A standard curve using bovine serum albumin standards (0, 25, 50, 75, 100 μg) was prepared for each protein determination. The alkaline copper reagent (reagent C, 5 ml) was added to 1 ml of the protein standards and the appropriately diluted unknown protein samples, then vortexed immediately upon addition. After a 30 min stand at room temperature, 0.5 ml of the Folin-Ciocalteau reagent (reagent D) was added to the samples and the samples were immediatelely vortexed. The absorbance (A_{660}) was measured after one h at room temperature. A standard curve of absorbance versus the amount of BSA was used to determine the amount of protein in the unknown samples.

2.5.2 SDS Polyacrylamide Gel Electrophoresis

Electrophoresis of protein samples through polyacrylamide gels (SDS-PAGE) was used to separate proteins to determine their size and purity (Laemmli, 1970). The Bio-Rad mini-gel apparatus was used to cast and run 12.5% polyacrylamide separating gels. After the separating gel polymerized for approximately 1 h, the stacking gel was poured. The samples were applied to the stacking gel within 30 min. Protein samples to be analyzed were initially dissolved in 2X SDS gel-loading buffer (4 volumes 30% SDS, 1.5 volumes of the following: stacking gel buffer, glycerol, β- mercaptoethanol and 0.1% bromophenol blue). An appropriate aliquot was then diluted with water to a final 1X loading buffer concentration in a 20 μl volume and loaded onto the gel. Samples were separated by electrophoresis at 150 V in reservoir buffer (0.025M Tris-HCl, 0.2 M glycine, pH 8.3, 0.1% SDS) for approximately 1 h until the dye front ran off the gel. The gels were then used for immunoblots or staining with Commassie Brilliant Blue or silver salts.

<u>30% acrylamide/bis solution:</u> 30% acrylamide, 0.75% bis-acrylamide

<u>Separating gel buffer:</u> 1.5 M Tris-HCl, pH 8.8

<u>Stacking gel buffer:</u> 0.5 M Tris-HCl, pH 6.8

<u>Separating gel:</u> reagents required to make one separating gel for a Bio-Rad mini-gel. 1.87 ml deionized/distilled H_2O; 1.5 ml separting gel buffer; 2.5 ml, 30% acrylamide/bis solution; 60 μl, 10% (w/v) SDS; 12 μL, 50% (v/v) glycerol; 2 μL TEMED; 45 μL, 10% (w/v) ammonium persulphate.

<u>Stacking gel:</u> reagents required to make one stacking gel for a Bio-Rad mini gel. 1.18 ml deionized/distilled H_2O; 0.5 ml, stacking gel buffer; 0.38 ml, 30% acrylamide/bis

solution; 10 µL, 10% (w/v) SDS; 4 µL, 50% (v/v) glycerol; 2 µL, TEMED; 12.5 µL, 10% (w/v) ammonium persulphate.

2.5.3 Protein Silver Staining

Silver staining was used to visualize proteins on polyacrylamide gels. After separating the protein samples by SDS-PAGE, the gel was placed in destaining solution (20% EtOH, 10% acetic acid) for 10 min. The gel was then washed twice for 20 min with 50% methanol, then three times for 20 min with distilled water. The gel was placed in 150 ml of water containing 5 µg/ml of DTT for 30 min. After removal of this solution, the gel was placed in silver nitrate solution (100 mg/100 ml water) for 30 min followed by two quick washes with distilled water. The gel was then placed in developing solution (12 g Na_2CO_3, 200 µl of 37% formaldehyde in 400 ml of distilled water) with gentle shaking back and forth until the desired staining intensity of the protein bands developed. The staining was stopped by the addition of 10% acetic acid.

2.5.4 Western Blotting

Western blotting was used to detect and quantitate UCP in yeast subcellular fractions based on the method of Towbin *et al.* (1979). Proteins were transferred electrophoretically from polyacrylamide gels to nitrocellulose either at 100 V for 1 h or 40 mA overnight in transfer buffer (25 mM Tris-HCl, 192 mM glycine, pH 8.3, 20% methanol). The nitrocellulose was then blocked with Carnation instant skim milk powder (5%) in Tris/saline solution (0.9% NaCl, 10 mM Tris-HCl, pH 7.4) for 30 min at 37°C. The antibody/antigen reaction took place in a seal-a-meal bag cut to the size of the nitrocellulose. The primary antibody (100 μl) was added to the nitrocellulose in 5 ml of Tris/saline blocking solution and incubated at room temperature for 90 min on a rocking platform. The nitrocellulose was then washed with shaking at 10 min intervals one time with Tris/saline, two times with Tris/saline containing 0.05% NP40 and one time with Tris/saline. The secondary antibody, either [^{125}I]protein A (5 μl/5 ml Tris/saline blocking solution) or anti-rabbit peroxidase linked antibody (0.25 μl/5 ml Tris/saline blocking solution) was added to the nitrocellulose and incubated for 30 min at room temperature on a rocking platform. The nitrocellulose was then washed as stated previously and dried thoroughly on whatman paper. The [^{125}I]protein A probed nitrocellulose was exposed directly to X-ray film for 2-7 days. The nitrocellulose probed with the peroxidase-linked antibody was incubated for 1 min with the chemiluminescence reagents from the ECL or Renaissance western blot kit, sandwiched between plastic wrap and exposed to X-ray film for 1-5 min.

2.5.5 Immunoprecipitation

UCP was immunoprecipitated from subcellular fractions using monospecific antibodies from rabbit following the method of Chien and Freeman (1984). Aliquots of subcellular fractions were added to adjusting buffer (10 mM Tris-HCl, 0.3 M NaCl, 5 mM EDTA, 1% Triton X-100, pH 7.2) to a 1 ml total volume. Soy bean trypsin inhibitor (5 μl of 5 mg/ml stock) and 20 μl of antiserum were added to the samples which were then rotated overnight at 4°C. Protein A-Sepharose CL-4B beads swollen in adjusting buffer (20 μl) were then added to the samples and rotated at 4°C for 3 h. The protein A-antibody-UCP complex attached to the sepharose beads was then pelleted using a microcentrifuge and washed 10 times with 1 ml of adjusting buffer. The antibody-UCP complex was stripped from the protein A-Sepharose CL-4B beads by incubating the pellet in 100 µl stripping buffer (8% SDS, 6.5% β-mercaptoethanol, 60 mM Tris-HCl, pH 6.8) for 1 h at room temperature. The protein A-Sepharose CL-4B beads were then pelleted by centrifugation and the supernatent transfered to a fresh tube. The supernatant protein samples were then separated by SDS-PAGE and detected by a western blot.

2.6 CONSTRUCTION OF UCP EXPRESSION VECTORS

2.6.1 Original UCP Expression Vector Containing Rat UCP cDNA

The *Kpn* I/*Pst* I fragment of the rat UCP cDNA from pSPT18UCP was cloned into the *Bam*H I site of pCGS110 beside the inducible *Gal* 1 promoter. This was achieved using two, 8-nucleotide-long bridges (AB264 and AB265) designed to join *Pst* I and *Kpn* I restriction site overhangs to a *Bam*H I overhang respectively.

2.6.2 Expression Vector Containing Altered 5' Region of UCP cDNA

The UCP cDNA altered at the 5' end was constructed in pGEM5Zf by cloning the UCP cDNA containing *Sph* I/*Taq* I fragment from pSPT18UCP into *Sph* I/*Pst* I cut pGEM5Zf using two complimentary oligonucleotides (AB439 and AB440) designed to have *Pst* I and *Taq* I restriction site overhangs at their ends and an altered UCP 5'region. The altered UCP cDNA was removed from pGEM5ZfUCP with *Pst* I and ligated into *Bam*H I cut pCGS110 with an 8-nucleotide-long bridge (AB264). DNA fragments used in the ligation reaction were separated by agarose gel electrophoresis (Sambrook *et al.*, 1989) and purified from low melting point agarose.

2.6.3 Modified pCGS110 Containing *Sac* I Site

A *Sac* I site was introduced into pCGS110 to simplify subcloning of UCP cDNA from M13mp19 into pCGS110 after site-directed mutagenesis. Two complimentary oligonucleotides (AB1703 and AB1704) designed to contain an internal *Sac* I site and *Bam*H I and *Sph* I restriction site overhangs on their ends were subloned into *Bam*H I/*Sph* I cut pCGS110. This enabled the *Sac* I/*Sph* I UCP cDNA containing fragments from M13mp19 to be directly subloned into *Sac* I/*Sph* I cut pCGS110.

2.7 YEAST EXPRESSION SYSTEM

2.7.1 Transformation of Yeast

Shuttle vector constructs were introduced into yeast cells by electroporation (Becker and Guarente, 1991) or into lithium treated competent cells following the method of Ito *et al.* (1983). For electroporation, a 50 ml YPD culture of yeast was harvested when the cells reached an A_{600} of 1.3 to 1.5. After the pelleted cells were washed with sterile water, they were concentrated and resuspended in 500 µl of sterile 1.0 M sorbitol. Plasmid DNA (3 µl of a plasmid mini-preparation) was added to 40 µl of concentrated cells and the cells were electroporated in 0.2 cm sterile electroporation cuvettes at 1.5 kV, 25 µF, 200 Ω using a BioRad gene pulser with pulse controller. Immediately following electroporation, 1 ml of cold, sterile 1.0 M sorbitol was added to the cells and the cells were spread on selective plates.

Yeast transformation with lithium treated cells required the 50 ml YPD yeast culture to be harvested at late log phase. After washing the cells with sterile water, the cell pellet was resuspended in 500 µl of lithium acetate solution (10 mM Tris-HCl, 1 mM

EDTA, 0.1 M lithium acetate, pH 7.5) and incubated for 1 h at 30°C with agitation. Carrier DNA (50 μg) and transforming DNA (1 μg) were added to 100 μl of cells and the transformation mix was incubated for 30 min at 30°C without agitation. DNA uptake was facilitated by adding 700 μl of solution containing 40% PEG, 0.1 M lithium acetate, 1X TE buffer to the transformation mix and incubating the mixture for another 30 min at 30°C without agitation. The cells were pelleted with a microcentrifuge, washed twice with TE buffer, resuspended in 100 μl TE buffer and spread on selective plates.

Transformed cells from either method were selected on ura- selective plates and became visible after several days growth at 30°C. From each independent transformation, the colonies on that plate were array plated onto a new selective plate. Then, an individual colony was chosen to be streaked onto a selective plate. The resultant yeast plate derived from a single colony was used to start liquid cultures and was replated as required or every two months, whichever came first.

2.7.2 Expression of UCP in Yeast

Starting cultures (100 ml) of yeast transformants were inoculated from the single colony yeast plates and were grown in selective medium in a 250 ml flask at a shaking rate of 180 rpm for approximately 2 days at 30°C. The starting cultures were then used to inoculate 500 ml of selective medium. These cultures were grown for an additional 5 h to an A_{600} of 0.3-0.4. Expression of UCP was then induced by addition of galactose to 0.2%. Cells were grown for an additional 8-12 h before harvesting the cells. Control yeast transformants not containing the UCP cDNA were grown following the same procedure outlined above. Yeast transformants not induced to express UCP were grown under the same conditions without the addition of galactose.

2.7.3 Mitochondrial Isolation from Yeast

Mitochondria were isolated from yeast essentially as described by Gasser (Gasser, 1983). Yeast cells were pelleted at 5000 rpm for 5 min using a GSA rotor and washed once with deionized/distilled water. Cell walls were prepared for digestion by incubating the cells for 10 min in 0.1 M Tris-sulfate, pH 9.4, 10 mM DTT at 0.5 g cell wet wt/ml. The cells were then pelleted at 5000 rpm for 5 min using an SS34 rotor, washed once with 1.2 M sorbitol and repelleted. The cells were resuspended in spheroplasing buffer (1.2 M sorbitol, 20 mM potassium phosphate pH 7.4, 1 mM PMSF) and the cell walls were digested using Zymolyase or Yeast Lytic Enzyme at 1 mg enzyme/g cell wet weight. The spheroplasts were pelleted at 3500 rpm for 5 min using an SS34 rotor, washed twice with 1.2 M sorbitol and then resuspended in chilled breaking buffer (0.6 M mannitol or sucrose, 20 mM HEPES-KOH, pH 6.5 or 7.4, 0.1% fatty acid-free BSA, 1 mM PMSF). Spheroplasts were disrupted using 20 strokes of a Dounce homogenizer. The nuclear fraction was recovered at 3500 rpm for 5 min and the mitochondrial fraction at 9000 rpm for 10 min using an SS34 rotor. The mitochondrial fraction was washed once with breaking buffer, any residual nuclear fraction was pelleted with a low speed spin and the mitochondrial fraction was again recovered from the supernatant. The final mitochondrial pellet was resuspended in 500 µl of breaking buffer without PMSF.

2.8 SUBCELLULAR LOCALIZATION OF UCP

2.8.1 Western Blot Analysis of Subcellular Fractions

To determine the subcellular location of UCP, aliquots of the nuclear, mitochondrial and post mitochondrial fractions were separated by 12.5% SDS-PAGE, transferred onto nitrocellulose and immunodetected using a rabbit monospecific antibody to UCP and [^{125}I]labelled protein A.

2.8.2 Hydroxylapatite Purification of UCP from Mitochondria

UCP was purified from yeast mitochondria following the hydroxylapatite column purification procedure outlined by Lin and Klingenberg (1980). Basically 2.5 mg of mitochondrial protein were extracted first with Lubrol WX, then with Triton X-100. The supernatant was added to a hydroxylapatite column, and 50 µl fractions were collected. Aliquots of each fraction (2-5 µl) were then separated by SDS-PAGE and the proteins visualized by silver staining. The identity of UCP was verified by a western blot of the fractions.

2.8.3 Yeast Mitochondrial Inner Membrane Preparation

The mitochondrial outer membrane was removed from approximately 6-8 mg of mitochondria in a 1.0-ml volume using a 0.4:1.0 ratio of digitonin to mitochondrial protein. After a 1 min incubation on ice, the resulting mitoplasts were recovered by microcentrifugation for 5 min at 4°C. The mitoplasts were resuspended in 500 µl of hypotonic medium containing 10 mM Tris-HCl, 1 mM EDTA, pH 7.2, and sonicated 3 X 20 s in a bath sonicator to release the matrix contents. Membranes were collected at 150,000 g for 20 min and resuspended in 500 µl of mitochondrial breaking buffer (0.6 M mannitol, 20 mM HEPES-KOH, pH 7.4, 0.1% fatty acid-free BSA). Marker enzyme assays were performed on each fraction according to published procedures and included the outer membrane marker, kynurenine hydroxylase (Hayaishi, 1962), the inner membrane marker, cytochrome *c* oxidase (Cooperstein and Lazarow, 1951), and the matrix marker, malate dehydrogenase (Gregory *et al.*, 1971).

2.9 UCP FUNCTIONAL ASSAYS

2.9.1 Respiration Assay

Two assays based on monitoring mitochondrial respiration were developed to assess the ability of UCP to uncouple oxidative phosphorylation in yeast mitochondria. Respiration of yeast mitochondria was determined using the YSI 5300 monitor, the 5357 micro oxygen probe and the 5356 micro oxygen chamber, which had a capacity of 0.6 ml. The reaction buffer contained 0.65 M sorbitol, 0.36 mM EDTA, 10 mM KCl, 10 mM KH_2PO_4, 10 mM Tris-HCl, and either 0.05% or 0.3% fatty acid-free bovine albumin adjusted to a final pH of 6.5. The reaction buffer was added to the oxygen chamber from the bottom outlet using an airtight syringe. Once a stable oxygen consumption signal was established, 10-20 µl of mitochondria (200-400 µg) were added to the chamber through the top porthole using a Hamilton syringe. All other additions to the chamber were made through this porthole.

Assay #1: Reaction buffer containing 0.3% fatty acid-free BSA was added to the oxygen chamber. After the addition of mitochondria containing or lacking UCP, succinate (10 mM) was added as a substrate. Coupling was determined by measuring the respiratory control ratio (RCR) after the addition of 60 nmol of ADP (100 µM) (see Figure 3-12 for illustration). Activation of UCP was tested by measuring the stimulation of the respiratory rate after oleate addition (0-300 µM) and the resultant effect of oleate on the coupled state of the mitochondria (see Figure 3-15 for illustration). Inhibition of UCP was tested by measuring the decrease in the respiratory rate after GDP addition (167 μM) and the resultant effect of GDP on the coupled state of the mitochondria (see Figure 3-15 for illustration) .

Assay #2: Reaction buffer containing 0.05% fatty acid-free BSA was added to the oxygen chamber. After the addition of mitochondria containing or lacking UCP, succinate (10mM) was added as the substrate. Oligomycin (66 μg/ml) was then added to the mitochondria to inhibit oxidative phosphorylation. Activation of UCP was tested by measuring the stimulation of the respiratory rate after the addition of oleate/BSA mixutres (see Figure 3-18 for illustration). Inhibition of UCP was tested by measuring the decrease in the respiratory rate after GDP addition (0- 2 mM) (see Figure 3-18 for illustration).

2.9.1.1 Determination of Free Oleate Concentration in Oleate/BSA Solutions

The stock oleate solutions used in the mitochondrial respiration assays were either premixed oleate/BSA solutions added to respiration buffer or oleate solutions added to respiration buffer containing 0.3% BSA. This requires that the concentration of free oleate not bound to BSA present in the respiration assays be determined. This was accomplished by determining the partitioning of oleate between aqueous and organic phases in the absence and presence of BSA following the procedure of Spector *et al.* (1969). First, the partitioning of oleate into heptane was determined. [^{3}H]Oleate solutions in mitochondrial reaction buffer without BSA, pH 6.5 were prepared at a range of concentrations from 1 to 500 μM oleate at 100 μCi/μmol and 0.8 to 2 mM oleate at 1 μCi/μmol. An aliquot of 620 μl of each solution was transferred into glass vials and an equal volume of heptane was added. After flushing the tubes with nitrogen to remove oxygen, the solutions were equilibrated overnight at 37°C with gentle shaking. Aliquots of each phase were removed and appropriate volumes of each phase were counted in 10 ml of ACS scintilation fluid. Based on the radioactivity recovered in each phase and the specific activity of [^{3}H]oleate, the concentration of oleate in each phase was determined. A standard curve of the (-log[oleate]$_{heptane}$) vs (-log[oleate]$_{aqueous}$) was plotted. The second stage was to determine the partitioning of oleate between heptane and the BSA present in the aqueous phase. [^{3}H]Oleate/BSA stock solutions were prepared from a stock of 35 mM [^{3}H]oleate/5 mM BSA at 100 µCi/µmol using 5 mM BSA as the diluent such that a range of [^{3}H]oleate/BSA solutions were made (oleate/BSA molar ratios ranging from 0.5 to 7) all at 100 µCi/µmol. Respiration reaction buffer, pH 6.5 (600 µl) containing 0.05% BSA was aliquoted into glass vials and then 20 µl of each [^{3}H]oleate/BSA stock solution was added to individual vials and mixed. Heptane (620 µl) was added to the vials and the samples were equilibrated overnight, aliquots from the phases were removed and appropriate volumes were counted as explained above. Based on the radioactivity recovered in each phase, the concentration of oleate in the heptane phase and the total concentration of oleate in the aqueous phase (which included oleate bound to BSA and unbound to BSA) was determined. As stated in Spector *et al.* (1969), two aqueous solutions (one with and one without BSA) that are in equilibrium with the same concentration of free fatty acid in heptane are, in turn, in equilibrium with each other. Based on this, the concentration of free, unbound oleate in the aqueous phase containing BSA can be read off of the standard curve of the (-log[oleate]$_{heptane}$) vs (-log[oleate]$_{aqueous}$) generated in the absence of BSA based on the concentration of oleate determined in the heptane phase (Spector *et al.*, 1969). A standard curve was then generated, plotting the molar ratio of oleate/BSA in the respiration reaction versus (-log[oleate]$_{aqueousfree}$), such that the free oleate concentration in the respiration assays could be determined from the curve.

2.9.2 GDP Binding Assay

The ability of UCP to bind purine nucleotides was tested by measuring the amount of [^{3}H]GDP bound to yeast mitochondria containing and lacking UCP. The centrifugation method of Desautels *et al* (1978) was followed measuring the amount of GDP bound to mitochondria in the presence and absence of ADP. [^{14}C]sucrose was used as a supernatant marker to measure the amount of unbound [^{3}H]GDP from the supernatant trapped in the mitochondrial pellet. Mitochondria were isolated from yeast and resuspended in the breaking buffer containing 0.6 M mannitol, pH 7.4. The binding assay took place in 1.5 ml microcentrifuge tubes. Mitochondria (500 µg) were added to reaction buffer (0.65 M sorbitol, 0.36 mM EDTA, 10 mM KCl, 10 mM KH_2PO_4, 10 mM Tris-HCl, pH 6.5, 0.05% fatty acid-free BSA) and mixed by inversion. At 30 s intervals, succinate (10 mM), oligomycin (66 µg/ml), fatty acid-free BSA (167 µM) and carboxyatractyloside (0.1 mM) were added to the mitochondria and mixed by inversion. One min after the addition of carboxyatractyloside, [^{3}H]GDP (0-25 µM) was added to the reaction and mixed by inversion. Binding proceeded at room temperature for 5 min. Mitochondria were then pelleted for 2 min using a microcentrifuge. The supernatant was removed from the mitochondrial pellet and saved. The bottom of the microcentrifuge tube containing the mitochondrial pellet was cut off and placed in 1 ml of tissue solubilizer.

A fraction of the supernatant (100 μl) was also placed in 1 ml of tissue solubilizer. The samples were incubated at 50°C for 2 h with gentle shaking. For liquid scintillation counting, 7 ml of toluene-omnifluor and 100 μl of 10% ascorbic acid were added to the samples. The samples remained in the counter overnight devoid of light and were counted the following morning. To measure binding in the presence of ADP, 2 mM ADP was added to the reaction 1 min prior to the GDP addition.

RESULTS AND DISCUSSION

3.1 EXPRESSION OF RAT UNCOUPLING PROTEIN IN YEAST

To study the functioning of UCP independently from brown adipose tissue mitochondrial components, an expression system for UCP was examined in yeast. If the protein functioned in yeast mitochondria, the long term goal of this project was to use site-directed mutagenesis of the UCP cDNA to investigate structure/function relationships of UCP.

3.1.1 Modified UCP cDNA Required for High Level Expression

To study the function of rat UCP in yeast mitochondria, an expression level of UCP in yeast mitochondria comparable to that found in rat brown adipose tissue mitochondria was desired. In cold-adapted animals when non-shivering thermogenesis is active, UCP can represent 10% of the mitochondrial protein (reviewed in Trayhurn and Milner, 1989). Since mitochondrial proteins represent approximately 10% of total cellular protein, an expression level of UCP representing approximately 1% of total cellular protein was desired.

The rat UCP cDNA (Ridley *et al.*, 1986) was inserted into the *S. cerevisiae/E. coli* shuttle vector pCGS110 at the *Bam*H I site such that the cDNA was under transcriptional control of the inducible *GAL* 1 promoter (Figure 3-1). Using this system, it was previously shown that UCP was synthesized at low levels under induction

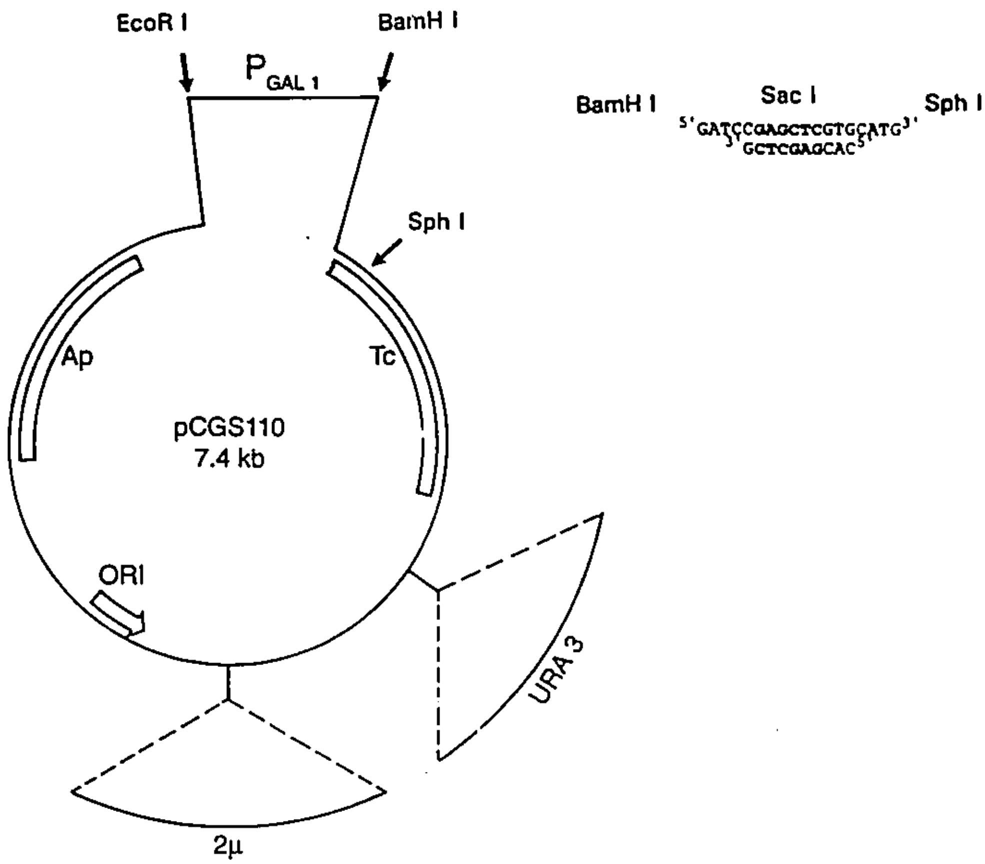

Figure 3-1. ***Saccharomyces cerevisiae/Escherichia coli*** **shuttle vector pCGS110**

A description of the vector can be found in the legend to Figure 1-3. The original rat UCP cDNA from pSPT18UCP was inserted into the vector at the unique *Bam*H I site beside the inducible *GAL* 1 promoter as outlined in the methods section **2.6.1 Original UCP Expression Vector Containing Rat UCP cDNA**. Rat UCP cDNA altered for high level expression in yeast from pGEM5ZfUCP was inserted into pCGS110 at the unique *Bam*H I site of pCGS110 as outlined in the methods section **2.6.2 Expression Vector Containing Altered 5' region of UCP cDNA**. A *Sac* I site was introduced into pCGS110 to simplify subcloning of UCP cDNA from M13mp19 into pCGS110 after site directed mutagenesis. Two complimentary oligonucleotides designed to contain an internal *Sac* I site with *Bam*H I and *Sph* I restriction site overhangs on their ends were subcloned into *Bam*H I/*Sph* I cut pCGS110 as explained in the methods section **2.6.3 Modified pCGS110 Containing *Sac* I site**. This enabled *Sac* I/*Sph* I UCP cDNA fragments from M13mp19 to be directly subcloned into *Sac* I/*Sph* I cut pCGS110.

conditions, but represented only 0.008% of the total [^{35}S]methionine-labelled cell protein (Murdza, 1988). The low level of UCP was not due to degradation of the protein, loss of plasmid from the cells or a low level of UCP mRNA (Murdza, 1988). Since the region around the start codon in yeast transcripts is very different from that found in mammalian mRNAs (Hamilton *et al.*, 1987) and there is a codon bias in highly expressed yeast genes (Sharp *et al.*, 1986), it appeared the low level of UCP observed in yeast was probably due to inefficient translation of the mRNA.

High level expression of UCP was achieved by altering the region around the start codon of the rat UCP cDNA as outlined in Figure 3-2. The 18 nucleotides upstream from the start codon were changed to match the sequence of a highly expressed *S. cerevisiae* glyceraldehyde-3-phosphate dehydrogenase gene (*G3PaD*) (Hamilton *et al.*, 1987) and the 5 nucleotides downstream from the start codon, coding for valine and serine, were changed to match the sequence of highly used valine and serine codons in yeast (Sharp *et al.*, 1986). An oligonucleotide incorporating these changes along with its complimentary strand were designed and used to construct the altered UCP cDNA as outlined in the methods section **2.6.2. Expression Vector Containing Altered 5' region of UCP cDNA**. Expression of the altered cDNA resulted in at least a 24 fold increase in the level of UCP present in the mitochondrial fraction over that obtained with the unmodified cDNA (Figure 3-3) as determined by scanning densitometry of the immunodetected protein bands on X-ray film. The level of UCP in yeast mitochondria was quantified from western blots of mitochondrial fractions to be 70-100 μg UCP/mg mitochondrial protein (Figure 3-4) with an average value of 88 ± 8 μg UCP/mg mitochondrial protein. The level of rat UCP in yeast mitochondria is very similar to the level of UCP found in

```
                                   Met  Val  Ser
rat UCP DNA:    TCTGCCCTCCGAGCCAAGATGGTGAGTT

                                   Met  Val  Arg
G3PDa DNA:      CACACATAAATAAACAAAATGGTTAGAG

                                   Met  Val  Ser
altered DNA:    GACACATAAATAAACAAAATGGTCTCTT
```

Figure 3-2. Altered Nucleotide Sequence in the Rat UCP cDNA Required for High Level Expression of UCP in Yeast

The 18 nucleotide upstream and the 5 nucleotide downstream regions around the start codon of rat UCP cDNA were changed to ones that closely resembled the sequence of a highly expressed yeast glyceraldehyde-3-phosphate dehydrogenase gene (G3PDa) and highly used codons in yeast.

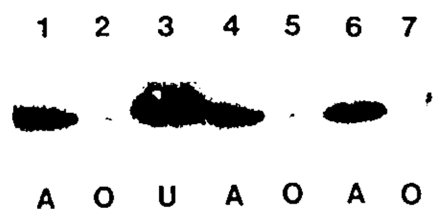

Figure 3-3. Immunoblot Analysis of Mitochondrial Fractions Isolated From Cells Having Either the Original or the Altered UCP cDNA

Yeast transformants containing the shuttle vector pCGS110 with either the original rat UCP cDNA (O) or the altered form (A) were induced to express uncoupling protein (U) by the addition of galactose to 0.2% for 10 h. After the cells were disrupted and fractionated, samples from the mitochondrial fractions were separated by SDS-12.5% PAGE, transferred to nitrocellulose and detected with monospecific antiserum against rat UCP and [^{125}I]-labelled protein A. Lanes 1, 4 and 6 contain 50 μg of mitochondria from cells containing the altered rat UCP cDNA; lanes 2, 5 and 7 contain 50 μg of mitochondria from cells containing the original rat UCP cDNA; lane 3 contains 7.1 μg rat UCP marker.

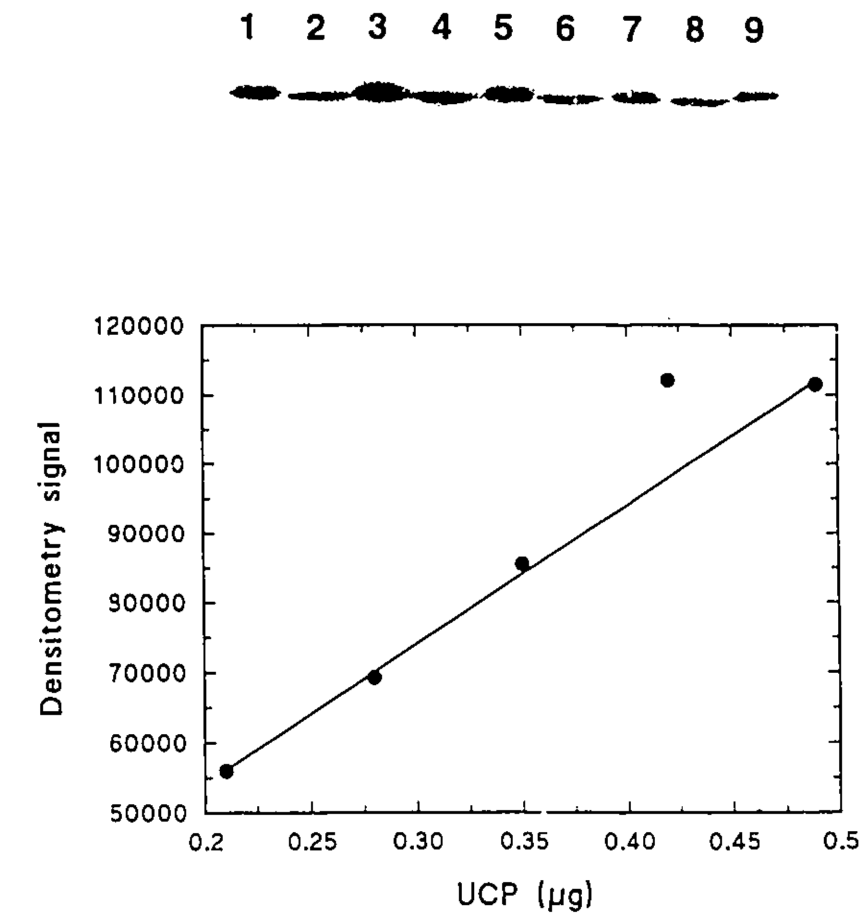

Figure 3-4. Quantification of UCP in a Yeast Mitochondrial Fraction

Purified rat UCP and yeast mitochondria isolated from transformants induced to express UCP were separated by SDS-12.5% PAGE, transferred to nitrocellulose and detected with monospecific antiserum against rat UCP and [^{125}I]-labelled protein A. Lanes 1,3,5,7,9 contain 0.49, 0.42, 0.35, 0.28 and 0.21 μg of rat UCP purified from brown adipose tissue mitochondria respectively. Lanes 2, 4, 6 and 8 each contain 5 μg of yeast mitochondria isolated from yeast transformant JB516pCGS110 UCP (which contains the altered UCP cDNA) that was induced to express UCP by galactose induction (0.2%) for 10 h. The accompanying graph shows the standard curve resulting from the densitometry signals from the western blot for the UCP standards shown in the above photograph versus the amount of protein applied to each lane. This curve was used to measure the amount of UCP in the mitochondrial samples based on their densitometry signals. The mitochondrial samples of lanes 2, 4, 6 and 8 contained 0.36, 0.45, 0.40 and 0.40 μg UCP respectively for 5 μg mitochondrial protein. This results in an average expression level of UCP in this mitochondrial preparation of 80 ± 4 μg UCP/mg mitochondrial protein.

brown adipose tissue mitochondria of cold-adapted rats, 75 ± 6 μg UCP/mg mitochondrial protein for rats acclimated at 4°C for 5 days (Peachey *et al.*, 1988) and 52 ± 3 μg UCP/mg mitochondrial protein for rats acclimated at 4°C for 3 weeks (Trayhurn *et al.*, 1987).

Using a similar galactose-inducible yeast expression system, Arechaga *et al.* (1993) reported expression of 24 μg UCP/mg mitochondrial protein after removal of the 5' and 3' non-coding sequences in the rat UCP cDNA in the expression vector. Other eukaryotic expression systems for UCP have been established by others throughout the course of this research, however, they have not been used for functional studies. UCP was expressed in *Xenopus laevis* oocytes and detected in the mitochondrial fraction, but the protein was not functional (Klaus *et al.*, 19[illegible]). UCP was functionally expressed in CHO cells, although the level of UCP was not reported and no further reports of structure/function studies have appeared using this expression system (Casteilla *et al.*, 1990).

3.1.2 Growth of Cells Expressing UCP

The growth of yeast in medium containing a non-fermentable carbon source such as lactate forces the cells to use mitochondrial oxidative phosphorylation to generate ATP as opposed to using glycolysis. Cells able to grow in this type of non-fermentable medium must contain functional mitochondria prior to their isolation. If mitochondria are partially uncoupled, the cells would grow at a slower rate. The growth of yeast transformants in selective lactate medium after addition of 0.2% galactose was monitored to determine whether the expression of UCP had any effect on cell growth. In comparing the growth curves in Figure 3-5, after the addition of 0.2% galactose, cells lacking UCP cDNA had a doubling time of 6.5 h and cells containing UCP cDNA had a doubling time of 7 h, which indicated that the expression of UCP did not significantly affect yeast cell growth.

3.2 LOCALIZATION OF UCP TO THE YEAST MITOCHONDRIAL INNER MEMBRANE

3.2.1 Subcellular Localization of UCP

Immunodetection of UCP from cell fractions of galactose-induced yeast transformants was performed to determine the subcellular location of UCP (Figure 3-6). UCP was detected in the post-nuclear fraction (lane 3) and the mitochondrial fraction (lane 5), but not in the post-mitochondrial fraction (lane 2) from cells containing the UCP cDNA. No protein at 32 kDa was immunodetected in cell fractions isolated from cells lacking the UCP cDNA (lanes 7-9).

3.2.2 Hydroxylapatite Purification of UCP

The first indication that UCP was imported into yeast mitochondria and not just bound to the outer mitochondrial membrane came from the purification of UCP from the yeast mitochondrial fraction. Using the standard method of Triton X-100 extraction and hydroxylapatite chromatography of mammalian brown adipose tissue mitochondria, UCP imported into the mitochondrial inner membrane does not bind to the column and comes out in the column void volume (Lin and Klingenberg, 1980). In contrast, UCP not imported into the mitochondrial inner membrane *in vitro*, but either bound to the

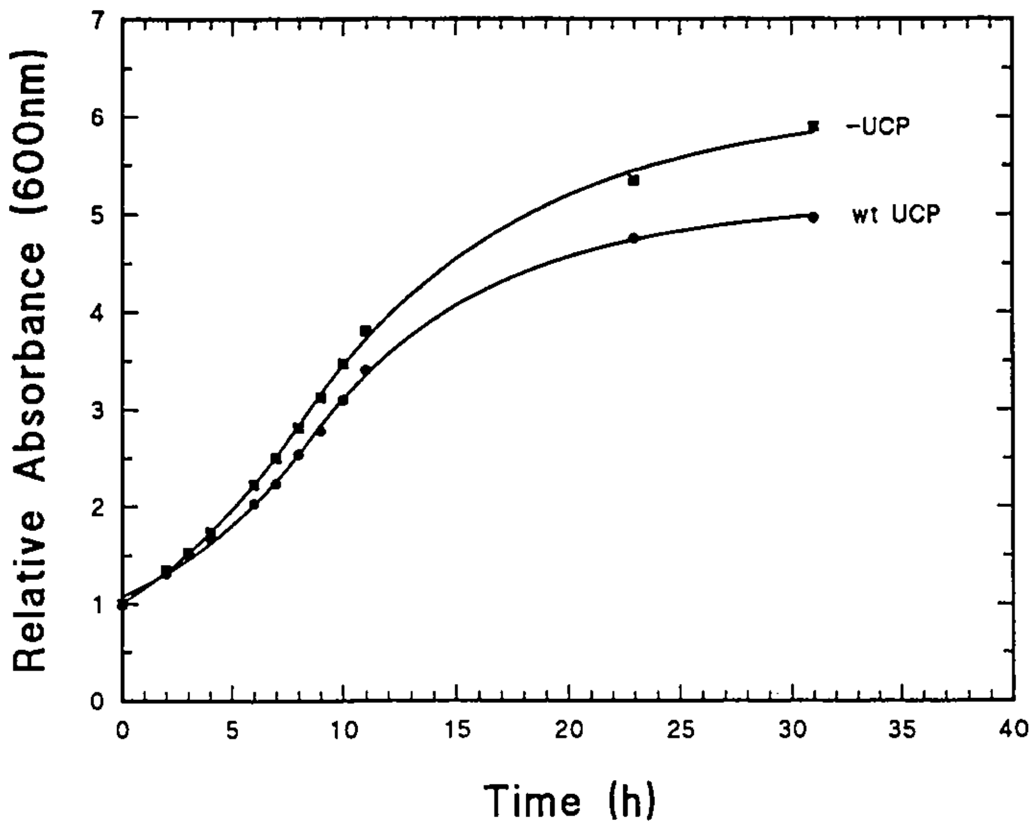

Figure 3-5. Growth Curves of Yeast Transformants Induced With Galactose

Yeast transformants containing pCGS110 either without the UCP cDNA or with the UCP cDNA altered for high level expression in yeast were grown in Ura- selective growth medium to an A_{600} of approximately 0.25. At that time (time 0 on the above graph), galactose was added to the cultures to a final concentration of 0.2% and the growth of the cultures were monitored over the next 32 h. The relative absorbance at each time point was calculated by dividing each A_{600} value at each time point by the initial A_{600} value at time 0 in order to more easily compare the growth rates of the cultures.

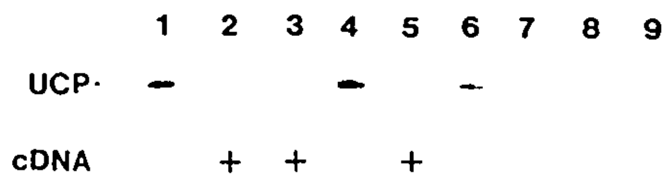

Figure 3-6. Imm[illegible]lot Analysis of Uncoupling Protein Distribution in Yeast Cell Frac[illegible]

Yeast transformants were induced to express UCP by the addition of galactose to 0.2% for 8 h and then cells were disrupted and fractionated. A portion of each cell fraction was immunoprecipitated using monospecific antiserum against rat UCP and protein A-Sepharose CL-4B. The immunoprecipitates were separated by SDS-12.5% PAGE, transferred to nitrocellulose and detected with monospecific antiserum against rat UCP and [^{125}I]-labelled protein A. Lanes 1, 4 and 6 contain rat 32 kDa UCP markers of 0.35, 0.28 and 0.21 μg, respectively. Lanes 2, 3 and 5 represent 0.14% of the post mitochondrial, 0.23% of the post nuclear and 0.42% of the mitochondrial fractions, respectively, isolated from galactose-induced yeast cells transformed with pCGS110 containing the altered UCP cDNA. Lanes 7, 8 and 9 represent the same percentages stated above for the mitochondrial, post nuclear and post mitochondrial fractions, respectively, from galactose induced cells transformed with pCGS110 lacking modified UCP cDNA.

mitochondrial outer membrane or other particulate matter in the import reaction, remains bound to the column using this purification procedure (K.B. Freeman, personal communication). Analysis of the hydroxylapatite column fractions from mitochondria of yeast containing and lacking UCP cDNA by SDS-12.5% PAGE and silver staining revealed two protein bands at 32 and 30 kDa in the column void volume. Immunoblot analysis of the fractions only detected UCP at 32 kDa from mitochondria of cells containing UCP cDNA (Figure 3-7a, lanes 3-5 and 7-9) but not from mitochondria of cells lacking UCP cDNA (Figure 3-7b, lanes 3-5 and 7-9). Since UCP could be isolated using this purification procedure, it was likely that UCP had been incorporated into mitochondrial membranes as in brown adipose tissue mitochondria rather than bound to mitochondria.

3.2.3 Submitochondrial Localization of UCP

The submitochondrial location of UCP was determined by comparing the level of UCP immunodetected in submitochondrial fractions to marker enzyme activities in the different submitochondrial fractions. The inner-to-outer membrane ratio of the level of UCP, cytochrome *c* oxidase activity (an inner membrane protein marker) and kynurenine hydroxylase activity (an outer membrane protein marker) were 3.0 ± 0.7, 3.8 ± 0.4 and 0.4 ± 0.1 respectively (Table 3-1). These data indicated that UCP was located in the mitochondrial inner membrane since its submitochondrial location correlated with the activity of the mitcohondrial inner membrane marker cytochrome *c* oxidase.

(a)

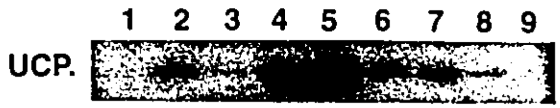

(b)

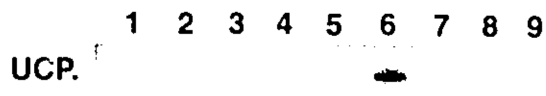

Figure 3-7. Immunoblot Analysis of a Triton X-100 Extract of the Yeast Mitochondrial Fraction Separated by Hydroxylapatite Chromatography

UCP was purified from a yeast mitochondrial fraction isolated from transformants containing the UCP cDNA that were induced with galactose (a). The standard methods of Triton X-100 extraction and hydroxylapatite purification were followed as outlined in the methods section **2.8.2 Hydroxylapatite Purification of UCP from Mitochondria**. The same procedure was also performed using yeast mitochondria isolated from non-induced transformants (b). One 150 μL fraction and six 50 μL fractions were collected from the hydroxylapatite column, 5 μL of each were separated by SDS-12.5% PAGE, transferred to nitrocellulose and detected with monospecific antiserum against rat uncoupling protein and [^{125}I]-labelled protein A. Lane 1, fraction 1; lane 2, 5 μg yeast mitochondrial protein; lanes 3, 4, 5, 7, 8 and 9, fractions 2,3,4,5,6 and 7, respectively; lane 6, 0.14 μg of rat uncoupling protein purified from brown adipose tissue mitochondria.

Table 3-1. Mitochondrial Location of UCP

Mitochondria isolated from yeast transformants induced to express UCP with 0.2% galactose for 8 h were subfractionated into an inner membrane fraction, outer membrane and intermembrane space fraction and matrix fraction following the method outlined in section **2.8.3 Yeast Mitochondrial Inner Membrane Preparation**. Marker enzyme assays were performed on the submitochondrial fractions. UCP levels were determined by Western blot analysis of the submitochondrial fractions. The outer membrane marker was kynurenine hydroxylase and the inner membrane marker was cytochrome *c* oxidase. The data presented is the average from two individual mitochondrial preparations ± SEM.

Protein Detected	Inner Membrane/Outer Membrane Level
Uncoupling Protein	3.0 ± 0.7
Cytochrome *c* Oxidase	3.8 ± 0.4
Kynurenine Hydroxylase	0.4 ± 0.1

3.3 FUNCTIONING OF UCP IN YEAST MITOCHONDRIA

3.3.1 GDP Binding to Yeast Mitochondria

3.3.1.1 GDP Binding to Brown Adipose Tissue Mitochondria

Several studies have shown that UCP exists in mitochondria in either a non-functional form with respect to proton conductance where GDP binding sites are masked resulting in a low level of bound [^{3}H]GDP or a functional form where GDP binding sites are unmasked resulting in a high level of bound [^{3}H]GDP (Ashwell *et al.*, 1985, Gribskov *et al.*, 1986, Trayhurn *et al.*, 1987, Swick and Swick, 1988, Peachy *et al.*, 1988). The molar ratio of GDP bound/UCP to brown adipose tissue mitochondria has been used as an index for the proton conductance activity of mitochondria specific to UCP rather than as a measure of mitochondrial UCP levels due to the masking/unmasking of GDP binding sites. The molar ratio has been reported to approach 1.0 mol GDP per mol $UCP_{monomer}$ (UCP_m) in brown adipose tissue mitochondria isolated from cold-adapted rats (Peachey *et al.*, 1988, Feil and Rafael, 1994) and for UCP purified from rat brown adipose tissue mitochondria (French *et al.*, 1988) in contrast to a molar ratio of 0.5 found for purified hamster UCP (Lin and Klingenberg, 1982). A molar binding ratio of 1 has been interpreted to mean that all of the UCP is in a fully active conformation for proton conductance with mitochondrial thermogenic activity at its maximum (Peachey *et al.*, 1988, Feil and Rafael, 1994). Peachey *et al.* (1988) showed that the maximum molar ratio measured was dependent on the length of time rats were exposed to the cold. They reported that within hours of cold exposure, initial unmasking of GDP binding sites occurred without an increase in UCP level (0.88 mol GDP/mol UCP_m) that was followed by an increase in UCP level and remasking of GDP binding sites after prolonged cold exposure (0.42 mol GDP/mol UCP_m). This response was interpreted to mean that upon cold exposure, rats acquired excess thermogenic capacity in order to allow them to respond quickly to additional cold stress by unmasking inactive UCP. Binding ratios less than 0.5 mol GDP/mol UCP_m have been measured in mitochondria from warm-adapted rats (Trayhurn *et al.*, 1987; Peachey *et al.*, 1988). However, Feil and Rafael found that the molar GDP/UCP_m ratio varied from 0.5 - 1.0 depending on the thermogenic activity of brown adipose tissue mitochondria. In this study, the molar ratio of bound GDP to UCP was 0.5 mol GDP/UCP_m in mitochondria from warm-adapted rats and 1.0 mol GDP/UCP_m in mitochondria from cold-adapted rats (Feil and Rafael, 1994). They also stated that brown fat mitochondria from warm-adapted guinea pigs and rats were coupled in the absence of GDP, whereas mitochondria from cold-adapted animals were uncoupled in the absence of GDP. Interpreting their results in terms of dimeric UCP (the functional unit of UCP in the mitochondrial inner membrane), Feil and Rafael (1994) suggest that the UCP dimer (UCP_d) binds one GDP in the inactive state, with this bound nucleotide having no regulatory relevance, and that the UCP_d binds two GDP molecules in its active state, with the bound nucleotides regulating UCP function.

The differences in the literature for the molar ratio of GDP bound/UCP_m may reside in the methods used to quantify UCP. Feil and Rafael (1994) stated that their purification of UCP from brown adipose tissue mitochondria by hydroxylapatite chromatography represented only 40-50% of the protein eluted from the column. They state that if UCP was purified only to this extent in previous studies, and was subsequently used as a standard for UCP quantification in mitochondria, molar GDP binding levels/UCP_m may have been underestimated. However, French *et al.* (1988)

purified UCP from rat brown adipose tissue mitochondria of cold-adapted animals using the standard hydroxylapatite chromatography method and measured 0.85 mol GDP bound/mol UCP_m using this purified UCP.

In summary, it appears that the GDP binding ratio in thermogenically active rat brown adipose tissue mitochondria can approach a value of 1 mol GDP bound/mol UCP_m with this ratio ranging from 0.5-1 and that the level of GDP bound to thermogenically inactive rat brown adipose tissue mitochondria is not certain, but is equal to or less than 0.5 mol GDP/mol UCP_m. The molar ratio of GDP bound to UCP for UCP in thermogenically active and inactive brown adipose tissue mitochondria is an important parameter to be accurately determined for several reasons. In terms of understanding the function of UCP, it must be determined whether the functional unit of UCP, UCP_d, binds one mol of GDP in its inactive state and two mol of GDP in its active state, or whether the molar GDP binding ratio can vary from zero mol GDP bound for completely inactive UCP_d and up to two mol GDP bound to active UCP_d. These parameters are also important in order to assess the functional state of UCP that is expressed in heterologous systems or reconstituted into proteoliposomes.

3.3.1.2 GDP Binding To Yeast Mitochondria: Optimization of Binding Conditions

GDP binding experiments to yeast mitochondria containing and lacking UCP were carried out to determine the extent of GDP bound per mol UCP in comparison to the molar GDP binding ratio found in the literature for rat brown adipose tissue mitochondria. Binding of $[^3H]$GDP to yeast mitochondria containing and lacking UCP in the presence and absence of ADP was carried out following the centrifugation method of Desautels *et* *al*. (1978) as outlined in the methods section **2.9.2 GDP Binding Assay**. [^{14}C]Sucrose was used as a supernatant marker to measure the amount of unbound [^{3}H]GDP from the supernatant trapped in the mitochondrial pellet.

In preliminary studies, binding of [^{3}H]GDP to mitochondria containing and lacking UCP was measured with 10 μM GDP at pH 7.4. Yeast mitochondria containing 80 μg UCP/mg mitochondrial protein bound 0.45 ± 0.02 nmol GDP/mg mitochondrial protein (Table 3-2). Control mitochondria isolated from non-induced transformants bound 0.05 ± 0.01 nmol GDP/mg mitochondrial protein and control mitochondria isolated from galactose induced transformants that contained the shuttle vector without the UCP cDNA bound 0.10 ± 0.01 nmol GDP/mg mitochondrial protein (Table 3-2). After subtracting the level of GDP bound to control mitochondria, yeast mitochondria containing UCP bound 0.12 - 0.14 mol GDP/mol UCP_m. This level of binding is comparable to that found for brown adipose tissue mitochondria isolated from cold-adapted rats that had been rewarmed to thermoneutral temperature (27°C) where GDP binding decreased from 0.30 to 0.12 mol GDP/mol UCP_m for 62 μg UCP/mg mitochondrial protein (Peachey *et al.*, 1988). The reduction in the molar ratio of GDP bound/UCP_m was thought to be due to remasking of GDP binding sites on UCP which occured concurrently with inactivation of mitochondrial proton conductance.

For the initial binding studies to yeast mitochondria, the buffer used for mitochondrial isolation and GDP binding contained 0.6 M mannitol, 20 mM HEPES and 0.1% BSA at a pH of 7.4. However, past studies have shown that the affinity of purine nucleotides for purified UCP and UCP present in brown adipose tissue mitochondria was dependent on the pH of the binding medium. The strongest binding was observed over

Table 3-2. GDP Binding to Isolated Yeast Mitochondria

Mitochondria were isolated from yeast transformants containing or lacking the UCP cDNA that were grown in the presence or absence of 0.2% galactose for 8 h. Both the mitochondrial isolation and the GDP binding were carried out in mitochondrial isolation buffer containing 0.6 M mannitol, 20 mM HEPES, pH 7.4, 0.1% BSA. Binding of [^{3}H]GDP to isolated mitochondria was carried out in the presence of carboxyatractyloside (0.1 M) as outlined in the method section **2.9.2 GDP Binding Assay** using 10 μM GDP without the addition of succinate, fatty acid free BSA or oligomycin. Data is presented as the mean of three replicate binding samples from single mitochondrial preparations ± SEM. Yeast mitochondria isolated from transformants containing the UCP cDNA that were induced with galactose contained 80 μg UCP/mg mitochondrial protein as determined by immunoblot analysis.

Yeast Transformant	**UCP Expression**	**GDP Bound (nmol/mg mitochondrial protein)**
+UCP cDNA +0.2% galactose for 8 h	+UCP	0.45 ± 0.02
+UCP cDNA -galactose	-UCP	0.05 ± 0.01
-UCP cDNA +0.2% galactose for 8 h	-UCP	0.1 ± 0.01

a pH range of 5.5 - 6.5 but the binding affinity decreased as the pH increased above 6.8 (Nicholls, 1976, Klingenberg, 1988, Rafael *et al.*, 1994). In addition, GDP inhibition of oleate activated uncoupling of yeast mitochondria containing UCP (results section **3.3.2.4 Oleate Stimulation and GDP Inhibition of Yeast Mitochondrial Respiration**) was observed and measured at pH 6.5 in mitochondrial respiration buffer (0.65 M sorbitol, 0.36 mM EDTA, 10 mM KCl, 10 mM KH_2PO_4, 10 mM Tris-HCl, 0.05% BSA). Binding of GDP to yeast mitochondria was then tested using the mitochondrial respiration buffer at pH 6.5 to determine optimal binding conditions using 10 μM GDP (Table 3-3).

Mitochondria were isolated as before at pH 7.4 and the binding assay was carried out in both the isolation buffer at pH 7.4 (0.6 M mannitol, 20 mM HEPES, 0.1% BSA, pH 7.4) and the respiration buffer at pH 6.5 (0.65 M sorbitol, 0.36 mM EDTA, 10 mM KCl, 10 mM KH_2PO_4, 10 mM Tris-HCl, 0.05% BSA, pH 6.5). Binding of GDP (10 μM) to yeast mitochondria containing UCP increased from 0.50 ± 0.02 to 0.93 ± 0.03 nmol GDP/mg mitochondrial protein for binding measured in isolation versus respiration buffer respectively (Table 3-3). GDP binding to control mitochondria lacking UCP also increased from 0.10 ± 0.01 to 0.4 ± 0.04 nmol GDP/mg mitochondrial protein for binding measured in isolation versus respiration buffer respectively (Table 3-3). Isolating mitochondria containing UCP in an isolation buffer containing 0.6 M sucrose at pH 6.5 (the conditions required to prepare coupled yeast mitochondria, results section **3.3.2.3 Respiratory Control of Yeast Mitochondria**) instead of 0.6 M mannitol at pH 7.4 decreased GDP binding measured in respiration buffer, pH 6.5 from 0.93 ± 0.03 to 0.23 ± 0.1 nmol GDP/mg mitochondrial protein (Table 3-3). The higher level of GDP bound measured at pH 6.5 to mitochondria isolated in isolation buffer containing mannitol at pH

Table 3-3. Comparison of GDP Binding in Different Buffers to Yeast Mitochondria Isolated in Different Buffers

Mitochondria were isolated from yeast transformants containing (+UCP) or lacking (-UCP) the UCP cDNA after growth in the presence of 0.2% galactose for 8-10 h. Mitochondrial isolation buffer either contained 0.6 M mannitol, 20 mM HEPES, pH 7.4, 0.1% BSA or 0.6 M sucrose, 20 mM HEPES, pH 6.5, 0.1% BSA. GDP binding to mitochondria was assayed in either mitochondrial isolation buffer containing 0.6 M mannitol, 20 mM HEPES, pH 7.4, 0.1% BSA or mitochondrial respiration buffer containing 0.65 M sorbitol, 0.36 mM EDTA, 10 mM KCl, 10 mM KH_2PO_4, 10 mM Tris-HCl, pH 6.5, 0.05% BSA. Binding of [^{3}H]GDP was carried out as outlined in the methods section **2.9.2 GDP Binding Assay** using 10 μM GDP. Data is presented as the mean ± SEM. Data for GDP binding to -UCP mitochondria in mitochondrial isolation buffer (0.6 M mannitol, 20 mM HEPES, pH 7.4, 0.1% GSA) was taken from Table 3-2 and GDP binding to -UCP mitochondria in respiration buffer was taken from Table 3-4. GDP binding to +UCP mitochondria was assayed in duplicate.

UCP Expression	Mitochondrial Isolation Buffer	GDP Binding Buffer	GDP Bound nmol/mg Mitochondrial Protein
+UCP	0.6 M mannitol 20 mM HEPES pH 7.4 0.1% BSA	**Isolation Buffer** (0.6 M mannitol, 20 mM HEPES, pH 7.4, 0.1% BSA)	0.50 ± 0.02
		Respiration Buffer (0.65 M sorbitol, 0.36 mM EDTA, 10 mM KCl, 10 mM KH_2PO_4, 10 mM Tris-HCl, pH [illegible] 05% BSA)	0.93 ± 0.03
+UCP	0.6 M sucrose 20 mM HEPES, pH 6.5, 0.1% BSA	**Respiration Buffer** (0.65 M sorbitol, 0.36 mM EDTA, 10 mM KCl, 10 mM KH_2PO_4, 10 mM Tris-HCl, pH 6.5, 0.05% BSA)	0.23 ± 0.10
-UCP	0.6 M mannitol 20 mM HEPES, pH 7.4, 0.1% BSA	**Isolation Buffer** (0.6 M mannitol, 20 mM HEPES, pH 7.4, 0.1% BSA)	0.10 ± 0.01
		Respiration Buffer (0.65 M sorbitol, 0.36 mM EDTA, 10 mM KCl, 10 mM KH_2PH_4 , 10 mM Tris-HCl, pH 6.5, 0.05% BSA)	0.40 ± 0.04

7.4 versus mitochondria isolated in isolation buffer containing sucrose at pH 6.5 may be due to a lower level of endogenous GDP bound to UCP in mitochondria isolated at the higher pH in comparison to that bound to UCP in mitochondria isolated at the lower pH resulting from the pH dependancy of nucleotide binding to UCP (see results section **3.3.3 Comparison of UCP Functions in Yeast Mitochondria** for further discussion).

Specific binding of GDP to UCP was measured as the difference between GDP binding to mitochondria containing and lacking UCP. From Table 3-3, for mitochondria isolated in isolation buffer at pH 7.4 with binding measured in the same buffer, specific binding of GDP to UCP in mitochondria was 0.4 nmol GDP for approximately 80 μg UCP (0.5 nmol GDP/mg mitochondrial protein minus 0.1 nmol GDP/mg mitochondrial protein), for a molar binding ratio of 0.16 mol GDP/UCP_m. For mitochondria isolated in isolation buffer at pH 7.4 with binding measured in respiration buffer at pH 6.5, specific binding of GDP to UCP in mitochondria was 0.53 nmol GDP for approximately 80 μg UCP (0.93 nmol/mg mitochondrial protein minus 0.40 nmol/mg mitochondrial protein), for a molar binding ratio of 0.21 mol GDP/UCP_m. The higher level of specific GDP binding to UCP measured in respiration buffer at pH 6.5 as compared to isolation buffer at pH 7.4 is probably due to the pH dependence of binding, since purine nucleotides have a higher affinity to UCP at lower pH (Nicholls, 1976; Klingenberg, 1988). For mitochondria isolated in sucrose isolation buffer at pH 6.5, specific binding of GDP to UCP could not be determined because the appropriate control of GDP binding to mitochondria lacking UCP isolated under these conditions was not measured. However, even if there was no GDP bound to control mitochondria under these condition, the specific binding of GDP to UCP would be 0.23 nmol GDP for 80 μg UCP (0.23 nmol

GDP/mg mitochondrial protein minus 0 nmol GDP/mg mitochondrial protein), for a molar binding ratio of 0.09 mol GDP/UCP_m. As stated above, the lower level of binding measured to mitochondria isolated under these conditions could be due to a higher level of endogenous GDP bound to UCP in these isolated mitochondria (see results section **3.3.3 Comparison of UCP Functions in Yeast Mitochondria**).

Since the highest specific binding of GDP to UCP was measured for mitochondria isolated in isolation buffer at pH 7.4 (0.6 M mannitol, 20 mM HEPES, 0.1% BSA) using respiration buffer at pH 6.5 for the binding reaction, these conditions were used for subsequent GDP binding studies. Using these binding conditions would also allow a direct comparison of the K_d for GDP binding and the K_i for GDP inhibition of fatty acid activated respiration in mitochondria containing UCP (results section **3.3.2.4 Oleate Stimulation and GDP Inhibition of Yeast Mitochondrial Respiration**) since the binding and respiration measurements would be done in the same buffer.

3.3.1.3 GDP Binding to Yeast Mitochondria: Effect of Carboxyatractyloside on GDP Binding

To determine if ADP could compete for the specific GDP binding to UCP in yeast mitochondria, GDP binding would have to be measured in the absence and presence of ADP. To avoid ADP binding to the ADP/ATP carrier, carboxyatractyloside, a potent inhibitor of the ADP/ATP carrier that binds to its adenine nucleotide binding site, was present in the GDP binding assay in order for ADP competition studies to be done (Nicholls, 1976; Desautels *et al.*, 1978). Although UCP belongs to the same mitochondrial carrier family as the ADP/ATP carrier and binds both guanine and adenine nucleotides, GDP binding to brown adipose tissue mitochondria was shown to be carboxyatractyloside insensitive (Nicholls, 1976). To determine if carboxyatractyloside had any effect on GDP binding to yeast mitochondria, GDP binding was measured in its absence and presence. In the absence of carboxyatractyloside, yeast mitochondria lacking UCP bound a substantial level of GDP, which increased approximately 2.5 fold when cells were grown in the presence of galactose (Table 3-4). Although both carboxyatractyloside (100 μM) and ADP (2 mM) reduced the level of GDP bound to yeast mitochondria lacking UCP by approximately 70 - 75%, this still left a background level of 0.4 nmol GDP bound/mg mitochondrial protein at 10 μM GDP for control mitochondria lacking UCP isolated from galactose induced cells. In contrast, rat liver mitochondria were found to bind only 0.05 nmol GDP/mg mitochondrial protein at 10 μM GDP in the presence of carboxyatractyloside (Nicholls, 1976). The carboxyatractyloside-sensitive binding of GDP that can be competed by ADP in yeast mitochondria (line 1 of Table 3-4), which has also been reported by Arechaga *et al.* (1993), has not been reported in other mitochondria. Further binding studies were done in the presence of carboxyatractyloside to reduce the background level of GDP bound to control yeast mitochondria.

To determine the molar ratio of GDP bound to UCP, the background level of GDP bound to control yeast mitochondria lacking UCP isolated from galactose-induced cells was subtracted from the level of GDP bound to mitochondria containing UCP. This correction for background GDP binding to control mitochondria was not done when binding data was analyzed for brown adipose tissue mitochondria, probably because Nicholls (1976) found that rat liver mitochondria showed a low level of GDP binding at 10 μM GDP, 0.05 nmol GDP/mg mitochondrial protein.

Table 3-4. Comparison of GDP Binding to Yeast Mitochondria in the Presence and Absence of Carboxyatractyloside and ADP

Mitochondria were isolated from yeast transformants containing or lacking the UCP cDNA that were grown in the absence or presence of 0.2% galactose for 8-10 h. Mitochondrial isolation buffer contained 0.6 M mannitol, 20 mM HEPES, pH 7.4, 0.1% BSA. GDP binding was determined at 10 μM GDP in respiration buffer (0.65 M sorbitol, 0.36 mM EDTA, 10 mM KCl, 10 mM KH_2PO_4, 10 mM Tris-HCl, pH 6.5, 0.05% BSA as outlined in the methods section **2.9.2 UCP Binding Assay**. Binding was measured in the presence or absence of carboxyatractyloside (0.1 mM) and in the presence or absence of ADP (2 mM). Data is presented as the mean ± SEM.

UCP Expression	**Galactose Induction**	**GDP Bound (nmol/mg mitochondrial protein)**			
		-carboxyatractyloside		+carboxyatractyloside	
		-ADP	+ADP	-ADP	+ADP
-UCP	-gal	0.59± 0.01*	0.15±0.01*	0.18±0.01*	0.20±0.02*
-UCP	+gal	1.55±0.04*	N.D.	0.40±0.04†	0.38±0.05†
+UCP	+gal	1.46±0.02*	N.D.	0.89±0.12†	0.66±0.04†

* Data were obtained from single mitochondrial preparations with each sample assayed in duplicate.

† Data are averages from three separate mitochondrial preparations.

N.D. - not determined.

3.3.1.4 GDP Binding to Yeast Mitochondria: Binding Using Optimized Conditions

GDP binding curves were generated for yeast mitochondria containing and lacking UCP isolated from cells grown under the same induction conditions (Figure 3-8). Mitochondria lacking UCP showed a maximum binding of 0.4 nmol GDP/mg mitochondrial protein with a K_d of 0.35 μM. A similar level of GDP binding to yeast mitochondria was observed by Arechaga *et al.* (1993) at 0.32 nmol GDP/mg mitochondrial protein with a higher dissociation constant of 1.3 μM GDP. Yeast mitochondria containing UCP bound between 0.68 - 1.08 nmol GDP/mg mitochondrial protein (Figure 3-8). The level of UCP was quantified for each mitochondrial preparation and the appropriate background level of GDP binding to mitochondria lacking UCP was subtracted from the binding data. The level of GDP binding was expressed as mol GDP bound per mol UCP dimer (UCP_d) (Figure 3-9). From Figure 3-9, a K_d of 0.8 ± 0.1 μM GDP with a maximum binding capacity of 0.35 ± 0.02 mol GDP/mol UCP_d or 0.18 ± 0.01 mol GDP/mol UCP_m was measured. The binding affinity compares well to the binding affinities found for UCP in rat brown adipose tissue mitochondria at pH 7.1: 0.4 μM GDP (Sundin and Cannon, 1980), 0.92 μM GDP (Trayhurn *et al.*, 1987), 0.38-0.73 μM GDP (Peachey *et al.*, 1988), 0.9 μM GDP (Rafael *et al.*, 1994) and for that found for UCP in yeast mitochondria at pH 6.8, 0.4 μM GDP (Arechaga *et al.*, 1993). The K_d for purified rat UCP at pH 6.8 was 3.3 μM GDP (French *et al.*, 1988). The binding capacity for the yeast expressed UCP in this thesis study (0.18 ± 0.01 mol GDP/mol UCP_m) was close to that found for UCP in brown adipose tissue mitochondria from cold-adapted rats that had been rewarmed (0.12 mol GDP/mol UCP_m) where it was thought that masking of GDP binding sites on UCP occurred. The molar ratio of GDP bound to UCP in yeast

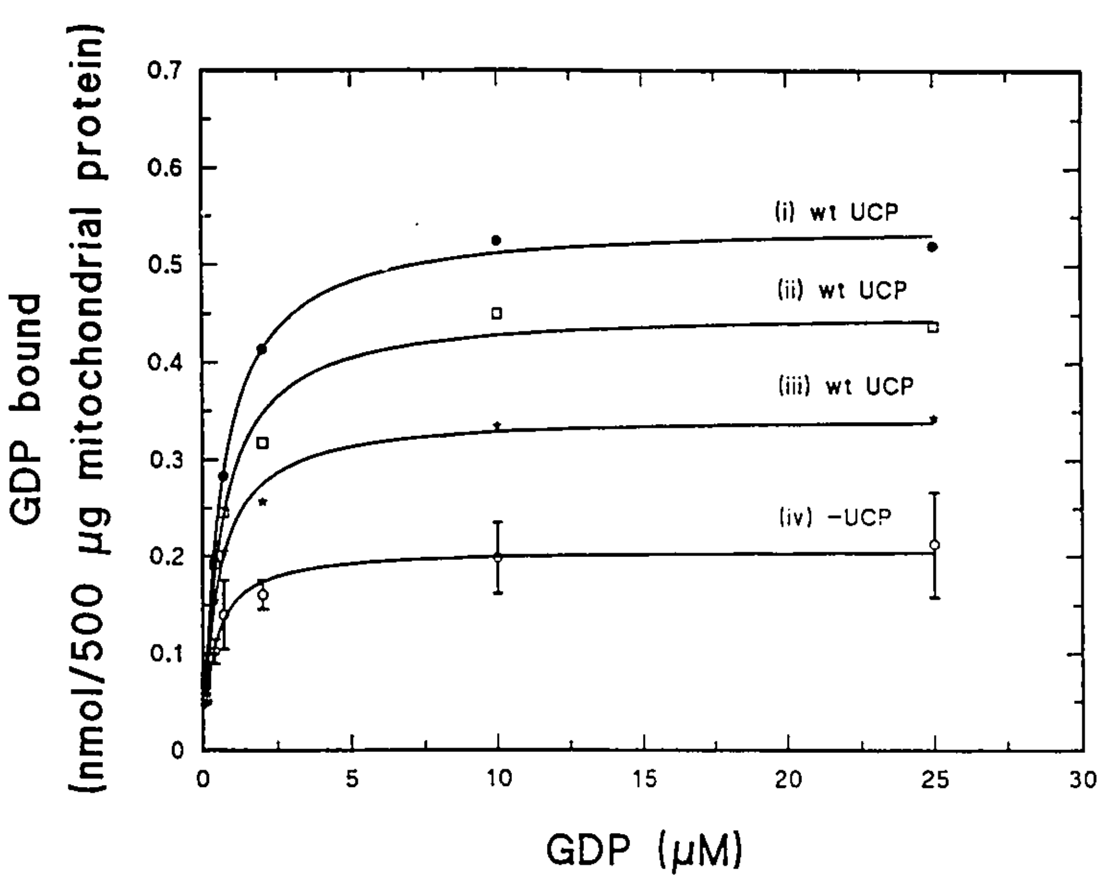

Figure 3-8. GDP Bound to Isolated Yeast Mitochondria

Mitochondria were isolated from galactose-induced yeast transformants as outlined in the methods section **2.7.3 Mitochondrial Isolation From Yeast** using isolation buffer containing 0.6 M mannitol, 20 mM HEPES, pH 7.4, 0.1% BSA. Binding of [^{3}H]GDP to 0.5 mg mitochondria was measured in mitochondrial respiration buffer, pH 6.5 in the presence of carboxyatractyloside at GDP concentrations ranging from 0.1-25 μM GDP as outlined in the methods section **2.9.2 GDP Binding Assay**. Three mitochondrial preparations containing wild type UCP ((i) wt UCP, 110 μg UCP/mg mitochondrial protein; (ii) wt UCP, 86 μg UCP/mg mitochondrial protein; (iii) wt UCP, 82 μg UCP/mg mitochondrial protein) were tested and three mitochondrial preparations lacking UCP ((iv) -UCP, data represents average of three experiments) were tested. Data is expressed as nmol GDP bound/500 μg mitochondrial protein for each concentration of GDP tested.

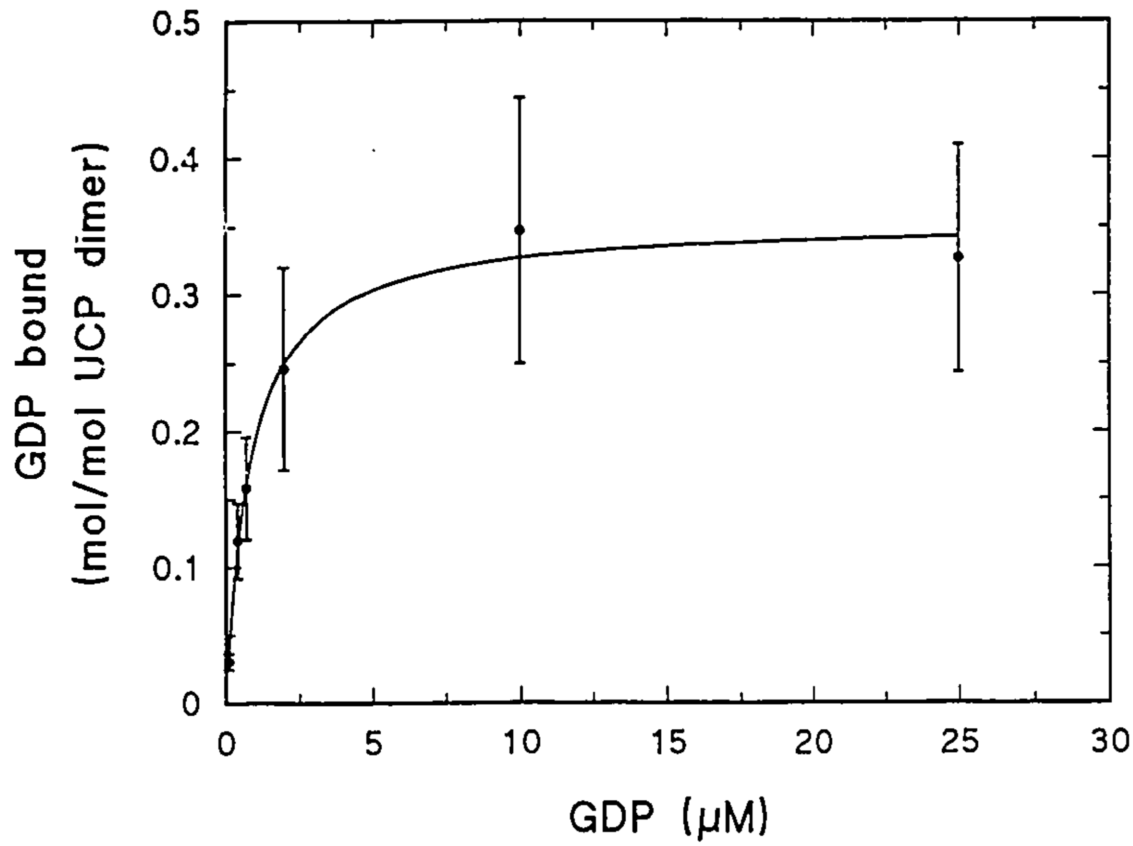

Figure 3-9. GDP Bound to Isolated Yeast Mitochondria Expressed Per Mol UCP_{dimer}

The level of GDP bound to mitochondria lacking UCP was subtracted from that bound to mitochondria containing UCP. The data is expressed as mol GDP bound/mol UCP_{dimer}. The data was calculated from experiments plotted in Figure 3-8 and represents the average from three independent mitochondrial preparations containing UCP ± SEM.

mitochondria from Arechaga *et al.* (1993) was not stated but could be calculated from their data. The binding capacity they attributed to UCP was 0.17 ± 0.1 nmol GDP/mg mitochondrial protein and the expression level of UCP was on average 24 μg/mg mitochondrial protein which would result in 0.23 ± 0.13 mol GDP/mol UCP_m. Therefore, the binding capacity of UCP in yeast mitochondria is comparable between the yeast experiments. It is not known if the low ratio of GDP bound/UCP in yeast mitochondria was due to UCP being inactive with respect to GDP binding because the protein had not been activated in this system and therefore, the majority of UCP resided in a masked, inactive state or because the protein (or a fraction of it) had been covalently modified or folded improperly into the mitochondria, impairing its ability to bind GDP.

3.3.1.5 GDP Binding to Yeast Mitochondria: ADP Competed GDP Binding

GDP binding experiments were also carried out in the presence of ADP since UCP binds both GDP and ADP in brown adipose tissue mitochondria (Nicholls, 1976, Desautels *et al.*, 1978) and in its purified form (Klingenberg, 1988, French *et al.*, 1988). If ADP was a competitive inhibitor of GDP, then the GDP binding curve in the presence of ADP should be shifted to the right with respect to the curve in the absence of ADP, such that there are lower levels of bound GDP in the presence of ADP at the tested GDP concentrations. Results shown in Figure 3-10(a) indicate that the GDP binding curves in the presence of 2 mM ADP to mitochondria containing UCP are shifted to the right. The ADP competed GDP binding, calculated from the difference between binding in the absence and presence of ADP, is shown in Figure 3-10(b). From these curves, the GDP binding at 25 μM GDP was determined to be, on average, 28% of that found for GDP

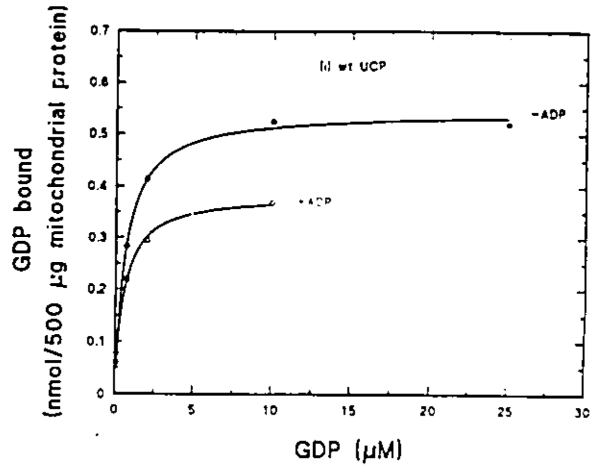

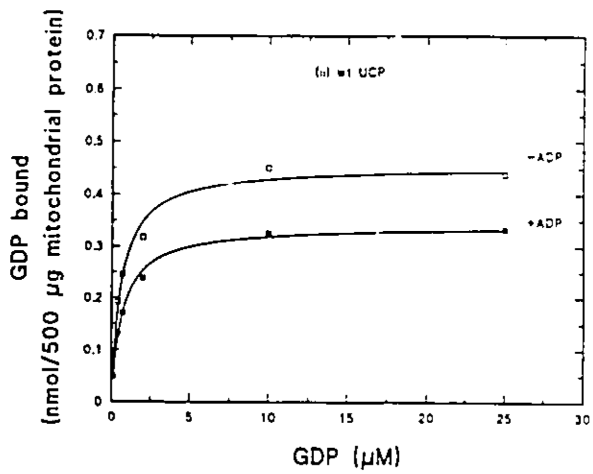

Figure 3-10(a). GDP Bound to Yeast Mitochondria in the Absence and Presence of ADP

GDP binding to yeast mitochondria was carried out as outlined in the legend to Figure 3-8 in the absence (-ADP) and presence (+ADP) of 2 mM ADP. Binding curves in the absence of ADP are reproduced from Figure 3-8. Graphs (i), (ii) and (iii) are for mitochondrial preparations containing 110, 86 and 82 μg wild type UCP/mg mitochondrial protein respectively. GDP binding to mitochondria lacking UCP is illustrated in graph (iv) and represents the average binding curves calculated from three independent mitochondrial preparations ± SEM.

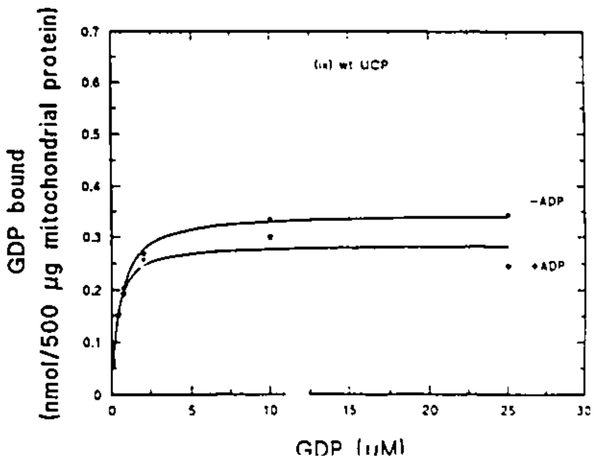
(iii) wt UCP
GDP bound
(nmol/500 μg mitochondrial protein)
GDP (μM)
−ADP
+ADP
0
0.1
0.2
0.3
0.4
0.5
0.6
0.7
0
5
10
15
20
25
30

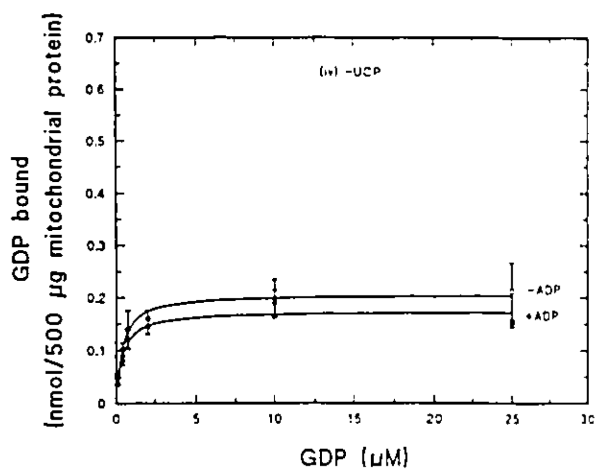
(iv) −UCP
GDP bound
(nmol/500 μg mitochondrial protein)
GDP (μM)
−ADP
+ADP
0
0.1
0.2
0.3
0.4
0.5
0.6
0.7
0
5
10
15
20
25
30

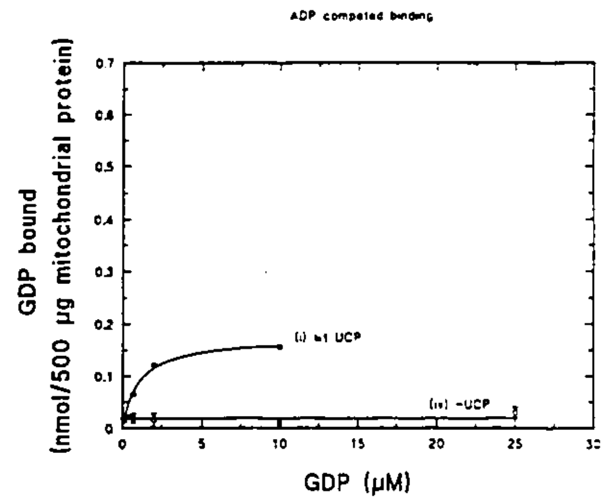

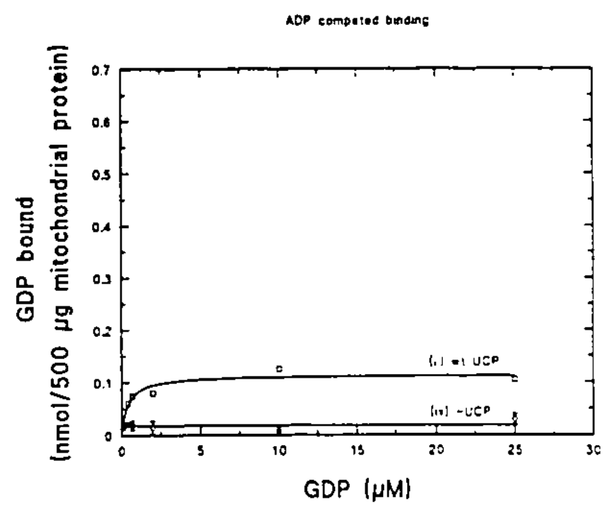

Figure 3-10(b). ADP competed GDP Binding to Yeast Mitochondria

The amount of bound GDP competed by ADP was calculated from the difference between the GDP binding curves of Fig. 3-10(a) in the absence (-ADP) and the presence (+ADP) of ADP. Binding curves (i), (ii) and (iii) are for mitochondrial preparations containing 110, 86 and 82 µg wild type UCP/mg mitochondrial protein respectively. Binding curve (iv) represents ADP competed GDP binding to yeast mitochondria lacking UCP which is the average curve calculated from three independent mitochondrial preparations ± SEM.

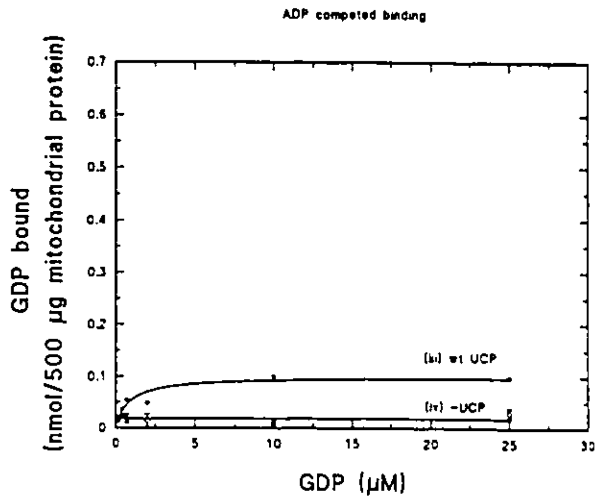
ADP competed binding
GDP bound
(nmol/500 μg mitochondrial protein)
0.7
0.6
0.5
0.4
0.3
0.2
0.1
0
wt UCP
-UCP
0
5
10
15
20
25
30
GDP (μM)

bound to mitochondria in Figure 3-8. From the data in Figure 10(b), the ADP competed GDP binding was recalculated after subtracting the data for mitochondria lacking UCP and expressed as the molar ratio of GDP bound/UCP_d (Figure 3-11). The ADP competed GDP binding had a binding capacity of 0.14 ± 0.02 mol GDP/mol UCP_d, which was only 40% of the GDP binding capacity measured in Figure 3-9 (0.35 ± 0.02 mol GDP/mol UCP_d). The binding affinity of GDP was 0.9 ± 0.4 μM GDP from Figure 3-11 which was within error of the binding affinity of 0.8 ± 0.1 μM GDP from Figure 3-9. In theory, the binding affinity of GDP and the molar ratio of GDP bound/UCP_d should be the same for GDP binding to UCP (Figure 3-9) and ADP competed GDP binding to UCP (Figure 3-11). It is not clear why 2 mM ADP did not compete all GDP binding to UCP. If it is assumed that GDP and ADP have equal binding affinity to UCP and ADP is a competitive inhibitor of GDP, then it can be calculated using the equation $1/V=1/V_{max} + K_M/V_{max} (1 + [I]/K_i)(1/[S])$ that in the presence of 2 mM ADP, GDP binding should have been reduced to 1% of its original value.

This lack of complete inhibition of GDP binding by ADP was also observed in rat brown adipose tissue mitochondria where a 10 fold excess of ADP reduced GDP binding to brown adipose tissue mitochondria from cold-adapted rats by 50% (Desautels *et al.*, 1978). In mouse brown adipose tissue mitochondria, the ADP competed GDP binding was also reported to be lower than GDP binding in the absence of ADP (Goodbody and Trayhurn, 1981). Rafael *et al.* (1994) have recently shown that UCP in rat brown adipose tissue mitochondria had an 18 fold higher affinity for GDP over that for ADP at pH 7.0. In the yeast experiment, if ADP was a competitive inhibitor of GDP binding, with a 67 fold excess of ADP, a K_d of 14 μM ADP (assuming the K_d is 18

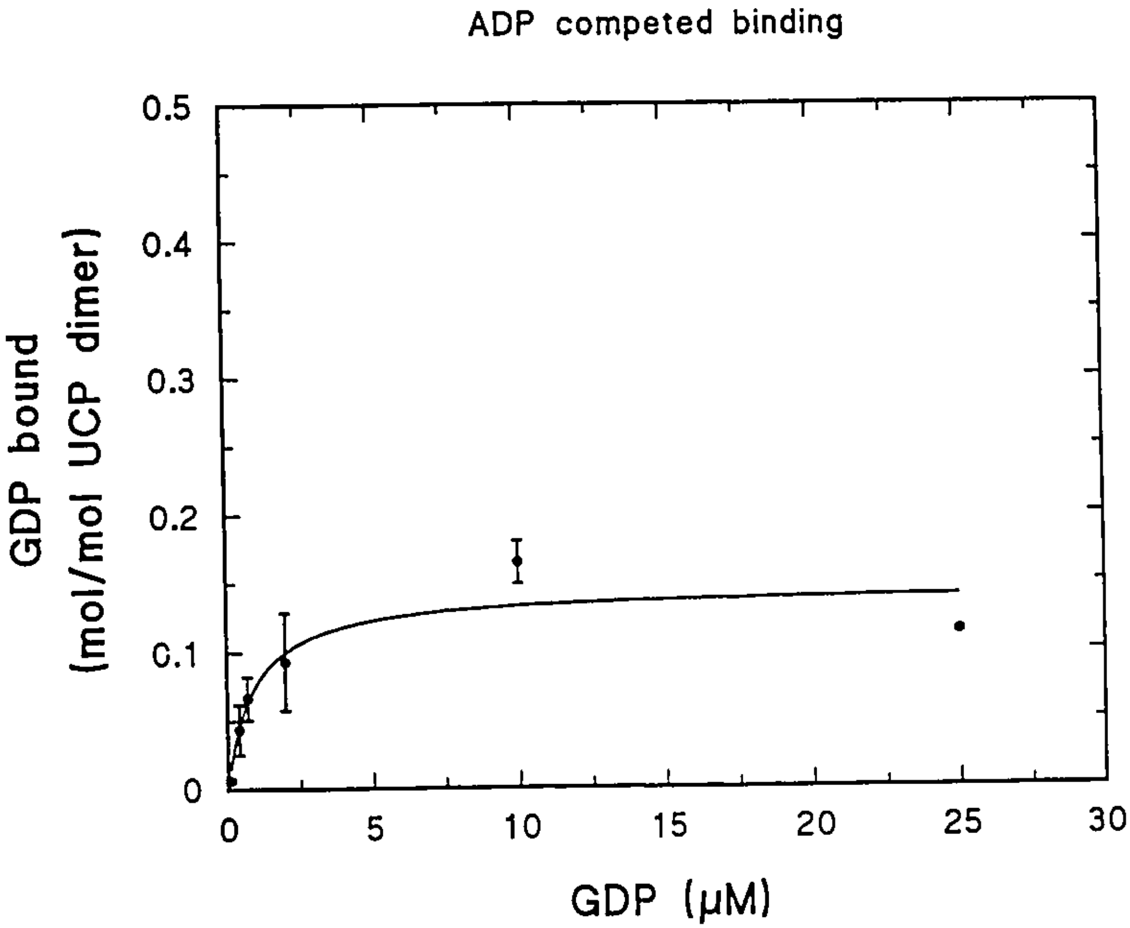

Figure 3-11. ADP Competed GDP Binding Expressed Per Mol UCP_{Dimer}

The level of GDP bound to yeast mitochondria lacking UCP that could be competed by ADP (Figure 3-10b(iv)) was subtracted from that bound to mitochondria containing wild type UCP (Figure 3-10b(i-iii)). The data is expressed as the mol GDP bound/mol UCP_{dimer}. Each point represents an average from three independent mitochondrial preparations ± SEM.

times higher for ADP than GDP), and a binding capacity equal to that found for GDP (0.35 mol ADP/mol UCP_d), then ADP would still have reduced binding to 17% of the original value. If this were so, then the binding capacity for the ADP competed GDP binding would be 83% of the original binding capacity. It is not known whether ADP only competes out 40% of the binding to UCP due to a lower affinity (K_d of 100 μM ADP required to compete out 40% of GDP binding at 2 mM ADP), or whether expression of UCP increases the background level of GDP binding in yeast mitochondria due to increased GDP binding to some other protein present in yeast mitochondria.

3.3.2 Uncoupling of Oxidative Phosphorylation in Yeast Mitochondria by UCP

3.3.2.1 Oxidative Phosphorylation and Respiratory Control

Oxidative phosphorylation refers to the flow of electrons through the mitochondrial respiratory chain to oxygen as ADP is simultaneously phosphorylated to ATP (as outlined in the Introduction, Figure 1-1). As electrons are transferred from the electron carriers of the respiratory chain to oxygen, protons are pumped out from the mitochondrial matrix across the mitochondrial inner membrane into the intermembrane space. Since the mitochondrial inner membrane is relatively impermeable to protons, respiration establishes an electrochemical gradient across the inner membrane which serves as a storage form for the energy of substrate oxidation. The stored electrochemical energy of the transmembrane proton gradient, termed the protonmotive force, is used to drive ATP synthesis. When protons flow down their electrochemical gradient back into the matrix through the ATP synthase, the energy released is used in the synthesis of ATP. As the proton electrochemical gradient collapses during this process, the rate of respiration (oxygen consumption) increases in order to pump protons back out of the matrix at a rate that balances proton re-entry into the matrix.

The regulation of oxidative phosphorylation by ADP is called respiratory control. Mitochondria are under tight respiratory control when oxidation occurs only as ADP is phosphorylated to ATP. Since oxidation and phosphorylation are coupled to the proton gradient under these circumstances, the mitochondria are termed "coupled". When protons re-enter the mitochondrial matrix through an alternative pathway, bypassing the ATP synthase, oxidation occurs without phosphorylation. These mitochondria are not under respiratory control and are termed "uncoupled". Respiratory control is measured by comparing the rate of mitochondrial oxygen consumption in the presence of ADP to the rate that results after all the ADP is converted to ATP (Figure 3-12). The ratio of these rates is known as the respiratory control ratio (RCR). The higher the RCR, the better the respiratory control and therefore, the more coupled the mitochondria are.

3.3.2.2 Brown Adipose Tissue Mitochondria

Mitochondria isolated from brown adipose tissue of cold-adapted animals are uncoupled, with no stimulation of respiration by ADP or uncouplers. The lack of respiratory control in brown adipose tissue mitochondria is due to the high proton conductance of the inner membrane resulting from the activity of UCP. UCP enables these mitochondria to dissipate the energy of oxidation as heat (non-shivering thermogenesis) rather than using it to drive ATP production. Past studies have shown that proton permeability and respiration of brown adipose tissue mitochondria is activated by fatty acids resulting in uncoupling and inhibited by GDP resulting in recoupling (reviewed

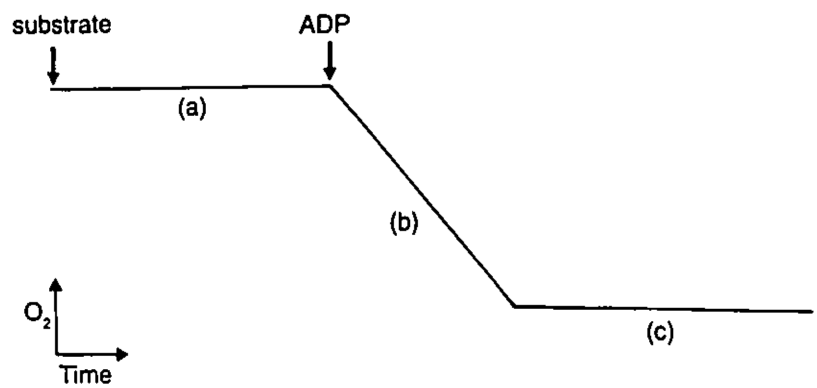

Figure 3-12. Respiratory Control

Mitochondria are depicted under idealized absolute respiratory control. In part (a), mitochondria with an established proton electrochemical gradient will not oxidize substrate in the absence of ADP, therefore, no O_2 consumption occurs. When ADP is added to the mitochondria, respiration (O_2 consumption) is stimulated (b) in order to pump protons back out of the matrix at a rate that balances proton re-entry through the ATP synthase as the proton electrochemical gradient is collapsed during ATP synthesis. When all the ADP is converted to ATP, respiration is no longer required once the proton electrochemical gradient is re-established (c). The respiratory control ratio (RCR) is measured as rate (b)/rate (c).

in Nicholls *et al.*, 1986). It is now known from reconstitution studies using purified UCP that UCP transports many different monovalent anions and that these ion transporting activities of UCP are inhibited by purine nucleoside di- and triphosphates (Jezek *et al.*, 1990, Jezek and Garlid, 1990; Jezek *et al.*, 1994). In addition, reconstitution studies have shown that proton flux across lipid bilayers mediated by UCP is activated by free fatty acids (Winkler and Klingenberg, 1994, Murdza-Inglis *et al.*, 1994; Jezek *et al.*, 1994), although it is not certain if UCP is involved directly in proton transport or indirectly as a fatty acid anion transporter, thus enabling fatty acids to act as protonophores (Skulachev, 1991).

3.3.2.3 Respiratory Control of Yeast Mitochondria

Respiratory control of yeast mitochondria containing and lacking UCP was examined to determine whether UCP could give yeast mitochondria the respiratory characteristics of brown adipose tissue mitochondria. The coupled state of yeast mitochondria containing and lacking UCP was measured using an oxidative phosphorylation assay. The mitochondrial respiratory rate was monitored using an oxygen electrode to measure the amount of oxygen consumed over time. Respiratory control was determined by measuring the respiratory control ratio (RCR), the ratio of the ADP stimulated rate to the rate re-established after ADP stimulation (Figure 3-12). The RCR was used as an indication of the coupled state of the mitochondria. Yeast mitochondria typically have RCRs in the range of 2.0 - 3.5 (Yaffee, 1991).

When mitochondria were isolated in isolation buffer containing 0.6 M mannitol, 20 mM HEPES at pH 7.4, 0.1% BSA with respiratory control measured in respiration buffer at pH 7.4, the RCR for mitochondria containing wild type UCP was only 1.6 ± 0.1. By changing the isolation buffer to one containing 0.6 M sucrose, 20 mM HEPES at pH 6.5, 0.1% BSA and changing the pH of the respiration buffer to pH 6.5, the RCR for yeast mitochondria containing UCP (Figure 3-13a) increased to 2.0 ± 0.1 (averaged from 11 independent mitochondrial preparations). It is likely that isolating yeast mitochondria at the lower pH resulted in more endogenously bound purine nucleotide, resulting in inhibition of UCP and better coupling of the mitochondria (see results section **3.3.3 Comparisons of UCP Functions in Yeast Mitochondria** for further discussion). The RCR for mitochondria lacking UCP (Figure 3-13b) was 2.8 ± 0.2 averaged from 5 independent preparations. Since mitochondria containing UCP are slightly less coupled than mitochondria lacking UCP, this could indicate a low level of UCP activity. However, it is also possible that UCP is inactive in yeast mitochondria. The integrity of the mitochondrial inner membrane may have been compromised due to the high level of UCP, thereby making the inner membrane leaky from non-specific effects which would result in some loss of respiratory control.

3.3.2.4 Oleate Stimulation and GDP Inhibition of Yeast Mitochondrial Respiration

To determine whether fatty acids could activate UCP in yeast mitochondria, the effects of oleate (a strong activator of UCP) and GDP (a strong inhibitor of UCP) on respiration and coupling of yeast mitochondria were examined using two assays.

The first assay was based on the oxidative phosphorylation assay. Normally, when mitochondria become uncoupled, protons re-enter the matrix by an alternative pathway bypassing the ATP synthase. The increase in proton re-entry rate causes an

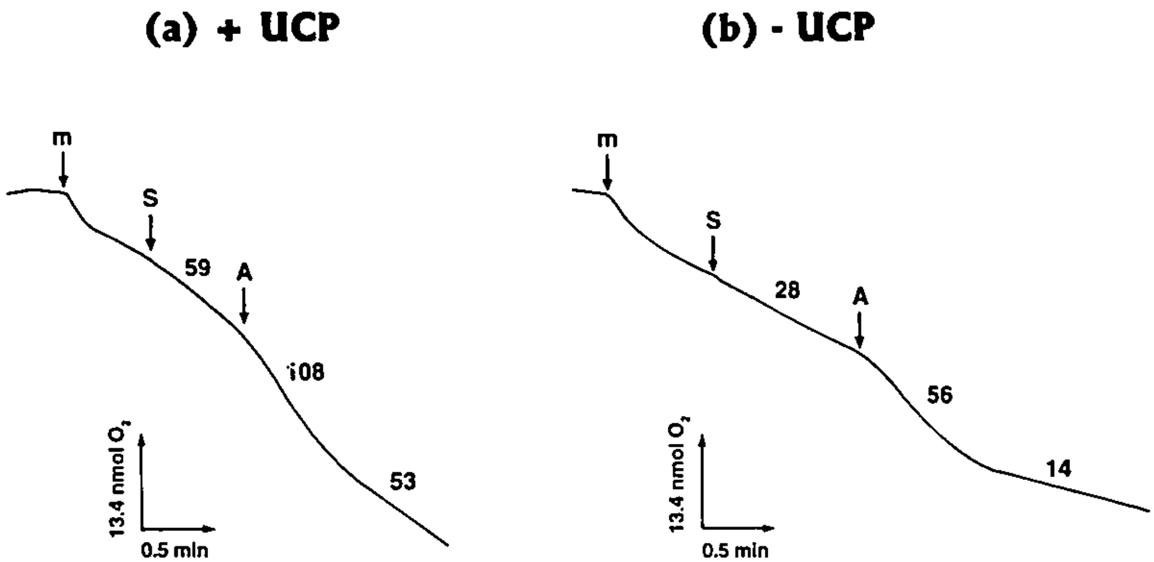

Figure 3-13. Respiratory Control in Yeast Mitochondria Containing and Lacking UCP

Respiration of yeast mitochondria containing (+UCP) and lacking (-UCP) uncoupling protein was monitored before and after ADP addition (as outlined in the methods section **2.9.1 Respiration Assay**). The addition of mitochondria (m), succinate (S) and ADP (A) to the reaction chamber are denoted on the traces. The respiratory rates recorded above the traces are in nmol 0_2/min/mg mitochondrial protein. The respiratory control ratios (RCRs) were calculated from the ADP stimulated rate divided by the cut off rate as outlined in the legend to Figure 3-12. The RCR for mitochondria containing UCP was 2.0 from the illustrated example. The RCR for mitochondria lacking UCP was 3.8 from the illustrated example.

increase in the respiratory rate, such that protons are pumped back out of the matrix at a rate that balances proton re-entry. The effect of the protonophore CCCP on yeast mitochondrial respiration illustrates the uncoupling effect on respiratory rate and ADP stimulation (Figure 3-14). As the concentration of CCCP was increased, the respiratory stimulation increased. The coupled state of the mitochondria was tested by ADP addition. ADP caused less of a stimulation in the respiratory rate as oxidation became uncoupled from phosphorylation. Recoupling of mitochondria would cause a decrease in the respiratory rate and a normal ADP respiratory stimulation. To test the effect of oleate on yeast mitochondrial respiration, oleate was added to respiring mitochondria and its effect on the respiratory rate recorded using an oxygen electrode. The coupled state of the mitochondria was assessed by ADP addition. GDP was then subsequently added to the mitochondria to test its effect on respiration and again the coupled state of the mitochondria was assessed by ADP addition. A schematic of the assay is presented in Figure 3-15. In theory, activation of UCP by oleate would cause an increase in the respiratory rate and uncoupling of the mitochondria (Figure 3-15a). Inhibition of UCP by GDP would cause a decrease in the respiratory rate and recoupling of the mitochondria (Figure 3-15a). If the oleate and GDP effects were specific to UCP, yeast mitochondria lacking UCP would show no effects from their addition (Figure 3-15b).

The effects of oleate and GDP on yeast mitochondrial respiration using this assay are presented in Figure 3-16a and b. The results from this assay are expressed as the respiratory stimulation versus free oleate concentration using 3 different curves: respiratory stimulation (i) after oleate addition, (ii) after the subsequent ADP addition (ADP_1) and (iii) after GDP and the subsequent ADP addition (ADP_2). The respiratory

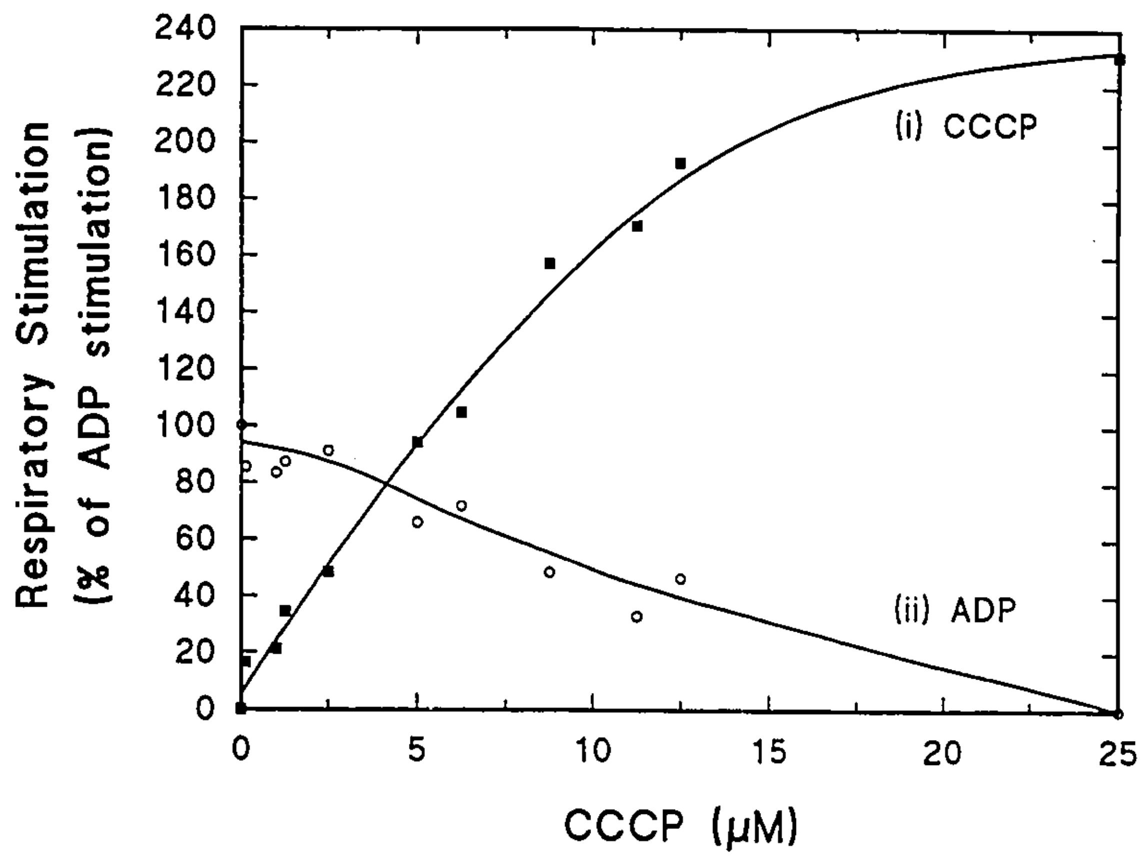

Figure 3-14. Effect of CCCP on Mitochondrial Respiration

The effect of the protonophore CCCP on yeast mitochondrial respiration was monitored for increasing concentrations of CCCP. Yeast mitochondria were isolated as outlined in the methods section **2.7.2 Mitochondrial Isolation From Yeast**. Mitochondrial respiration was monitored using an oxygen electrode as outlined in the methods section **2.9.1 Respiration Assay**. After the addition of succinate to the mitochondria, CCCP was added to the concentration indicated on the graph and the respiratory rate was measured ((i) CCCP). Subsequently, ADP (100 μM) was added to test the coupled state of the mitochondria and the respiratory rate was measured ((ii) ADP). The respiratory stimulations caused by CCCP and the subsequent ADP additions are expressed as a percentage of the respiratory rate stimulation caused by ADP addition in the absence of CCCP.

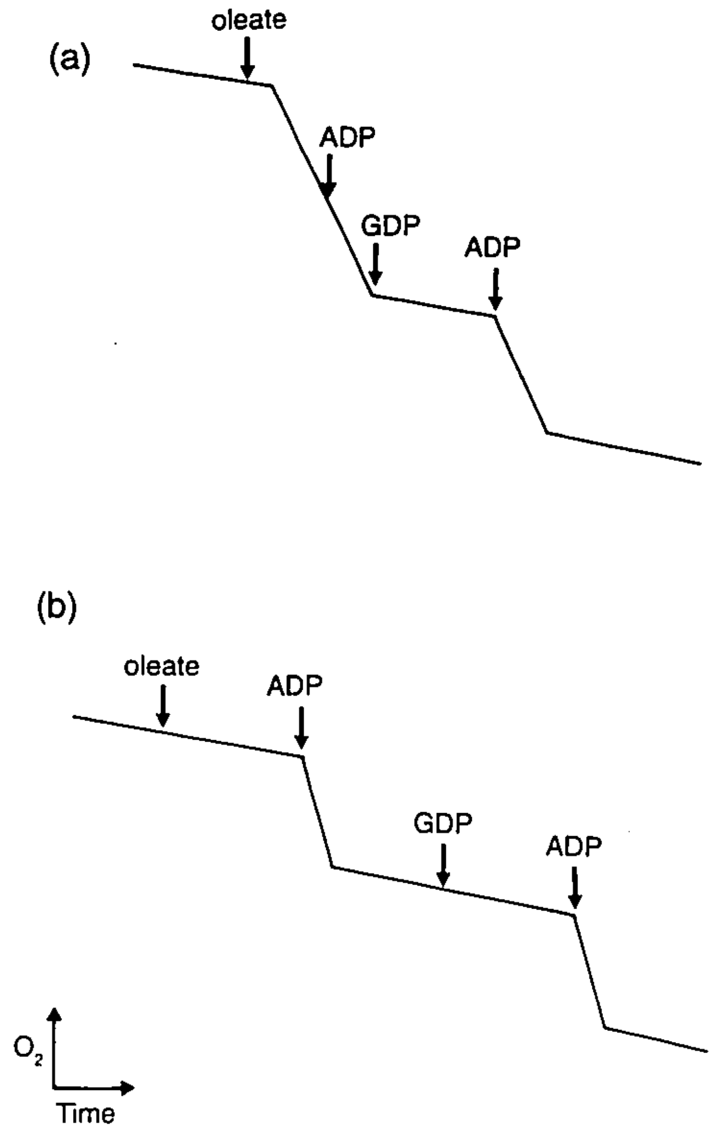

Figure 3-15. Schematic of Assay 1 Used to Test the Effects of Oleate and GDP on Yeast Mitochondrial Respiration

Yeast mitochondrial respiration was monitored using an oxygen electrode as outlined in the methods section **2.9.1 Respiration Assay**. Once the mitochondria established a steady state respiratory rate using succinate for substrate oxidation, oleate was added (at varying concentrations) and the resulting respiratory rate recorded. Coupling was tested by ADP addition. Subsequently, GDP (167 μM) was added and the resulting respiratory rate recorded. Coupling was again tested by ADP addition. Figure (a) depicts the expected result if oleate caused uncoupling and GDP caused recoupling of the mitochondria. Figure (b) depicts the expected result if oleate and GDP had no effect on the coupled state of the mitochondria.

stimulation was calculated as the difference between the stimulated rate and the previous rate, expressed as a percentage of the ADP stimulation measured in the absence of oleate or GDP. Since 45 μM BSA was present in the reaction medium and BSA binds oleate, the free oleate concentration in the reaction was calculated and plotted. In mitochondria lacking UCP (Figure 3-16a(i)), oleate had no effect on respiration from 0 to 6 μM oleate, above which oleate started to cause respiratory stimulation. The mitochondria were coupled up to 6 μM oleate (Figure 3-16a(ii)). This was evident from the respiratory stimulation caused by the first ADP addition which only started to drop below 80% of its original value above 6 μM oleate. GDP had no recoupling effect on the mitochondria since the respiratory stimulation after the second ADP addition (Figure 3-16a(iii)) was very similar to, and in fact less than, the stimulation after the first ADP addition.

In contrast, respiration of mitochondria containing UCP increased over the 0 to 6 μM oleate range (Figure 3-16b(i)). The respiratory stimulation appeared to plateau at 6 μM oleate, reaching 53% of the original ADP stimulation before increasing again. Above 6 μM oleate, oleate caused a further increase in respiration as observed for mitochondria lacking UCP. As oleate increased respiration, the subsequent ADP respiratory stimulation decreased (Figure 3-16b(ii)), which indicated that oleate was uncoupling the mitochondria. GDP had a recoupling effect on the mitochondria up to 7.6 μM oleate (Figure 3-16b(iii)) evident from the respiratory stimulation by the second ADP addition after GDP, which was greater than the stimulation by the first ADP addition prior to GDP. By 11 μM oleate addition, irreversible uncoupling of the mitochondria had occurred. From Figure 3-16b, at 11 μM oleate , the ADP stimulation before and after GDP addition were both low at 8.3 and 15.6 % of the original value respectively. The

Figure 3-16. Effects of Oleate and GDP on Yeast Mitochondrial Respiration Using Assay 1

The effects of oleate and GDP on yeast mitochondrial respiration were tested using Assay 1 outlined in the methods section **2.9.1 Respiration Assay** and in the legend to Figure 3-15. Mitochondria were isolated as outlined in the methods section **2.7.3 Mitochondrial Isolation From Yeast** in isolation buffer containing 0.6 M sucrose, 20 mM HEPES, pH 6.5, 0.1% BSA. Mitochondria lacking UCP (-UCP, (a)) were isolated from yeast transformants containing the UCP cDNA that were not induced with galactose. Mitochondria containing wild type UCP (b) were isolated from yeast transformants containing the UCP cDNA that were induced to express UCP by galactose addition. The respiratory stimulation after the addition of oleate ((i) oleate, -■-); the first ADP addition ((ii) ADP1, -o-); and the subsequent GDP and second ADP addition ((iii) ADP2, -★-) is expressed as a percentage of the ADP stimulation in the absence of oleate or GDP. ADP stimulation was measured as the difference between the respiratory rates (r) in the presence of ADP and succinate, [ADP_r-$succinate_r$]. The oleate stimulation was measured as the difference between the respiratory rates in the presence of oleate and succinate, [$oleate_r$-$succinate_r$]. The ADP1 stimulation was measured as the difference between the respiratory rates in the presence of ADP1 and oleate, [$ADP1_r$-$oleate_r$]. The ADP2 stimulation was measured as the difference between the respiratory rates in the presence of ADP2 and GDP, [$ADP2_r$-$succinate_r$]. The results are averaged from 3 independent mitochondrial preparations containing wild type UCP and 2 independent mitochondrial preparations lacking UCP ± SEM.

(a) −UCP

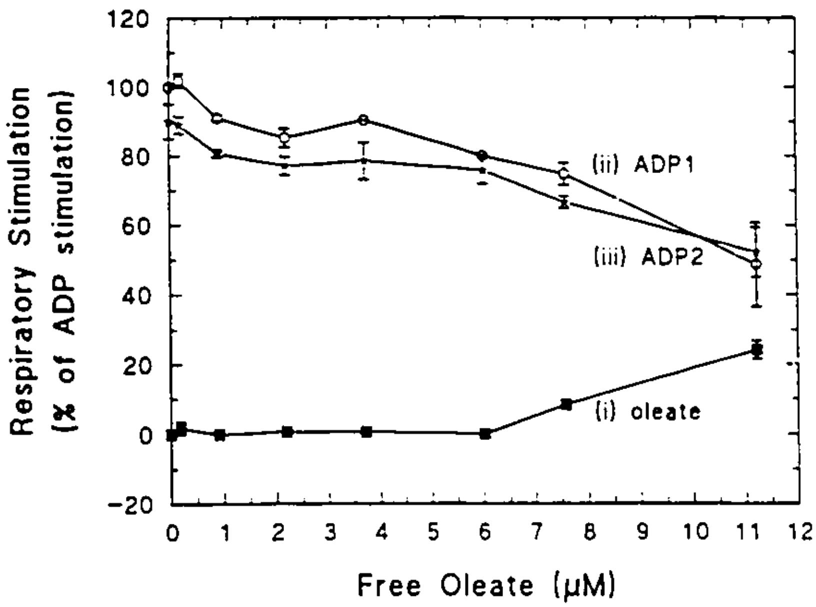

(b) wild type UCP

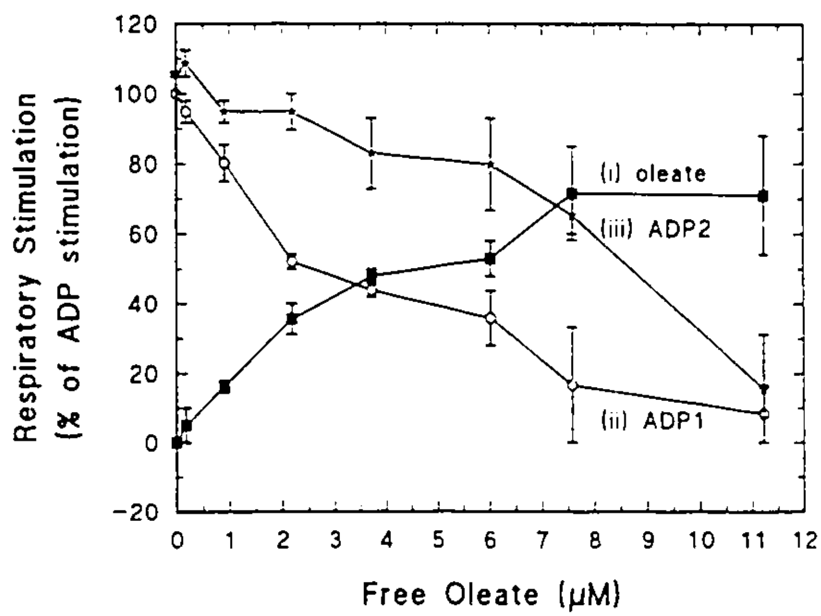

uncoupling and recoupling effects of oleate and GDP respectively are most clearly observed in this figure from 2 to 6 μM oleate. At 6 μM oleate, oleate addition caused a respiratory stimulation equal to 53% of the original ADP stimulation; the subsequent ADP stimulation dropped to 36% of its original value; the ADP stimulation after the subsequent GDP addition increased to 80% of its original value. GDP also had a recoupling effect in mitochondria containing UCP even when no oleate was added. This was evident from the second ADP stimulation (after GDP addition) at zero oleate addition which was greater than the first ADP stimulation, in contrast to mitochondria lacking UCP (Figure 3-16a).

From these experiments, it appears that there is a low basal level activity of UCP in isolated yeast mitochondria since GDP has a recoupling effect on yeast mitochondria containing UCP in the absence of oleate. No such effect was observed in yeast mitochondria lacking UCP. A low basal level activity of UCP in yeast mitochondria is also in agreement with the RCR values reported for mitochondria containing and lacking UCP. Yeast mitochondria containing UCP have a lower RCR (2.0) as compared to mitochondria lacking UCP (2.8), indicating that mitochondria containing UCP are more uncoupled.

Oleate was proven to be ineffective as an uncoupler of yeast mitochondria in the absence of UCP. However, since low concentrations of oleate uncoupled yeast mitochondria containing UCP and GDP reversed these effects; it is clear that oleate can activate UCP and GDP can inhibit UCP in yeast mitochondria. Oleate uncoupling appeared to saturate at about 6 μM oleate in mitochondria containing UCP. The concentration of oleate required for half maximal respiratory stimulation ($K_{0.5}$) was determined using Michaelis-Menten kinetics. The data for oleate respiratory stimulation was replotted for mitochondria containing and lacking UCP and is presented in Figure 3-17. The $K_{0.5}$ was calculated to be 3.0 ± 0.6 μM oleate. This value is higher than that found for palmitate in guinea pig brown adipose tissue mitochondra where the $K_{0.5}$ was 0.1 μM palmitate (Cunningham *et al.*, 1986). However, the concentration of laurate required for 50% maximal GDP-sensitive proton efflux for hamster brown adipose tissue UCP reconstituted into proteoliposomes was 16-33 μM laurate (Orosz, 1993).

The second assay used to assess the effects of oleate and GDP on yeast mitochondrial respiration was based on first inhibiting the ATP synthase in the mitochondria. Phosphorylation can be inhibited in mitochondria using oligomycin, a potent inhibitor of the ATP synthase, which in turn stops protons from re-entering the mitochondrial matrix through the ATP synthase. In the presence of oligomycin, any mitochondrial oxidation that occurs must be in response to protons re-entering the mitochondrial matrix by pathways other than through the ATP synthase. In the absence of ATP synthesis, mitochondrial respiration is mainly controlled by the proton leak across the mitochondrial inner membrane, but there is also significant control by the succinate utilization reactions (reactions that catalyze transport of succinate into the mitochondria and its oxidation by the electron transport chain) (Groen *et al.*, 1982; reviewed in Nicholls and Ferguson, 1992). To test the effects of oleate and GDP on yeast mitochondria using this assay, oligomycin was first added to respiring mitochondria. Oleate was then added to the mitochondria and its effect on the respiratory rate was recorded. GDP was subsequently added and its effect on the respiratory rate was recorded. A schematic of the assay is presented in Figure 3-18. In theory, activation of UCP by oleate would cause

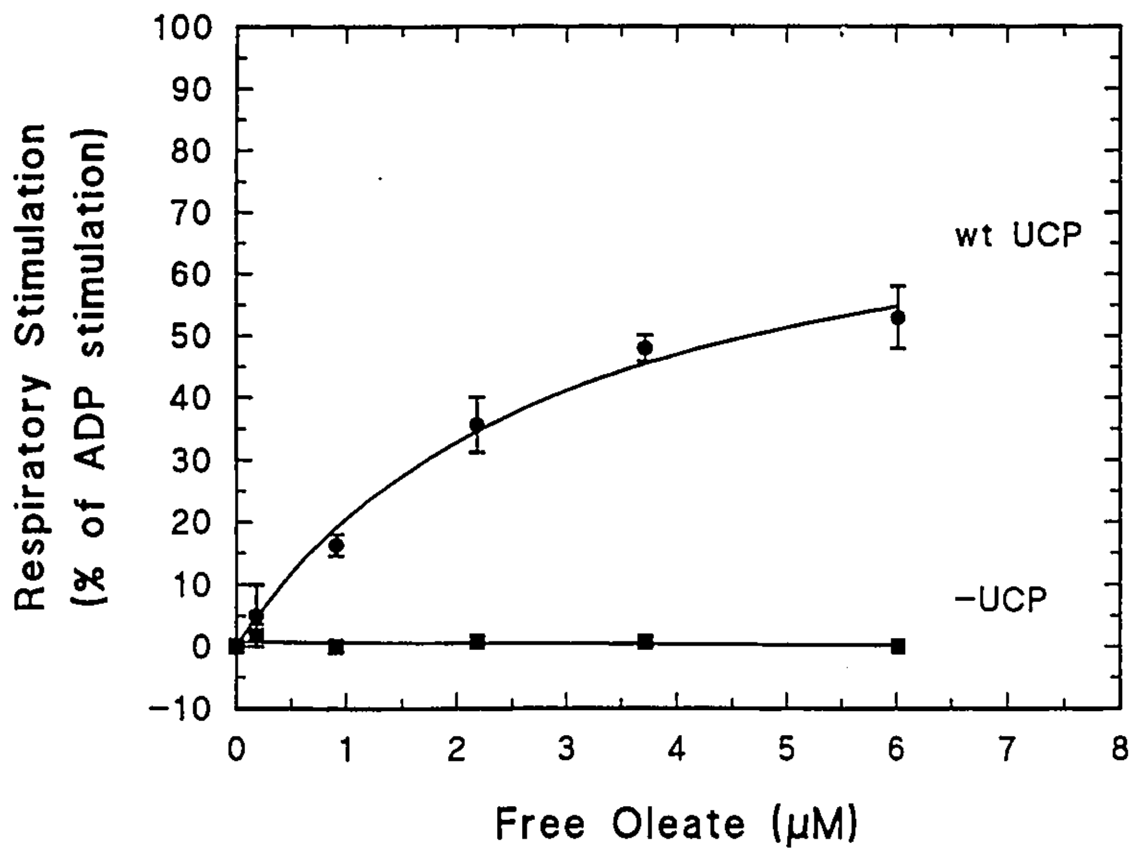

Figure 3-17. Yeast Mitochondrial Respiratory Stimulation After Oleate Addition

The data for the respiratory stimulation measured after oleate addition from Figure 3-16 a and b were replotted for mitochondria containing wild type UCP (wt UCP) and lacking UCP (-UCP). The concentration of oleate required for half maximal respiratory stimulation ($K_{0.5}$) of mitochondria containing UCP was calculated from a curve fit of the data to a one site binding model (Michaelis-Menten kinetics, $V_mS/(K_m+S)$). The $K_{0.5}$ was 3.0 ± 0.6 μM oleate.

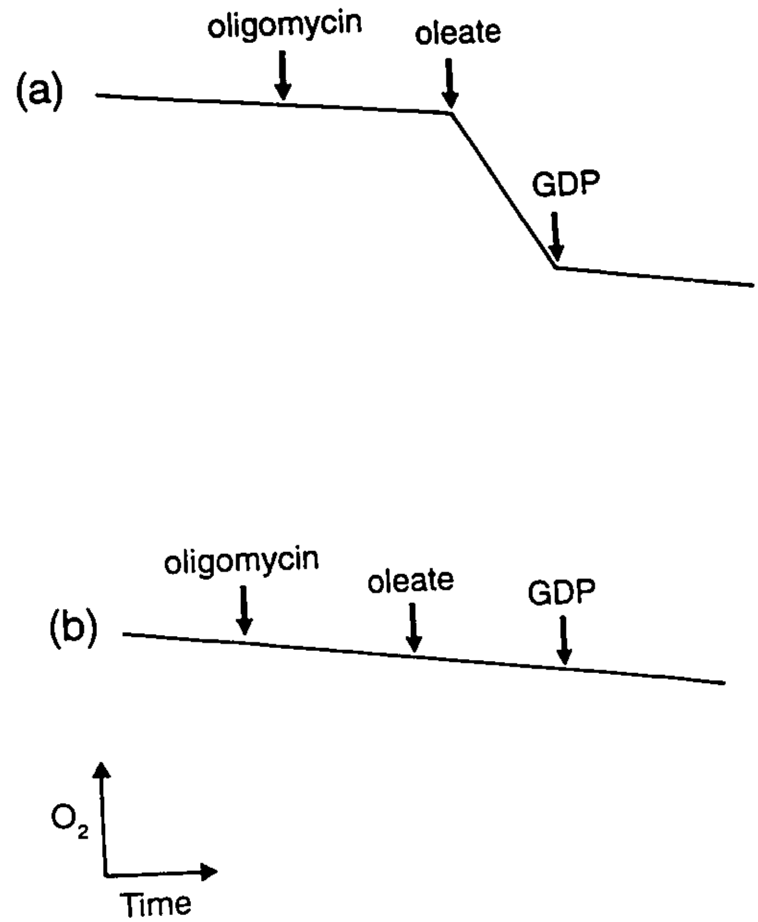

Figure 3-18. Schematic of Assay 2 Used to Test the Effects of Oleate and GDP on Yeast Mitochondrial Respiration

Yeast mitochondrial respiration was monitored using an oxygen electrode as outlined in the methods section **2.9.1 Respiration Assay**. Once the mitochondria established a steady state respiratory rate using succinate for substrate oxidation, oligomycin was added (66 µg/ml) to inhibit the ATP synthase. Oleate was then added (as mixtures of oleate/BSA solutions) and the resulting respiratory rate recorded. Subsequently, GDP (167 µm) was added and the resulting respiratory rate recorded. Oleate/BSA mixtures added to the reaction ranged from a molar ratio of 1:1 oleate:BSA to 7:1 oleate:BSA, where the BSA concentration was held constant at 5 mM. For control reactions without the addition of oleate, 5 mM BSA was added to the reaction. The concentration of free oleate in the reaction was determined as outlined in the methods section **2.9.1.1 Determination of Free Oleate Concentration in Oleate/BSA Solutions**. Plot (a) depicts the expected result if oleate caused uncoupling and GDP caused recoupling of the mitochondria. Plot (b) depicts the expected result if oleate and GDP had no effect on the mitochondria.

an increase in the mitochondrial respiratory rate (Figure 3-18a). Subsequent inhibition of UCP by GDP would decrease the respiratory rate, reversing the oleate effect (Figure 3-18a). If the oleate and GDP effects were specific to UCP, mitochondria lacking UCP would show no effects from oleate or GDP (Figure 3-18b).

The effect of oleate on yeast mitochondrial respiration was plotted as the respiratory stimulation versus free oleate concentration (Figure 3-19). The respiratory stimulation by oleate was calculated as the difference between the oleate stimulated respiratory rate and the rate in the absence of oleate, expressed as a percentage of the ADP stimulation in the absence of oligomycin and oleate. Since oleate was added as pre-equilibrated oleate/BSA mixtures, the free oleate concentration was calculated and plotted. Oleate did not cause any respiratory stimulation in mitochondria lacking UCP over the oleate concentration range tested (Figure 3-19) again indicating oleate is ineffective as an uncoupler in yeast mitochondria lacking UCP. However, oleate did cause a saturable respiratory stimulation in mitochondria containing UCP over the oleate concentration range tested (Figure 3-19). The oleate respiratory stimulation measured using the two different assays were very similar, evident by comparing Figures 3-17 and 3-19. The oleate concentration that caused 50% of the maximum oleate stimulation ($K_{0.5}$) using the second assay was 3.4 ± 0.5 μM oleate, which was within error of the $K_{0.5}$ calculated using the first assay, 3.0 ± 0.6 μM oleate.

The observed oleate stimulation in mitochondria containing UCP using the second assay was also reversible by GDP as shown in Figure 3-20. Here, the value of the oleate respiratory stimulation was calculated from the difference between the oleate stimulated rate and the subsequent GDP inhibited rate rather than from the difference between the

Figure 3-19. The Effect of Oleate on Yeast Mitochondrial Respiration Using Assay 2

The effect of oleate on yeast mitochondrial respiration was tested using the oligomycin Assay 2 outlined in the methods section **2.9.1 Respiration Assay** and in the legend to Figure 3-18. Yeast mitochondria were isolated from cells containing the UCP cDNA that were either induced with galactose to express wild type UCP (wt UCP) or were not induced with galactose and lack UCP (-UCP) as outlined in the methods section **2.7.3 Mitochondrial Isolation From Yeast**. Mitochondria were isolated in isolation buffer containing 0.6 M sucrose, 20 mM HEPES, pH 6.5, 0.1 % BSA. The respiratory stimulation after oleate addition is presented as a percentage of the respiratory stimulation measured for ADP in the absence of oleate and GDP: [oleate respiratory stimulation/ADP respiratory stimulation]×100. The reference reaction, to which the respiratory stimulation by ADP or oleate was compared to, included the addition of succinate, oligomycin, BSA and GDP to mitochondria as explained in the legend to Figure 3-18. All respiratory rates (r) were normalized to the succinate rate of that reaction. Respiratory stimulation for oleate was calculated as the difference between the oleate stimulated respiratory rate (recorded after the addition of oleate/BSA mixtures to a reaction) and the rate in the absence of oleate (recorded after the addition of BSA only in the reference reaction): $[(\text{oleate/BSA})_r/\text{succinate}_r]-[\text{BSA}_r/\text{succinate}_r]$. Respiratory stimulation for ADP was calculated as the difference between the ADP stimulated rate in the absence of oligomycin and oleate, and the rate in the presence of BSA only in the reference reaction: $[\text{ADP}_r/\text{succinate}_r]-[\text{BSA}_r/\text{succinate}_r]$. The plotted results were averaged from 3 independent mitochondrial preparations containing wild type UCP and 2 independent mitochondrial preparations lacking UCP ± SEM. The concentration of oleate required for 50% maximal stimulation ($K_{0.5}$), measured as described in the legend to Figure 3-17, was 3.4 ± 0.5 μM oleate.

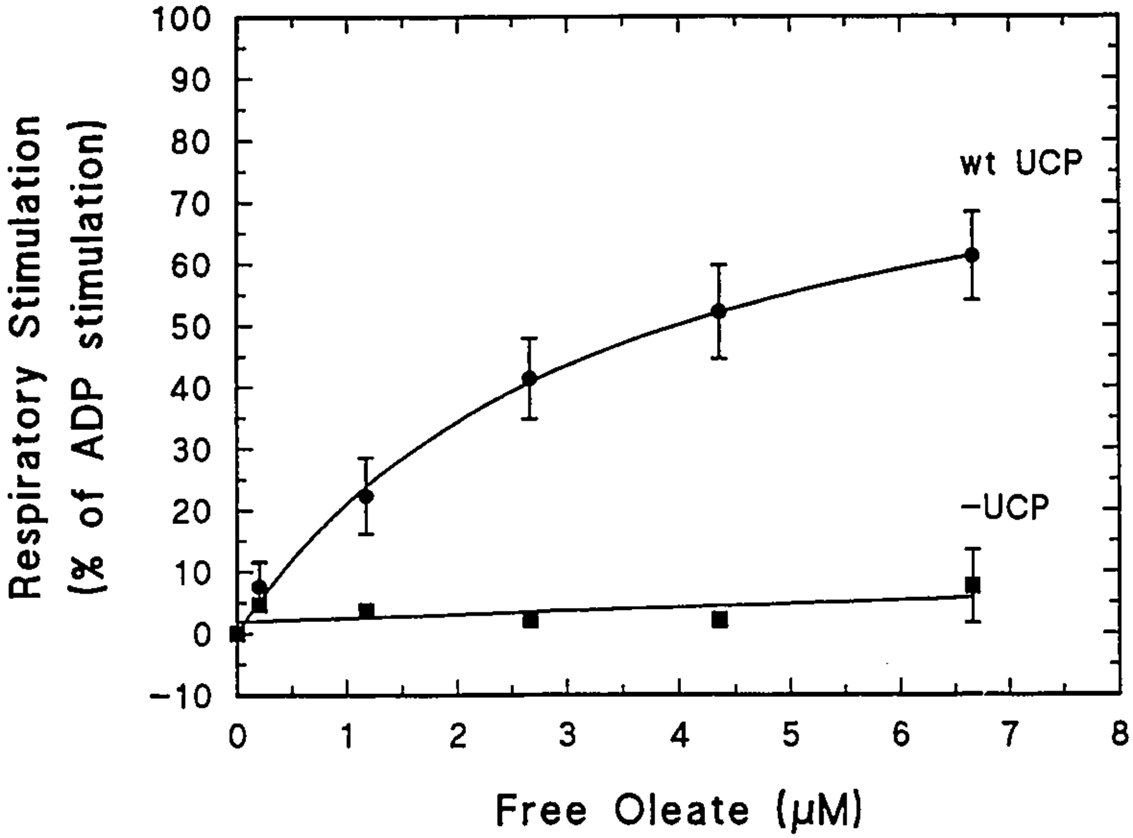
Respiratory Stimulation
(% of ADP stimulation)
Free Oleate (μM)
wt UCP
−UCP
100
90
80
70
60
50
40
30
20
10
0
−10
0
1
2
3
4
5
6
7
8

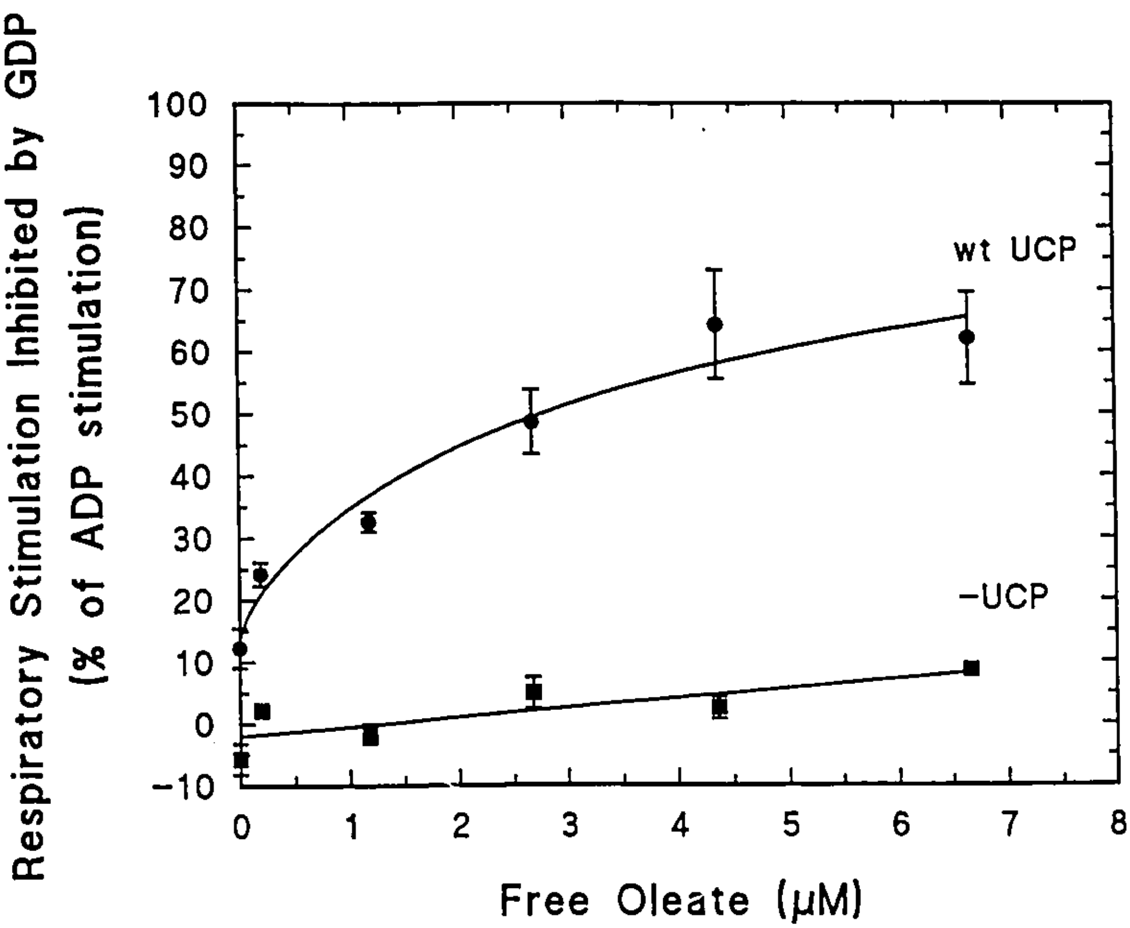

Figure 3-20. Oleate Respiratory Stimulation Relative to the GDP Inhibited Rate

Oleate respiratory stimulation from the experiment of Figure 3-19 was replotted such that the oleate stimulation was measured as the difference between the oleate stimulated rate and the GDP inhibited rate, rather than as the difference between the oleate stimulated rate and the BSA only rate (see schematic of assay 2 in Figure 3-18). All rates were normalized to the succinate respiratory rate. The respiratory stimulation was still expressed as a percentage of the ADP stimulation which was measured in the absence of oligomycin and oleate as outlined in the legend to Figure 3-19.

oleate stimulated rate and the rate in the absence of oleate. Clearly, GDP reversed the effects of oleate. In comparing Figure 3-19 and 3-20, GDP inhibited the respiratory rate of mitochondria containing UCP at zero oleate addition by 12.3%, but did not show this effect in mitochondira lacking UCP. The slight respiratory stimulation in mitochondria containing UCP in the absence of oleate that could be inhibited by GDP indicated a low basal level of UCP activity in yeast mitochondria. This low basal level of activity of UCP in isolated yeast mitochondria was also supported from the results of the first assay where GDP addition recoupled yeast mitochondria in the absence of oleate and from the lower RCR determined for mitochondria containing UCP in comparison to mitochondria lacking UCP.

In order to determine the GDP concentration required to decrease oleate-activated respiration by 50% (K_i), the decrease in the oleate-activated respiratory rate was titrated using a range of GDP concentrations. The respiratory rate was stimulated using a 4:1 oleate/BSA molar ratio which is equal to 4.4 µM free oleate. The effect of GDP on the oleate-stimulated respiratory rate was plotted as the respiratory inhibition versus GDP concentration (Figure 3-21). The respiratory inhibition was calculated as the difference between the oleate-stimulated and GDP-inhibited respiratory rates. The inhibition was expressed as a percent decrease of the oleate stimulation. The oleate stimulation was calculated from the difference between the oleate stimulated rate and the rate in the absence of oleate. The inhibition constant was calculated as the concentration of GDP that caused 50% of the maximum inhibition using Michaelis-Menten kinetics. The K_i was determined to be 26 ± 1 µM GDP. Nicholls (1974a) reported the concentration of GDP required for 50% inhibition of mitochondrial proton conductance for isolated brown

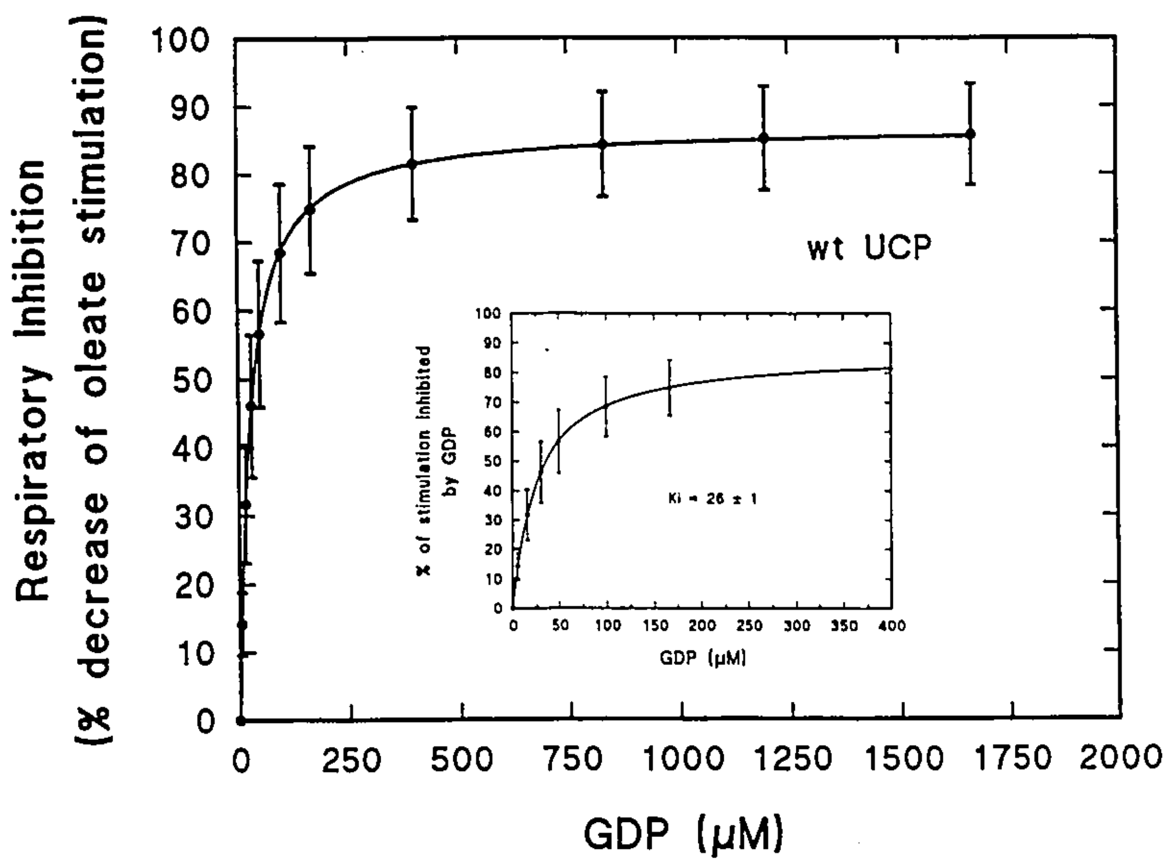

Figure 3-21. Inhibition of Oleate Stimulation by GDP

The effect of GDP on the oleate-stimulated respiratory rate for the mitochondrial preparations tested in Figure 3-19 was measured for a range of GDP concentrations. The respiratory rate (r) was stimulated using a solution of oleate/BSA containing a molar ratio of 4:1 oleate:BSA, which is equivalent to 4.4 μM free oleate. The effect of GDP on the oleate-stimulated respiratory rate was plotted as the respiratory inhibition versus GDP concentration. The inset shows an expanded scale for GDP concentrations ranging from 0-400 μM. The respiratory inhibition was calculated as the difference between the oleate-stimulated and GDP-inhibited respiratory rates with all rates normalized to the succinate respiratory rate: $[(\text{oleate/BSA})_r/\text{succinate}_r]-[\text{GDP}_r/\text{succinate}_r]$. The inhibition was expressed as a percent decrease of the oleate stimulation: [(respiratory inhibition/respiratory stimulation)×100]. The oleate stimulation was calculated from the difference between the oleate stimulated rate and the rate in the absence of oleate as outlined in the legend to Figure 3-19. The results are averaged from 3 independent mitochondrial preparations containing wild type UCP and 2 independent mitochondrial preparations lacking UCP ± SEM. The concentration of GDP required to decrease oleate-activated respiration by 50% (Ki), calculated from Michaelis-Menten kinetics ($V_mS/(K_m+S)$), was 26 ± 1 μM GDP.

adipose tissue mitochondria in the presence of albumin was 10 μM GDP at pH 7.1 which agrees with the K_i determined for GDP inhibition of oleate-activated respiration in yeast mitochondria containing UCP. GDP inhibition of laurate-activated proton efflux for reconstituted hamster brown adipose tissue UCP had a K_i of 16 μM GDP (Jezek *et al.*, 1994,). GDP inhibition of laurate-activated proton efflux for reconstituted yeast expressed rat UCP had a K_i of 8-10 μM GDP (Murdza-Inglis *et al.*, 1994). Therefore, GDP inhibition of UCP in yeast mitochondria agrees well with GDP inhibition of UCP determined in brown adipose tissue mitochondria and in proteoliposomes.

In contrast to the GDP-sensitive, fatty acid-activation of respiration found in yeast mitochondria containing UCP or for reconstituted UCP in proteoliposomes, exogenous fatty acid activation of respiration in brown adipose tissue mitochondria is not overcome by GDP (Rial *et al.*, 1983). Fatty acids can override the nucleotide induced respiratory control in brown adipose tissue mitochondria. However, GDP can inhibit fatty acid-induced proton permeability in non-respiring brown adipose tissue mitochondria (Rial *et al.*, 1983) and endogenous proton conductance in respiring brown adipose tissue mitochondria (Nicholls, 1974a).

The discrepancy in the effect of fatty acid and GDP in respiring and non-respiring brown adipose tissue mitochondria is thought to reside in the magnitude of the membrane potential under respiring and non-respiring conditions and the type of proton conductance observed for the inner membrane at each potential (Rial *et al.*, 1983). Mitochondrial proton conductance is the measure of proton current (derived from the respiratory rate) per mV of membrane potential. In all mitochondria, the inner membrane is not completely impermeable to protons in the absence of ATP synthesis. Therefore, respiration continues to pump protons back out of the matrix at a rate that balances proton re-entry thus maintaining the membrane potential. For mitochondria respiring at rates below their maximum rate, the magnitude of the membrane potential increases as substrate supply increases. Because the proton leak across the inner membrane also increases as the membrane potential increases, the steady-state respiratory rate, which is required to maintain the potential, also increases. Under these circumstances, the proton conductance across the inner membrane is constant, following an ohmic relationship where proton current increases in proportion to membrane potential (reviewed in Nicholls and Ferguson, 1992). However, a point is reached where the membrane potential plateaus but the respiratory rate continues to increase with substrate supply. At this high membrane potential termed the breakpoint, the proton conductance shifts to a non-ohmic relationship, where proton current increases without an increase in membrane potential (Nicholls and Ferguson, 1992). Nicholls and Ferguson (1992) state that non-ohmic conductance occurs possibly to limit the magnitude of the potential across the membrane. Respiration increases during non-ohmic conductance without an increase in membrane potential either because the inner membrane becomes increasingly leaky to protons at high membrane potentials or because the respiratory chain "slips" at high membrane potentials, pumping out less protons than it normally does (Nicholls and Ferguson, 1992). A maximum respiratory rate is reached during non-ohmic conductance in the presence of excess substrate, which is limited by the substrate utilization reactions (Nicholls and Ferguson, 1992).

GDP has the effect of converting a very high ohmic conductance in brown adipose tissue mitochondria to a very low ohmic conductance which is only 4% of the conductance level in the absence of GDP, until the breakpoint potential is reached (Nicholls, 1977). Above the breakpoint potential (approximately 180 mV), GDP can not inhibit the non-ohmic proton conductance, where respiration increases without increasing membrane potential (Nicholls, 1977). In brown adipose tissue mitochondria, in the presence of excess GDP, fatty acids have the overall effect of lowering the breakpoint potential (Rial *et al.*, 1983). In addition, in the presence of GDP, fatty acids only increase the respiratory rate of brown adipose tissue mitochondria that have membrane potentials above the breakpoint potential prior to fatty acid addition (Rial *et al.*, 1983).

In summary, fatty acid addition in the presence of GDP to brown adipose tissue mitochondria with membrane potentials above the breakpoint has the effect of lowering the membrane potential and increasing the respiratory rate. However, fatty acid addition in the presence of GDP to brown adipose tissue mitochondria with membrane potentials below the breakpoint has no effect on the respiratory rate (Rial *et al.*, 1983). Therefore, in non-respiring mitochondria, where the membrane potential is well below the breakpoint, GDP can inhibit the fatty acid-activated proton permeability (Rial *et al.*, 1983). Analagous to non-respiring brown adipose tissue mitochondria, it is possible that respiring yeast mitochondria maintain a membrane potential below the breakpoint potential necessary for fatty acid stimulation of respiration uncontrolled by GDP. The ability of GDP to inhibit fatty acid-activated respiration in yeast mitochondria containing UCP was also observed by other groups (Arechaga *et al.*,1993; Bouillaud *et al.*, 1994). GDP was also able to inhibit fatty-acid induced proton flux in proteoliposomes reconstituted with UCP (Murdza-Inglis *et al.*, 1994; Jezek *et al.*, 1994, Winkler and Klingenberg, 1994).

3.3.3 Comparison of UCP Functions in Yeast Mitochondria

3.3.3.1 Comparison of Yeast Mitochondrial Isolation Conditions and Assay Conditions Required to Analyze UCP Activity

Respiration studies (results sections **3.3.2.3 Respiratory Control of Yeast Mitochondria, 3.3.2.4 Oleate stimulation and GDP inhibition of Yeast Mitochondrial Respiration**) indicated that UCP in yeast mitochondria had a low basal level of activity when mitochondria were isolated in buffer containing 0.6 M sucrose, 20 mM HEPES, pH 6.5, 0.1% BSA and tested in respiration buffer (0.65 M sorbitol, 0.36 mM EDTA, 10 mM KCl, 10 mM KH_2PO_4, 10 mM Tris-HCl, pH 6.5, 0.05% BSA). Under these conditions, oleate activated UCP, causing uncoupling of mitochondria. In comparison, yeast mitochondria were more uncoupled when they were isolated in 0.6 M mannitol, 20 mM HEPES, pH 7.4, 0.1% BSA.

In comparing the conditions tested to measure GDP binding to UCP in yeast mitochondria (results section **3.3.1.2 GDP Binding to Yeast Mitochondria: Optimization of Binding Conditions**), the lowest level of binding to yeast mitochondria was observed using mitochondria isolated in the buffer that was required to prepare coupled yeast mitochondria (0.6 M sucrose, 20 mM HEPES, pH 6.5, 0.1 % BSA; 0.09 mol GDP/mol UCP_m) and the highest level of binding was observed using mitochondria isolated in the buffer in which the mitochondria were more uncoupled (0.6 M mannitol, 20 mM HEPES, pH 7.4, 0.1% BSA; 0.21 mol GDP/mol UCP_m).

It has been established that purine nucleotide binding to UCP is pH dependent, with the tightest binding observed at pH 5.5 - 6.5, and with the affinity decreasing above pH 6.8 (Nicholls, 1976; Klingenberg, 1988). It is possible to infer from the above experimental observations that there is less endogenous purine nucleotide bound to UCP in yeast mitochondria when the mitochondria are isolated in buffer at pH 7.4, resulting in two observed effects: (a) the UCP has a higher basal activity level resulting in a lower RCR and (b) there are more available purine nucleotide binding sites, leading to a higher level of bound [^{3}H]GDP per UCP. In contrast, it appears that there is more endogenous purine nucleotide bound to UCP in yeast mitochondria when the mitochondria are isolated in sucrose isolation buffer at pH 6.5, resulting in two observed effects: (a) the UCP has a relatively lower basal activity level resulting in a higher RCR and (b) there are fewer purine nucleotide binding sites available leading to a lower level of bound [^{3}H]GDP. Experiments monitoring tryptic digest of UCP in yeast mitochondria support this theory. It is known that nucleotide binding to UCP protects UCP from tryptic cleavage, presumably due to a conformational change in UCP induced by binding purine nucleotide (Eckerskorn and Klingenberg, 1987). Trypsin digested UCP in yeast mitochondria more efficiently when the mitochondria were isolated in 0.6 M mannitol, 20 mM HEPES, pH 7.4, 0.1% BSA where presumably there is less endogenous purine nucleotide bound to UCP. Trypsin had little effect on UCP in yeast mitochondria that were isolated in 0.6 M sucrose, 20 mM HEPES, pH 6.5, 0.1% BSA, where presumably higher levels of endogenous purine nucleotides are bound to UCP (data not shown).

3.3.3.2 Comparison of K_d for GDP binding to UCP and K_i for GDP Inhibition of Fatty Acid-Activated Respiration

The K_i for GDP inhibition of fatty acid-activated respiration in yeast mitochondria was 26 ± 1 μM GDP but the K_d for GDP binding to yeast mitochondria containing UCP was 0.8 ± 0.1 μM GDP. The binding and respiration assays were both measured in the same respiration reaction medium at pH 6.5, although the K_d for binding was measured in the absence of oleate, to mitochondria that were isolated under conditions where there was most likely less endogenously bound GDP. Rial *et al.* (1983) showed that fatty acids could modulate the affinity of UCP for purine nucleotides in brown adipose tissue mitochondria. Although palmitate had little effect on the K_d for GDP binding to hamster brown adipose tissue mitochondria, the K_d for ATP increased from 10 to 30 μM in the presence of palmitate (Rial *et al.*, 1983). In contrast to this study, binding studies using purified reconstituted UCP showed no competition between inhibitory nucleotides and fatty acids (Winkler and Klingenberg, 1994). The level of GDP bound to yeast mitochondria at 10 and 25 μM GDP was not altered by the presence of 4.4 μM oleate (a level sufficient to cause activation of uncoupling). Although the K_d was not determined in the presence of oleate, it appears unlikely that oleate affected the GDP binding affinity to UCP.

If the GDP binding site on UCP is a regulatory site where binding of GDP causes inhibition of transport, then it is expected that the K_d for GDP binding would equal the K_i for GDP inhibition of transport. The reason for the discrepancy between the K_d and the K_i is not known, but has been observed by others as discussed below. Nicholls (1974a) reported that the K_i for GDP inhibition of the endogenous mitochondrial proton conductance in isolated brown adipose tissue mitochondria in the presence of albumin was 10 μM GDP whereas the dissociation constant of GDP binding to brown adipose tissue mitochondria in the presence of albumin was 1.1 μM GDP (Rial *et al.*, 1983). Kopecky *et al.* (1987) found a non-linear relationship between occupancy of the nucleotide binding site and the inhibitory effect on proton permeation in brown adipose tissue mitochondria where up to 50% occupancy of the binding site had no inhibitory effect on proton permeation, with full inhibition observed by 100% saturation of binding sites. They state that these results strongly suggest that there is not a simple direct link between binding of purine nucleotides to UCP and inhibition of transport. Eckerskorn and Klingenberg (1987) suggested that protection of UCP from tryptic cleavage by purine nucleotides was due to an induced conformational change in UCP that resulted from binding the nucleotide, and that protection was not just from the binding of nucleotide itself. Their suggestion was based on the fact that an ATP derivative, which bound UCP but did not inhibit proton transport, also did not protect UCP from tryptic cleavage, presumably because the analogue could not induce the conformational change in UCP required for inhibition of both proton transport and tryptic digest. However, Klingenberg (1994) has found that fatty acid-activated proton flux catalyzed by UCP reconstituted into proteoliposomes was inhibited by GDP in proportion to the occupancy of the GDP binding site on UCP, with the K_i for GDP inhibition appearing to equal the K_d for GDP binding, although the K_i was not calculated.

Discrepancies between the dissocation constant for GDP binding and the inhibition constant for GDP inhibition of anion transport also have been observed in brown adipose tissue mitochondria. In a recent study by Nedergaard and Cannon (1994), discrepancies were reported between the dissociation constant for GDP binding to hamster brown adipose tissue mitochondria, K_d = 1.3 μM, and the concentration of GDP required for 50% inhibition of anion transport (EC_{50}) in the mitochondria, 32 μM GDP for Cl^- transport, 324 μM GDP for benzenesulfonate transport and 4074 μM GDP for hexanesulfonate transport. Although the apparent affinity of GDP for its binding site was lowered by the anions in the transport medium (apparent K_ds were 3 μM GDP in KCl medium, 12 μM GDP in benzenesulfonate medium and 20 μM GDP in hexanesulfonate medium), the lowered affinity for GDP binding was still always higher than its potency as an inhibitor of transport (Nedergaard and Cannon, 1994). Their observation that better transported species showed larger discrepancies between affinity and potency of GDP lended support to Rial and Nicholls idea that there is a competition between the anion transporting and GDP binding forms of UCP (Rial and Nicholls, 1989, Nedergaard and Cannon, 1994). If fatty acid anion is being transported by UCP (Skulachev, 1991; Jezek *et al.*, 1994) in yeast mitochondria, the discrepancy between the affinity of GDP binding to UCP and the potency of GDP as an inhibitor of fatty acid-activation of UCP in yeast mitochondria is analogous to the discrepancies observed between the K_d for GDP binding to brown adipose tissue mitochondria and the K_i for GDP inhibition of anion transport observed by Nedergaard and Cannon (1994).

3.4 ANALYSIS OF SITE-DIRECTED MUTANTS OF UCP

3.4.1 Cysteine Residues

The seven cysteines in UCP are conserved in UCP of all known species (Figure 3-22). Past chemical studies using sulfhydryl reagents implied that cysteines were involved in ion transport, GDP binding and GDP inhibition of ion transport, although specific residues and their roles could not be identified (Rial and Nicholls, 1986; Jezek, 1987; Kopecky *et al.*, 1987; Jezek and Drahota, 1989). Steric hindrence of function due to the introduction of chemical groups by the sulfhydryl reagents could not be ruled out to account for the observed effects.

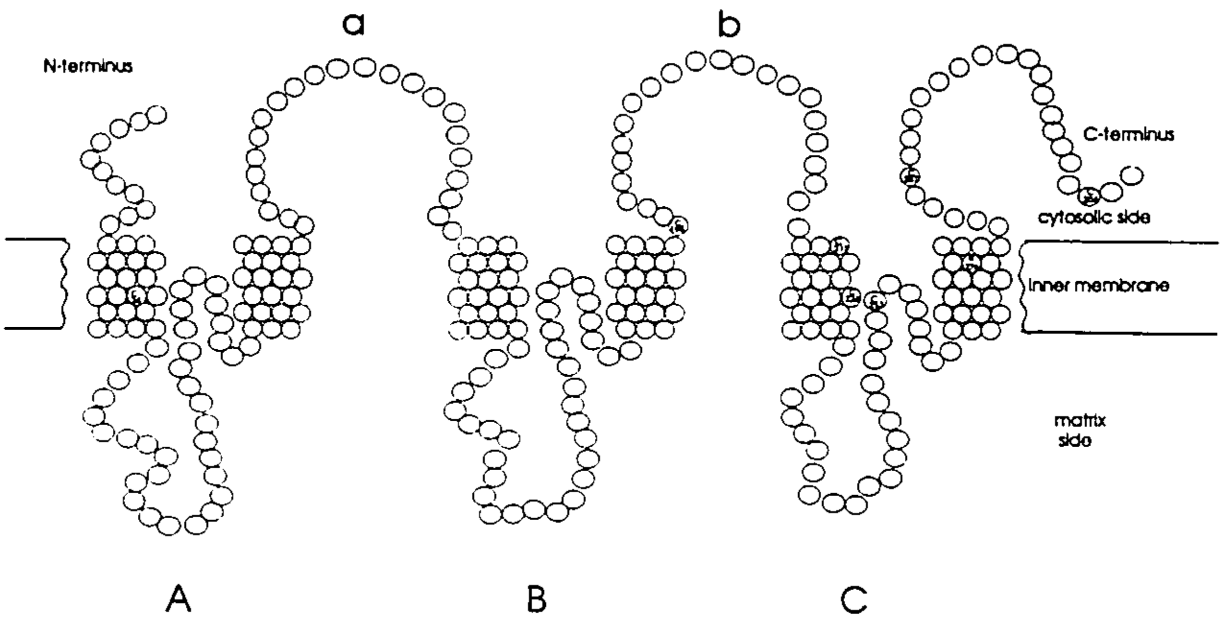

Figure 3-22. Location of the Seven Cysteines and Arginine276 in UCP

The membrane disposition model of UCP from Figure 1-2 is presented with the seven cysteines (cys24, cys188, cys213, cys224, cys253, cys287, cys304) and arginine276 highlighted.

3.4.1.1 Cysteine to Serine Changes in UCP

The cysteine side chain contains a thiol group which can have many different functions in proteins. Disulfide bonds, formed from the oxidation of two thiol groups, can provide a protein with structural stability. Alternatively, dithiol-disulfide interchange has been shown to be involved in solute transport systems (Robillard and Konings, 1982). Cysteines are also part of catalytic active sites such as in thiol proteases (Rawlings and Barrett, 1994) and in transglutaminases (Yee *et al.*, 1994) where catalysis proceeds through a thioester intermediate. In some metalloproteinases, a cysteine thiol present in the active site regulates enzyme activity by binding to the active-site zinc in the inactive zymogen, thereby blocking the active site (Springman *et al.*, 1990). Fatty acylation through a thioester linkage to an active site cysteine residue may also be used to regulate enzyme activity (Berthiaume *et al.*, 1993). Cysteines can be involved in hydrogen bonding, such as in stabilizing transition state complexes or for protein structure (Gregoret *et al.*, 1991) although this role is not very common and usually requires a negative charge on the sulfur atom (Gregoret *et al.*, 1991, Mangani and Hakansson, 1992). Further, the cysteine side chain is relatively hydrophobic in comparison to other amino acid side chains (Engelman *et al.*, 1986). Therefore, its hydrophobic character may be important for protein structure.

To determine which, if any, thiol groups in UCP are necessary for the protein's functions, each cysteine was changed independently to serine by site-directed mutagenesis of the rat UCP cDNA and mitochondria containing the mutant proteins were tested for oleate-activated, GDP-sensitive uncoupling. Serine substitution removed the cysteine thiol group and replaced it with a hydroxyl group. In comparing the polarity of serine and cysteine based on the free energy required for the transfer of the amino acids from a hydrophobic environment (an α-helix in a membrane interior) into water, the transfer free energy for cysteine is 2.0 kcal/mol and for serine, 0.6 kcal/mol (Stryer, 1995; Engelman *et al.*, 1986), which indicates that both residues are hydrophobic. Also, this isosteric substitution minimizes steric changes at each substitution. Therefore, both polarity and steric changes were minimized at each cysteine position while the functional importance of the thiols were assessed by the cys to ser substitutions. Due to the variability of the response to oleate and GDP of independent yeast mitochondria preparations containing wild type UCP, subtle differences in mitochondrial response to oleate and GDP would not be considered significant. Only dramatic differences in response of multiple mitochondria preparations containing mutant UCP would be considered significant changes in UCP activity.

Immunoblot analysis of yeast mitochondrial fractions showed that all the cys to ser mutant proteins were expressed and localized to yeast mitochondria at levels similar to that found for the wild type protein (Figure 3-23). Expression of these mutant proteins did not effect yeast cell growth (Figure 3-24). The respiratory control ratios (RCR) for yeast mitochondria containing the cys to ser mutant UCPs were similar to the RCR measured for yeast mitochondria containing wild type UCP (Table 3-5), but all RCRs including that measured for mitochondria containing wild type UCP were lower than that found for mitochondria lacking UCP (Table 3-5).

Yeast mitochondria containing each cys to ser mutant UCP all showed oleate-activated, GDP sensitive uncoupling (Figure 3-25). None of the mitochondria containing the cys to ser mutant UCPs showed any dramatic differences in response to oleate and

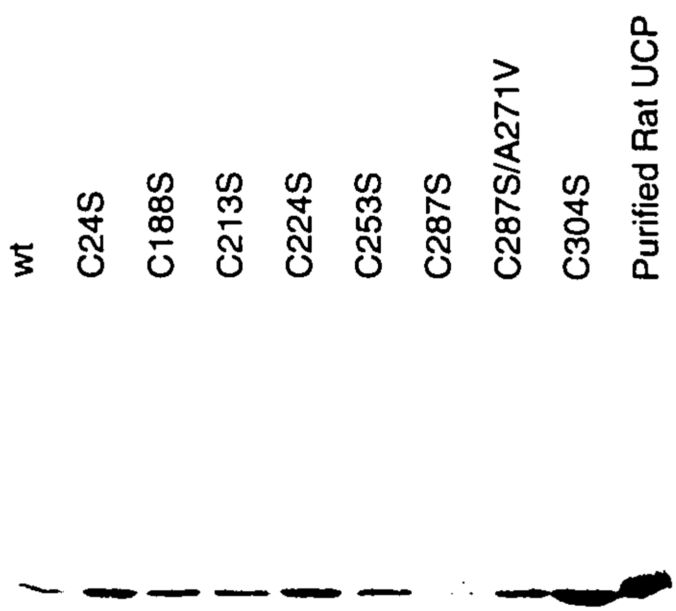

Figure 3-23. Immunoblot Analysis of Mitochondrial Fractions Isolated From Yeast Transformants Containing UCP cDNA Encoding Either Wild Type UCP or Cysteine to Serine Mutated UCP

Yeast transformants containing the shuttle vector pCGS110 with the cDNA coding for wild type rat UCP or UCP mutated at one of seven cysteines were induced to express UCP by the addition of galactose to 0.2% for 11 h. Ten μg of mitochondrial protein isolated from each of the transformants were separated by SDS-12.5% PAGE and analyzed by an immunoblot using monospecific antibody against rat UCP and [^{125}I]-labelled protein A. The type of UCP expressed is indicated above each lane: wild type, wt; cys24ser, C24S; cys188ser, C188S; cys213ser, C213S; cys224ser, C224S; cys253ser, C253S; cys287ser, C287S; double mutant cys287ser/ala271val, C287S/A271V; cys304ser, C304S. Purified rat UCP (1 μg) from brown adipose tissue mitochondria was run as a standard.

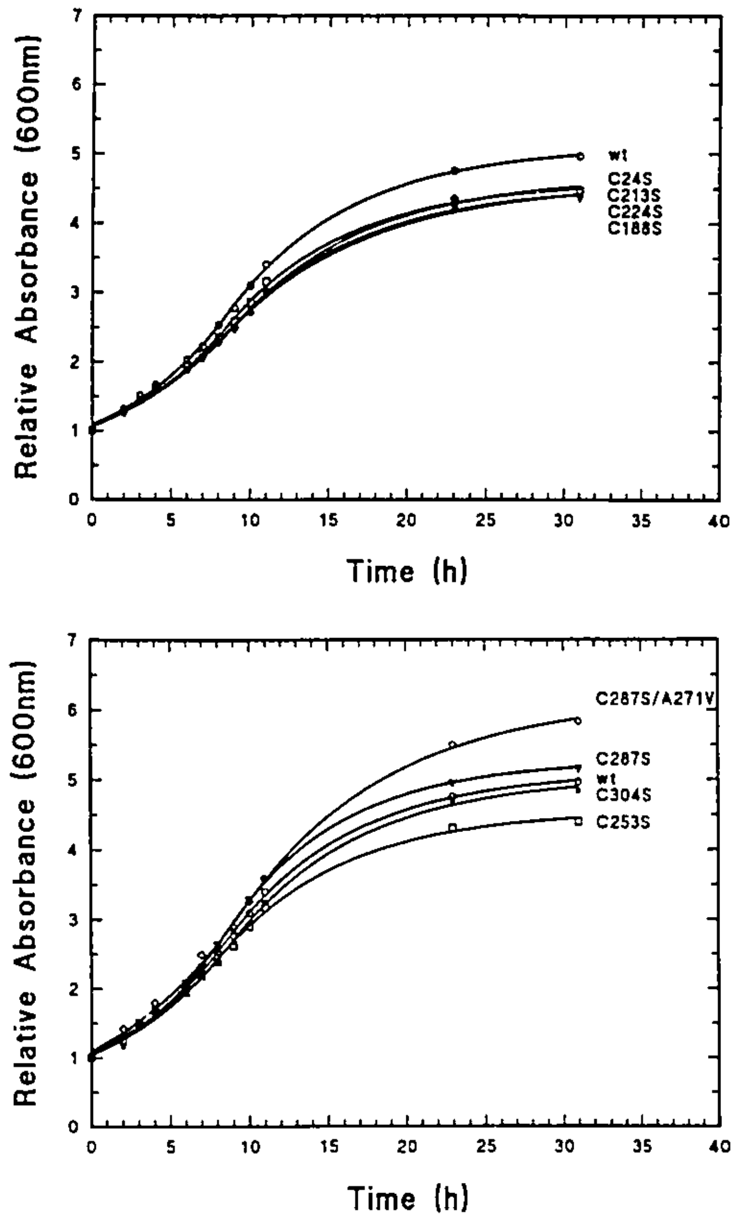

Figure 3-24. Growth Curves of Yeast Transformants Expressing Wild Type and Mutant UCP

The growth of yeast transformants expressing wild type or cys to ser mutant UCP was monitored as explained in the legend of Figure 3-5. Galactose was added to yeast cultures at time 0 to induce expression of UCP and growth was monitored for 32 h. The type of UCP expressed is indicated beside each growth curve. In graph (a): wild type, wt -o-; cys24ser, C24S -□-; cys188ser, C188S -▽-; cys213ser, C213S -◊-; cys224ser, -★-. In graph (b): wild type, wt -o-; cys253ser, C253S -□-; cys287ser, C287S -▽-; cys287ser/ala271val, C287S/A271V -◊-; cys304ser, C304S -★-.

Table 3-5. Respiratory Control Ratios (RCR) for Yeast Mitochondria Preparations Containing cys to ser Mutant UCP

Mitochondria were isolated from yeast transformants expressing either wild type or mutant UCP or lacking UCP as outlined in the methods section **2.7.3 Mitochondrial Isolation From Yeast** using mitochondrial isolation buffer containing 0.6 M sucrose, 20 mM HEPES, pH 6.5, 0.1% BSA. Respiratory control ratios (RCR) were determined using an oxygen electrode as outlined in the methods section **2.9.1 Respiration Assay** using respiration buffer containing 0.65 M sorbitol, 0.36 mM EDTA, 10 mM KCl, 10 mM KH_2PO_4, 10 mM Tris-HCl, pH 6.5, 0.3% BSA. Data are presented as the mean ± SEM. The calculated RCRs are for: 5 mitochondrial preparations lacking UCP (-UCP); 11 mitochondrial preparations containing wild type UCP; and single mitochondrial preparations containing cys to ser mutant UCP (C24S, C188C, C213S, C224S, C253S, C287S, C287S/A271V, C304S).

UCP	RCR
-UCP	2.8 ± 0.2
wild type	2.0 ± 0.1
C24S	1.7 ± 0.1
C188S	1.7 ± 0.1
C213S	1.9 ± 0.2
C224S	1.8 ± 0.1
C253S	2.1 ± 0.1
C287S	2.4 ± 0.2
C287S/A271V	1.6 ± 0.1
C304S	2.0 ± 0.1

Figure 3-25 Effects of Oleate and GDP on Yeast Mitochondrial Respiration Using Assay 1: Results For Mitochondria Containing Cys to Ser Mutant UCP

The effects of oleate and GDP on yeast mitochondrial respiration were tested using Assay 1 as outlined in the legend to Figure 3-16. Mitochondria containing cys to ser or cys253 to ala mutant UCP were isolated from yeast transformants 10 h after the addition of galactose. The respiratory stimulation was measured after the addition of oleate ((i) oleate, -■-), the first ADP addition ((ii) ADP1, -o-), and the subsequent GDP and second ADP addition ((iii) ADP2, -★-). The respiratory stimulation is expressed as a percentage of the ADP stimulation measured in the absence of oleate and GDP as explained in the legend to Figure 3-16. The results are from single mitochondrial preparations containing cys24ser, cys188ser, cys213ser, cys224ser, cys253ser, cys287ser, cys287ser/ala271val, cys304ser and cys253ala UCP. The type of UCP in each mitochondrial preparation is indicated above each graph.

C24S UCP

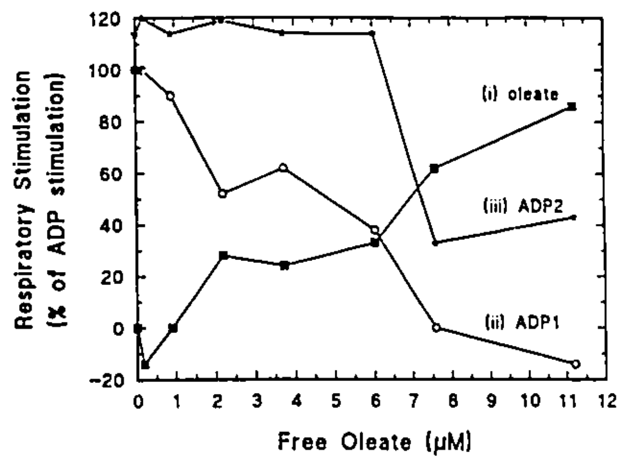

C188S UCP

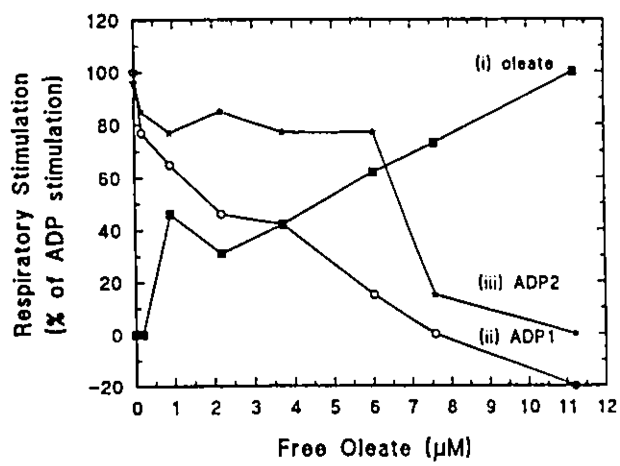

C213S UCP

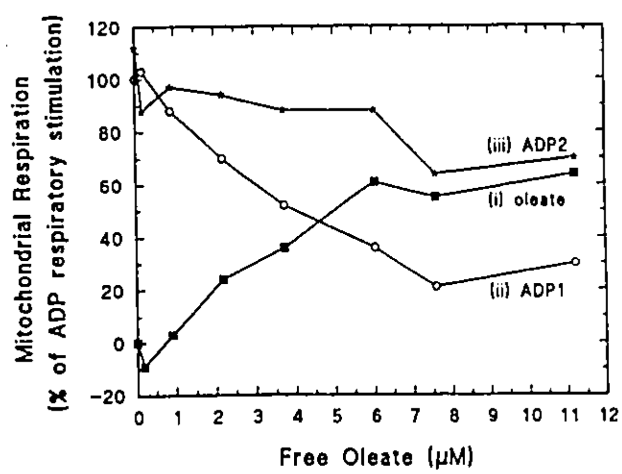

C224S UCP

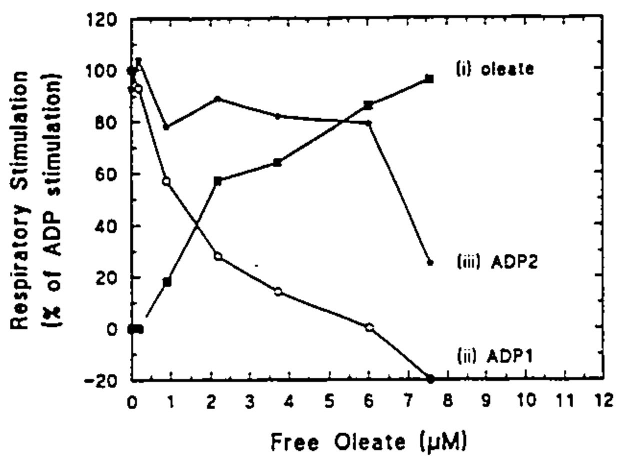

C253S UCP

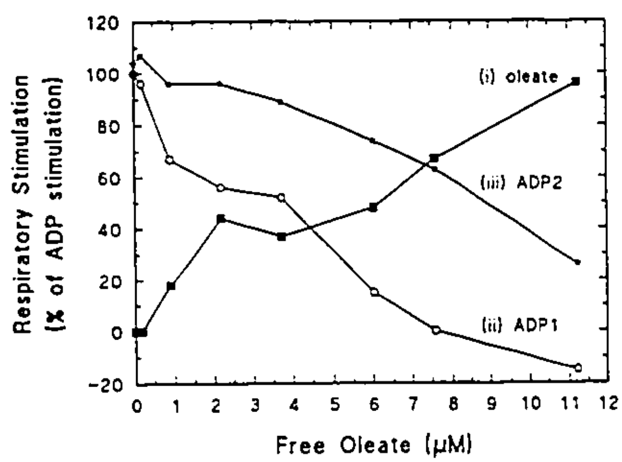

C287S UCP

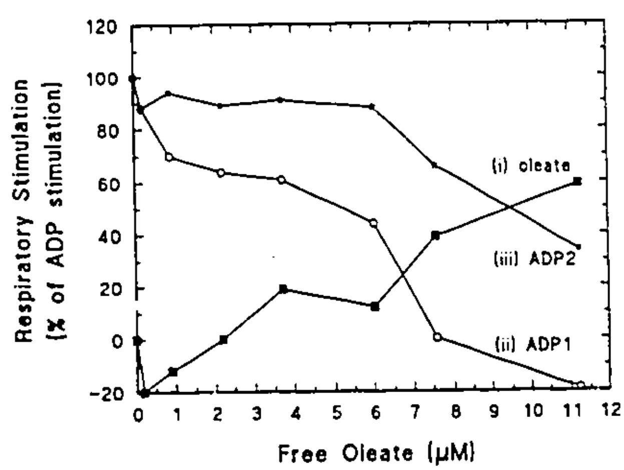

C287S / A271V UCP

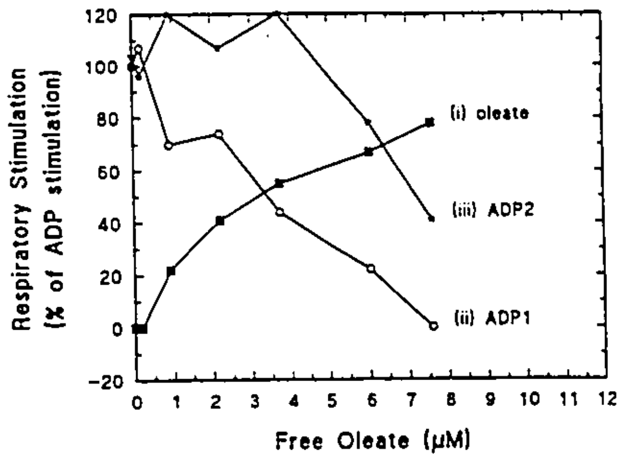

C304S UCP

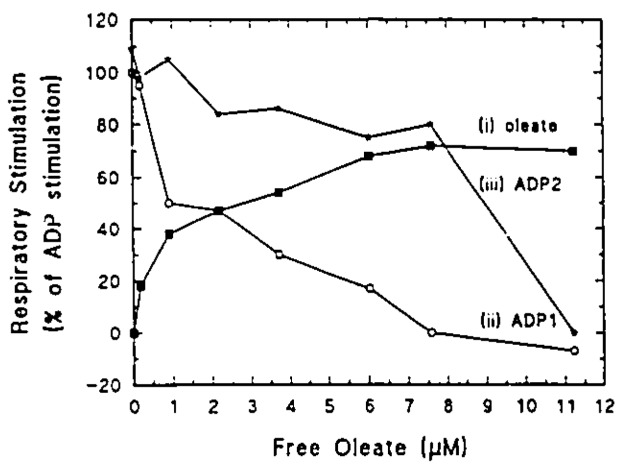

C253A UCP

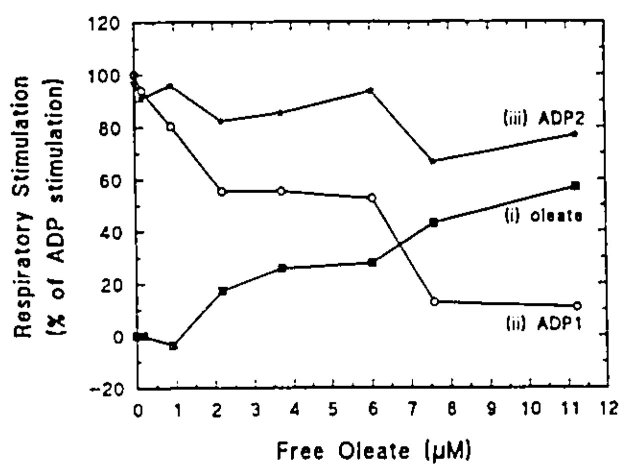

GDP from mitochondria containing wild type UCP. For mitochondria containing wild type UCP, oleate-activated uncoupling reversible by GDP was observed up to 7.6 μM oleate, with irreversible uncoupling observed by 11 μM oleate (Figure 3-16b). Mitochondria containing C253S, C287S, C304S showed this same response to oleate and GDP. Mitochondria containing C24S, C188S, C224S, C287S/A271V showed oleate-activated uncoupling reversible by GDP up to 6 μM oleate, above which uncoupling started to become irreversible. Mitochondria containing C213S still showed GDP-reversible uncoupling at 11 μM oleate. In general, oleate uncoupling appeared to saturate by 6 μM oleate in mitochondria containing the cys to ser mutant UCPs, as was observed for mitochondria containing wild type UCP.

Although the RCRs for mitochondria containing the cys to ser mutant UCPs were similar to that found for mitochondria containing wild type UCP, GDP did not appear to have a recoupling effect in the absence of oleate in mitochondria containing C188S, C213S, C224S, C287S and C287S/A271S which possibly indicated no basal activity level for these mutant UCPs. Since all eight mitochondria preparations containing individually each cys to ser mutant UCP showed a similar response to oleate and GDP as mitochondria containing wild type UCP, only one preparation of each cys to ser UCP containing mitochondria was tested.

In summary, mitochondria containing cys to ser mutant UCPs all showed oleate-activated, GDP-sensitive uncoupling, indicating that none of the thiol groups individually in UCP are neccessary for oleate-activated, GDP-sensitive uncoupling specific to UCP. This conclusion was verified for these mutant UCPs that were purified from yeast mitochondria and reconstituted into proteoliposomes. Changing all cysteines to serines was without effect on GDP inhibition of UCP-mediated proton or anion transport (Murdza-Inglis *et al.*, 1994). Arechaga *et al.* (1993) also found cysteine residues were not essential for UCP function. Since serine can substitute for all cysteines in UCP, it can be concluded that there are no essential disulphide bonds in UCP. The ion transport model for UCP suggested by Jezek (1987) involving a dithiol-disulphide interconversion (Robillard and Konings, 1982) can be discounted based on the cysteine to serine substitution results.

The transport function of another member of the mitochondrial carrier family, the phosphate transport protein (PTP) of yeast, was also sensitive to sulfhydryl reagents (Phelps *et al.*, 1991). However, of the three cysteines present in the yeast PTP and the eight present in the beef heart mitochondrial PTP, only one cysteine was conserved between the two species (Phelps *et al.*, 1991). Replacement of any or all of the three cysteines in the yeast PTP with serine produced yeast that were able to grow on a non-fermentable carbon source and the reconstituted transport activity for the mutant PTPs were normal (Phelps and Wohlrab, 1993). In addition, for the yeast mitochondrial ADP/ATP carrier (AAC), replacement of the three cysteines with serine also produced yeast that were able to grow on a non-fermentable carbon source, indicating the mutant carriers were functional. However, the C73S mutation caused the loss of bound cardiolipin on isolation and purification of the protein from the mitochondria which was required for the reconstituted activity (Hoffmann *et al.*, 1994). Since all the cys to ser mutants of UCP, PTP and AAC were functional in yeast mitochondria, these observations suggest that cysteines are not essential residues in the mitochondrial carrier family of proteins.

3.4.1.2 Cysteine 253 of UCP

The ability of serine to substitute for cysteine without affecting the functions of UCP does not rule out functional roles for the cysteine side chains where a hydroxyl group could substitute for the thiol group. Labelling studies using ATP analogues have localized the purine nucleotide binding region of UCP to the third domain of the protein (Mayinger and Klingenberg, 1992; Winkler and Klingenberg, 1992). Because Mayinger and Klingengerg (1992) deduced that cys253 was the most likely residue covalently labeled by the ATP analog 3'-O-(5-fluoro-2,4-dinitrophenyl)adenosine 5'-triphosphate, an because chemical modification of cysteines were shown to affect both GDP binding to UCP and GDP inhibition of anion transport (Rial and Nicholls, 1986; Kopecky *et al.*, 1987; Jezek and Drahota, 1989), cys253 was further modified using site-directed mutagenesis to determine if this residue was important for the functioning of UCP. Cys253 was altered to alanine to remove the potentially reactive thiol group (or the hydroxyl group of serine) replacing it with a hydrogen. This substitution still maintained the hydrophobic nature of position 253 since the transfer free energy for alanine from a hydrophobic to an aqueous environment was 1.6 kcal/mol as compared to that for cysteine of 2.0 kcal/mol (Engelman *et al.*, 1986). In addition, cys253 was altered to phenylalanine to determine whether oleate-activated uncoupling or GDP-inhibition of uncoupling could be sterically blocked by this bulkier substitution at position 253. In making the phenylalanine substitution at position 253, an extra point mutation also arose in the UCP cDNA, changing arginine 152 to serine. Positive charge is known to be important for mitochondrial protein import into the mitochondria (Freeman *et al.*, 1995). Chemical studies using arginine-modifying reagents previously implied that arginine is a critical functional residue for purine nucleotide binding and regulation of UCP (Katiyar and Shrago, 1989). Therefore, the double mutant C253F/R152S UCP was also tested for expression, import and function.

The three mutant forms of UCP (C253A, C253F, C253F/R152S) were expressed in yeast and were immunodetected in yeast mitochondrial fractions at levels similar to that found for wild type UCP (Figure 3-26). The respiratory control ratios listed in Table 3-6 indicated that the mitochondria were coupled to the same extent as mitochondria containing wild type UCP, with mitochondria containing the double mutant, C253F/R152S, having an RCR closer to that found for yeast mitochondria lacking UCP.

Mitochondria containing UCP mutated from cys253 to alanine were tested for UCP activity using both respiratory assays (Figures 3-15 and 3-18). Mitochondria containing UCP mutated from cys253 to phenylalanine were tested using the oligomycin respiratory assay only (Figure 3-18). The mitochondrial respiratory response to oleate and GDP observed for mitochondria containing these mutant UCPs was the same as that observed for mitochondria containing wild type UCP. Using the first respiratory assay, mitochondria containing cys253ala UCP showed oleate-activated, GDP-sensitive uncoupling (Figure 3-25) very similar to that observed for mitochondria containing wild type UCP (Figure 3-16b). Mitochondria containing individually the three mutant forms of UCP (C253A, C253F, C253F/R152S) showed a similar oleate-induced respiratory stimulation in the presence of oligomycin (Figure 3-27a,b,c) and GDP-inhibited respiration (Figure 3-28a,b,c) as that observed for mitochondria containing wild type UCP. GDP inhibition of the oleate stimulated respiratory rate had inhibition constants (K_i) of 20 ± 4 μM GDP for mitochondria containing C253A UCP, 28 ± 1 μM GDP for mitochondria

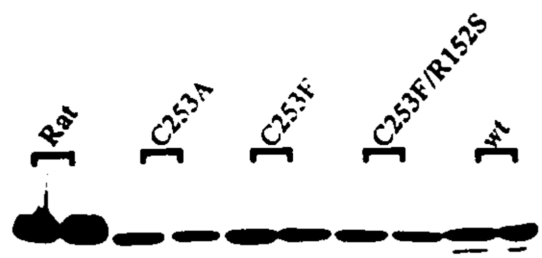

Figure 3-26. Immunoblot Analysis of Mitochondrial Fractions Isolated From Yeast Transformants Containing UCP cDNA Encoding Either Wild Type UCP or UCP Mutated at Cys253

Yeast transformants containing the shuttle vector pCGS110 with the cDNA coding for wild type rat UCP or UCP mutated at cys253 were induced to express UCP by the addition of galactose to 0.2% for 11 h. Ten μg of mitochondrial protein isolated from each of the transformants were separated by SDS-12.5% PAGE and analyzed by an immunoblot using monospecific antibody against rat UCP and HRP-conjugated anti-rabbit antibody. Chemiluminescence was used to detect protein. The type of UCP expressed is indicated above each lane. Purified rat UCP (1 μg) from brown adipose tissue mitochondria was run as a marker.

Table 3-6. Respiratory Control Rates (RCR) for Yeast Mitochondria Preparations Containing UCP Mutated at cys253

Mitochondria were isolated from yeast transformants as described in the legend to Table 3-5. For mitochondria containing UCP mutated at cys253, the RCRs were determined in respiration buffer containing 0.05% BSA. The -UCP and wild type data are taken from Table 3-5 for comparison. Data is presented as the mean ± SEM. The calculated RCRs for mitochondria containing UCP mutated at cys253 are for single mitochondrial preparations.

UCP	RCR
-UCP	2.8 ± 0.2
wild type	2.0 ± 0.1
C253A	2.1 ± 0.1
C253F	2.2 ± 0.2
C253F/R152S	3.1

(a)

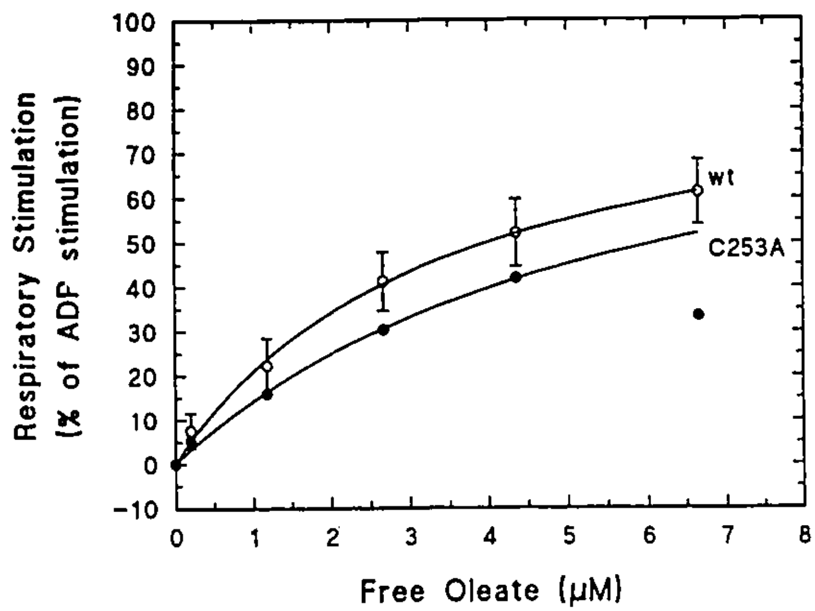

Figure 3-27. The Effect of Oleate on Yeast Mitochondrial Respiration Using Assay 2: Results For Mitochondria Containing UCP Mutated at Cys253

The effect of oleate on yeast mitochondrial respiration was tested using the oligomycin Assay 2 as outlined in the legend to Figure 3-19. Mitochondria contained: (a) cys253ala (C253A) UCP; (b) cys253phe (C253F) UCP; or (c) cys253phe/arg152ser (C253F/R152S) UCP. Results include the data for mitochondria containing wild type UCP taken from Figure 3-19 for comparison. The respiratory stimulation was calculated as the difference between the oleate stimulated rate and the rate in the absence of oleate as explained in the legend of Figure 3-19, and is plotted as a percentage of the ADP respiratory stimulation. The results for mitochondria containing the mutant UCPs are from single mitochondrial preparations.

(b)

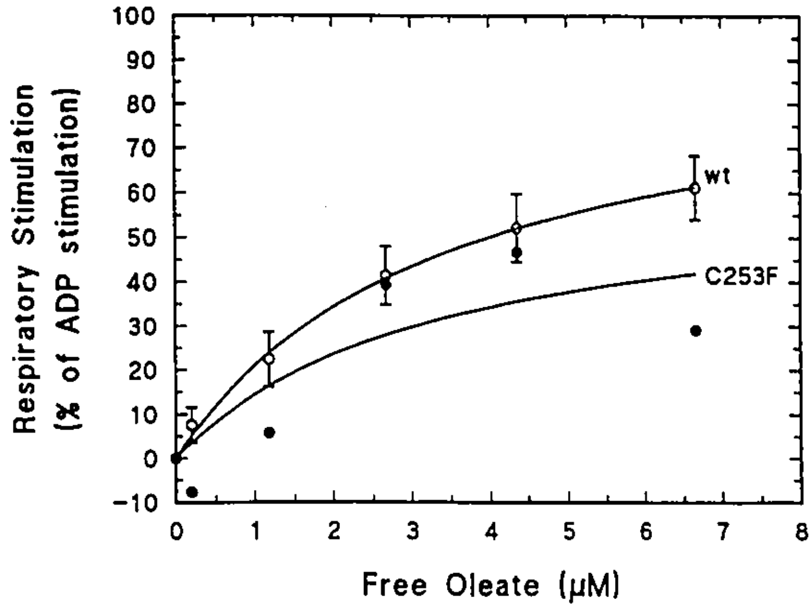

100
90
80
70
60
50
40
30
20
10
0
-10
Respiratory Stimulation
(% of ADP stimulation)
wt
C253F
0
1
2
3
4
5
6
7
8
Free Oleate (μM)

(c)

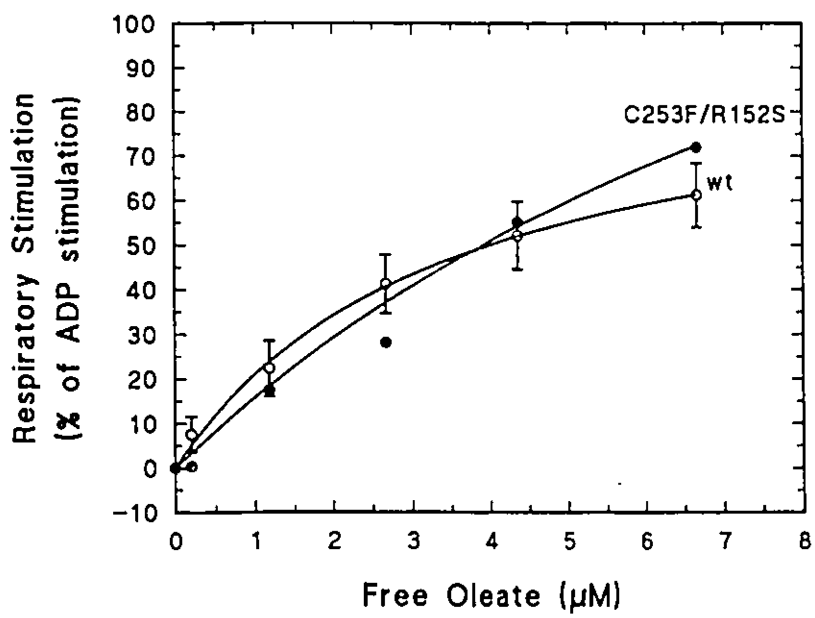

100
90
80
70
60
50
40
30
20
10
0
-10
Respiratory Stimulation
(% of ADP stimulation)
C253F/R152S
wt
0
1
2
3
4
5
6
7
8
Free Oleate (μM)

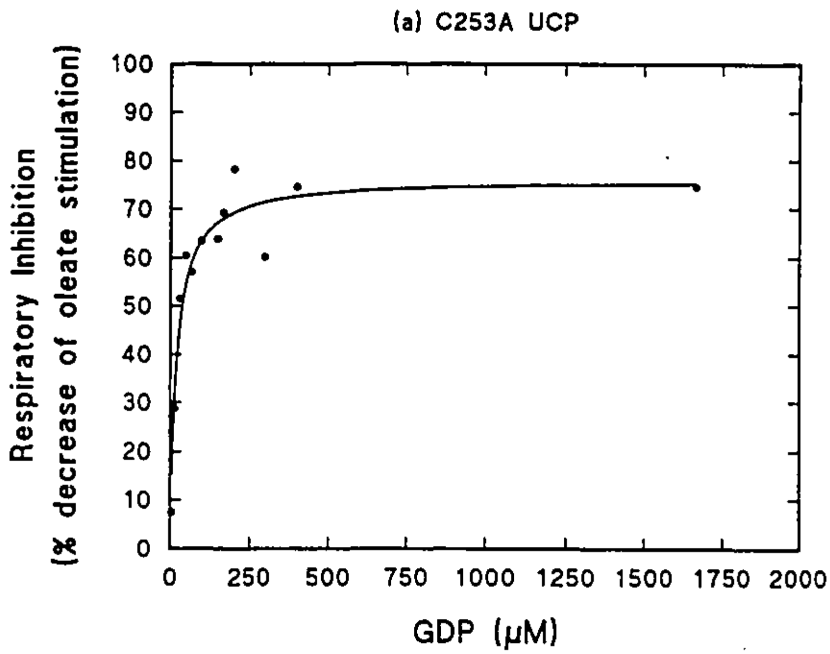

Figure 3-28 Inhibition of Oleate Stimulation by GDP: Results For Mitochondria Containing UCP Mutated at Cys253

The inhibitory effect of GDP on oleate-stimulated respiration was measured for the mitochondrial preparations of Figure 3-27 following the procedure outlined in the legend to Figure 3-21. The respiratory rate was stimulated using a solution of oleate/BSA containing a molar ratio of 4:1 oleate:BSA, which is equivalent to 4.4 μM free oleate. The effect of a range of GDP concentrations on the oleate-stimulated respiratory rate was plotted as the respiratory inhibition versus GDP concentration. The respiratory inhibition was calculated as the difference between the oleate-stimulated and GDP-inhibited respiratory rates, expressed as a percent decrease of the oleate stimulation as explained in the legend to Figure 3-21. Mitochondrial preparations contained: (a) cys253ala (C253A) UCP, K_i of 20 ± 4 μM GDP; (b) cys253phe (C253F) UCP, K_i of 28 ± 1 μM GDP; and (c) cys253phe/arg152ser (C253F/R152S) UCP, K_i of 16 ± 3 μM GDP. Single mitochondrial preparations containing the mutant proteins were tested.

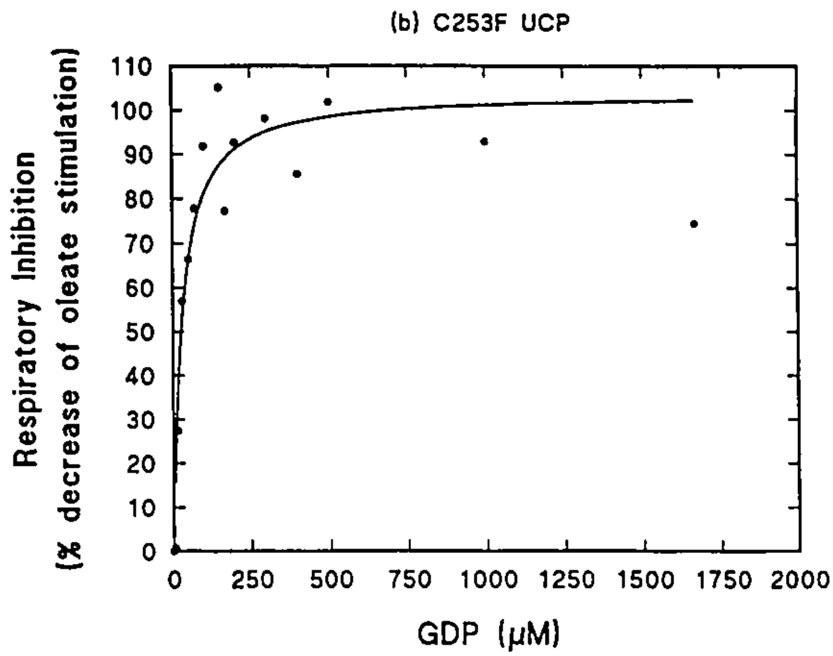
(b) C253F UCP
Respiratory Inhibition
(% decrease of oleate stimulation)
110
100
90
80
70
60
50
40
30
20
10
0
0
250
500
750
1000
1250
1500
1750
2000
GDP (μM)

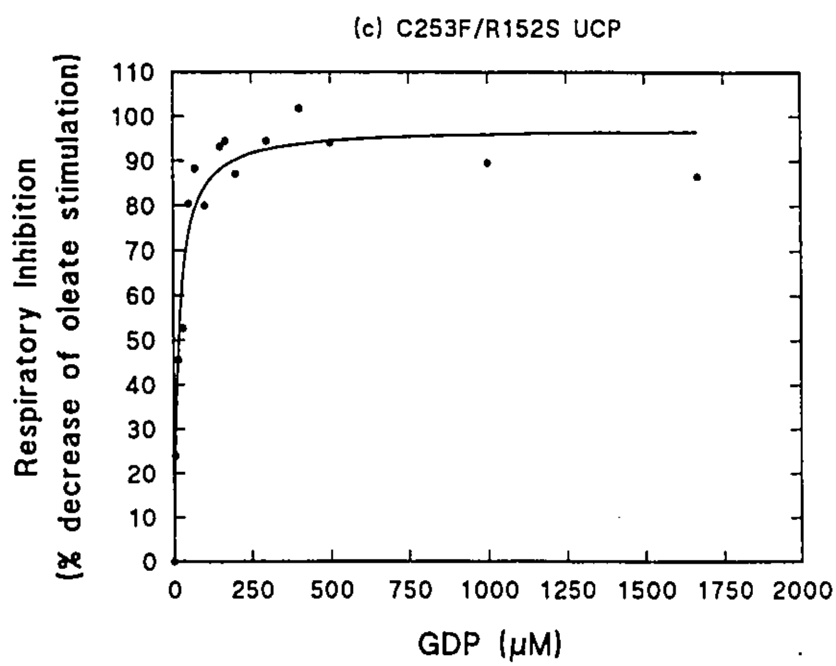
(c) C253F/R152S UCP
Respiratory Inhibition
(% decrease of oleate stimulation)
110
100
90
80
70
60
50
40
30
20
10
0
0
250
500
750
1000
1250
1500
1750
2000
GDP (μM)

containing C253F UCP and 16 ± 3 μM GDP for mitochondria containing C253F/R152S UCP. These inhibition constants were similar to that found for mitochondria containing wild type UCP, where the K_i was 26 ± 1 μM GDP.

In summary, all the cys253 mutant forms of UCP showed a normal wild type response to oleate and GDP. These results clearly indicate that a reactive thiol at position 253 in UCP is not required for uncoupling or GDP inhibition of uncoupling of yeast mitochondria. Furthermore, position 253 in UCP can accommodate the sterically bulky phenylalanine substitution without any effect on function, indicating that this position is in a flexible part of the protein. Since mitochondria contained the same levels of wild type, C253F and C253F/R152S UCP, the positive charge at position 152 is not a major contributor to mitochondrial targeting information in UCP. Furthermore, substitution of arg152 with serine did not effect oleate-activated, GDP-sensitive uncoupling indicating that arg152 is not critical for UCP function.

3.4.2 Arginine Residues

Based on the pH dependence of nucleotide binding to UCP, Klingenberg proposed that both acidic and basic residues are present in the purine nucleotide binding site (Klingenberg, 1987; Huang and Klingenberg, 1995). As previously mentioned, past chemical studies using arginine-modifying reagents implied that arginine is a critical functional residue in UCP required for purine nucleotide binding to UCP and purine nucleotide regulation of UCP (Katiyar and Shrago, 1989). Labeling studies using ATP analogs localized the purine nucleotide binding region of UCP to the third domain of the protein. There are three arginines present in this region of UCP that are conserved in

UCP of all species known, arg238, arg276 and arg299 of rat UCP (Nelson *et al.*, 1993). The transmembrane arrangement of the third domain proposed by Mayinger and Klingenberg (1992) depicts a nucleotide binding pocket in UCP between transmembrane helices 5 and 6, with a portion of the matrix region connecting these helices looping up into the region between the helices forming the base of the pocket (see Figure 1-2). In this proposed arrangement, the nucleotide binding site would only be accessible to cytosolic purine nucleotides which are known to regulate UCP from the outer face of the inner membrane (Nicholls, 1976). Arg276 is present in the proposed nucleotide binding pocket of UCP, spacially close to residues covalently labeled by ATP analogues and accessible to cytosolic purine nucleotides. Arg238 is excluded from this binding pocket and is inaccessible to nucleotides in this arrangement. Based on the size of ATP in its extended *anti* conformation (Zheng *et al*, 1993) and the location of residues covalently labeled by the ATP analogues (at the bottom of the proposed binding pocket), it is unlikely that arg299 could interact with ATP. Further, arg276 is conserved in all mitochondrial carrier family members except the phosphate carrier (Nelson *et al.*, 1993). Based on this information, arg276 was modified using site-directed mutagenesis to determine if this residue was involved in GDP inhibition of uncoupling and GDP binding to UCP.

3.4.2.1 Arginine 276

Arginines are important residues in proteins for non-covalent inter- or intra-molecular interactions. The positively charged side chain of arginine can interact with negatively charged groups to form electrostatic interactions and the side chain can supply hydrogen donor groups for hydrogen bonding between groups.

The role of arg276 in UCP was investigated by replacing the arginine with glutamine and leucine using site-directed mutagenesis of the rat UCP cDNA. The glutamine substitution maintained some hydrogen-bonding ability but removed positive charge. Leucine removed both these characteristics and introduced a non-polar side chain into this position. The transfer free energy for arginine from a hydrophobic to an aqueous environment is -12.3 kcal/mol, which makes it the most hydrophilic of all the amino acids. The glutamine substitution maintains the hydrophilic nature of this position (transfer free energy of -4.1 kcal/mol), but the leucine substitution is hydrophobic (transfer free energy of 2.8 kcal/mol) (Engelman *et al.*, 1986). In each case, the substituted side chain was shorter which should minimize steric interference of function.

Immunoblot analysis of yeast mitochondrial fractions prepared from cells induced to express the mutant forms of the protein indicated that both mutant UCPs were expressed and localized to yeast mitochondria, but mitochondrial levels were lower than that obtained for wild type UCP (Figure 3-29). Quantification of western blots using standards of purified rat UCP indicated that yeast mitochondrial fractions contained on average 16 μg arg276leu UCP/mg mitochondrial protein and 4 μg arg276gln UCP/mg mitochondrial protein. Based on these protein levels, arg276leu UCP and arg276gln UCP were present at approximately 18% and 4% of the level of wild type UCP (88 μg UCP/mg mitochondrial protein) respectively in yeast mitochondria. The respiratory control ratios listed in Table 3-7 indicated that the mitochondria were as coupled as mitochondria containing wild type UCP. The respiratory response of mitochondria containing arg276leu or arg276gln UCP to oleate and GDP was tested using the oligomycin respiratory assay (Figure 3-18). Oleate addition to mitochondria containing

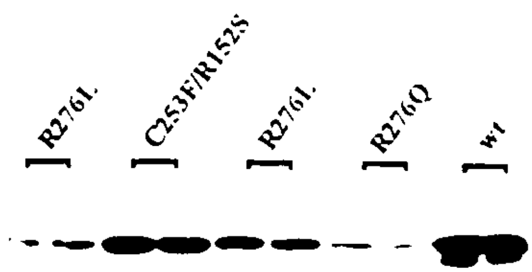

Figure 3-29. Immunoblot Analysis of Mitochondrial Fractions Isolated From Yeast Transformants Containing UCP cDNA Encoding Either Wild Type UCP or UCP Mutated at arg276

Yeast transformants containing the shuttle vector pCGS110 with the cDNA coding for wild type rat UCP or UCP mutated at arg276 were induced to express UCP by the addition of galactose to 0.2% for 11 h. Ten μg of mitochondrial protein isolated from each of the transformants were separated by SDS-12.5% PAGE and analyzed by an immunoblot using monospecific antibody against rat UCP and HRP-conjugated anti-rabbit antibody. Chemiluminescence was used to detect protein. The type of UCP expressed is indicated above each lane.

Table 3-7. Respiratory Control Ratios (RCR) for Yeast Mitochondria Preparations Containing UCP Mutated at arg276

Mitochondria containing UCP mutated at R276 were isolated and assayed as described in the legend to Table 3-6. The -UCP and wild type data are taken from Table 3-5 for comparison. Data is presented as the mean ± SEM. The calculated RCRs for mitochondria containing UCP mutated at arg276 are for duplicate mitochondrial preparations.

UCP	RCR
-UCP	2.8 ± 0.2
wild type	2.0 ± 0.1
R276L	1.9 ± 0.2
R276Q	1.6 ± 0.1

the mutant UCPs caused respiratory stimulation to the same extent as that observed for mitochondria containing wild type UCP (Figure 3-30a,b). However, the subsequent GDP addition (166 μM) had little effect on decreasing the stimulated respiratory rate. This was shown by measuring the oleate respiratory stimulation relative to the GDP inhibited rate (Figure 3-31a,b) rather than relative to the respiratory rate prior to oleate addition (Figure 3-30a,b). Because GDP did not decrease the respiratory rate, the stimulation relative to the GDP rate was less than 15% of the ADP stimulated rate and did not follow a saturation curve. GDP inhibition of the respiratory stimulation induced by 4.4 μM free oleate was titrated using a range of GDP concentrations for mitochondria containing either arg276leu or arg276gln UCP (Figure 3-32). The K_i was increased from 26 ± 1 μM GDP for mitochondria containing wild type UCP to 1250 ± 415 μM GDP for mitochondria containing arg276leu UCP. GDP inhibition was abolished in mitochondria containing arg276gln UCP.

To determine whether the lack of GDP inhibition was due to a lack of GDP binding to the mutant forms of the protein, GDP binding to mitochondria containing either arg276leu or arg276gln UCP was measured. GDP binding to mitochondria containing arg276leu UCP was measured for four independent mitochondrial preparations (Figure 3-33a-d). The level of GDP bound to mitochondria containing arg276leu UCP was just above the background level of GDP bound to control mitochondria lacking UCP. However, the amount of arg276leu UCP present in the mitochondria preparations (8 ± 2 μg R276L UCP/500 μg mitochondrial protein) was much lower than the wild type level of UCP (44 ± 4 μg wild type UCP/500 μg mitochondrial protein). The theoretical amount of GDP bound to mitochondria containing only 8 μg of wild type UCP was

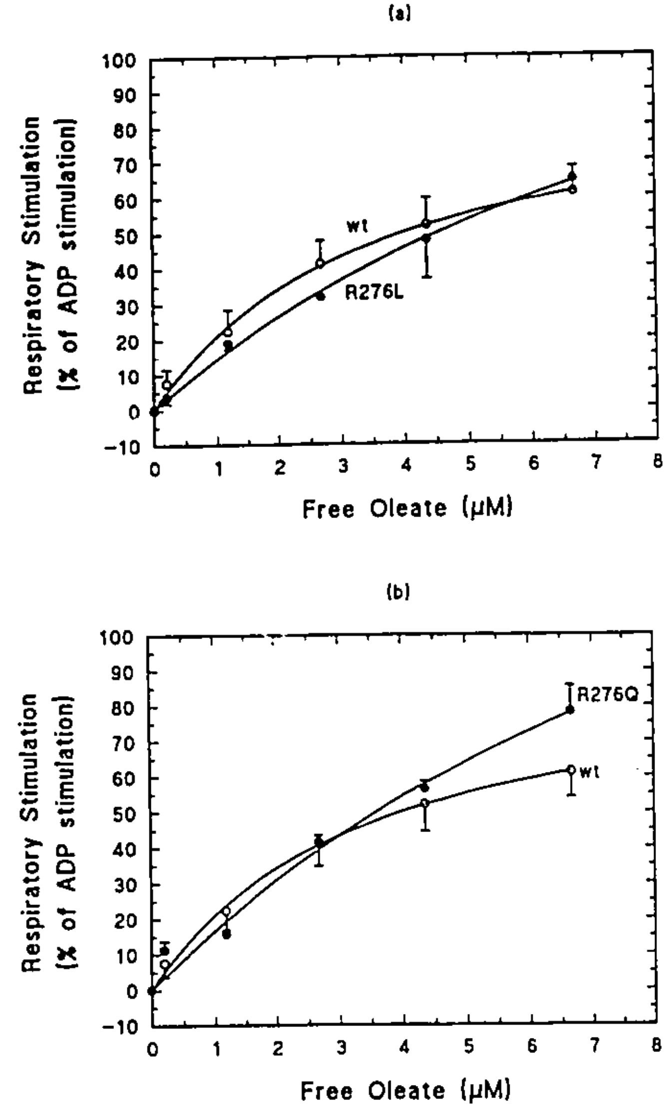

Figure 3-30 The Effect of Oleate on Yeast Mitochondrial Respiration Using Assay 2: Results For Mitochondria Containing UCP Mutated at Arg276

The effect of oleate on yeast mitochondrial respiration was tested using the oligomycin Assay 2 as outlined in the legend to Figure 3-19. Mitochondria contained (a) arg276leu (R276L) UCP or (b) arg276gln (R276Q) UCP. Results include the data for mitochondria containing wild type UCP taken from Figure 3-19 for comparison. The respiratory stimulation was calculated as the difference between the oleate stimulated rate and the rate in the absence of oleate as explained in the legend of Figure 3-19, and is plotted as a percentage of the ADP respiratory stimulation. The results for mitochondria containing the mutant UCPs are from duplicate mitochondrial preparations ± SEM.

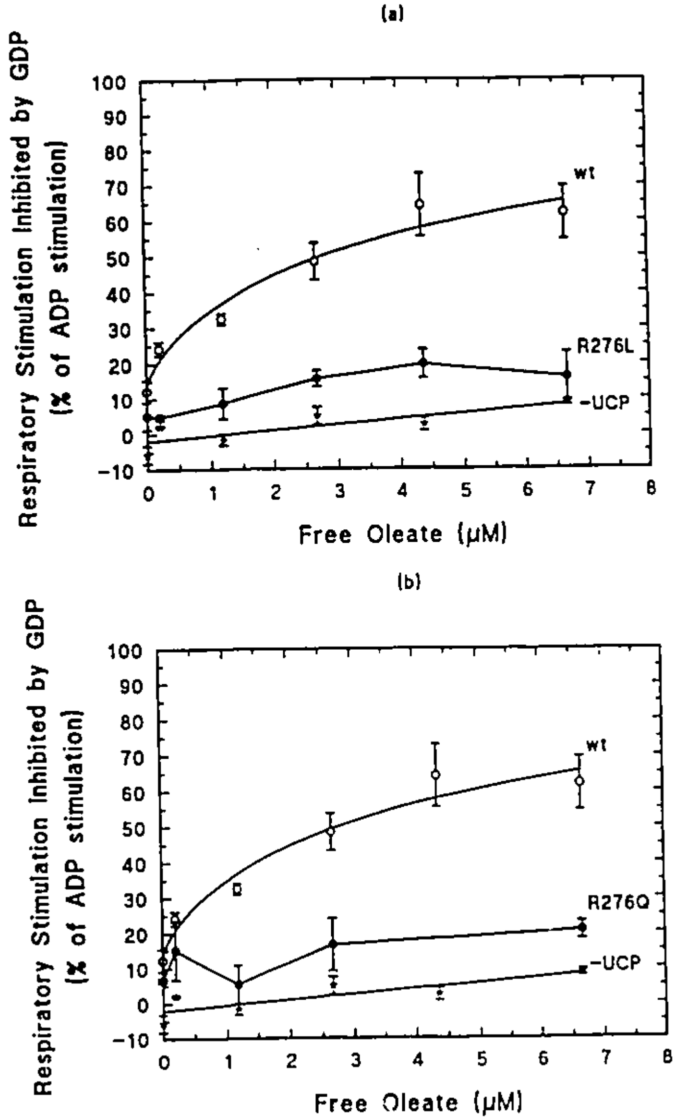

Figure 3-31. Oleate Respiratory Stimulation Relative to the GDP Inhibited Rate: Results For Mitochondria Containing UCP Mutated at Arg276

Oleate respiratory stimulation from the experiment of Figure 3-30 was replotted such that the oleate stimulation was measured as the difference between the oleate stimulated rate and the GDP inhibited rate, rather than as the difference between the oleate stimulated rate and the BSA rate, as outlined in the legend of Figure 3-20 (see also Figure 3-18 for schematic of assay). The respiratory stimulation was still expressed as a percentage of the ADP stimulation. Mitochondria contained (a) arg276leu (R276L) UCP or (b) arg276gln (R276Q) UCP. Results include data for mitochondria containing wild type (wt) UCP or lacking UCP (-UCP) taken from Figure 3-20. The results for mitochondria containing the mutant UCPs are from duplicate mitochondrial preparations ± SEM.

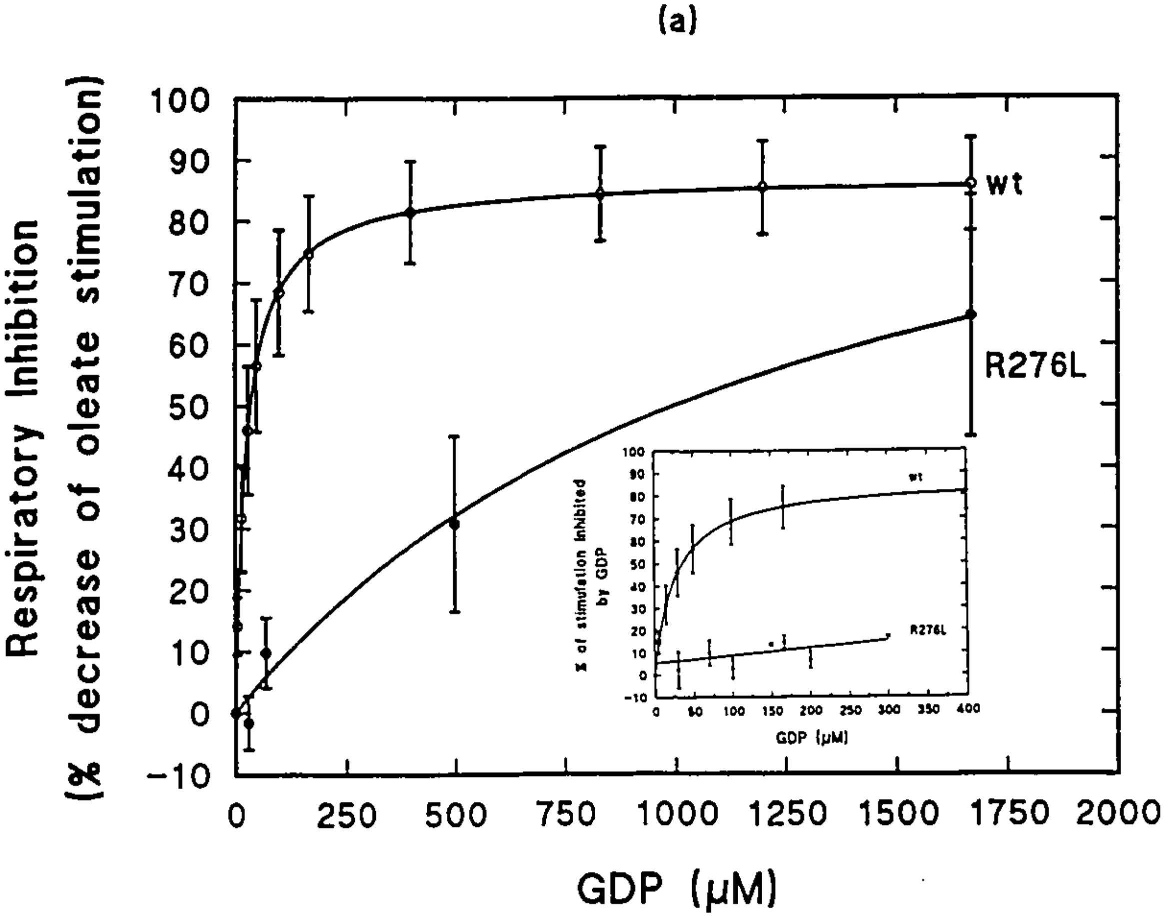

Figure 3-32. Inhibition of Oleate Stimulation by GDP: Results For Mitochondria Containing UCP Mutated at Arg276

The inhibitory effect of GDP on oleate-stimulated respiration was measured for the mitochondrial preparations of Figure 3-27 following the procedure outlined in the legend to Figure 3-21. The respiratory rate was stimulated using a solution of oleate/BSA containing a molar ratio of 4:1 oleate:BSA, which is equivalent to 4.4 μM free oleate. The effect of a range of GDP concentrations on the oleate-stimulated respiratory rate was plotted as the respiratory inhibition versus GDP concentration. The respiratory inhibition was calculated as the difference between the oleate-stimulated and GDP-inhibited respiratory rates, expressed as a percent decrease of the oleate stimulation as explained in the legend to Figure 3-21. Mitochondrial preparations contained: (a) arg276leu (R276L) UCP, K_i of 1250 ± 415 μM GDP or (b) arg276gln (R276Q) UCP. Three mitochondrial preparations containing R276L UCP and duplicate mitochondrial preparations containing R276Q UCP were tested. The results in each graph represent the averages from two preparations ± SEM. The data for mitochondria containing wild type UCP was taken from Figure 3-21.

(b)

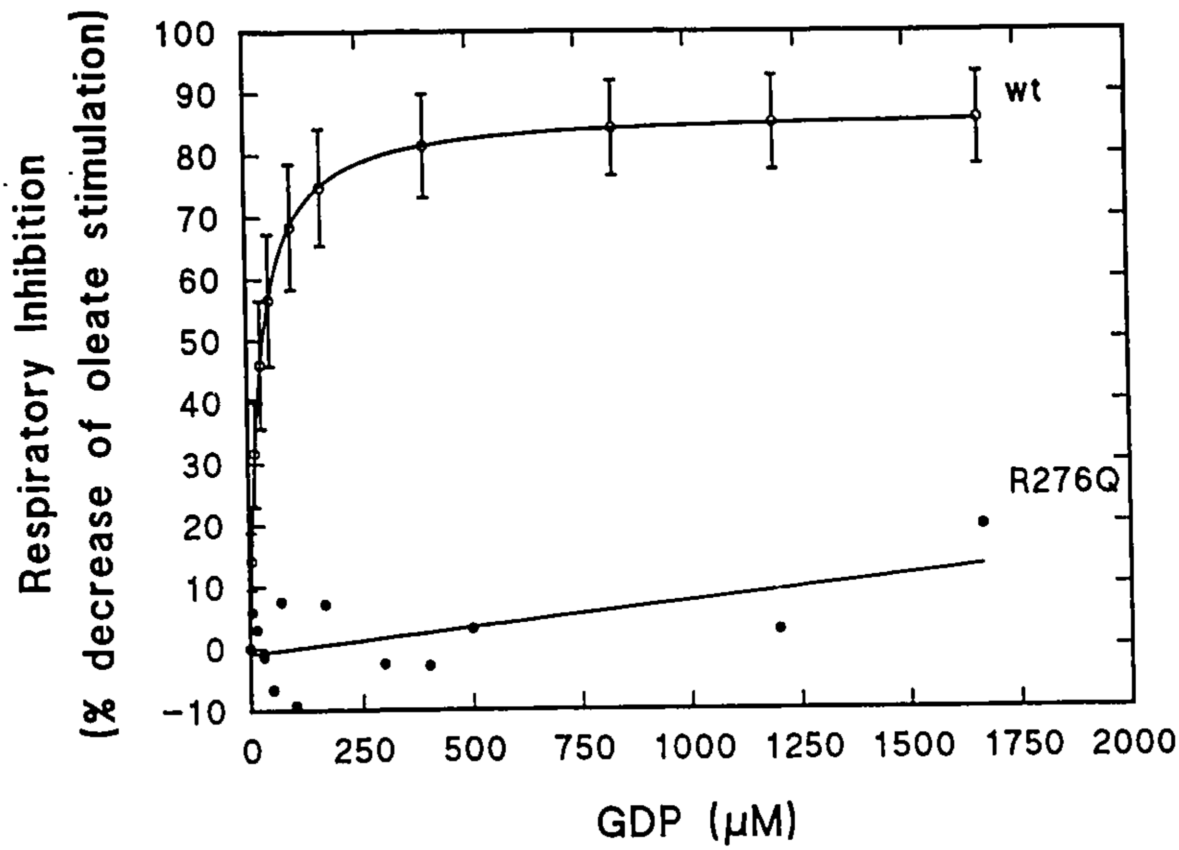
Respiratory Inhibition
(% decrease of oleate stimulation)
100
90
80
70
60
50
40
30
20
10
0
−10
0
250
500
750
1000
1250
1500
1750
2000
GDP (μM)
wt
R276Q

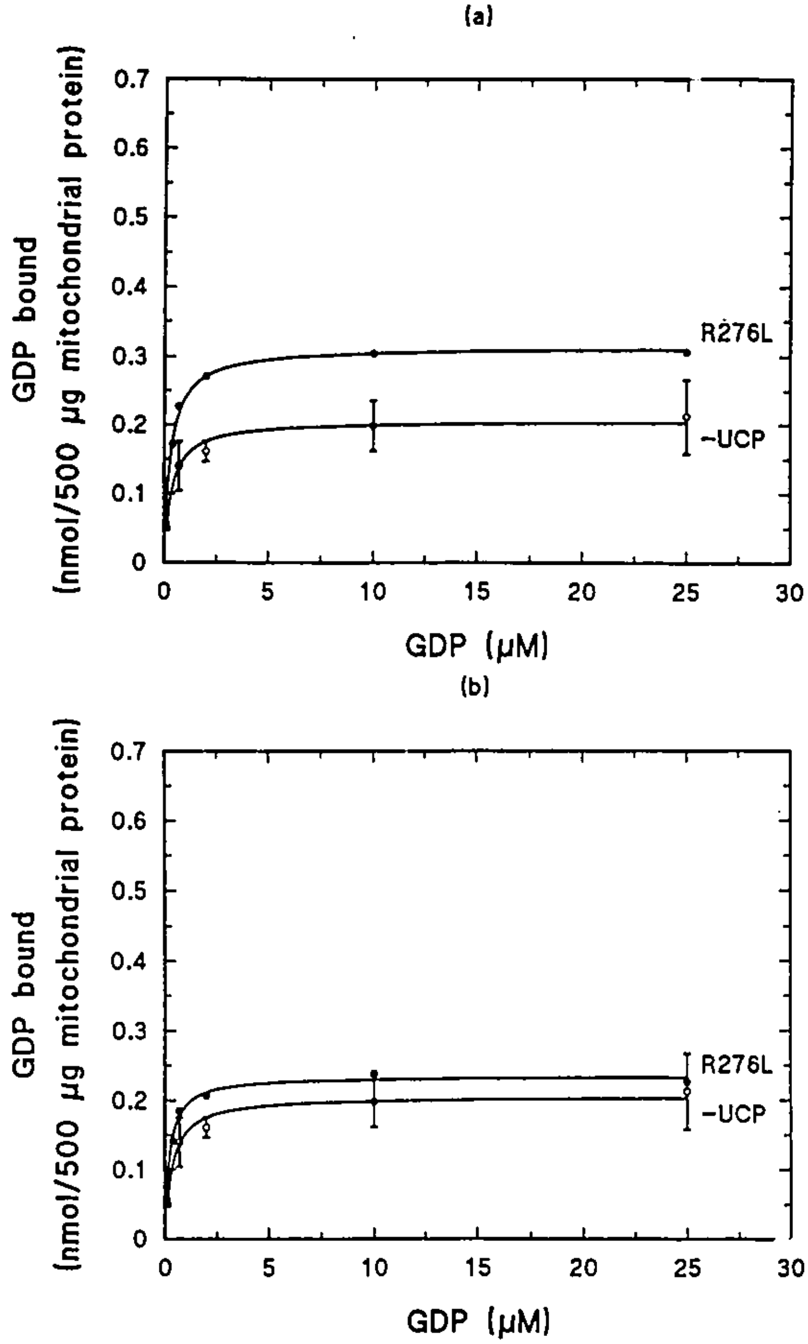

Figure 3-33. GDP Bound to Isolated Yeast Mitochondria: Results for Mitochondria Containing Arg276Leu UCP

Binding of [^{3}H]GDP to 0.5 mg of mitochondria containing arg276leu (R276L) UCP was measured as described in the legend to Figure 3-8. Four mitochondrial preparations (a), (b), (c) and (d) each contained 6, 5, 14, and 7 µg of arg276leu (R276L) UCP/500 µg mitochondrial protein respectively. Data for GDP bound to mitochondria lacking UCP (-UCP) was taken from Figure 3-8.

(c)

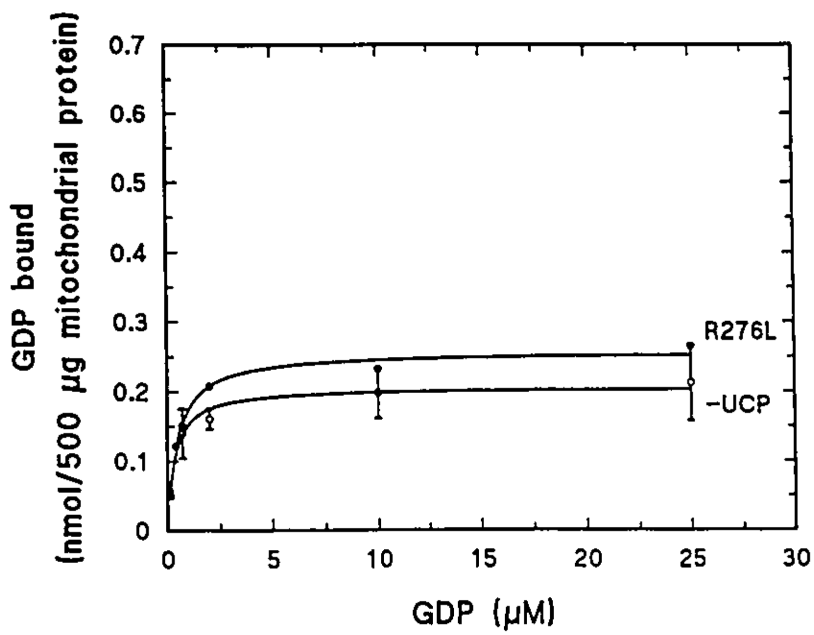
GDP bound
(nmol/500 µg mitochondrial protein)
0.7
0.6
0.5
0.4
0.3
0.2
0.1
0
0
5
10
15
20
25
30
GDP (µM)
R276L
-UCP

(d)

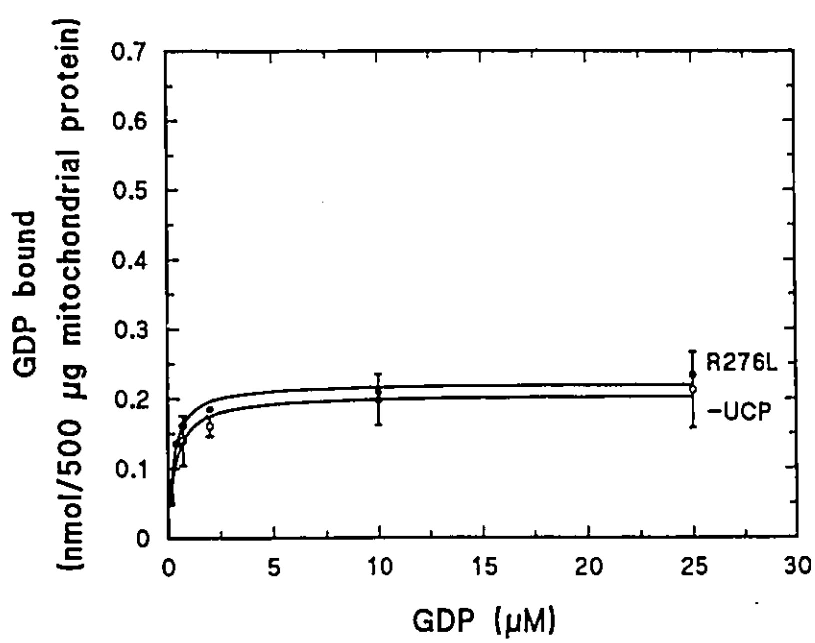
GDP bound
(nmol/500 µg mitochondrial protein)
0.7
0.6
0.5
0.4
0.3
0.2
0.1
0
0
5
10
15
20
25
30
GDP (µM)
R276L
-UCP

calculated from previous binding data (Figure 3-8) and plotted with the average arg276leu binding data calculated from the four independent mitochondria preparations. From Figure 3-34, the theoretical binding curve for GDP bound to mitochondria containing 8 μg wild type UCP was the same as GDP bound to mitochondria containing arg276leu UCP. Because the arg276leu UCP binding curves were very close to and sometimes within error of the background level of GDP bound to control mitochondria (Figure 3-33a-d), the molar ratio of GDP bound per arg276leu UCP dimer could not be calculated.

The ADP competed binding was also very low for each mitochondria preparation containing arg276leu UCP (Figure 3-35a-d). The average ADP competed binding curve for mitochondria containing arg276leu UCP was also very similar to the theoretical binding curve calculated for mitochondria containing 8 μg wild type UCP (Figure 3-36). Again, because the ADP competed GDP binding curves for mitochondria containing arg276leu UCP were very close to and sometimes within error of the background level of ADP competed GDP binding to control mitochondria (Figure 3-35a-d), the molar ratio of GDP bound per arg276leu UCP dimer could not be calculated. GDP binding (Figure 3-37) and the ADP competed GDP binding (Figure 3-38) to mitochondria containing arg276gln UCP was found to be below or within error of the average background level of GDP bound to control mitochondria. Binding studies were not continued with mitochondria containing arg276gln UCP due to the low level of mutant UCP (2 μg arg276gln UCP/500 μg mitochondrial protein).

In summary, mitochondria containing either arg276leu or arg276gln UCP showed the same oleate-activated respiratory stimulation as mitochondria containing wild type UCP (Figure 3-30a,b) but lacked GDP inhbition of oleate respiratory stimulation (Figure

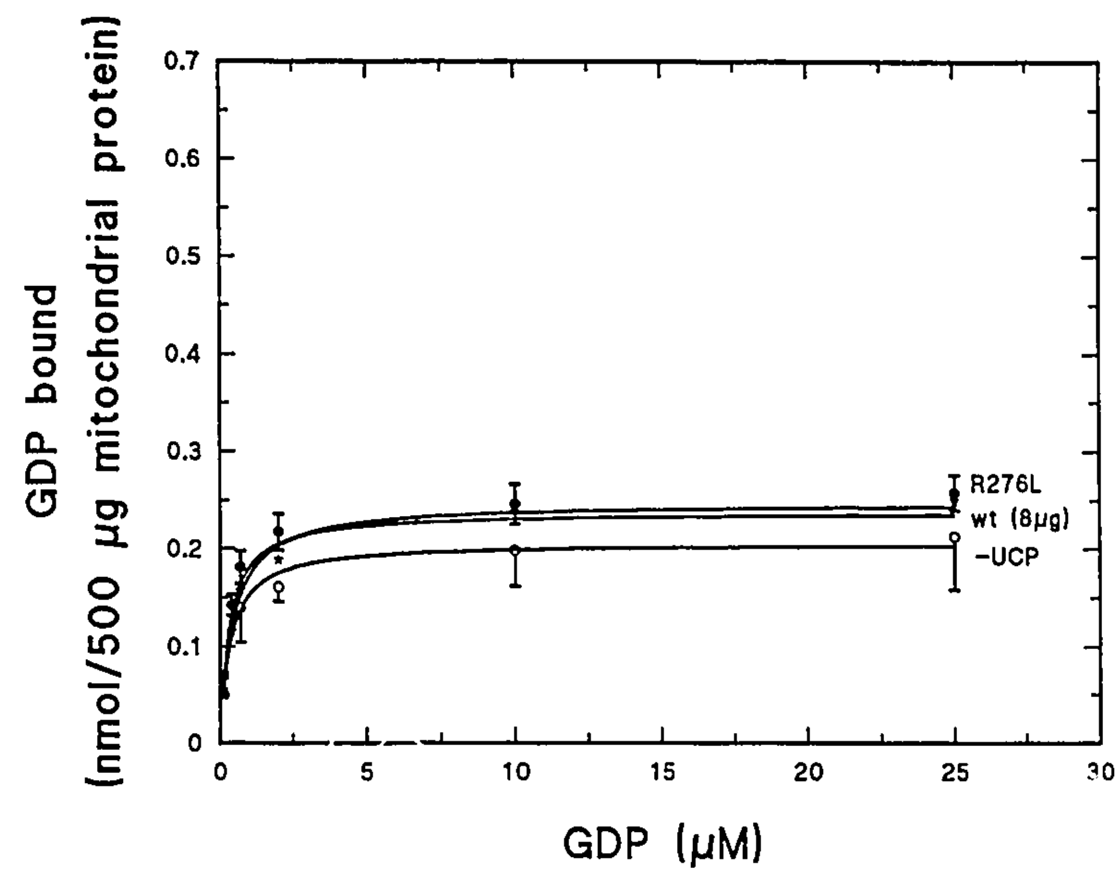

Figure 3-34. GDP Bound to Isolated Yeast Mitochondria: Comparison of Mitochondria Containing R276L UCP and 8 μg of Wild Type UCP

The binding data from the four mitochondrial preparations containing arg276leu UCP of Figure 3-33 was averaged and plotted ± SEM and compared to the theoretical level of GDP bound to mitochondria containing only 8 μg of wild type (wt) UCP, determined from Figure 3-8. The data for mitochondria lacking UCP (-UCP) was taken from Figure 3-8. Arg276leu UCP: R276L, -•-; wild type UCP: wt, -★-; no UCP: -UCP, -o-.

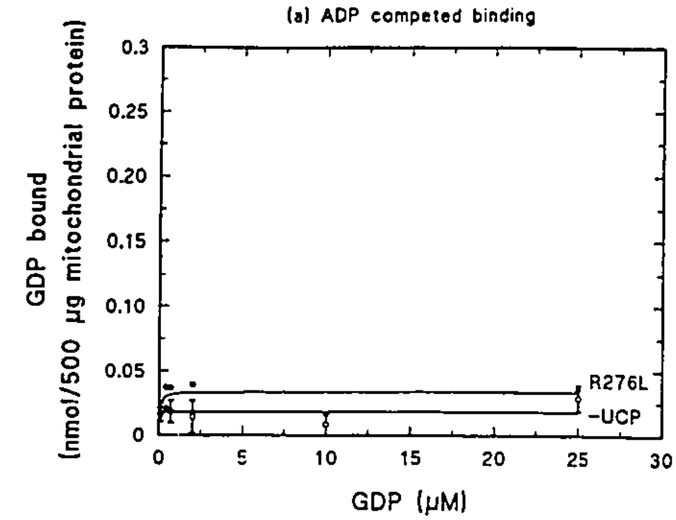

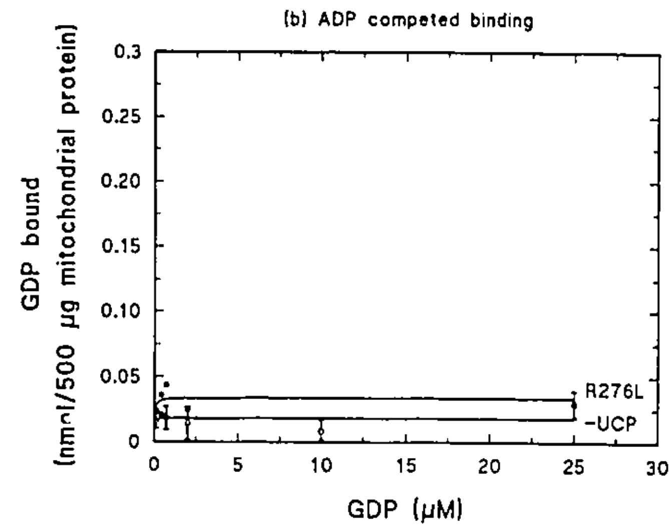

Figure 3-35. ADP Competed GDP Binding to Yeast Mitochondria: Results for Mitochondria Containing Arg276Leu UCP

The amount of bound GDP competed by ADP for the mitochondrial preparations of Figure 3-34 was calculated from the difference between GDP binding in the absence and presence of ADP, as outlined in the legend to Figure 3-10b. Binding curves (a), (b), (c) and (d) are for mitochondrial preparations containing 6, 5, 14 and 7 μg arg276leu (R276L) UCP/500 μg mitochondrial protein respectively. The binding curve for mitochondria lacking UCP (-UCP) was taken from Figure 3-10b(iv).

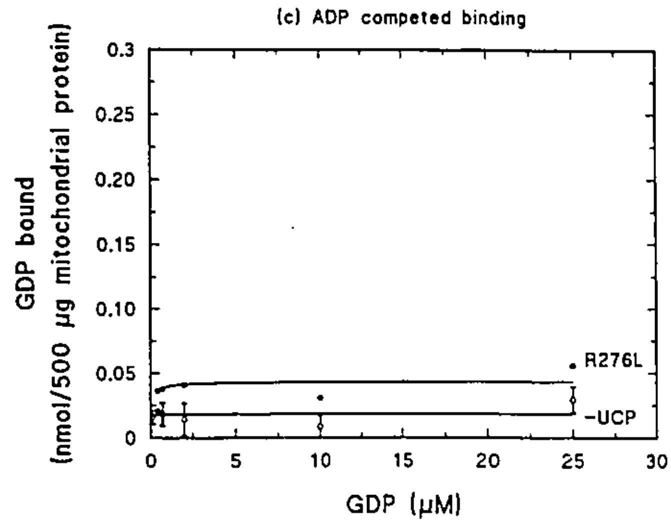
(c) ADP competed binding
GDP bound
(nmol/500 μg mitochondrial protein)
0.3
0.25
0.20
0.15
0.10
0.05
0
R276L
-UCP
0
5
10
15
20
25
30
GDP (μM)

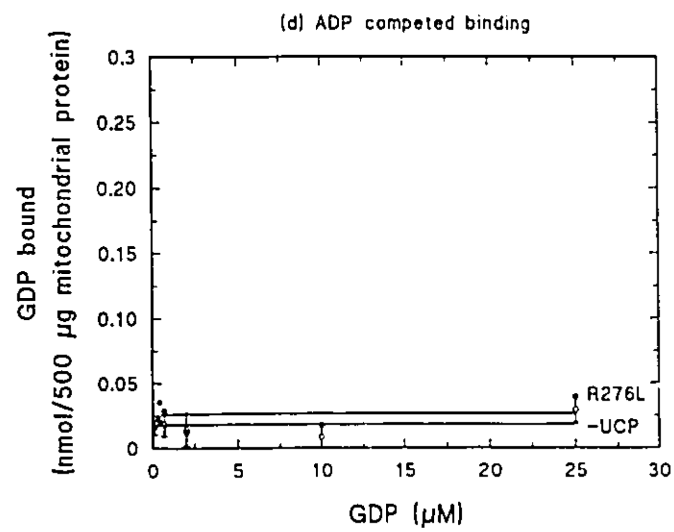
(d) ADP competed binding
GDP bound
(nmol/500 μg mitochondrial protein)
0.3
0.25
0.20
0.15
0.10
0.05
0
R276L
-UCP
0
5
10
15
20
25
30
GDP (μM)

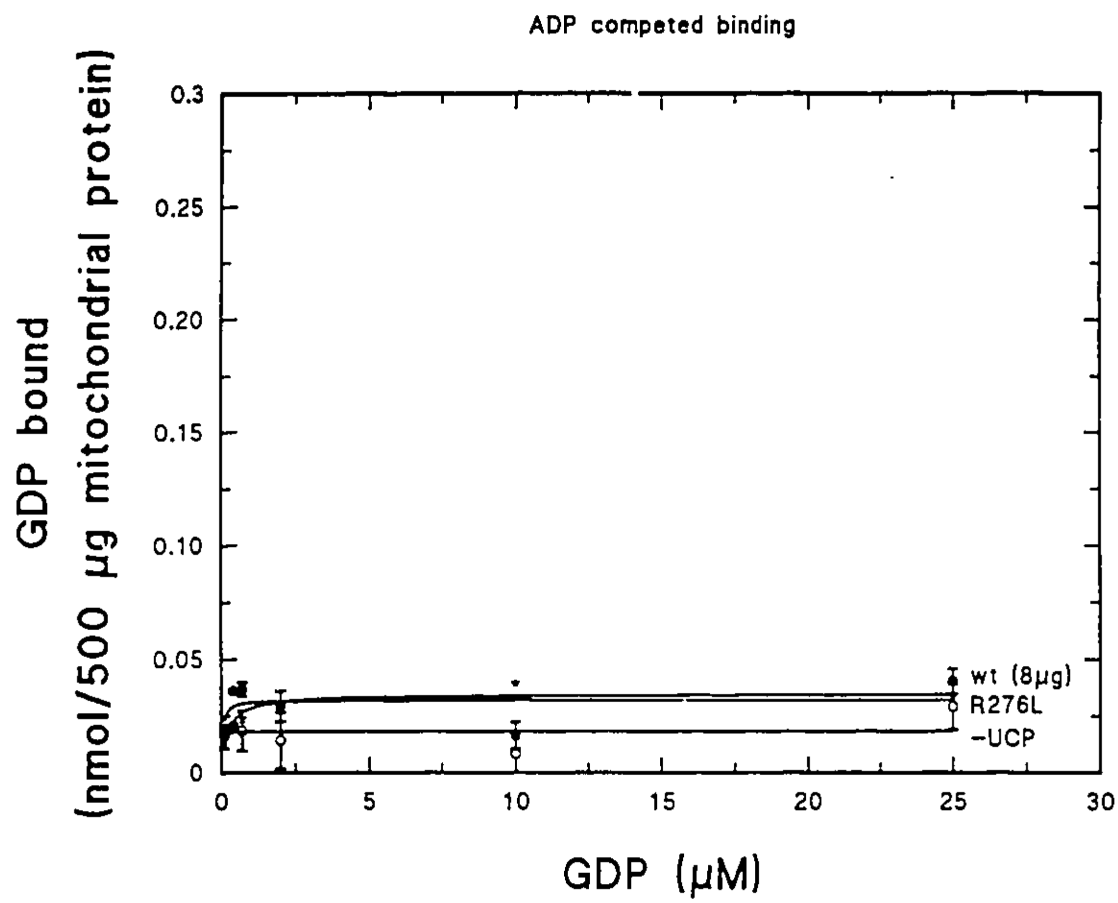

Figure 3-36. ADP Competed GDP Binding to Yeast Mitochondria: Comparison of Mitochondria Containing R276L UCP and 8 µg of Wild Type UCP

The binding data from the four mitochondrial preparations containing arg276leu UCP of Figure 3-35 was averaged and plotted ± SEM and compared to the theoretical level of bound GDP competed by ADP for 0.5 mg of mitochondria containing only 8 µg of wild type (wt) UCP, determined from Figure 3-10b. The data for mitochondria lacking UCP (-UCP) was taken from Figure 3-8. Arg276leu UCP: R276L, -•-; wild type UCP: wt,-★-; no UCP: -UCP, -o-.

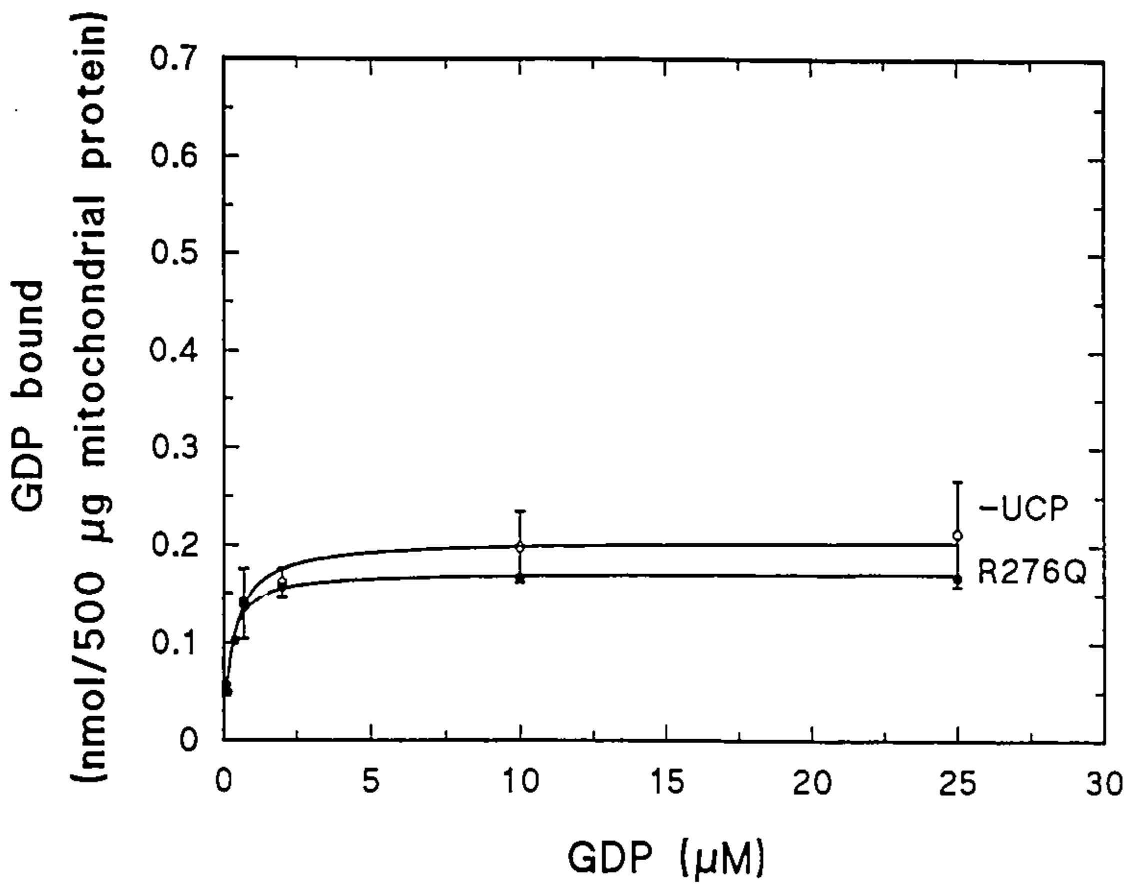

Figure 3-37. GDP Bound to Isolated Yeast Mitochondria: Results for Mitochondria Containing Arg276Gln UCP

Binding of [^{3}H]GDP to 0.5 mg of mitochondria containing arg276gln (R276Q) UCP was measured as described in the legend to Figure 3-8. A single mitochondrial preparation containing 2 μg of arg276gln (R276Q) UCP/500 μg mitochondrial protein was tested (-•-). Data for GDP bound to mitochondria lacking UCP (-UCP, -o-) was taken from Figure 3-8.

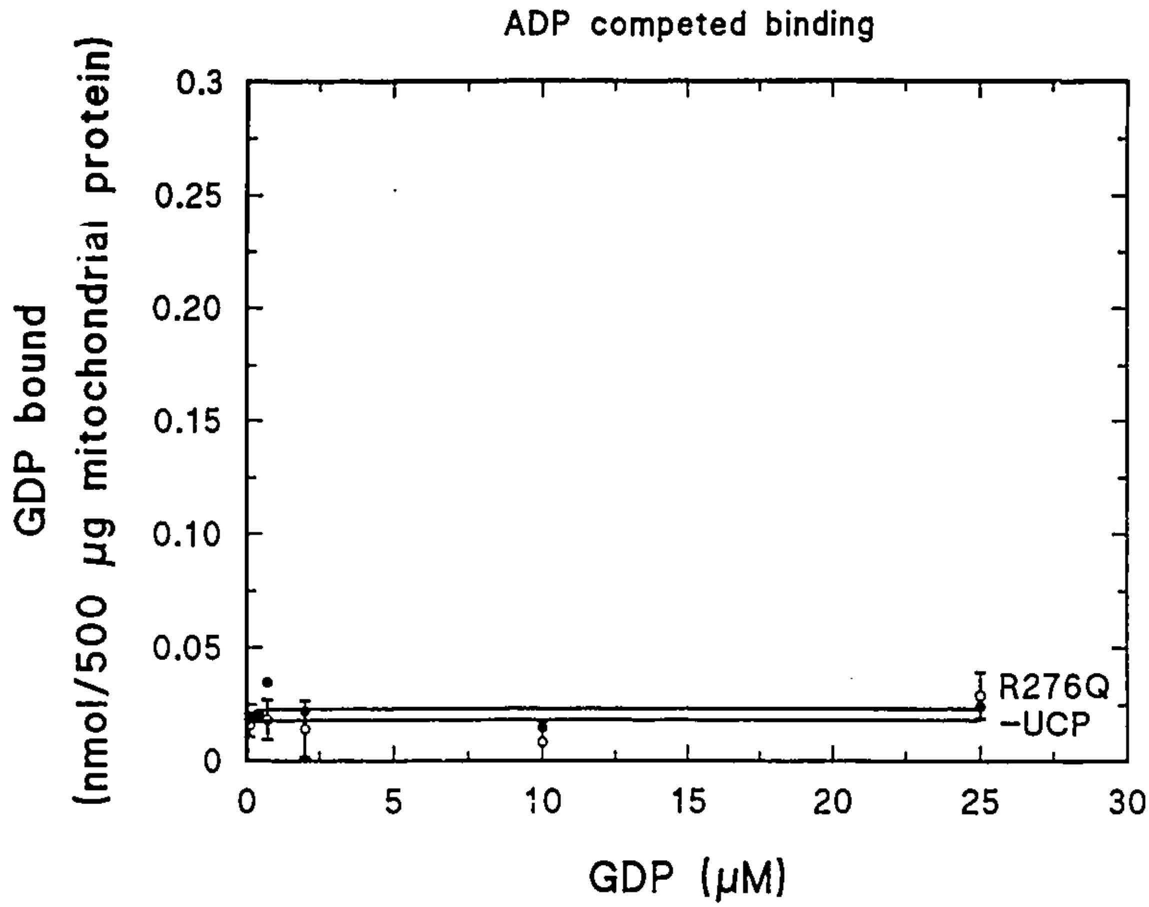

Figure 3-38. ADP Competed GDP Binding to Yeast Mitochondria: Results for Mitochondria Containing Arg276Gln UCP

The amount of bound GDP competed by ADP for the mitochondrial preparation in Figure 3-37 was calculated from the difference between GDP binding in the absence and presence of ADP, as outlined in the legend to Figure 3-10b. ADP competed GDP binding was determined for a single mitochondrial preparation containing 2 µg arg276gln (R276Q) UCP/500 µg mitochondrial protein (-•-). The binding curve for mitochondria lacking UCP (-UCP, -o-) was taken from Figure 3-10b(iv).

3-32a,b). Quantification of the arg276 mutant UCPs in yeast mitochondria revealed that arg276leu UCP was present at 18% the level and arg276gln UCP was present at 4% the level of wild type UCP in yeast mitochondria, yet the oleate stimulation was the same for each mitochondrial preparation.

Several reasons could account for these results. It is not possible that the mutant proteins have an elevated transport rate since reconstitution of the purified arg276leu UCP had the same fatty-acid catalyzed proton efflux rate per mg of UCP as purified wild type UCP from yeast and the proton efflux rate for purified arg276gln UCP was 50% of the wild type UCP rate (Murdza-Inglis *et al.*, 1994).

It is possible that only a certain amount of UCP in yeast mitochondria is activatable by oleate giving rise to the observed oleate respiratory stimulation. The rest of the UCP above a certain level may be inactive and thus not affected by oleate. The inactivation could be due to overcrowding of UCP in the membrane which could lead to improper folding of UCP in yeast mitochondria or possibly due to covalent modification of excess UCP in yeast mitochondria. In support of this theory, reconstituted UCP-catalyzed fatty acid-activated proton efflux for equal amounts of purifed hamster brown adipose tissue UCP and rat UCP purified from yeast mitochondria showed that the hamster UCP had a 2 fold higher maximum transport rate over that measured for the yeast purified UCP (M. Modriansky, personal communication). This indicates that up to 50% of the rat UCP in yeast mitochondria is inactive with respect to fatty acid-activated transport, unless the transport rate of hamster UCP is greater than that of rat UCP.

It is also possible that the majority of wild type UCP is inactive due to endogenous purine nucleotides bound to the protein, retaining it in an inactive state (see results section **3.3.3 Comparison of UCP Functions in Yeast Mitochondria**). It should be noted that in yeast mitochondria, oleate can not overcome GDP inhibition of uncoupling (data not shown). Therefore, if yeast mitochondria were isolated with GDP bound to UCP, oleate may only be able to activate UCP that is not inhibited by GDP. Since mitochondria containing UCP mutated at arg276 is impaired in GDP inhibition of oleate respiratory stimulation, lower levels of mutant protein may be able to cause the same respiratory stimulation as the higher level of wild type protein. Although reconstitution of purified arg276leu UCP showed that the mutant protein catalyzed fatty acid-activated proton efflux at the same rate per mg of protein as wild type UCP purified from yeast, bound GDP that inhibits UCP in yeast mitochondria may have been lost during purification of the protein from yeast mitochondria.

A third possibility to explain the same oleated-activated respiratory rate for different levels of wild type and mutant UCP in yeast mitochondria may lie in the steps that control respiration in mitochondria. Control of the mitochondrial respiratory rate is shared among the many steps involved in respiration (succinate utilization reactions including cytochrome *c* oxidase, proton leak, ATP turnover reactions) such that there is not one reaction step that alone controls the respiratory rate (Groen *et al.*, 1982, reviewed in Nicholls and Ferguson, 1992). The respiratory rate in the absence of ATP synthesis (state 4 respiration) is mainly controlled by the proton leak across the mitochondrial inner membrane, but there is also significant control by the succinate utilization reactions (reactions that catalyze transport of succinate into the mitochondria and its oxidation by the electron transport chain). As respiratory rate increases, there is less control from the proton leak, and more control by the succinate utilization reactions. Therefore, as oleate addition causes an increase in the respiratory rate, there may be less control of the respiratory rate due to the activity of UCP at higher respiratory rates and the respiratory rate may become limited by other steps. Therefore, even though mitochondria contain different amounts of wild type and mutant UCPs, the oleate stimulated rate may not be controlled by UCP activity at high respiratory rates and hence, oleate stimulated respiratory rates may not correlate with the level of UCP in the mitochondria. However, in the reconstituted system, fatty acid-activated proton efflux is only dependent on the activity of UCP. Therefore, direct measurements of transport rates per mg of UCP can be compared. Transport rates per mg of protein were identical between wild type and arg276leu UCP (Murdza-Inglis *et al.*, 1994), giving support to the control theory of oleate-activated respiration (if it is assumed there was no change of endogenous purine nucleotide bound to UCP during purification).

Lastly, if UCP does transport fatty acid anion out of the mitochondria as opposed to protons back into the matrix (Skulachev, 1991), the transport rate may be limited by the slow rate of oleic acid diffusion back across the mitochondrial inner membrane, rather than by UCP catalyzed transport of anion out of the matrix. If this is the case, the rate would not be dependent on the level of UCP if the anion efflux rate was greater than the fatty acid influx rate.

In order to resolve the reason for the same oleate-activated respiration for different levels of UCP in yeast mitochondria, oleate respiratory stimulation would have to be measured for varying levels of wild type UCP in yeast mitochondria. It could then be determined if the oleate respiratory stimulation was or was not proportional to the level of UCP in yeast mitochondria. Fatty acid-catalyzed proton efflux would then have to be measured for the different expression levels of UCP that were purified and reconstituted. Comparison of the transport rates per mg of UCP would determine whether the specific activity of UCP was constant or varied for different expression levels of UCP in yeast. Results from the mitochondrial and reconstitution experiments together could possibly then distinguish if the same oleate-activated respiratory rate for different amounts of wild type UCP in yeast mitochondria was observed, whether it was due to different levels of inactive protein at different expression levels or due to respiratory rate control by steps other than UCP catalyzed uncoupling.

It is possible that a combination of the factors listed above are involved in UCP activity in yeast mitochondria. A fraction of UCP in yeast mitochondria may be inactive and control of the respiratory rate may be shared among different steps in mitochondrial oxidation of succinate and fatty acid transport across the membrane.

Both mutations of arg276 to leucine and glutamine impaired GDP inhibition of oleate respiratory stimulation (Figure 3-32a,b). It is not known why changing arg276 to glutamine completely abolished GDP inhibition whereas changing arg276 to leucine decreased inhibition approximately 50 fold. It may be possible that the glutamine substitution, even though it is closer in polarity to arginine than leucine, disrupted the local conformation in UCP more so than the leucine substitution. In comparing the structures of these three residues, the third carbon in the side chain from the α-carbon in glutamine is planar due to the carbonyl group (Wingrove and Caret, 1981) whereas the third carbon in arginine and leucine are both tetrahedral. In addition, glutamine is both a hydrogen bond donor and acceptor. Thus, with its different spacial orientation and its ability to hydrogen bond, glutamine may have distorted the local conformation around position 276 in UCP, resulting in a greater loss of GDP inhibition than the leucine substitution. These mutant proteins were both purified from yeast mitochondria and reconstituted into proteoliposomes. Both mutant forms of UCP catalyzed proton efflux, but GDP inhibition of transport was abolished for both mutants (Murdza-Inglis *et al.*, 1994). The difference in response of the mutant proteins in yeast mitochondria and in proteoliosomes may be due to slightly different conformations of the proteins in the two systems resulting from purification and refolding in proteoliposomes.

To further investigate the loss of GDP inhibition, GDP binding studies to mitochondria containing these mutant proteins were carried out. Unfortunately, the background level of GDP binding to yeast mitochondria lacking UCP was quite high. Because of the lower levels of mutant proteins present in yeast mitochondria, it was difficult to measure GDP bound specifically to the mutant proteins above the background level. However, mitochondria containing arg276leu UCP bound the same level of GDP as that proposed for mitochondria containing the same amount of wild type UCP, which assumed a proportional relationship between the level of wild type UCP in yeast mitochondria and the amount of GDP bound to UCP at different wild type UCP levels in yeast mitochondria. If this is true, then the comparison indicated that GDP binding was not impaired in the arg276leu mutant UCP, even though GDP inhibition was 50 fold lower. The level of GDP bound to mitochondria containing arg276gln UCP was too low to make any inference.

It appears from the data that arginine 276 is a residue in UCP involved in GDP inhibition of transport, but does not affect transport itself and possibly does not affect GDP binding to the protein. It is thought that GDP binding to UCP induces a change in the protein, causing the protein to reside in an inactive state for ion transport (Eckerskorn and Klingenberg, 1987; Kopecky *et al*, 1987; Jezek *et al.*, 1988). The role of arg276 may be one involved in responding to GDP binding, acting as an effector residue as proposed by Jezek *et al.* (1988) to participate in the transfer of the binding signal to cause the conformational change, rather than being involved directly in binding. It is hard to conceive that all binding energy for GDP to UCP is lost by the substitution of arg276 with gln and leu, especially since the mutant proteins were found to have normal transport function, ruling out gross conformational changes in protein structure. Binding studies on the purified mutant proteins will have to be done to determine whether GDP binding was impaired in these arg276 mutant UCPs.

This is the first identification of a single residue in UCP that is directly involved in purine nucleotide regulation of UCP transport function. It is hoped that any information gained on the functional organization of UCP may also be applied to the other members of the mitochondrial transport protein family. The homologous residue of arg276 of UCP in AAC was shown to be required for growth of yeast on a non-fermentable carbon source, indicating that this residue was important in the functioning of AAC (Nelson *et al.*, 1993), although the transport function of the mutant AAC was not tested directly. It has been reported that deletion of three residues in the third domain of UCP close to arg276 (phe267, lys268 and gly269) abolished GDP inhibition of fatty acid-activated respiration of yeast mitochondria (Bouillaud *et al*, 1994). However, fatty acid-stimulation of the respiratory rate of mitochondria containing the mutant UCP was also reduced by 50% in comparison to that found for mitochondria containing the wild type protein, indicating that the mutation was not only specific to purine nucleotide inhibition and may involve a change in the overall protein conformation. Purine nucleotide binding studies to mitochondria containing the mutant UCP were not carried out in this study which would be required for further speculation as to the significance of this result.

CONCLUSIONS

4.1 SUMMARY OF RESULTS

A functional, high level heterologous expression system for UCP was established in yeast, whereby UCP gave yeast mitochondria the respiratory characteristics of brown adipose tissue mitochondria. The results clearly show that UCP is responsible for fatty acid-activated uncoupling of yeast mitochondria. The fatty acid-induced uncoupling was reversed by GDP. UCP in yeast mitochondria was found to bind GDP with a comparable affinity to that found for UCP in brown adipose tissue mitochondria, although the level of binding was lower than that measured for activated UCP in brown adipose tissue mitochondria. The seven cysteines in UCP do not serve a critical role in fatty acid-activated, GDP-inhibited uncoupling. Arginine 276 is involved in purine nucleotide regulation of UCP, but it is not known if this residue is involved directly in the binding of purine nucleotides or in propagating the response in the protein to the bound nucleotide.

The yeast expression system has proven itself to be a useful system for investi ting structure/function relationships in UCP. It provides a convenient system for expressing mutant forms of UCP such that the function of the mutant proteins can be analyzed in both yeast mitochondria and in proteoliposomes following purification and reconstitution.

4.2 FUTURE RESEARCH

Due to the tripartite nature of UCP, residues homologous to arg276 in putative transmembrane α-helices 2 and 4 corresponding to arg83 and arg182 have also been substituted with glutamine to determine any effects on function. Preliminary results from these mutant proteins purified from yeast mitochondria and reconstituted into proteoliposomes indicate that they both show the same function as UCP mutated at arg276; wild type fatty acid-activated proton flux, but nucleotide inhibition of proton flux is abolished (M. Modriansky, personal communication). Purine nucleotide binding studies to the mutant proteins have not been done. Other positively charged residues in putative membrane spanning regions have also been mutated to gln (His214, Lys267) to determine their effects, if any, on the functions of UCP. These results are not yet available.

REFERENCES

Andreyev A.Y., Bondareva, T.O., Dedukhova, V.I., Mokhova, E.N., Skulachev, V.P., Tsofina, L.M., Volkov, N.I. and Vygodina, T.V. (1989) The ATP/ADP antiporter is involved in the uncoupling effect of fatty acids. In *Anion Carriers of Mitochondrial Membranes*, A. Azzi, K.A. Nalecz, M.J. Nalecz and L. Wojtezak (eds.), Springer-Verlag, Berlin, p159-168.

Aquila, H., Link, T.A. and Klingenberg, M.K. (1987) Solute carriers involved in energy transfer of mitochondria form a homologous protein family. *FEBS Lett.* **212**, 1-9.

Aquila, H., Misra, D., Eulitz, M. and Klingenberg, M. (1982) Complete amino acid sequence of the ADP/ATP carrier from beef heart mitochondria. *Hoppe-Seyler's Z. Physiol. Chem.* **363**, S345-S349.

Arch, J.R.S. (1989) The brown adipocyte β-adrenoceptor. *Proc. Nutr. Soc.* **48**, 215-223.

Arch, J.R.S., Ainsworth, A.T., Cawthorne, M.A., Piercy, V., Sennitt, M.V., Thody, V.E., Wilson, C. and Wilson, S. (1984) Atypical β-adrenoceptor on brown adipocytes as target for anti-obesity drugs. *Nature (London)* **309**, 163-165.

Arechaga, I., Raimbault, S., Prieto, S., Levi-Meyrueis, C., Zaragoza, P., Miroux, B., Ricquier, D., Bouillaud, F. and Rial, E. (1993) Cysteine residues are not essential for uncoupling protein function. *Biochemistry* **296**, 693-700.

Ashwell, M., Holt, S., Jennings, G., Stirling, D.M., Trayhurn, P. and York, D.A. (1985) Measurement by radioimmunoassay of the mitochondrial uncoupling protein from brown adipose tissue of obese (ob/ob) mice and Zucker (fa/fa) rats at different ages. *FEBS Lett.* **179**, 233-237.

Becker, D.M. and Guarente, L. (1991) High-efficiency transformation of yeast by electroporation. *Method. Enzymol.* **194**, 182-187.

Berthiaume, L., Deichaite, I., Peseckis, S. and Resh, M.D. (1994) Regulation of enzymatic acitivity by active site fatty acylation. A new role for long chain fatty acid acylation of proteins. *J. Biol. Chem.* **269**, 6498-6505.

Birnboim, H.C. (1983) A rapid alkaline extraction method for the isolation of plasmid DNA. *Method. Enzymol.* **100**, 243-255.

Bisaccia, F., Capobianco, L., Brandolin, G. and Palmieri, F. (1994) Transmembrane topology of the mitochondrial oxoglutarate carrier assessed by peptide-specific antibodies and enzymatic cleavage. *Biochemistry* **33**, 3705-3713.

Bouillaud, F., Ricquier, D., Gulik-Krzywicki, T. and Gary-Bobo, C.M. (1983) The possible proton translocating activity of the mitochondrial uncoupling protein of brown adipose tissue. *FEBS Lett.* **164**, 272-276.

Bouillaud, F., Arechaga, I., Petit, P.X., Raimbault, S., Levi-Meyrueis, C., Casteilla, Laurent, M., Rial, E. and Ricquier, D. (1994) A sequence related to a DNA recognition element is essential for the inhibition by nucleotides of proton transport through the mitochondrial uncoupling protein. *EMBO J.* **13**, 1990-1997.

Brandolin, G., Boulay, F. Dalbon P and Vignals, P.V. (1989) Orientation of the N-terminal region of the membrane-bound ADP/ATP carrier protein explored by antipeptide antibodies and an arginine-specific endoprotease. Evidence that the accessibility of the N-terminal residues depends on the conformational state of the carrier. *Biochemistry* **28**, 1093-1100.

Brustovetsky, N. and Klingenberg, M. (1994) The reconstituted ADP/ATP carrier can mediate H+ transport by free fatty acids, which is further stimulated by mersalyl. *J. Biol. Chem.* **269**, 27329-27336.

Capobianco, L., Brandolin, G. and Palmieri, F. (1991) Transmembrane topography of the mitochondrial phosphate carrier explored by peptide-specific antibodies and enzymatic digestion. *Biochemistry* **30**, 4963-4969.

Casteilla, L., Blondel, O., Klaus, S., Raimbault, S., Diolez, P., Moreau, F., Bouillaud, F. and Ricquier, D. (1990) Stable expression of functional mitochondrial uncoupling protein in Chinese hamster ovary cells. *Proc. Natl. Acad. Sci. (USA)* **87**, 5124-5128.

Cheng, M.Y., Pollock, R.A., Hendrick, J.P. and Horwich, A.L. (1987) Import and processing of human ornithine transcarbamoylase precursor by mitochondria from *Saccharomyces cerevisiae*. *Proc. Natl. Acad. Sci. USA* **84**, 4063-4067.

Chien, S.M. and Freeman, K.B. (1984) Import of rat liver mitochondrial malate dehydrogenase: synthesis, transport and processing *in vitro* of its precursor. *J. Biol. Chem.* **259**, 3337-3342.

Cooperstein, S.J. and Lazarow, A. (1951) A microspectrophotometric method for the determination of cytochrome oxidase. *J. Biol. Chem.* **189**, 665-670.

Cunningham, S.A., Wiesinger, H. and Nicholls, D.G. (1986) Quantification of fatty acid activation of the uncoupling protein in brown adipocytes and mitochondria from the guinea-pig. *Eur. J. Biochem.* **157**, 415-420.

Desautels, M., Zaror-Behrens, G. and Himms-Hagen, J. (1978) Increased purine nucleotide binding, altered polypeptide composition, and thermogenes in brown adipose tissue mitochondria of cold-acclimated rats. *Can. J. Biochem.* **56**, 378-383.

Eckerskorn, C. and Klingenberg, M. (1987) In the uncoupling protein from brown adipose tissue the C-terminus protrudes to the c-side of the membrane as shown by tryptic cleavage. *FEBS Lett.* **226**, 166-170.

Emr, S.D. (1990) Heterologous gene expression in yeast. *Method. Enzymol.* **185**, 231-233.

Engelman, D.M., Steitz, T.A. and Goldman, A. (1986) Identifying nonpolar transbilayer helices in amino acid sequences of membrane proteins. *Annu. Rev. Biophys. Biophys. Chem.* **15**, 321-353.

Etcheverry, T. (1990) Induced expression using yeast copper metallothionein promoter. *Method. Enzymol.*, **185**, 319-329

Feil, S. and Rafael, J. (1994) Effect of acclimation temperature on the concentration of uncoupling protein and GDP binding in rat brown fat mitochondria. *Eur. J. Biochem.* **219**, 681-690.

Fernandez, M., Nicholls, D.G. and Rial, E. (1987) The uncoupling protein from brown-adipose-tissue mitochondria. Chymotrypsin-induced structural and functional modifications. *Eur. J. Biochem.* **164**, 675-680.

Freeman, K.B., Hartlen, R. and Inglis, D.L. (1995) Protein import into yeast mitochondria, in *Plant Metabolism*, in press.

French, R.R., Gore, M.G. and York, D.A. (1988) A study of GDP binding to purified thermogenin protein from brown adipose tissue. *Biochem. J.* **251**, 385-389.

Futcher, A.B. (1988) The 2 μm circle plasmid of *Saccharomyces cerevisiae*. *Yeast* **4**, 27-40.

Gasser, S.M. (1983) Import of polypeptides into isolated yeast mitochondria. *Method. Enzymol.*, **97**, 329-336.

Goubern, M., Chapey, M.-F., Laury, M.-C. and Portet, R. (1993) *In vivo* β-adrenergic induction of the unmasking of the uncoupling protein in rat brown fat. *Comp. Biochem. Physiol.* **106C**, 171-177.

Goubern, M., Chapey, M.-F., Senault, C., Laury, M.-C., Yazbeck, J., Miroux, B., Ricquier, D. and Portet, R. (1992) Effect of sympathetic de-activation on thermogenic function and membrane lipid composition in mitochondria of brown adipose tissue. *Biochim. Biophys. Acta* **1107**, 159-164.

Granneman, J.G. and Whitty, C.J. (1991) CGP 12177A modulates brown fat adenylate cyclase activity by interacting with two distinct receptor sites. *J. Pharm. Exper. Therap.* **256**, 421-425.

Gregoret, L.M., Rader, S.D., Fletterick, R.J. and Cohen, F.E. (1991) Hydrogen bonds involving sulfur atoms in proteins. *Proteins: Structure, Function, and Genetics* **9**, 99-107.

Gregory, E.M., Yost, F.J., Jr., Rohrback, M.S. and Harrison, J.M. (1971) Selective chemical modification of malate dehydrogenase. N-Ethylmaleimide modification of active center sulfhydryl residues. *J. Biol. Chem.* **246**, 5491-5497.

Gribskov, C.L., Henningfield, M.F., Swick, A.G. and Swick, R.W. (1986) Evidence for unmasking of rat brown-adipose-tissue mitochondrial GDP-binding sites in response to acute cold exposure. Effects of washing with albumin on GDP binding. *Biochem. J.* **233**, 743-747.

Groen, A.K., Wanders, R.J.A., Westerhoff, H.V., van der Meer, R. and Tager, J.M. (1982) Quantification of the contribution of various steps to the control of mitochondrial respiration. *J. Biol. Chem.* **257**, 2754-2757.

Hamilton, R., Watanabe, C.K. and de Boer, H.A. (1987) Compilation and comparison of the sequence context around the AUG start codons in *Saccharomyces cerevisiae* mRNAs. *Nucl. Acids Res.* **15**, 3581-3593.

Hayaishi, O. (1962) Kynurenine Hydroxylase. *Methods Enzym.* **5**, 807-809.

Heaton, G.M. and Nicholls, D.G. (1977) The structural specificity of the nucleotide-binding site and the reversible nature of the inhibition of proton conductance induced by bound nucleotides in brown adipose tissue mitochondria. *Biochem. Soc. Trans.* **5**, 210-212.

Heaton, G.M., Wagenvoord, R.J., Kemp, A. Jr. and Nicholls, D.G. (1978) Brown-adipose-tissue mitochondria: photoaffinity labelling of the regulatory site of energy dissipation. *Eur. J. Biochem.* **82**, 515-521.

Henningfield, M.F. and Swick, R.W. (1991) Unmasking of GDP binding sites on hamster brown adipose tissue mitochondria and uncoupling protein. *Comp. Biochem. Physiol.* **99B**, 821-825.

Himms-Hagen, J. (1990) Brown adipose tissue thermogenesis: interdisciplinary studies. *FASEB J.* **4**, 2890-2898.

Hoffman, B., Stöckl, A., Schlame, M., Beyer, K. and Klingenberg, M. (1994) The reconstituted ADP/ATP carrier activity has an absolute requirement for cardiolipin as shown in cysteine mutants. *J. Biol. Chem.* **269**, 1940-1944.

Huang, S-G. and Klingenberg, M. (1995) Fluorescent nucleotide derivatives as specific probes for the uncoupling protein: Thermodynamics and kinetics of binding and the control by pH. *Biochemistry* **34**, 349-360.

Ito, H., Fukuda, Y., Murata, K. and Kimura, A. (1983) Transformation of intact yeast cells treated with alkali cations. *J. Bacteriol.* **153**, 163-168.

Ježek, P. (1987) Sulfhydryl groups are involved in H^+ translocation via the uncoupling protein of brown adipose tissue mitochondria. *FEBS Lett.* **211**, 89-93.

Ježek, P. and Drahota, Z. (1989) Sulfhydryl groups of the uncoupling protein of brown adipose tissue mitochondria. *Eur. J. Biochem.* **183**, 89-95.

Ježek, P. and Garlid, K.D. (1990) New substrates and competitive inhibitors of the Cl^- translocating pathway of the uncoupling protein of brown adipose tissue mitochondria. *J. Biol. Chem.* **265**, 193303-19311.

Ježek, P. and Freisleben, H.-J. (1994) Fatty acid binding site of the mitochondrial uncoupling protein. Demonstration of its existence by EPR spectroscopy of 5-DOXYL-stearic acid. *FEBS Lett.* **343**, 22-26.

Ježek, P., Drahota, Z. and Ring, K. (1990) The activating effect of fatty acid on the mitochondrial uncoupling protein reconstituted in liposomes. *J. Lipid Mediators* **2**, 85-94.

Ježek, P., Orosz, D.E. and Garlid, K.D. (1990) Reconstitution of the uncoupling protein of brown adipose tissue mitochondria, demonstration of GDP-sensitive halide anion uniport. *J. Biol. Chem.* **265**, 19296-19302.

Ježek, P., Orosz, D.E., Modriansky, M. and Garlid, K.D. (1994) Transport of anions and protons by the mitochondrial uncoupling protein and its regulation by nucleotides and fatty acids. *J. Biol. Chem.* **269**, 26184-26190.

Johnston, M. and Davis, R.W. (1984) Sequences that regulate the divergent *Gal1-Gal10* promoter in *Saccharomyces cerevisiae*. *Mol. Cell. Biol.* **4**, 1440-1448.

Kamp, F. and Hamilton, J.A. (1992) pH gradients across phospholipid membranes caused by fast flip-flop of unionized fatty acids. *Proc. Nat'l. Acad. Sci. (USA)* **89**, 11367-11370.

Kaplan, R.S., Mayor, J.A. and Wood, D.O. (1993) The mitochondrial tricarboxylate transport protein. *J. Biol. Chem.* **268**, 13682-13690.

Katiyar, S.S. and Shrago, E. (1989) Reconstitution of purified brown adipose tissue mitochondria uncoupling protein: Demonstration of separate identity of nucleotide binding and proton translocation sites by chemical probes. *Proc. Natl. Acad. Sci. (USA)* **86**, 2559-2562.

Katiyar, S.S. and Shrago, E. (1991) Differential interaction of fatty acids and fatty acyl CoA esters with the purified/reconstituted brown adipose tissue mitochondrial uncoupling protein. *Biochem. Biophys. Res. Commun.* **175**, 1104-1111.

Kaufman, R.J. (1990) Vectors used for expression in mammalian cells. *Method. Enzymol.* **185**, 487-511.

Klaus, S., Casteilla, L., Bouillaud, F., Raimbault, S. and Ricquier, D. (1990) Expression of the brown fat mitochondria uncoupling protein in *Xenopus* oocytes and import into mitochondrial membrane. *Biochem. Biophys. Res. Commun.* **167**, 784-789.

Klingenberg, M. (1988) Nucleotide binding to uncoupling protein. Mechanism of control by protonation. *Biochemistry* **27**, 781-791.

Klingenberg, M. (1990) Mechanism and evolution of the uncoupling protein of brown adipose tissue. *TIBS* **10**, 108-112.

Klingenberg, M. (1993) Dialectics in carrier research: the ADP/ATP carrier and the uncoupling protein. *J. Bioenerg. Biomem.* **225**,, 447-457.

Klingenberg, M. and Winkler, E. (1985) The reconstituted isolated uncoupling protein is a membrane potential driven H^+ translocator. *EMBO J.* **4**, 3087-3092.

Klingenberg, M. and Appel, K. (1989) The uncoupling protein dimer can form a disulfide cross-link between the mobile C-terminal SH groups. *Eur. J. Biochem.* **180**, 123-131.

Kopecký, J., Ježek, P., Drahota, Z. and Houštěk, J. (1987) Control of uncoupling protein in brown-fat mitochondria by purine nucleotides. Chemical modification by diazobenzenesulfonate. *Eur. J. Biochem.* **164**, 687-694.

Kopecký, J., Guerrieri, F., Ježek, P., Drahota, Z. and Houštěk, J. (1984) Molecular mechanism of uncoupling in brov adipose tissue mitochondria. *FEBS Lett.* **170**, 186-190.

Kuan J. and Saier, H. Jr. (1993) The mitochondrial carrier family of transport proteins: Structural, functional, and evolutionary relationships. *Crit. Rev. Biochem. Mol. Biol.* **23**, 209-233.

Kunkel, T.A., Roberts, J.D. and Zakour, R.A. (1987) Rapid and efficient site-specific mutagenesis without phenotypic selection. *Method. Enzymol.* **154**, 367-382.

Laemmli, U.K. (1970) Cleavage of structural proteins during the assembly of the head of bacteriophage T4. *Nature (London)*, **227**, 680-685.

Lehninger, A.L., Nelson, D.L. and Cox, M.M. (1993) Principles of Biochemistry, Worth Publishers, New York, p559.

Levinson, A.D. (1990) Expression of heterologous genes in mammalian cells. *Method. Enzymol.* **185**, 485-487.

Lin, C.S. and Klingenberg, M. (1980) Isolation of the uncoupling protein from brown adipose tissue mitochondria. *FEBS Lett.* **113**, 299-303.

Lin, C.S. and Klingenberg, M. (1982) Characteristics of the isolated purine nucleotide binding protein from brown fat mitochondria. *Biochemistry* **21**, 2950-2956.

Lowry, O.H., Rosebrough, N.J., Farr, A.L. and Randall, R.J. (1951) Protein measurement with the folin phenol reagent. *J. Biol. Chem.* **193** 265-275.

Mangani, S. and Håkansson, K. (1992) Crystallographic studies of the binding of protonated and unprotonated inhibitors to carbonic anhydrase using hydrogen sulphide and nitrate anions. *Eur. J. Biochem.* **210**, 867-871.

Mayinger, P. and Klingenberg, M. (1992) Labeling of two different regions of the nucleotide binding site of the uncoupling protein from brown adipose tissue mitochondria with two ATP analogs. *Biochemistry* **31**, 10536-10543.

Miroux, B., Frossard, V., Raimbault, S., Ricquier, D. and Bouillaud, F. (1993) The topology of the brown adipose tissue mitochondrial uncoupling protein determined with antibodies against its antigenic sites revealed by a library of fusion proteins. *EMBO J.* **12**, 3739-3745.

Miroux, B., Casteilla, L., Klaus, S., Raimbault, S., Grandin, S., Clement, J.M., Ricquier, D. and Bouillaud, F. (1992) Antibodies selected from whole antiserum by fusion proteins as tools for the study of the topology of mitochondrial membrane proteins. *J. Biol. Chem.* **267**, 13603-13609.

Mohell, N. and Dicker, A. (1989) The β-adrenergic radioligand [^{3}H]CGP-12177, generally classified as an antagonist, is a thermogenic agonist in brown adipose tissue. *Biochem. J.* **261**, 401-405.

Murdza, D.L. (1988) 4B6 Thesis, McMaster University. Examination for the expression of uncoupling protein in *Saccharomyces cerevisiae*, 71 p.

Murdza-Inglis, D.L., Modriansky, M., Patel, H.V., Woldegiorgis, G., Freeman, K.B. and Garlid. K.D. (1994) A single mutation in uncoupling protein of rat brown adipose tissue mitochondria abolishes GDP sensitivity of H^+ transport. *J. Biol. Chem.* **269**, 7435-7438.

Mylin, L.M., Hofmann, K.J., Schultz, L.D. and Hopper, J.E. (1990) Regulated *GAL4* Expression Cassette Providing Controllable and High-Level Output from High-Copy Galactose Promoters in Yeast. *Method. Enzymol.* **185**, 297-308.

Nedergaard, J. and Cannon, B. (1992) The uncoupling protein thermogenin and mitochondrial thermogenesis in *Molecular Mechanisms in Bioenergetics*, New Comprehensive Biochemistry **23**, L. Ernster (ed.), Elsevier Science Publishers, 385-420.

Nedergaard, J. and Cannon, B. (1994) Sulfonates are low-affinity ligands for the GDP-binding site of brown-fat mitochondria. *Biochim. Biophys. Acta* **1185**, 311-317.

Nelson, D.R., Lawson, J.E., Klingenberg, M. and Douglas, M.G. (1993) Site-directed mutagenesis of the yeast mitochondrial ADP/ATP translocator. *J. Mol. Biol.* **230**, 1159-1170.

Nicholls, D.G. (1974a) Hamster brown adipose tissue mitochondria: the control of respiration and the proton electrochemical potential gradient by possible physiological effectors of the proton conductance of the inner membrane. *Eur. J. Biochem.* **49**, 573-583.

Nicholls, D.G. (1974b) The influence of respiration and ATP hydrolysis on the proton-electrochemical gradient across the inner membrane of rat-liver mitochondria as determined by ion distribution. *Eur. J. Biochem.* **50**, 305-315.

Nicholls, D.G. (1976) Hamster brown-adipose tissue mitochondria: purine nucleotide control of the ion conductance of the inner membrane, the nature of the nucleotide binding site. *Eur. J. Biochem.* **62**, 223-228.

Nicholls, D.G (1977) The effective proton conductance of the inner membrane of mitochondria from brown adipose tissue: dependancy on proton electrochemical potential gradient. *Eur. J. Biochem.* 77, 349-356.

Nicholls, D.G. and Lindberg, O. (1973) Brown-adipose-tissue mitochondriaL the influence of albumin and nucleotides on passive ion permeability. *Eur. J. Biochem.* *37*, 523-530.

Nicholls, D.G. and Ferguson, S.J. (eds.) (1992) Bioenergetics 2. Academic Press Ltd., San Diego., 255p.

Nicholls, D.G., Snelling, R. and Rial, E. (1984) Proton and calcium circuits across the mitochondrial inner membrane. *Biochem. Soc. Trans.* p388-390.

Nicholls, D.G., Cunningham, S.A. and Rial, E. (1986) The bioenergetic mechanisms of brown adipose tissue thermogenesis. in *Brown Adipose Tissue*, P. Trayhurn and D.G. Nicholls (eds.), Edward Arnold Publishers Ltd., London, p53-85.

Orosz, D.E. (1993) PhD. Thesis: Kinetics of ion transport mediated by the uncoupling protein of brown adipose tissue mitochondria. Medical College of Ohio, 221p.

Palmieri, F. (1994) Mitochondrial carrier proteins. *FEBS Lett.* **346**, 48-54.

Palmieri, F., Bisaccia, F., Capobianco, L., Dolce, V., Fiermonte, G., Iacobazzi, V. and Zara, V. (1993) Transmembrane topology, genes, and biogenesis of the mitochondrial phosphate and oxoglutarate carriers. *J. Bioenerg. Biomem.* **25**, 493-501.

Peachey, T., French, R.R. and York, D.A. (1988) Regulation of GDP binding and uncoupling-protein concentration in brown-adipose-tissue mitochondria: the effects of cold-acclimation, warm acclimation and noradrenaline. *Biochem. J.* **249**, 451-457.

Phelps, A., Schobert, C.T. and Wohlrab, H. (1991) Cloning and characterization of the mitochondrial phosphate transport protein gene from the yeast *Saccharomyces cerevisiae*. *Biochemistry* **30**, 248-252.

Phelps, A. and Wohlrab, H. (1993) Cys28 of the mitochondrial phosphate transport protein is responsible for the inhibition the transport by oxygen. *FASEB J.* 7(Abs.), 321.

Price, V.L., Taylor, W.E., Clevenger, W., Worthington, M. and Young, E.T. (1990) Expression of heterologous proteins in *Saccharomyces cerevisiae* using *ADH2* promoter. In *Gene Expression Technology*, D.V. Goeddel (ed.), Academic Press, Inc., San Diego, CA. *Methods in Enzymology* **185**, 308-318.

Rafael, J., Pampel, I. and Wang, X. (1994) Effect of pH and MgCl2 on the binding of purine nucleotides to the uncoupling protein in membrane particles from brown fat mitochondria. *Eur. J. Biochem.* **223**, 971-980.

Rawlings, N.D. and Barrett, A.J., eds. (1994) Families of cysteine peptidases. *Method. Enzymol.* **244**, 461-487.

Rial, E. and Nicholls, D.G. (1986) Chemical modification of the brown-fat-mitochondrial uncoupling protein with tetranitromethane and *N*-ethylmaleimide. A cysteine residue is implicated in the nucleotide regulation of anion permeability. *Eur. J. Biochem.* **161**, 689-694.

Rial, E. and Nicholls, D.G. (1989) On the mechanism of transport by the uncoupling protein from brown adipose tissue mitochondria. In *Anion Carriers of Mitochondrial Membranes*, A. Azzi et al. (eds.), Springer-Verlag, Berlin, p.261-267.

Rial, E., Poustie, A. and Nicholls, D.G. (1983) Brown adipose tissue mitochondria: the regulation of the 32000 Mr uncoupling protein by fatty acids and purine nucleotides. *Eur. J. Biochem.* **137**, 197-203.

Ridley, R.G., Patel, H., Gerber, G.E., Morton, R. and Freeman, K.B. (1986) Complete nucleotidee and derived amino acid sequence of cDNA encoding the mitochooondrial uncoupling protein of rat brown adipose tissue: lack of a mitochondrial targeting presequence. *Nucl. Acid. Res.* **10**, 4025-4035.

Robillard, G.T. and Konings, W.N. (1982) A hypothesis for the role of dithiol-disulfide interchange in solute transport and energy-transducing processes. *Eur. J. Biochem.* **127**, 597-604.

Rose, A.B. and Broach, J.R. (1990) Propogation and expression of cloned genes in yeast: 2 μM circle-based vectors. *Method. Enzymol.* **185**, 234-279.

Runswick, M.J., Powell, S.J., Nyren, P. and Walker, J.E. (1987) Sequence of the bovine mitochondrial phosphate carrier protein: structural relationship to ADP/ATP translocase and the brown fat mitochondrial uncoupling protein. *EMBO J.* **6**, 1367-1373.

Runswick, M.J., Walker, J.EE., Biasaccia, F., Iacobazzi, V. and Palmieri, Ferdinando. (1990) Sequence of the bovine 2-oxoglutarate/malate carrier protein: structural relationship to other mitochondrial transport proteins. *Biochemistry* **29**, 11033-11040.

Sambrook, J., Fritsch, E.F. and Maniatis, T. (1989) Molecular Cloning. A Laboratory Manual, Volumes 1, 2 and 3. Cold Spring Harbor Laboratory Press, Cold Spring Harbor, NY.

Saraste M. and Walker, J.E. (1982) Internal sequence repeats and the path of polypeptide in mitochondrial ADP/ATP translocase. *FEBS Lett.* **144**, 250-254.

Scarpace, P.J. and Matheny, M. (1991) Adenylate cyclase agonist properties of CGP-12177A in brown fat: evidence for atypical β-adrenergic receptors. Am. J. Physiol. **260**, E226-E231.

Schleyer, M., Schmidt, B. and Neupert, W. (1982) Requirement of a membrane potential for the posttranslational transfer of proteins into mitochondria. *Eur. J. Biochem.* **125**, 109-116.

Sharp, P.M. Tuohy, T.M.F. and Mosurski, K.R. (1986) Codon usage in yeast: cluster analysis clearly differentiates highly and lowly expressed genes. *Nucl. Acid. Res.* **14**, 5125-5143.

Skulachev, V.P. (1991) Fatty acid circuit as a physiological mechanism of uncoupling of oxidative phosphorylation. *FEBS Lett.* **294**, 158-162.

Spector, A.A., John, K. and Fletcher, J.E. (1969) Binding of long-chain fatty acids to bovine serum albumin. *J. Lipid Res.* **10**, 56-66.

Springman, E.B., Angleton, E.L., Birkedal-Hansen, H. and Van Wart, H.E. (1990) Multiple modes of activation of latent human fibroblast collagenase: Evidence for the role of a Cys^{73} active-site zinc complex in latency and a "cysteine switch" mechanism for activation. *Proc. Nat'l. Acad. Sci. (USA)* **87**, 364-368.

Sterns, T., Ma, H. and Botstein, D. (1990) Manipulating yeast genome using plasmid vectors. *Method. Enzymol.* **185**, 280-296.

Strieleman, P.J., Schalinske, K.L. and Shrago, E. (1985) Partial purification and functional reconstitution of GDP sensitive brown adipose tissue mitochondria uncoupling protein using octyl glucoside. *Biochem. Biophys. Res. Commun.* **127**, 509-516.

Strieleman, P.J., Schalinske, K.L. and Shrago, E. (1985b) Fatty acid activation of the reconstituted brown adipose tissue mitochondria uncoupling protein. *J. Biol. Chem.* **260**, 13402-13405.

Stryer, L. (1995) Biochemistry, Fourth Edition, W.H. Freeman and Company, New York, p284.

Sundin, U. and Cannon, B. (1980) GDP-binding to the brown fat mitochondria of developing and cold-adapted rats. *Comp. Biochem. Physiol.* **65B**, 463-471.

Swick, A.G. and Swick, R.W. (1986) Rapid changes in number of GDP binding sites on brown adipose tissue mitochondria. *Am. J. Physiol.* **251**, E192-E195.

Swick, A.G. and Swick, R.W. (1988) Changes in GDP binding to brown adipose tissue mitochondria and the uncoupling proteins. *Am. J. Physiol.* **251**, E865-E870.

Towbin, H., Staehelin, T. and Gordon, J. (1979) Electrophoretic transfer of proteins from polyacrylamide gels to nitrocellulose sheets: Procedure and some applications. *Proc. Nat'l. Acad. Sci. USA* **76**, 4350-4354.

Trayhurn, P., Ashwell, M., Jennings, G., Richard, D. and Stirling, D.M. (1987) Effect of warm or cold exposure on GDP binding and uncoupling protein in rat brown fat. *Am. Physiol. Soc.*, E237- E243.

Trayhurn, P. and Milner, R.E. (1989) A commentary on the interpretation of in vitro biochemical measures of brown adipose tissue thermogenesis. *Can J. Physiol. Pharmacol.* **67**, 811-819.

Walker, J.E., and Runswick, M.J. (1993) The mitochondrial transport protein superfamily. *J. Bioener. Biomem.* **25**, 435-446.

Winkler, E. and Klingenberg, M. (1992) Photoaffinity labeling of the nucleotide-binding site of the uncoupling protein from hamster brown adipose tissue. *Eur. J. Biochem.* **203**, 295-304.

Winkler, E. and Klingenberg, M. (1994) Effect of fatty acids on H^+ transport activity of the reconstituted uncoupling protein. *J. Biol. Chem.* **269**, 2508-2515.

Wojtczak, L. and Schonfeld, P. (1993) Effect of fatty acid on energy coupling processes in mitochondria. *Biochim. Biophys. Acta.* **1183**, 41-57.

Yaffe, M.P. (1991) Analysis of Mitochondrial Function and Assembly. *Method. Enzymol.* **194**, 627-643.

Yee, V.C., Pedersen, L.C., Trong, I.L., Bishop, P.D., Stenkamp, R.E. and Teller, D.C. (1994) Three-dimensional structure of a transglutaminase: Human blood coagulation factor XIII. *Proc. Nat'l. Acad. Sci. (USA)* **91**, 7296-7300.

Zhao, J., Unelius, L., Bengtsson, T., Cannon, B. and Nedergaard, J. (1994) Coexisting β-adrenoceptor subtypes: significance for thermogenic process in brown fat cells. *Am. J. Physiol.* **267**, C969-C979.

Zheng, J., Knighton, D.R., Eyck, L.F.T., Karlsson, R., Xuong, N-H., Taylor, S.S. and Sowadski, J.M. (1993) Crystal structure of the catalytic subunit of cAMP-dependent protein kinase complexed with MgATP and peptide inhibitor. *Biochemistry* **32**, 2154-2161.

APPENDIX

Publications

Murdza-Inglis, D.L., Patel, H.V., Freeman, K.B., Jezek, P., Orosz, D.E. and Garlid, K.D. (1991) Functional reconstitution of rat uncoupling protein following its high level expression in yeast. *J. Biol. Chem.* **266**, 11871-11875.

Murdza-Inglis, D.L., Modriansky, M., Patel, H.V., Woldegiorgis, G., Freeman, K.B. and Garlid, K.D. (1994) A single mutation in uncoupling protein of rat brown adipose tissue mitochondria aoolishes GDP sensitivity of H^+ transport. *J. Biol. Chem.* **269**, 7435-7438.

THE JOURNAL OF BIOLOGICAL CHEMISTRY
Vol. 266, No. 18, Issue of June 25, pp. 11871-11875, 1991
Printed in U.S.A.

Functional Reconstitution of Rat Uncoupling Protein Following Its High Level Expression in Yeast*

(Received for publication, November 7, 1990)

Debra L. Murdza-Inglis‡§, Hasmukh V. Patel‡, Karl B. Freeman‡¶, Peter Jezek||, David E. Orosz||, and Keith D. Garlid¶||

From the ‡Department of Biochemistry, McMaster University, Hamilton, Ontario L8N 3Z5, Canada and the ||Department of Pharmacology, Medical College of Ohio, Toledo, Ohio 43699

Small mammals, including human infants, rely on nonshivering thermogenesis for a substantial portion of their body heat during exposure to cold. This thermogenesis is mediated in large part by the uncoupling protein, which is found exclusively within the inner membrane of brown adipose tissue mitochondria. The sole function of uncoupling protein is to provide a regulated transport pathway for electrophoretic back-flux of H^+ ions into the mitochondrial matrix, thereby dissipating the protonmotive force and producing heat. Thus, uncoupling protein is unique with respect to both its physiological role and its tissue expression. We have now achieved high level expression of rat uncoupling protein in yeast, with import into yeast mitochondria at levels, 70–100 μg/mg of mitochondrial protein, similar to those observed in brown adipose tissue mitochondria from cold-adapted rats. When the expressed protein was purified and reconstituted into liposomes, the proteoliposomes exhibited GDP-sensitive proton and chloride uniports that were inhibited by GDP with K_i values similar to those obtained with native protein. Moreover, the molecular activities of the expressed protein with respect to Cl^- and H^+ transport were indistinguishable from those of native protein. The availability of unlimited amounts of functional, expressed uncoupling protein will now permit application of site-directed mutagenesis to the many intriguing aspects of uncoupling protein structure and function.

The uncoupling protein (UCP)[1] provides a regulated transport pathway for electrophoretic back-flux of protons into the mitochondrial matrix, thereby dissipating protonmotive force and producing heat. H^+ transport is inhibited by purine nucleotides and activated by fatty acids, but the detailed mechanism of H^+ transport and its regulation remain unknown (1–3). UCP also transports monovalent anions electrophoretically, and transported anions range in size from halides to large, unipolar, amphiphilic anions such as alkylsulfonates (4, 5). The hydrophobic alkylsulfonates are potent competitive inhibitors of Cl^- transport and are also transported at faster rates than smaller hydrophilic anions (4, 5). Anion transport is inhibited by purine nucleotides whose K_i values increase with anion hydrophobicity (5). Hydrophilic sulfhydryl reagents selectively inhibit proton transport without inhibiting anion transport (6). These results support a hypothesis that anions and protons are transported through different pathways (7) and that anions must surmount a hydrophobic surface barrier before entering their channel (5). Structural similarities between some of the new UCP substrates and fatty acids led Garlid (8) to propose that UCP contains a fatty acid-docking site that lowers the energy barrier to anions, thereby permitting unintentional electrophoretic anion transport. According to this hypothesis, anion transport through UCP is a probe of the fatty acid regulatory site.

Although UCP is found exclusively in brown adipose tissue mitochondria, it exhibits pronounced structural homologies, including dimeric character, with the P_i-H^+ symporter and the adenine nucleotide antiporter, which are found in all mitochondria. It was considered difficult to understand how these homologies manifest themselves, given that the three porters exhibit different transport properties (8, 9). However, the adenine nucleotide antiporter and UCP share a nucleotide-binding site and a hydrophobic region that interacts with fatty acid hydrocarbon tails (10–12). Jezek and Garlid (5) pointed out that all three porters may possess an internal translocation pathway for protons (which may be blocked in the adenine nucleotide antiporter) and that specific changes in their sequences may account for the different charge specificities and transport modes (5). To understand these differences and similarities will require an extensive study of mutants of all three porters.

An expression system will be necessary in order to address questions about the structure-function relationships of UCP using site-directed mutagenesis. Casteilla *et al.* (13) have reported functional expression of UCP in Chinese hamster ovary cells; however, function was measured in intact mitochondria, whose complexity complicates evaluation of the results. Thus, the scientific obstacle at present is that we do not know whether the expressed protein functions normally with respect to anion and proton transport and regulation. It will be necessary to show definitively that expressed UCP has the properties claimed for it, and this will require studies on the purified protein. The technical obstacle is that high level expression, which heretofore has not been achieved, is necessary for discriminating structure-function studies, because the molecular activity of UCP is exceedingly low (14).

* This study was supported by Grant MT-1910 (to K. B. F.) from the Medical Research Council of Canada and Grants GM-31086 and HL-36573 (to K. D. G.) from the National Institutes of Health. The costs of publication of this article were defrayed in part by the payment of page charges. This article must therefore be hereby marked "*advertisement*" in accordance with 18 U.S.C. Section 1734 solely to indicate this fact.

§ Recipient of a Medical Research Council of Canada Studentship.

¶ To whom reprint requests should be addressed.

[1] The abbreviations used are: UCP, uncoupling protein; HEPES, 4-(2-hydroxyethyl)-1-piperazineethanesulfonic acid; SDS, sodium dodecyl sulfate; PAGE, polyacrylamide gel electrophoresis; TEA, tetraethylammonium; TES, N-tris(hydroxymethyl)methyl-2-aminoethanesulfonic acid; PBFI, potassium-binding benzofuran isopthalate.

We now report expression of 70–100 μg of UCP/mg of yeast mitochondrial protein. This high level of expression, which is similar to that achieved in brown adipose tissue mitochondria of cold-adapted rats (15), is shown to provide amounts of UCP that have the activities of the native protein and are more than adequate for quantitative assays of function *in vitro*.

EXPERIMENTAL PROCEDURES

Materials—The *Escherichia coli/Saccharomyces cerevisiae* shuttle vector pCGS110 was a kind gift of Dr. D. T. Moir, Collaborative Research Inc. pGEM 5Zf(+) was from Promega, and pSPT18 was from Pharmacia LKB Biotechnology Inc. The *S. cerevisiae* strain JB 516 (*MATa,ura3,ade1,leu2,his4,gal*$^{+}$) was the kind gift of Dr. A. B. Futcher (McMaster University). Yeast lytic enzyme (1×10^{5} units/g) was obtained from ICN Biochemicals. Fatty acid-free bovine serum albumin was obtained from Sigma. Oligonucleotides were purchased from the Central Facility of the Institute for Molecular Biology and Biotechnology at McMaster University. The fluorescent probes 6-methoxy-*N*-(3-sulfopropyl)quinolium and PBFI were obtained from Molecular Probes, Inc.

Yeast Expression System—The *S. cerevisiae* strain JB 516 was transformed with the *E. coli/S. cerevisiae* multicopy shuttle vector pCGS110 containing the *Kpn*I/*Pst*I fragment of rat UCP cDNA (16) inserted at the unique *Bam*HI site beside the inducible *Gal*I promoter. The vector contained the *ura3* gene as the yeast selectable marker. To increase the level of expression of UCP in yeast, the 5′ region around the initiating ATG of UCP cDNA was altered to resemble the sequence of a highly expressed yeast glyceraldehyde-3-phosphate dehydrogenase gene (G3PDa) (17) and highly used codons in yeast (18).

Rat UCP DNA:	TCTGCCCTCCGAGCCAAGATGGTGAGTT
G3PDa DNA:	CACACATAAATAAACAAAATGGTTAGAG
Altered DNA:	GACACATAAATAAACAAAATGGTCTCTT
	ACGTCTGTGTATTTATTTGTTTTACCAGAGAAGC

The altered UCP cDNA was constructed in pGEM5Zf by cloning the *Sph*I/*Taq*I fragment from pSPT18UCP into *Sph*I/*Pst*I cut pGEM5Zf using two complementary oligonucleotides designed to have *Pst*I and *Taq*I sites at their ends and the altered 5′ region. The modified UCP cDNA was removed from pGEM5ZfUCP with *Pst*I, ligated into *Bam*HI cut pCGS110 with an 8-nucleotide-long bridge and then transformed into yeast. Yeast transformants were grown at 30 °C in selective medium containing 0.17% yeast nitrogen base, 0.5% $(NH_4)_2SO_4$, and 0.005% each of adenine, leucine, and histidine. The carbon source was 2% lactate, 0.05% glucose (19).

Mitochondrial Isolation—Mitochondria were isolated from yeast transformants as described by Gasser (20) from cells induced with 0.2% galactose for 8–10 h (21, 22). The nuclear fraction was recovered at 3500 rpm for 5 min, and the mitochondrial fraction, at 9000 rpm for 10 min. Mitochondria were resuspended in a solution containing 0.6 M mannitol, 20 mM Hepes-KOH, pH 7.4, and 0.1% fatty acid-free bovine serum albumin.

Inner Membrane Preparation—Yeast mitochondria were fractionated in a 1.0-ml volume using a 0.4:1.0 ratio of digitonin to mitochondrial protein (23). The resulting mitoplasts were resuspended in 500 μl of hypotonic medium containing 10 mM Tris, 1 mM EDTA, pH 7.2, and sonicated 3 × 20 s in a bath sonicator to release the matrix contents. Membranes were collected at 150,000 × *g* for 20 min and resuspended in 500 μl of the mitochondrial resuspension buffer described above. The Lowry method was used to determine protein concentration in the fractions. Marker enzyme assays were performed on each fraction according to published procedures and included the outer membrane marker, kynurenine hydroxylase (24), the inner membrane marker, cytochrome oxidase (25), and the matrix marker, malate dehydrogenase (26).

Mitochondrial Respiration—Respiration of yeast mitochondria was determined using the YSI 5300 monitor, the 5357 micro oxygen probe and the 5356 micro oxygen chamber, which had a capacity of 0.6 ml. The reaction buffers contained 0.65 M sorbitol, 10 mM KCl, 0.36 mM EDTA, 10 mM KH_2PO_4, 10 mM Tris-HCl, and 0.3% fatty acid-free bovine albumin adjusted to a final pH of 6.5 (27).

Purification of Uncoupling Protein from Yeast Mitochondria—UCP was purified from yeast mitochondria using the same protocols that have been described for hamster brown adipose tissue mitochondria (4). Briefly, a paste containing octylpentaoxyethylene-extracted yeast mitochondria, lipid, and hydroxylapatite was packed in a column and centrifuged at low speed. The ionic composition of the eluate was adjusted to the desired "internal medium" and then stirred with a Bio-Beads SM-3 (Bio-Rad) for 150 min at 4 °C to remove detergent and form proteoliposomes. Remaining traces of detergent and external probe were removed by centrifugation through a second Bio-Beads SM-2 column and a Sephadex column (4).

Electrophoretic Cl^- Transport—UCP was purified as described above with "internal medium" containing 0.14 mM KCl, 50 mM TEA sulfate, 100 mM TEA-TES, pH 7.2, and 1 mM of the Cl^--sensitive fluorescent probe 6-methoxy-*N*-(3-sulfopropyl)quinolium. For assay, 150-μl aliquots of stock proteoliposomes were added to 1.85 ml of 150 mM KCl and 25 mM TEA-TES, pH 7.2, resulting in a final KCl concentration of 138 mM. Rates of Cl^- uptake were obtained from measured rates of fluorescence decrease using Stern-Volmer calibration curves, as previously described (4). Fluorescence intensity was converted to internal $[Cl^-]$ using a numerical iteration procedure.[2] Internal volume and protein content of proteoliposomes were measured (4) for conversion to uptake rates per milligram of UCP.

Electrophoretic H^+ Transport—UCP was purified as described above with "internal medium" containing 0.14 mM K-TES, 75 mM TEA sulfate, 75 mM TEA-TES, pH 7.2, and 50 μM of the K^+-sensitive fluorescent probe, PBFI. H^+ transport was assayed indirectly as the K^+ counterflux in the presence of valinomycin (28). 150-μl aliquots of stock proteoliposomes were added to 1.85 ml of 75 mM K_2SO_4, 75 mM TEA-TES, pH 7.2, resulting in a final K^+ concentration of 138 mM. The fluorescent probe response was calibrated, and fluorescence intensity was converted to internal $[K^+]$, as previously described (29).

RESULTS

Expression of Uncoupling Protein in Yeast—We developed an expression system in yeast to enable us to investigate structure-function relationships using site-directed mutagenesis. The rat UCP cDNA that we had previously cloned (16) was inserted into the shuttle vector pCGS110 under control of the inducible *Gal*I promoter. A high level of expression of UCP was achieved in yeast transformants by altering the 18-nucleotide upstream region and the 5-nucleotide downstream region around the initiating ATG of the UCP cDNA to resemble the sequence of a highly expressed yeast glyceraldehyde-3-phosphate dehydrogenase gene and highly used codons in yeast. These changes resulted in a 24-fold increase in the level of UCP over that obtained with unmodified cDNA. Cell fractionation of galactose-induced yeast transformants containing the altered UCP cDNA showed that UCP localized to the mitochondrial fraction (Fig. 1) at a level of 70–100 μg of UCP/mg of mitochondrial protein.

The inner membrane-to-outer membrane ratio of the level of UCP, cytochrome oxidase activity (an inner membrane protein marker) and kynurenine hydroxylase activity (an outer membrane protein marker) were 3.6, 4.3, and 0.2, respectively, showing that UCP was located in the mitochondrial inner membrane. Further studies have shown that yeast mitochondria containing UCP exhibit GDP binding to the extent of 0.4 nmol of GDP/mg of mitochondrial protein, which may be compared to a value of 0.9 obtained by Lin and Klingenberg (30) in brown adipose tissue mitochondria isolated from cold-adapted rats and hamsters.

Effect of Expressed Uncoupling Protein on Yeast Mitochondrial Function—In brown adipose tissue mitochondria, fatty acids activate the UCP, causing stimulation of respiration and uncoupling of oxidative phosphorylation (1). These effects of fatty acids are reversed by purine nucleoside di- and triphosphates. To determine whether UCP imparted these characteristics of brown adipose tissue mitochondria to yeast mitochondria, we examined the effects of oleate and GDP on the respiratory rates of yeast mitochondria that contained or lacked UCP. As illustrated in Fig. 2, isolated mitochondria

[2] P. Jezek, unpublished data.

containing (*a*) and lacking (*c*) UCP were both coupled with similar ADP:O and respiratory control ratios. The higher rate of respiration in transformed mitochondria was consistently observed and may be due in part to activity of UCP. This explanation is supported by the finding that respiratory rate in mitochondria containing UCP was depressed by one-third in the presence of GDP.

The addition of oleate to mitochondria containing UCP caused a further 1.3-fold increase in the rate of respiration and prevented the normal stimulation of respiration by ADP addition (Fig. 2*b*). In contrast, mitochondria lacking UCP were not affected by oleate addition and had a 2.1-fold stimulation in the rate of respiration after ADP addition (Fig. 2*d*). Furthermore, the subsequent GDP addition to mitochondria containing UCP caused a 37% decrease in the rate of respiration, after which ADP addition caused a 1.8-fold stimulation in the rate. Mitochondria lacking UCP were relatively unaffected by the GDP addition showing an 8% decrease in the respiratory rate, after which ADP addition caused a 1.4-fold stimulation in the rate.

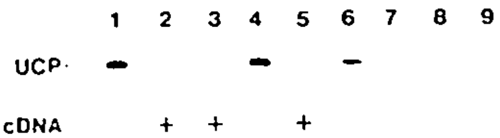

FIG. 1. **Immunoblot analysis of uncoupling protein (UCP) distribution in yeast cell fractions.** Yeast transformants were induced to express UCP by the addition of galactose to 0.2% for 8 h (21, 22); then cells were disrupted and fractionated (20). A portion of each cell fraction was immunoprecipitated using monospecific antiserum against rat UCP and protein A-Sepharose CL-4B. The immunoprecipitates were separated by SDS-12.5% PAGE, transferred to nitrocellulose, and detected with monospecific antiserum against rat UCP and ^{125}I-labeled protein A. *Lanes 1, 4,* and *6* contain rat 32-kDa UCP markers of 0.35, 0.28, and 0.21 μg, respectively. *Lanes 2, 3,* and *5* represent 0.14% of the postmitochondrial, 0.23% of the postnuclear, and 0.42% of the mitochondrial fractions, respectively, isolated from galactose induced yeast cells transformed with pCGS110 containing the altered UCP cDNA. *Lanes 7–9* represent the same percentages stated above for the mitochondrial, postnuclear and postmitochondrial fractions, respectively, from galactose-induced cells transformed with pCGS110 lacking modified UCP cDNA.

These results, showing that oleate causes stimulation and uncoupling of respiration in mitochondria from transformed yeast cells, are consistent with activation of UCP. Furthermore, the demonstration that GDP reverses respiratory stimulation and restores coupling are consistent with normal function of the expressed UCP in yeast mitochondria. It is of interest to note that mitochondria containing UCP isolated from transformed CHO cells were uncoupled without requiring the addition of oleate and were recoupled by GDP addition (13). The differing activity of UCP in these two expression systems may derive in part from differences in the fatty acid content of the host mitochondria. These differences illustrate the complexity of the integrated system containing respiratory chain, ATPase, UCP, and other endogenous transporters. Thus, although our experiments indicate that UCP confers onto yeast mitochondria the respiratory characteristics of brown adipose tissue mitochondria, quantitative comparisons of activities for the purpose of structure/function studies would be difficult in this complex system. This emphasizes the need for a reconstitution system in which to examine the properties of the purified protein.

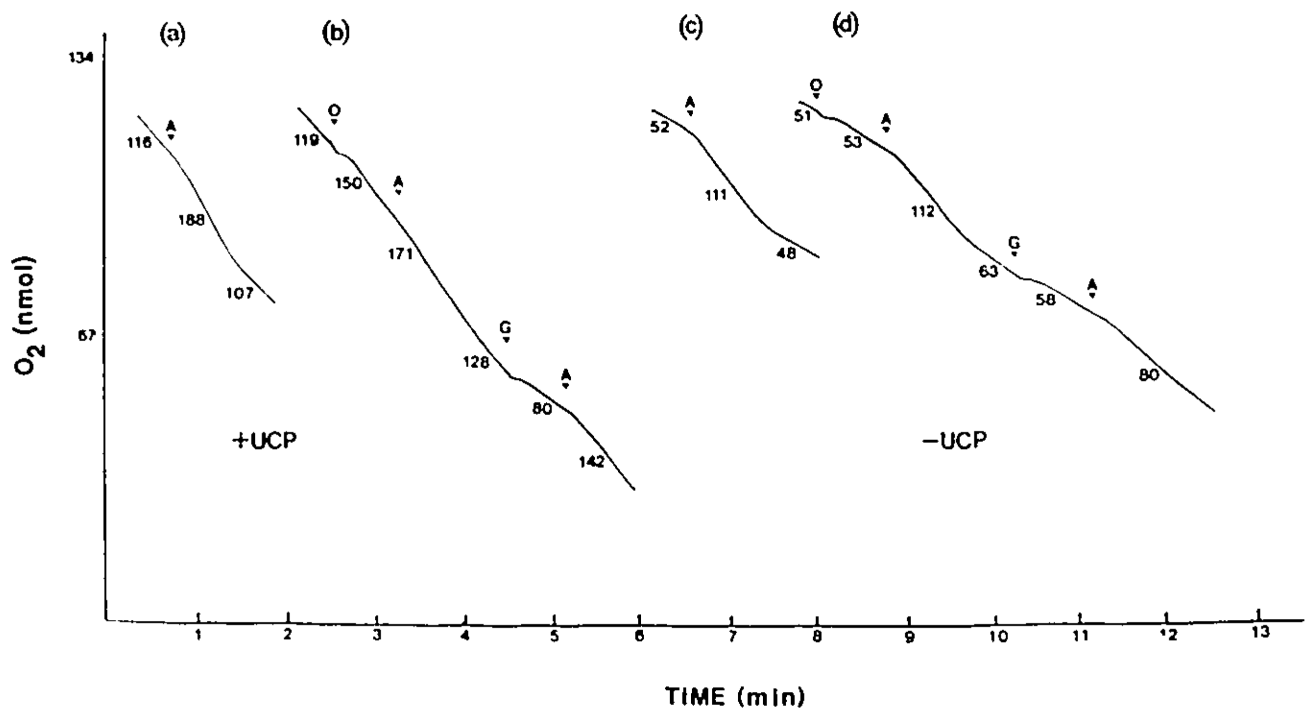

FIG. 2. **The effects of oleate and GDP on oxidative phosphorylation and respiration of yeast mitochondria.** Mitochondria containing UCP were isolated from yeast transformants that were grown in the presence of 0.2% galactose for 9 h. Control mitochondria were isolated from nontransformed yeast. Mitochondria containing UCP (187 μg) or lacking UCP (244 μg) were added to 0.6 ml of reaction buffer followed by the addition of succinate to 8 mM. Coupling was determined by the addition of 60 nmol of ADP (*A*). Activation and inhibition of UCP were tested by the addition of 170 μM oleate (*O*) and 170 μM GDP (*G*) where indicated. The respiration rates quoted on the graphs are in nmol of O_2/min/mg of mitochondrial protein. The ADP:O ratio in experiments *a* and *c* were 1.4 for mitochondria containing and lacking UCP. The respiratory control ratios were 1.8 and 2.3, respectively.

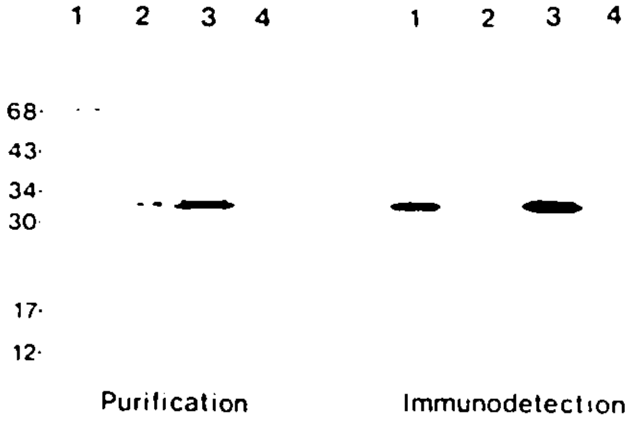

FIG. 3. **SDS-PAGE analysis of uncoupling protein isolated from yeast mitochondria.** Purification (*left panel*). UCP was purified from a yeast mitochondrial fraction as outlined under "Experimental Procedures." The resultant protein from the hydroxylapatite eluate was separated by SDS-12.5% PAGE and detected by silver staining. *Lane 1*, molecular mass markers (kDa); *lane 2*, 0.36 μg of rat UCP marker; *lanes 3* and *4*, protein purified from mitochondria isolated from yeast transformants containing (*lane 3*) and lacking (*lane 4*) the altered UCP cDNA. Immunodetection (*right panel*), isolated yeast mitochondria and hydroxylapatite-purified protein were separated by SDS-12.5% PAGE, transferred to nitrocellulose, and detected with monospecific antiserum against rat UCP and ^{125}I-labeled protein A. *Lanes 1* and *2*, mitochondria isolated from transformants containing (*lane 1*) or lacking (*lane 2*) altered UCP cDNA. *Lanes 3* and *4*, hydroxylapatite-purified protein obtained from transformants containing (*lane 3*) or lacking (*lane 4*) UCP cDNA.

Chloride and Proton Transport Mediated by the Heterologously Expressed Uncoupling Protein—Heterologously expressed UCP was purified from yeast mitochondria and reconstituted into proteoliposomes using protocols identical with those described for brown adipose tissue mitochondria (4). Typically, a single batch of transformed yeast (8 g, wet weight) yielded 10 mg of mitochondrial protein and 500–700 μg of purified UCP, an amount sufficient to carry out 15–20 reconstitution assays. Electrophoretic analysis of the purified protein revealed a single band at 32 kDa, which was confirmed to be UCP by immunodetection (Fig. 3).

The reconstituted UCP catalyzed rapid, GDP-sensitive Cl^- uptake (Fig. 4) and H^+ ejection (measured as K^+ uptake, Fig. 5) following addition of valinomycin to proteoliposomes suspended in medium containing 138 mM K^+. When excess GDP was present on both sides of the membrane, the rates of Cl^- uptake and H^+ ejection were comparable with the respective rates in liposomes and in proteoliposomes containing extract from mitochondria of yeast transformants lacking the UCP insert (data not shown). This confirms that the observed GDP-sensitive Cl^- transport is mediated entirely by the reconstituted 32-kDa protein. In further experiments not shown, we observed that Cl^- uniport is inhibited almost completely (98%) by the newly discovered UCP substrate, hexanesulfonate (5). Additionally, we observed that H^+ uniport is greatly stimulated when fatty acids are reconstituted with both the native[2] and the expressed UCP.

The average rates of Cl^- and H^+ uniport catalyzed by UCP were 3600 nmol Cl^-/min mg and 2100 nmol H^+/min mg of reconstituted protein. Assuming that these rates reflect operation of a 66-kDa dimeric protein (16), the corresponding turnover numbers are 4 s^{-1} for Cl^- and 2.3 s^{-1} for H^+. These are similar to values obtained with the hamster UCP, which are 4.3 s^{-1} for Cl^- (4) and 2 s^{-1} for H^+ ions (31).

[2] P. Jezek and K. D. Garlid, manuscript in preparation.

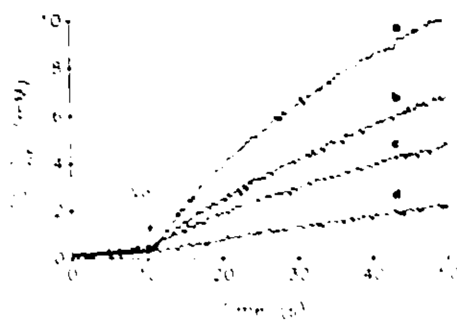

FIG. 4. **Electrophoretic chloride uptake into proteoliposomes reconstituted with uncoupling protein purified from yeast mitochondria.** The purified, reconstituted UCP catalyzed rapid, GDP-sensitive Cl^- uptake following addition of valinomycin (*Val*) to proteoliposomes suspended in 138 mM KCl medium (*curve a*). Cl^- uptake was inhibited 52% when 200 μM GDP was added to external medium (*curve c*). Cl^- uptake was inhibited 45% in proteoliposomes reconstituted with 200 μM internal GDP (*curve b*) and 90% when 200 μM GDP was present on both sides of the membrane (*curve d*). Cl^- flux was also measured in proteoliposomes reconstituted with extract from mitochondria of yeast transformants lacking the UCP cDNA sequence but containing the promoter vector. These rates, 1.2 nmol/min mg of lipid, were very similar to the rate, 2 nmol/min mg of lipid, observed when 200 μM GDP was present on both sides of the membrane.

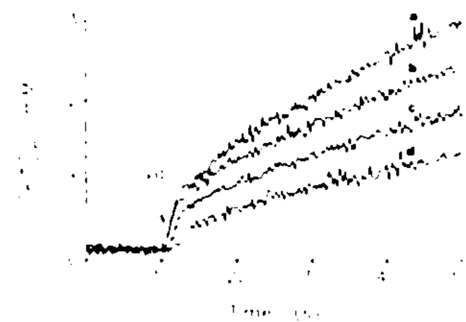

FIG. 5. **Electrophoretic proton ejection from proteoliposomes reconstituted with uncoupling protein purified from yeast mitochondria.** The purified, reconstituted UCP catalyzed rapid, GDP-sensitive K^+ uptake following addition of valinomycin (*Val*) to proteoliposomes suspended in 138 mM K^+ medium (*curve a*). Because the proteoliposomes were suspended in medium containing impermeant anions, the rate of valinomycin induced K^+ uptake is limited by H^+ efflux. We identify the pathway with the UCP because K^+ uptake is inhibited by GDP. H^+ ejection was inhibited 39% when 200 μM GDP was added to external medium (*curve c*). H^+ ejection was inhibited 32% in proteoliposomes reconstituted with 200 μM internal GDP (*curve b*) and 73% when 200 μM GDP was present on both sides of the membrane (*curve d*). H^+ flux in liposomes, 2.4 nmol/min mg of lipid, was somewhat less than the rates in proteoliposomes, 11 nmol/min mg of lipid, obtained when 200 μM GDP was present on both sides of the membrane. The initial jump in [K^+], which may reflect membrane charging following addition of valinomycin, was also observed in liposomes and was not used to calculate rates.

GDP Inhibition of Chloride and Proton Transport Mediated by the Heterologously Expressed Uncoupling Protein—In the mitochondrion, the GDP-binding sites occur on the cytosolic side of UCP (32). The effects of internal *versus* external GDP on both the Cl^- uniport and the H^+ uniport (Figs. 4 and 5) suggest a mixed orientation of reconstituted UCP, with about 50% of the sites facing the exterior of the proteoliposomes. This is in accord with findings on UCP isolated from hamster brown adipose tissue (4). Fig. 6 contains dose-response curves for GDP inhibition of Cl^- uniport and H^+ uniport. The observed k_i values at pH 7.2 were 7 and 10 μM, respectively. These compare well with k_i values of 15 μM for GDP inhibition

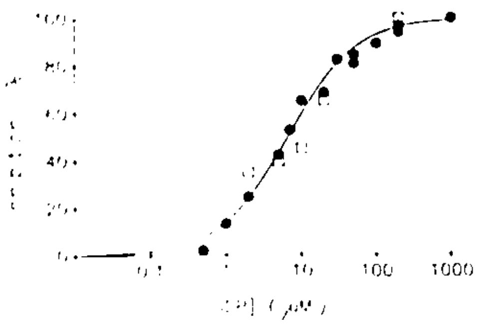

FIG. 6. **GDP titrations of H^+ and Cl^- transport through heterologously expressed, purified uncoupling protein.** The figure contains the dose-responses for inhibition of the Cl^- uptake (●) and the H^+ efflux (□) by external GDP in proteoliposomes containing expressed, purified UCP and 200 μM internal GDP. Measurements were performed as described in the legends to Figs. 4 and 5. Basal rates, obtained with 200 μM GDP on both sides of the membrane, were subtracted from measured rates to obtain percent inhibition. The theoretical dose-response curve (*solid line*) was plotted using a Hill coefficient of 1.0 and K_i value of 6.6 μM. Linear regressions of Hill plots yielded Hill coefficients and K_i values of 0.96 and 6.6 μM for GDP inhibition of Cl^- uptake and 0.75 and 10 μM for GDP inhibition of H^+ efflux.

of Cl^- transport (4) and 20 μM for GDP inhibition of H^+ transport[3] obtained with hamster UCP.

DISCUSSION

Our demonstration of functional reconstitution of purified, heterologously expressed uncoupling protein having properties indistinguishable from those of the native protein is the first such example for a mammalian mitochondrial inner membrane transport protein. This result establishes that UCP retains its functional properties following heterologous expression in yeast.

We have also demonstrated that mitochondria isolated from transformed yeast contain 70–100 μg of UCP/mg of mitochondrial protein, that the expressed protein is localized to the inner membrane, and that the yeast mitochondria respond to fatty acids and nucleotides in the same way as native brown adipose tissue mitochondria. The physiological competence of the expressed UCP *in situ* is important and will be presented in greater detail in a separate paper.[4] Nevertheless, intact mitochondria are biochemically and physiologically complex, and discerning analyses of functional properties require the purified, reconstituted preparation.

A major objective of these studies was to develop an expression system that is suitable for structure-function studies, including site-directed mutagenesis. Such a system must be cost-effective and amenable to quantitative assays of function. It must be shown to yield a protein that exhibits properties characteristic of native UCP. Moreover, it must be capable of high levels of stable expression, because the molecular activity of UCP is extremely low. (The molecular activity of UCP is about 2 orders of magnitude less than the activities of the K^+/H^+ antiporter (33) and the P_i-H^+ symporter (34), for example.) Although other expression systems have been reported for UCP (35, 13), it is only the transformed yeast system that satisfies these criteria.

Since the availability of expressed UCP is effectively unlimited, these studies can now readily be extended to define the molecular mechanisms of anion and H^+ translocation and of regulation of transport by fatty acids and purine nucleotides. Site-directed mutagenesis studies to elucidate the structural basis of the many intriguing aspects of UCP function are now underway in our laboratories.

[4] D. I. Murdza-Inglis, H. V. Patel, and K. B. Freeman, manuscript in preparation.

REFERENCES

1. Nicholls, D. G. (1979) *Biochim. Biophys. Acta* **549**, 1–29
2. Cunningham, S. A., Weisinger, H., and Nicholls, D. G. (1986) *Eur. J. Biochem.* **157**, 415–420
3. LaNoue, K. F., Strzelecki, T., Strzelecki, D., and Koch, C. (1986) *J. Biol. Chem.* **261**, 298–305
4. Jezek, P., Orosz, D. E., and Garlid, K. D. (1990) *J. Biol. Chem.* **265**, 19296–19302
5. Jezek, P., and Garlid, K. D. (1990) *J. Biol. Chem.* **265**, 19303–19311
6. Jezek, P. (1987) *FEBS Lett.* **211**, 89–93
7. Kopecky, J., Guerrieri, F., Jezek, P., Drahota, Z., and Houstek, J. (1984) *FEBS Lett.* **170**, 186–190
8. Garlid, K. D. (1990) *Biochim. Biophys. Acta* **1018**, 151–154
9. Klingenberg, M. (1990) *Trends Biochem. Sci.* **15**, 108–112
10. Wojtczak, L., and Zaluska, H. (1967) *Biochem. Biophys. Res. Commun.* **28**, 76–81
11. Andreyev, A. Y., Bondareva, T. O., Dedukhova, V. I., Mokhova, E. N., Skulachev, V. P., Tsofina, L. M., Volkov, N. I., and Vygodina, T. V. (1989) *Eur. J. Biochem.* **182**, 585–592
12. Schonfeld, P. (1990) *FEBS Lett.* **264**, 246–248
13. Casteilla, L., Blondel, O., Klaus, S., Raimbault, S., Diolez, P., Moreau, F., Bouillaud, F., and Ricquier, D. (1990) *Proc. Natl. Acad. Sci. U. S. A.* **87**, 5124–5128
14. Klingenberg, M., and Winkler, E. (1985) *EMBO J.* **4**, 3087–3092
15. Trayhurn, P., Ashwell, M., Jennings, G., Richard, D., and Stirling, D. M. (1987) *Am. J. Physiol.* **252**, E237–E243
16. Ridley, R. G., Patel, H. V., Gerber, G. E., Morton, R. C., and Freeman, K. B. (1986) *Nucleic Acids Res.* **14**, 4025–4035
17. Hamilton, R., Watanabe, C. K., and de Bohr, H. A. (1987) *Nucleic Acids Res.* **15**, 3581–3593
18. Sharp, P. M., Tuohy, T. F. F., and Mosurski, K. R. (1986) *Nucleic Acids Res.* **14**, 5125–5143
19. Daum, G., Bohni, P. C., and Schatz, G. (1982) *J. Biol. Chem.* **257**, 13028–13033
20. Gasser, S. M. (1983) *Methods Enzymol.* **97**, 329–336
21. Adams, B. G. (1972) *J. Bacteriol.* **111**, 308–315
22. Brown, C. M., and Johnson, B. (1970) *J. Gen. Microbiol.* **64**, 279–287
23. Velours, J., Guerin, B., and Duvert, M. (1977) *Arch. Biochem. Biophys.* **182**, 295–304
24. Hayaishi, O. (1962) *Methods Enzymol.* **5**, 807–809
25. Cooperstein, S. J., and Lazarow, A. (1951) *J. Biol. Chem.* **189**, 665–670
26. Gregory, E. M., Yost, F. J., Jr., Rohrback, M. S., and Harrison, J. M. (1971) *J. Biol. Chem.* **246**, 5491–5497
27. Guerin, B., Labbe, P., and Somlo, M. (1979) *Methods Enzymol.* **55**, 149–159
28. Krishnamoorthy, G., and Hinkle, P. (1984) *Biochemistry* **23**, 1640–1645
29. Jezek, P., Mahdi, F., and Garlid, K. D. (1990) *J. Biol. Chem.* **265**, 10522–10526
30. Lin, C. S., and Klingenberg, M. (1980) *FEBS Lett.* **113**, 299–303
31. Jezek, P., Drahota, Z., and Ring, K. (1990) *J. Lipid Mediators* **2**, 85–94
32. Lin, C. S., and Klingenberg, M. (1982) *Biochemistry* **21**, 2950–2956
33. Martin, W. H., DiResta, D. J., and Garlid, K. D. (1986) *J. Biol. Chem.* **261**, 12300–12305
34. Ligeti, E., Brandolin, G., Dupont, Y., and Vignais, P. V. (1985) *Biochemistry* **24**, 4423–4428
35. Klaus, S., Casteilla, L., Bouillaud, F., Raimbault, S., and Ricquier, D. (1990) *Biochem. Biophys. Res. Commun.* **167**, 784–789

The Journal of Biological Chemistry
© 1994 by The American Society for Biochemistry and Molecular Biology, Inc.

Vol. 269, No. 10, Issue of March 11, pp. 7435-7438, 1994
Printed in U.S.A.

A Single Mutation in Uncoupling Protein of Rat Brown Adipose Tissue Mitochondria Abolishes GDP Sensitivity of H⁺ Transport*

(Received for publication, November 4, 1993)

Debra L. Murdza-Inglis‡§, Martin Modriansky¶§, Hasmukh V. Patel‡, Gebre Woldegiorgis¶, Karl B. Freeman‡‖, and Keith D. Garlid¶‖

From the ‡Department of Biochemistry, McMaster University, Hamilton, Ontario L8N 3Z5, Canada and the ¶Department of Chemistry, Biochemistry, and Molecular Biology, Oregon Graduate Institute of Science and Technology, Portland, Oregon 97291-1000

The uncoupling protein is one of a family of mitochondrial transport proteins involved in energy metabolism. It dissipates oxidative energy to generate heat, either by catalyzing proton transport directly or by catalyzing fatty acid anion transport, thus enabling fatty acids to act as cycling protonophores. This transport process is tightly regulated by purine nucleotides. We have expressed uncoupling protein in yeast and examined its proton transport activity after its reconstitution into proteoliposomes. A directed change of Arg^{276} to Leu or Gln completely abolished nucleotide inhibition of protonophoretic action of the reconstituted mutant uncoupling proteins without affecting the transport process. Arg^{276} is the first residue of functional importance to be identified in uncoupling protein. Mutation of the homologous residue in the yeast ADP/ATP translocator prevented the growth of yeast on a nonfermentable carbon source, presumably by interfering with nucleotide exchange (Nelson, D. R., Lawson, J. E., Klingenberg, M., and Douglas, M. G. (1993) *J. Mol. Biol.* 230, 1159–1170). Demonstration of the essential role of a single homologous residue in protein-nucleotide interaction within these two transporters is the first direct evidence that uncoupling protein and the ADP/ATP translocator belong to the same gene family.

Uncoupling protein (UCP)[1] belongs to a family of mitochondrial anion porters involved in energy metabolism, including the ADP/ATP translocator, the phosphate-H⁺ symporter, and the oxoglutarate carrier. These porters do not exhibit prominent homologies of primary structure; however, they have similar molecular masses, and all contain three homologous domains of about 100 amino acid residues, each of which contains two transmembrane helical sequences (1–4). UCP has the specific role of generating heat in mammalian brown adipose tissue, either by permitting proton flux directly or by catalyzing fatty acid anion transport across the mitochondrial inner membrane, thus enabling the fatty acids to act as protonophores (4, 5).

Chemical modification studies on UCP using sulfhydryl reagents or arginine-modifying reagents have suggested that these residues might have functional significance, but in this approach the specific residues could not be identified (6, 7). Moreover, these effects could be due to introduction of bulky side groups resulting in steric interference with function. In a different approach, photoaffinity labeling with purine nucleotide analogs shows that the third domain of UCP is involved in nucleotide binding but does not identify functionally important residues (8, 9).

We have approached the question of locating such residues in UCP by developing a system of high level expression of functional rat UCP in yeast (10) and sensitive fluorescent assays of proton (11) and anion (12) transport in proteoliposomes reconstituted with expressed UCP purified from yeast. These protocols were used to evaluate the effects on GDP-sensitive proton transport of changing the individual cysteine residues to serine and Arg^{276} to glutamine and leucine. Mutation of Arg^{276} resulted in complete loss of GDP inhibition of proton transport mediated by reconstituted UCP.

EXPERIMENTAL PROCEDURES

Materials—The *Escherichia coli*/*Saccharomyces cerevisiae* shuttle vector pCGS110 was the kind gift of Dr. D. T. Moir, Collaborative Research Inc. M13mp19 was from Life Technologies, Inc. Zymolyase 100T was obtained from ICN Biochemicals. D(+)-galactose G 0750 and fatty acid-free bovine serum albumin A 6003 were obtained from Sigma. Oligonucleotides were purchased from the Central Facility of the Institute for Molecular Biology and Biotechnology at McMaster University. SPQ was purchased from Calbiochem. Bovine serum albumin (Factor IV), fatty acids, and ionophores were purchased from Sigma. Alkylsulfonates were purchased from Research Plus, Inc. (New Jersey). Materials for protein purification and liposome formation were obtained from sources described in Jezek *et al.* (12).

Mutagenesis—Rat UCP cDNA altered around the 5′-translation start site for efficient translation in yeast was originally constructed in pGEM5Zf (10). The *Sal*I/*Sph*I fragment containing the altered rat UCP cDNA from this construct was cloned into *Sal*I/*Sph*I-cut M13mp19 for site-directed mutagenesis. Oligonucleotides were designed to alter UCP codons for Arg^{276} (CGA) to Gln (CAA) and Leu (CTA) and Cys[illegible] (TGT) to Ala (GCT). Site-directed mutagenesis was carried out using the method of Kunkel (13). A unique *Sac*I site was engineered into the *E. coli*/*S. cerevisiae* shuttle vector pCGS110 between the *Bam*HI and *Sph*I sites of the vector. This permitted subcloning of *Sac*I/*Sph*I fragments from M13mp19 containing wild-type or mutated forms of UCP cDNA into *Sac*I/*Sph*I-cut pCGS110 such that the cDNAs were under transcriptional control of the inducible *Gal*I promoter. The *S. cerevisiae* strain JB516 (*MATa, ura3, ade1, leu2, his4, gal⁺*) was transformed by electroporation with the shuttle vector constructs at 1.5 kV, 25 microfarads, 200 ohm. The yeast transformants were grown at 30 °C in selective medium as previously described (10).

Mitochondrial Isolation—Expression of UCP was induced in yeast transformants with 0.2% galactose for 12 h, after which mitochondria

* This research was supported by Grants GM 31086 and HL 43814 (to K. D. G.) from the National Institutes of Health, Grant MT-1940 (to K. B. F.) from the Medical Research Council of Canada, and a Medical Research Council of Canada studentship (to D. L. M-I.). The costs of publication of this article were defrayed in part by the payment of page charges. This article must therefore be hereby marked "*advertisement*" in accordance with 18 U.S.C. Section 1734 solely to indicate this fact.

§ This work was submitted in partial fulfillment of requirements for the Ph.D. degree.

‖ To whom correspondence and reprint requests should be addressed: Dept. of Chemistry, Biochemistry, and Molecular Biology, Oregon Graduate Institute, P.O. Box 91000, Portland, OR 97291-1000. Tel.: 503-690-1680; Fax: 503-690-1464.

[1] The abbreviations used are: UCP, uncoupling protein; SPQ, 6-methoxy-*N*-(3-sulfopropyl)quinolinium; TES, *N*-tris(hydroxymethyl)methyl-2-aminoethanesulfonic acid; FDNP-ATP, 3′-*O*-(5-fluoro-2,4-dinitrophenyl)adenosine 5′-triphosphate.

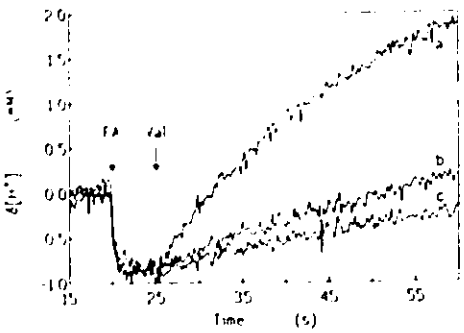

FIG. 1. Electrophoretic H⁺ efflux from proteoliposomes reconstituted with expressed, purified wild-type UCP. Fluorescence traces from proteoliposomes containing SPQ and 1 mM GDP were converted to changes in intraliposomal acidity ($\delta[H^+]$) and plotted *versus* time. Proton efflux was initiated by addition of valinomycin (*Val*) in the presence of 30 µM laurate (*FA*). *Trace a*, no further additions; *trace b*, 1 mM GDP was present in assay medium; *trace c*, 300 µM undecanesulfonate was present in assay medium.

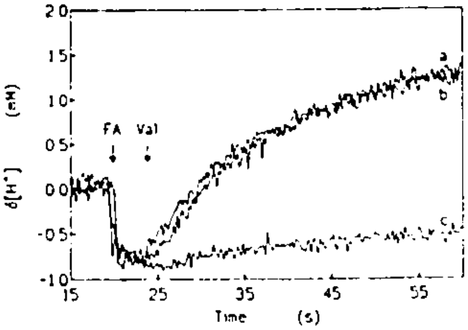

FIG. 2. Electrophoretic H⁺ efflux from proteoliposomes reconstituted with expressed, purified Arg²⁷⁶ → Leu mutant UCP. Fluorescence traces from proteoliposomes containing SPQ and 1 mM GDP were converted to changes in intraliposomal acidity ($\delta[H^+]$) and plotted *versus* time. Proton efflux was initiated by addition of valinomycin (*Val*) in the presence of 30 µM laurate (*FA*). *Trace a*, no further additions; *trace b*, 1 mM GDP was present in assay medium; *trace c*, 300 µM undecanesulfonate was present in assay medium.

were isolated and resuspended in a solution containing 0.6 M sucrose, 20 mM HEPES-KOH (pH 6.5) containing 0.1% fatty acid-free bovine serum albumin as previously described (10).

Preparation of Proteoliposomes Containing the Expressed, Purified Mutant and Wild-type UCPs—Purification and reconstitution followed protocols previously described (12). Briefly, yeast mitochondria were solubilized in 13% octylpentaoxyethylene in the presence of L-α-phosphatidylcholine, cardiolipin, and L-α-phosphatidic acid, and this mixture was applied to a hydroxyapatite column. The internal medium was adjusted to the desired concentrations, and the fluorescent probe SPQ was added. Vesicle formation and external probe removal were accomplished by treatment with Bio-beads SM-2 and Sephadex G-25, respectively. Final lipid concentration was approximately 40 mg/ml.

Proton Flux Measurements Using SPQ—Proteoliposomes were added to 2 ml of assay medium to a final concentration of 0.5 mg of lipid/ml. The intravesicular medium contained 1 mM GDP and tetraethylammonium salts of TES (28.8 mM), EGTA (0.6 mM), and SO_4 (84.4 mM), pH 7.2. The external medium, also at pH 7.2, contained tetraethylammonium salts of TES (28.8 mM), EGTA (0.6 mM), and SO_4 (24.4 mM), and 120 mM K^+ as the SO_4 salt. Proton efflux from the liposomes was initiated by adding 30 µM laurate followed by 0.1 µM valinomycin. As we have reported (11), TES anion quenches SPQ fluorescence whereas TES zwitterion does not; therefore, changes in fluorescence in this medium result from changes in total acid, *i.e.* from proton flux across the liposomal membrane. In each experiment, the quench coefficient was determined by calibration curves carried out on the proteoliposomes. Internal liposomal volume, determined from the volume of distribution of SPQ, was 1.1–1.6 µl/mg of lipid. Protein content, estimated by the Amido Black method, was 1–3 µg of protein/mg of lipid.

RESULTS

Proton Transport Phenotype of Wild-type UCP—Fig. 1 contains typical traces of H^+ efflux from vesicles reconstituted with wild-type UCP. The large internal acidification following laurate addition is due to partitioning of laurate/lauric acid in the membrane, followed by rapid flip-flop equilibration and delivery of protons to the internal medium (14). Addition of valinomycin caused internal alkalinization (Fig. 1, *trace a*), which implies an underlying movement of protons and charge. This electrophoretic proton efflux may be the result of proton transport directly by UCP (4) or of laurate anion transport by UCP, with the proton carried by nonionic diffusion of lauric acid (5). That proton efflux required mediation of UCP is demonstrated by its inhibition by external GDP (Fig. 1, *trace b*). The K_i values for GDP inhibition of proton transport by wild-type UCP ranged between 8 and 10 µM in three experiments where it was measured. Proton efflux was also inhibited by the laurate analogue, undecanesulfonate (Fig. 1, *trace c*). Undecanesulfonate is transported by UCP, and its inhibition of UCP-catalyzed H^+ transport is competitive with laurate.[2]

Proton Transport Phenotypes of Cysteine Mutants of UCP—We mutated all cysteines to serines independently, and we also mutated Cys²⁵³ to alanine. For each mutant, we assayed proton transport and its inhibition by GDP and undecanesulfonate. As we have reported in a preliminary communication (15), each of these mutations was without effect on transport and inhibition (data not shown).

Proton Transport Phenotypes of Arg²⁷⁶ Mutants of UCP—We mutated Arg²⁷⁶ to leucine and glutamine. Fig. 2 contains representative traces from an Arg²⁷⁶ → Leu mutant reconstituted into liposomes. UCP-catalyzed H^+ transport (Fig. 1, *trace a*) was unaffected in the leucine mutant, and it was reduced by about 50% in the glutamine mutant (see Table I). The striking feature of these mutants is that GDP had no effect on H^+ transport (Fig. 1, *trace b*), and this defect was apparent at doses up to 1 mM, as shown in the GDP dose-response curves of Fig. 3. Confirming that laurate-induced H^+ transport was qualitatively unaffected by these mutations, the competitive inhibitor undecanesulfonate was effective in inhibiting transport (Fig. 2, *trace c*; Table I).

DISCUSSION

Mechanism of UCP-catalyzed Proton Transport—It is agreed that fatty acids cause UCP to catalyze electrophoretic proton transport and that UCP also catalyzes electrophoretic transport of monovalent anions, including undecanesulfonate (4, 12, 16–21). Undecanesulfonate is an analogue of lauric acid, but it is incapable of inducing H^+ transport through UCP. These analogues differ in that lauric acid rapidly equilibrates across lipid membranes, whereas undecanesulfonic acid is incapable of nonionic diffusion (Fig. 1). Finally, undecanesulfonate is competitive with laurate in inhibiting UCP-mediated H^+ transport.[2] These results favor a mechanism proposed by Skulachev (5), in which UCP is an anion channel whose physiological substrate is fatty acid anions. In this model, fatty acids act as protonophores, and regulation of H^+ back flux is provided by nucleotide inhibition of the anion uniport half-cycle.

The mechanism of UCP-catalyzed proton transport is still under active investigation, but the present results are most simply understood using the Skulachev model. Thus, the data in Fig. 1 show that H^+ efflux can be inhibited either by GDP, an allosteric non-competitive inhibitor of fatty acid anion transport, or by undecanesulfonate, a channel substrate and com-

[2] D. E. Orosz, M. Modriansky, P. Jezek, and K. D. Garlid, unpublished data.

TABLE I

Transport activity of reconstituted, yeast-expressed rat uncoupling protein

Proton fluxes were measured as described under "Experimental Procedures." Fluxes are given as means ± S.E. of *n* independent experiments for each uncoupling protein genotype. Proton fluxes were measured in the presence or absence of either external GDP or undecanesulfonate. Rates for Arg[276] → Gln are averages of two separate experiments.

Uncoupling protein	*n*	Undecanesulfonate	GDP	Proton flux
		μM	mM	nmol min⁻¹ mg⁻¹
Wild type	4	0	0	3860 ± 310
		0	1	1240 ± 180
		300	0	720 ± 280
Arg[276] → Leu	3	0	0	4250 ± 490
		0	1	4230 ± 440
		300	0	280 ± 280
Arg[276] → Gln	2	0	0	1940
		0	1	2040
		300	0	600

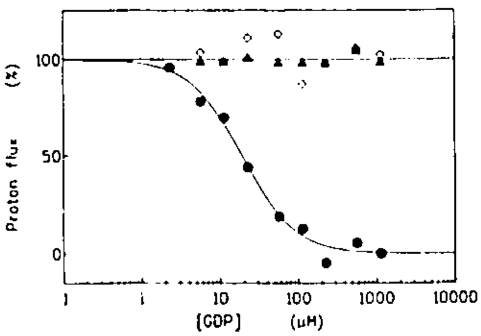

FIG. 3. **Effects of GDP on H⁺ efflux from proteoliposomes reconstituted with wild-type and mutant UCPs.** Proton fluxes, as percent of control rate in the absence of external GDP, are plotted *versus* external [GDP]. The figure contains data from three separate preparations: ●, wild-type UCP; ▲, Arg[276] → Leu mutant UCP; ◇, Arg[276] → Gln mutant UCP. The K_i for GDP inhibition of proton transport in the wild type was 10 μM. Control rates and rates in the presence of 1 mM GDP are contained in Table I.

petitive inhibitor of laurate anion transport.[2] The data in Fig. 2 show a dissociation of these effects. Protonophoretic cycling of laurate and lauric acid is unaffected by the mutation, as is inhibition by the competitive substrate, undecanesulfonate. On the other hand, GDP is no longer able to inhibit laurate transport through the mutant protein. Thus, the Arg[276] → Leu mutant is unimpaired in transport function but has completely lost its nucleotide regulatory capacity.

Role of Cysteines in UCP Transport and Regulation—The seven cysteines in UCP are conserved in UCP of all known species. Past chemical studies have implied that cysteines may be involved in both ion transport and GDP inhibition of this transport (6). However, changing all cysteines to serines independently was without effect on GDP inhibition of UCP-mediated proton or anion transport (15), indicating that a hydroxyl group can functionally substitute for each thiol group in UCP. Curiously, 5 of the 7 cysteines are found in the third domain of UCP, the region containing the GDP binding site. Because Mayinger and Klingenberg (8) deduced that Cys[253] was the most likely residue covalently labeled by the ATP analog FDNP-ATP, we replaced this residue with alanine to remove hydrogen-bonding ability while maintaining the hydrophobic nature of the side chain. This mutation was also without effect on transport function or regulation. These results show that the thiol group *per se* is not decisive for these functions. We are carrying out further studies, using bulkier substitutions, to determine whether the effects of thiol reagents on function may be steric rather than chemical.

Role of Arginine 276 in UCP Transport and Regulation—Based on the pH dependence of nucleotide binding to UCP, Klingenberg and co-workers (1) proposed that both acidic and basic residues are present in the purine nucleotide binding site of UCP. Chemical studies using arginine-modifying reagents had previously indicated that arginine is a critical functional residue for purine nucleotide binding (7). The most likely location of the arginine is in the third domain of UCP because labeling studies using ATP analogs have localized the purine nucleotide binding region of UCP to this area. Peptides labeled by the ATP analogs contained amino acids 258–283 and 238–255 (8, 9). From membrane disposition models of UCP, these peptides reside in helix 6 and in the matrix region connecting transmembrane helices 5 and 6, respectively (8, 20). It has been proposed that this region comprises a nucleotide binding pocket accessible to the cytosol side because it is known that purine nucleotides regulate UCP from this side of the inner membrane (8).

Of the 3 arginine residues in the third domain of UCP, we chose to modify Arg[276]. Based on the size of ATP in its extended *anti* conformation and the location of residues covalently labeled by the ATP analogs, it is unlikely that Arg[299] could interact with ATP. Although Arg[238] is about the same linear distance from the covalently labeled residues as Arg[276], the transmembrane arrangement of the third domain proposed by Mayinger and Klingenberg (8) depicts Arg[276] as being present in the proposed nucleotide binding pocket, spatially close to residues covalently labeled by ATP analogs and accessible to cytosolic purine nucleotides. Arg[238] is excluded from this binding pocket and is inaccessible to nucleotides in this arrangement. Further, Arg[276] is conserved in all mitochondrial carrier family members except the phosphate carrier, and the homologous residue in the yeast ADP/ATP translocator has recently been found to be required for growth, although its role in the transport function of the ADP/ATP translocator was not tested (22).

The functional role of Arg[276] was investigated by replacing the arginine with glutamine and leucine. The glutamine substitution maintains some hydrogen-bonding ability but removes positive charge. Leucine removes both these characteristics. In each case, the substituted side chain was shorter to minimize steric interference of function. Our results with purified, reconstituted UCP show that both mutations caused total abolition of GDP inhibition of proton transport. On the other hand, both mutant forms of UCP catalyzed proton efflux, and this transport was completely inhibited by the competitive inhibitor, undecanesulfonate. Because transport was normal with the Arg[276] → Leu mutant, the results are difficult to reconcile with a gross conformation change in the protein structure. They indicate that the effect of the mutation was on purine nucleotide sensitivity and not on transport function.

This is the first identification of a single residue that is directly involved in purine nucleotide regulation of UCP transport function and the first evidence that directly relates functionally important residues between the ADP/ATP translocator and UCP.

REFERENCES

1. Aquila, H., Link, T. A., and Klingenberg, M. (1987) *FEBS Lett.* **212**, 1–9
2. Runswick, M. J., Walker, J. E., Bisaccia, F., Iacobazzi, V., and Palmieri, F. (1990) *Biochemistry* **29**, 11033–11040
3. Casteilla, L., Bouillaud, F., Forest, C., and Ricquier, D. (1989) *Nucleic Acids Res.* **17**, 2131
4. Klingenberg, M. (1990) *Trends Biochem. Sci.* **15**, 108–112
5. Skulachev, V. P. (1991) *FEBS Lett.* **294**, 158–162
6. Jezek, P. (1987) *FEBS Lett.* **211**, 89–93
7. Katiyar, S. S., and Shrago, E. (1989) *Proc. Natl. Acad. Sci. U. S. A.* **86**, 2559–2562
8. Mayinger, P., and Klingenberg, M. (1992) *Biochemistry* **31**, 10536–10543
9. Winkler, E., and Klingenberg, M. (1992) *Eur. J. Biochem.* **203**, 295–304

10. Murdza-Inglis, D. L., Patel, H. V., Freeman, K. B., Jezek, P., Orosz, D. E., and Garlid, K. D. (1991) *J. Biol. Chem.* **266**, 11871–11875
11. Orosz, D. E., and Garlid, K. D. (1993) *Anal. Biochem.* **210**, 7–15
12. Jezek, P., Orosz, D. E., and Garlid, K. D. (1990) *J. Biol. Chem.* **265**, 19296–19302
13. Kunkel, T. A. (1985) *Proc. Natl. Acad. Sci. U. S. A.* **82**, 488–492
14. Kamp, F., and Hamilton, J. A. (1992) *Proc. Natl. Acad. Sci. U. S. A.* **89**, 11367–11370
15. Murdza-Inglis, D. L., Patel, H. V., Freeman, K. B., Orosz, D. E., Modriansky, M., and Garlid, K. G. (1993) *FASEB J.* **7**, A1108
16. Klingenberg, M., and Winkler, E. (1985) *EMBO J.* **4**, 3087–3092
17. Strieleman, P. J., Schalinske, K. L., and Shrago, E. (1985) *J. Biol. Chem.* **260**, 13402–13406
18. Cunningham, S. A., Weisinger, H., and Nicholls, D. G. (1986) *Eur. J. Biochem.* **157**, 415–420
19. Jezek, P., and Garlid, K. D. (1990) *J. Biol. Chem.* **265**, 19303–19311
20. Nedergaard, J., and Cannon, B. (1992) in *New Comprehensive Biochemistry: Molecular Mechanisms in Bioenergetics* (Ernster, L., ed) Vol. 23, pp. 385–420, Elsevier Science Publishers B.V., Amsterdam
21. Himms-Hagen, J. (1990) *FASEB J.* **4**, 2890–2898
22. Nelson, D. R., Lawson, J. E., Klingenberg, M., and Douglas, M. G. (1993) *J. Mol. Biol.* **230**, 1159–1170